Flexture and Shear Behaviour of Damaged RC Beams Repaired By Plate Bonding

by

Munawar Hussain

A Thesis Presented to the

FACULTY OF THE COLLEGE OF GRADUATE STUDIES

KING FAHD UNIVERSITY OF PETROLEUM & MINERALS

DHAHRAN, SAUDI ARABIA

In Partial Fulfillment of the
Requirements for the Degree of

MASTER OF SCIENCE

In

CIVIL ENGINEERING

July, 1992

INFORMATION TO USERS

This manuscript has been reproduced from the microfilm master. UMI films the text directly from the original or copy submitted. Thus, some thesis and dissertation copies are in typewriter face, while others may be from any type of computer printer.

The quality of this reproduction is dependent upon the quality of the copy submitted. Broken or indistinct print, colored or poor quality illustrations and photographs, print bleedthrough, substandard margins, and improper alignment can adversely affect reproduction.

In the unlikely event that the author did not send UMI a complete manuscript and there are missing pages, these will be noted. Also, if unauthorized copyright material had to be removed, a note will indicate the deletion.

Oversize materials (e.g., maps, drawings, charts) are reproduced by sectioning the original, beginning at the upper left-hand corner and continuing from left to right in equal sections with small overlaps. Each original is also photographed in one exposure and is included in reduced form at the back of the book.

Photographs included in the original manuscript have been reproduced xerographically in this copy. Higher quality 6" x 9" black and white photographic prints are available for any photographs or illustrations appearing in this copy for an additional charge. Contact UMI directly to order.

U·M·I

University Microfilms International
A Bell & Howell Information Company
300 North Zeeb Road, Ann Arbor, MI 48106-1346 USA
313/761-4700 800/521-0600

Order Number 1354026

Flexure and shear behaviour of damaged RC beams repaired by plate bonding

Hussain, Munawar Hussain, M.S.

King Fahd University of Petroleum and Minerals (Saudi Arabia), 1992

U·M·I
300 N. Zeeb Rd.
Ann Arbor, MI 48106

FLEXURE AND SHEAR BEHAVIOUR OF DAMAGED RC BEAMS REPAIRED BY PLATE BONDING

BY

MUNAWAR HUSSAIN

A Thesis Presented to the

FACULTY OF THE COLLEGE OF GRADUATE STUDIES

KING FAHD UNIVERSITY OF PETROLEUM & MINERALS

DHAHRAN, SAUDI ARABIA

In Partial Fulfillment of the
Requirements for the Degree of

MASTER OF SCIENCE
In
CIVIL ENGINEERING

JULY, 1992

KING FAHD UNIVERSITY OF PETROLEUM & MINERALS

DHAHRAN, SAUDI ARABIA

This thesis, written by

MUNAWAR HUSSAIN

under the direction of his thesis committee, and approved by all the members, has been presented to and accepted by the Dean, College of Graduate Studies, in partial fulfillment of the requirements for the degree of

MASTER OF SCIENCE IN CIVIL ENGINEERING

Thesis Committee

Chairman (Dr. Islem A. Basunbul)

Co-Chairman (Dr. Alfarabi M. Sharif)

Member (Dr. Ghazi J. Sulaimani)

Member (Dr. Mohammad H. Baluch)

Dr. Alfarabi M. Sharif
Department Chairman

Dr. Ala H. Rabeh
Dean College of Graduate Studies

Date : 1/11/92

كلية الدراسات العليا
COLLEGE OF GRADUATE STUDIES

This thesis is dedicated to

my beloved parents, wife, brothers and sisters

and

whose sacrifices made this task possible

ACKNOWLEDGEMENT

Praise and gratitude to Allah the Almighty, with whose gracious help it was possible to accomplish this work. Acknowledgement is due to King Fahd University of Petroleum and Minerals for extending all facilities and providing financial support.

I would offer my indebtedness and sincere appreciation to my advisor and committee chairman, Dr. Islem A. Basunbul, who has been a constant source of help and encourgement during my thesis work. I also greatly appreciate the invaluable co-operation and guidance extended by Dr. Alfarabi M. Sharif who was the co-chairman of the thesis committee. I am also thankful to Dr. Ghazi J. Sulaimani and Dr. Mohammad H. Baluch for their guidance, help and encouragement who were the members of the thesis committee. I am again thankful to Dr. Mohammad H. Baluch for his valuable guidance in carrying out the theoretical part of the thesis.

I owe the spirit of my thesis program to my family for inculcating in me the zeal and enthusiasm which has always been a source of inspiration for me. I am also greatful for their patience, understanding and encouragement.

Lastly, but not least, I am thankful to all faculty, staff, colleagues and friends who made my stay at K.F.U.P.M., a memorable experience.

TABLE OF CONTENTS

FORM SIGNED BY THESIS COMMITTEE ii

DEDICATION iii

ACKNOWLEDGEMENT iv

THESIS ABSTRACT xxiv

Chapter I: INTRODUCTION 1

PLATE BONDING 3
ADVANTAGES OF PLATE BONDING 4
HISTORICAL BACKGROUND OF PLATE BONDING 5
PROBLEM DEFINITION 29
SCOPE OF PRESENT RESEARCH WORK 30
RESEARCH SIGNIFICANCE 31

Chapter II: LITERATURE SURVEY 33

REFERENCE 28 33
REFERENCE 33 34
REFERENCE 26 35
REFERENCE 27 45
DEFORMATIONAL BEHAVIOUR 45
COMPOSITE ACTION 47
CRACKING 47
EFFECT OF PLATES ON THE COMPRESSION FACE 47
EFFECTS OF PLATE THICKNESS 48
REFERENCE 29 48
TYPE OF ADHESIVE 48
PLATE GEOMETRY 49
EFFECT OF PRECRACKING 49
EFFECT OF MULTIPLE PLATES 49
EFFECT OF PARTIAL BONDING 50
EFFECT OF GLUELINE THICKNESS 50
EFFECT OF JOINTED PLATE 51
ULTIMATE LOADS 51
EFFECT OF PLATING ON STIFFNESS 51
REFERENCE 34 51

REFERENCE 30 52
FIRST CRACK LOAD 52
DEFORMATIONAL BEHAVIOUR 53
COMPOSITE ACTION 54
SERVICEABILITY 56
ULTIMATE LOADS 56
MODES OF FAILURE 56
REFERENCE 19 57
REFERENCE 31 65
REFERENCE 20 69
REFERENCE 32 72
DEFORMATIONAL BEHAVIOUR 72

Chapter III: EXPERIMENTAL PROGRAM 74

PREPARATION OF BEAMS 74
BEAMS OF SERIES-B 74
BEAMS OF SERIES-MF 77
DAMAGING OF BEAMS 79
STRENGTHENING OPERATION 82
STRENGTHENING DETAIL OF BEAMS 84
INSTRUMENTATION DETAIL 100
TESTING OF THE REPAIRED BEAMS 100

Chapter IV: PRESENTATION OF TEST RESULTS AND DISCUSSION 101

DEFORMATIONAL BEHAVIOUR 101
ULTIMATE STRAINS 127
EFFECT OF PLATE THICKNESS ON ULTIMATE LOADS 130
EFFECT OF PLATE THICKNESS ON THE DUCTILITY 133
EFFECT OF PLATE THICKNESS ON STIFFNESS 135
SHEAR STRESSES AT THE INTERFACE 136
EXTERNAL STRENGTHENING WITHOUT GLUE BUT ANCHOR BOLTS 148
MODES OF FAILURE 150

Chapter V: PREDICTION OF SHEAR AND PEELING STRESSES AT INTERFACE 186

INTRODUCTION 186
PROGRAM NEW1 188
ASSUMPTIONS 188
ANALYSIS 190
BOUNDARY CONDITIONS 194
APPLICATIONS 197

ROBERTS APPROACH 204
VERIFICATION OF PROGRAM ROB1 216
STRESSES AT INTERFACE IN PLATED BEAMS 218
SHEAR STRESSES AT INTERFACE 218
PEELING STRESSES AT INTERFACE 223
VERIFICATION OF THE PROGRAM ROB9 226
COMPARISON OF EXPERIMENTAL AND THEORETICAL RESULTS 247

Chapter VI: LITERATURE SURVEY 250

INTRODUCTION 250
SHEAR FORCE 250
SHEAR STRESS BASED ON LINEAR STRESS DISTRIBUTION 253
BEHAVIOUR OF BEAMS WITHOUT SHEAR REINFORCEMENT 256
SHEAR STRENGTH OF CONCRETE BEAMS WITHOUT SHEAR REINFORCEMENT 267

Chapter VII: EXPERIMENTAL PROGRAM 270

PREPARATION OF BEAMS 270
MATERIAL PROPERTIES 272
DAMAGING THE BEAMS IN SHEAR 274
STRENGTHENING OF BEAMS 278
INSTRUMENTATIN OF BEAMS 280
STRENGTHENING DETAIL OF BEAMS 280
TESTING OF THE REPAIRED BEAMS 287

Chapter VIII: TEST RESULTS AND DISCUSSION 288

LOAD VS CENTRAL DEFLECTION 288
MODE OF FAILURES 301

Chapter IX: CONCLUSIONS AND RECOMMENDEDATIONS . . . 309

CONCLUSIONS 309
FLEXURE PART 309
SHEAR PART 314
RECOMMENDATIONS 315
FLEXURE PART 315
SHEAR PART 316

NOMENCLATURE 317

REFERENCES 323

Appendix A: BEAMS OF SERIES B 331

FLEXURE STRENGTH OF ORIGINAL BEAMS 333
FLEXURE STRENGTH OF BEAMS BONDED WITH 1.0 MM THICK PLATES 334
FLEXURE STRENGTH OF BEAMS BONDED WITH 1.5 MM PLATES 335
FLEXURE STRENGTH OF BEAMS BONDED WITH 2.00 MM THICK PLATES 337
FLEXURE STRENGTH OF BEAMS BONDED WITH 3.0 MM THICK PLATES 338
SHEAR STRENGTH OF BEAMS OF SERIES B 339

Appendix B: BEAMS OF MF-SERIES 341

FLEXURE STRENGTH OF ORIGINAL BEAMS 342
FLEXURE STRENGTH OF BEAMS BONDED WITH 1.0 MM THICK PLATES 343
FLEXURE STRENGTH OF BEAMS BONDED WITH 2.0 MM THICK PLATES 344
FLEXURE STRENGTH OF BEAMS BONDED WITH 3.0 MM THICK PLATES 346
SHEAR STRENGTH OF BEAMS OF MF-SERIES 347

Appendix C: BEAMS OF MS-SERIES 349

FLEXURAL STRENGTH OF BEAMS 350
SHEAR STRENGTH OF BEAMS 351

Appendix D: PRECEDURE FOR FINDING CURVATURE 352

Appendix E: LISTING AND A TYPICAL DATA FILE FOR PROGRAM NEW1 355

PROGRAM NEW1 355
EXPLANATION OF THE TERMS IN THE DATA FILE 355

Appendix F: LISTING AND A TYPICAL DATA FILE FOR PROGRAM ROB1 363

PROGRAM ROB1 363
EXPLANATION OF THE TERMS IN THE DATA FILE 363

Appendix G: LISTING AND A TYPICAL DATA FILE FOR PROGRAM ROB9 374

PROGRAM ROB9 374
EXPLANATION OF THE TERMS IN THE DATA FILE 374

LIST OF TABLES

1. Detail of beams of series A 36
2. Detail of plain concrete test beams of series B 39
3. Detail of beams of series C from C1 to C8 42
4. Detail of beams C13 to C15. 43
5. Summary of strengthening detail of beams 61
6. Table showing the extent of damage in flexure 82
7. Summary of strengthening detail of beams. 85
8. Ultimate loads, modulus of toughness and modes of failure 125
9. Flexural rigidities of the beams. 126
10. ULtimate strains at mid-span of beams 129
11. Average ultimate loads and modulus of toughness 133
12. Average values of flexural rigidities 136
13. Comparison of theoretical and experimental results 249
14. Original Loading 277
15. Average Width of Diagonal Cracks 278
16. Summary of the strengthening detail of beams 281
17. Summary of the test results 299
18. Average values of ultimate load and modulus of toughness 300

LIST OF FIGURES

Figure *Page*

1. Reinforcement of the haunched ceiling in the Hottingerstrasse telephone exchange, Zurick 7

2. Anchoring detail of a beam reinforcement in the Hottingerstrasse telephone exchange, Zurick 8

3. Reinforcement of floor above underground garage in shopping centre at Spreitenbach. Insulation has been cut out in the vicinity of the external reinforcement 9

4. Supplementary reinforcement between the new floor openings in Neue Hard, Zurick. Heat insulation has already been applied 10

5. Lattice reinforced mushroom slab in Contraves AG, Zurick 12

6. Strengthened concrete frame in Aluminium Smelter Bahrein 13

7. Installation of frame immediately following the application of the adhesive in the Swiss industries fair parking garage 14

8. Strengthened prestressed structure at the underside of the passage in Selnau telephone, Zurick 16

9. Bonded reinforcement for absorbing lateral tensile loads anchored at sides in Selnau telephone exchange, Zurick 17

10. Prestressed side girders with strengthened reinforced concrete slab as seen from underneath in Selnau telephone exchange, Zurick 18

11. Reinforcement of an end span in Swanley bridges 20

12. Reinforcement of the plate on the underside of the roadway in Swanley bridges 21

13. Bonding of the plates to the top of the slab above the pier. The sand bags were used to weigh down the plates until the

hardening of the adhesive in Swanley bridges 22

14. Testing of the Gizenen bridge following the reinforcement of the roadway slab 23

15. The reinforced main girders and cross-ties of the Gizenen bridge. The butt straps are clearly visible on the outer main girders 24

16. Reinforcement of end sections in Quinton bridges. The steel plates were shotblasted at the site 26

17. Installation of plate in Quinton bridges. Pressing is being done by means of wooden wedges 27

18. One of the reinforced end spans of the Quinton bridges 28

19. Load deflection curves for beams of series A 37

20. Load deflection curves of beams of series B 40

21. Strain distributions for beams A2 and B5 41

22. Load deflection curves for beams C13, C14, C15, C16, C3, C4 44

23. Load deflection curves of beams URB1, URB2, URB3, URB4 and URB5 46

24. Load deflection curves for beams 201, 202, 203, 204, 205 and 206 respectively 55

25. Element of a typical plated beam 58

26. End region of a plated beam 60

27. Strengthening detail of beams F31, F32, F34 and F35 62

28. Strengthening detail of beams F36 and F37 63

29. Load deflection curves for beams F31, F32, F33, F34, F35, F36 and F37 64

30. Load deflection curves of beams of series II (F12, F13 and F14). These beams were strengthened after unloading 67

31. Load deflection curves of beams of series III (F22, F23 and

F24). These beams were strengthened in loaded state 68

32. Cross-sectional view of a plated beam 71

33. Reinforcement detail of beams of series-B 76

34. Reinforcement detail of beams of MF-series 78

35. Beam marking and loading setup. 25 tons INSTRON machine was used for loading 80

36. Load vs central deflection. The loading was done upto 10 mm central deflection and then the load was gradually removed 81

37. Strengthening detail of beams B5 and B25. These beams were bonded with 1100 mm long, 100 mm wide and 1.00 mm thick steel plates. No end anchorage was given to the steel plate 86

38. Strengthening detail of beams B10 and B17. These beams were bonded with 1100 mm long, 100 mm wide and 1.5 mm thick steel plates. No end anchorage was given to the plates 87

39. Strengthening detail of beam B8. This beam was bonded with 1000 mm long, 100 mm wide and 2 mm thick steel plate. No end anchorage was given to the steel plate 88

40. Strengthening detail of beam B4. This beam was bonded with 1100 mm long, 100 mm wide and 2 mm thick steel plate. End anchorage was given to the steel plate 89

41. Strengthening detail of beams B1. This beam was bonded with 1000 mm long, 100 mm wide and 3 mm thick steel plates. No end anchorage was given the steel plate 90

42. Strengthening detail of beams B11 and B13. These beams were bonded with 1100 mm long, 100 mm wide and 1.5 mm thick steel plates. End anchorage was given to the plates 91

43. Strengthening detail of beams B14 and B16. These beams were bonded with 1100 mm long, 100 mm wide and 1.5 mm thick steel plates. End anchorage was given to the steel plates 92

44. Strengthening detail of beams B21 abd B24. These beams were bonded with 1100 mm long, 100 mm wide and 1.5 mm

thick steel plates. End anchorage was given to the steel plates 93

45. Strengthening detail of beams B19 and B23. These beams were bonded with 1100 mm long, 100 mm wide and 1.5 mm thick steel plates. End anchorage was given to the steel plates 94

46. Strengthening detail of beams B15 and B22. These beams were bonded with 1100 mm long, 100 mm wide and 1.5 mm thick steel plates. End anchorage was given to the steel plates 95

47. Strengthening detail of beams B3 and B18. These beams were strengthened with 1100 mm long, 100 mm wide and 1.5 mm thick steel plates. The plates were anchored by bolts at the ends. These plates were not bonded to the beams..... 96

48. Strengthening detail of beam MF1. This beam was bonded with 1000 mm long, 100 mm wide and 3 mm thick steel plate. No end anchorage was given to the steel plate 97

49. Strengthening detail of beams MF2 and MF4. These beams were bonded with 1000 mm long, 100 mm wide and 3 mm thick steel plate. End anchorage was given to the steel plates..... 98

50. Strengthening detail of beam MF3. This beam was bonded with 1000 mm long, 100 wide and 2 mm thick steel plate. End anchorage was given to the steel plate..... 99

51. Load vs central deflection for beam B6. This beam was reloaded without strengthening 102

52. Load vs central deflection for beam B7. This beam was reloaded without strengthening 103

53. Load vs central deflection for beam B5. This beam was strengthened with 1100 mm long, 100 mm wide and 1.00 mm thick steel plate. No end anchorage was given to the plate..... 104

54. Load vs central deflection for beam B25. This beam was strengthened with 1100 mm long, 100 mm wide and 1.00 mm thick steel plate. No end anchorage was given to the steel plate..... 105

55. Load vs central deflection for beam B10. This beam was

bonded with 1100 mm long, 100 mm wide and 1.5 mm thick steel plate. No end anchorage was given to the plate 106

56. Load vs central deflection for beam B17. This beam was bonded with 1100 mm long, 100 mm wide and 1.5 mm thick steel plate. No end anchorage was given to the plate 107

57. Load vs central deflection for beam B8. This beam was bonded with 1000 mm long, 100 mm wide and 2.00 mm thick steel plate. No end anchorage was given to the steel plate 108

58. Load vs central deflection for beam B4. This beam was bonded with 1100 mm long, 100 mm wide and 2.00 mm thick steel plate. End anchorage was given to the steel plate 109

59. Load vs central deflection for beam B1. This beam was bonded with 1000 mm long, 100 mm wide and 3.00 mm thick steel plate. No end anchorage was given to the steel plate 110

60. Load vs central deflection for beam B11. This beam was bonded with 1100 mm long, 100 mm wide and 1.5 mm thick steel plate. End anchorage was given to the steel plate 111

61. Load vs central deflection for beam B13. This beam was bonded with 1100 mm long, 100 mm wide and 1.5 mm thick steel plate. End anchorage was given to the plate 112

62. Load vs central deflection beam B14. This beam was bonded with 1100 mm long, 100 mm wide and 1.5 mm thick steel plate. End anchorage was given to the plate 113

63. Load vs central deflection for beam B16. This beam was bonded with 1100 mm long, 100 mm wide and 1.5 mm thick steel plate. End anchorage was given to the steel plate 114

64. Load vs central deflection for beam B21. This beam was bonded with 1100 mm long, 100 mm wide and 1.5 mm thick steel. End anchorage was given to the plate 115

65. Load vs central deflection for beam B24. This beam was bonded with 1100 mm long, 100 mm wide and 1.5 mm thick steel plate. End anchorage was given to the plate 116

66. Load vs central deflection for beam B15. This beam was bonded with 1100 mm long, 100 mm wide and 1.5 mm thick

steel plate. End anchorage was given to the plate 117

67. Load vs central deflection for beam B22. This beam was bonded with 1100 mm long, 100 mm wide, and 1.5 mm thick steel plate. End anchorage was given to the steel plate 118

68. Load vs central deflection for beam B19. This beam was bonded with 1100 mm long, 100 mm wide and 1.5 mm thick steel plate. End anchorage was given to the plate 119

69. Load vs central deflection for beam B23. This beam was bonded with 1100 mm long, 100 wide and 1.5 mm thick steel plate. End anchorage was given to the steel plate 120

70. Load vs central deflection for beam MF1. This beam was bonded with 1000 mm long, 100 mm wide and 3.0 mm thick steel plate. No end anchorage was given to the steel plate 121

71. Load vs central deflection for beam MF2. This beam was bonded with 1000 mm long, 100 mm wide and 3.0 mm thick steel plate. End anchorage was given to the steel plate 122

72. Load vs central deflection for beam MF4. This beam was bonded with 1000 mm long, 100 mm wide and 3.0 mm thick steel plate. End anchorage was given to the steel plate 123

73. Load vs central deflection for beam MF3. This beam was bonded with 1000 mm long, 100 mm wide and 2.0 mm thick steel plate. End anchorage was given to the steel plate 124

74. Strain distributions along plate for beam B25. This beam was bonded with 1.00 mm thick, 100 mm wide and 1100 mm long plate. No end anchorage was given to the plate 138

75. Strain distributions along plate for beam B10. This beam was bonded with 1.5 mm thick, 100 mm wide and 1100 mm long plate. No end anchorage was given to the plate 139

76. Strain distributions along plate for beam B17. This beam was strengthened by 1.5 mm thick, 100 mm wide and 1100 mm long steel plate. No end anchorage was given to the plate 140

77. Strain distributions along plate for beam B8. This beam was strengthened by 2.00 mm thick, 100 mm wide and 1000 mm long plate. No end anchorage was given to the plate 141

78. Strain distributions along plate for beam B1. This beam was strengthened by 3.00 mm thick, 100 mm wide and 1000 mm long plate. No end anchorage was given to the plate 142

79. Strain distributions along plate for beam B11. This beam was strengthened by 1.5 mm thick, 100 mm wide and 1100 mm long plate. End anchorage was given to the plate 144

80. Strain distributions along for beam B16. This beam was strengthened by 1.5 mm thick, 100 mm wide and 1100 mm long plate. End anchorage was given to the plate 145

81. Strain distributions along plate for beam B23. This beam was strengthened by 1.5 mm thick, 100 mm wide and 1100 mm long plate. End anchorage was given to the plate 146

82. Strain distributions along plate for beam B22. This beam was strengthened by 1.5 mm thick, 100 mm wide and 1100 mm long plate. End anchorage was given to the plate 147

83. Load vs central deflection curves for beams B3, B11 and B17 respectively. These beams were strengthened by 1.5 mm thick, 100 mm wide and 1100 mm long plates. In beam B3 plate was not bonded to the concrete beam. In beam B3 and B11 plates were anchored 149

84. Photograph showing the mode of failure for beam B25. This beam was strengthened by 1.00 mm thick, 100 mm wide and 1100 mm long plate. No end anchorage was given to the plate 151

85. Load vs strains 5, 6 and 7 for beam B25. This beam was strengthened by 1.00 mm thick, 100 mm wide and 1100 mm long plate. No end anchorage was given to the plate 152

86. Strains 5, 6 and 7 vs central deflection for beam B25. This beam was strengthened by 1.00 mm thick, 100 mm wide and 1100 mm long plate. No end anchorage was given to the plate 154

87. Load vs strains 2, 3 and 4 for beam B10. This beam was strengthened by 1.5 mm thick, 100 mm wide and 1100 mm long plates. No end anchorage was given to the plate 155

88. Photograph showing the mode of failure for beam B10. This beam was strengthened by 1.5 mm thick, 100 mm wide and 1100 mm long plate. No end anchorage was given to

the plate 156

89. Load vs strains 1, 2 and 3 for beam B17. This beam was strengthened by 1.5 mm thick, 100 mm wide and 1100 mm long plate. No end anchorage was given to the plate 157

90. Load vs strains 5, 6 and 7 for beam B17. This beam was strengthened by 1.5 mm thick, 100 mm wide and 1100 mm long steel plate. No end anchorage was given to the plate 158

91. Load vc strains 11, 12 and 13 for beam B8. This beam strengthened by 2.00 mm thick, 100 wide and 1000 mm long plate. No end anchorage was given to the plate 160

92. Load vs strains 1, 2 and 3 for B8. This beam was strengthened by 2.00 mm thick, 100 mm wide and 1000 mm long plate. No end anchorage was given to the plate 161

93. Photograph showing the mode of failure of beam B8. This beam was strengthened by 2.00 mm thick, 100 wide and 1000 mm long plate. No end anchorage was given to the plate 162

94. Photograph showing the mode of failure for beam B1. This beam was strengthened by 3.00 mm thick, 100 mm wide and 1000 mm long plate. No end anchorage was given to the plate 164

95. load vs strains 1, 3 and 4 for beam B1. This beam was strengthened by 3.00 mm thick, 100 mm wide and 1000 mm long plate. No end anchorage was given to the plate 165

96. Load vs strains 13, 14 and 15 for beam B1. This beam was strengthened by 3.00 mm thick, 100 mm wide and 1000 mm long plate. No end anchorage was given to the plate 166

97. Load vs strains 9, 10 and 13 for beam B11. This beam was strengthened by 1.50 mm thick, 100 mm wide and 1100 mm long plate. End anchorage was given to the plate 168

98. Load vs strains 19, 20 and 23 for beam B11. This beam was strengthened by 1.5 mm thick, 100 wide and 1100 mm long plate. End anchorage was given to the plate 169

99. Photograph showing the mode of failure for beam B14. This beam was strengthened by 1.5 mm thick, 100 mm wide and 1100 mm long plate. End anchorage was given to the plate 170

100. Load vs strains 6, 7 and 8 for beam B16. This beam was strengthened by 1.50 mm thick, 100 mm wide and 1000 mm long plate. End anchorage was given to the plate..... 171

101. Load vs strains 13, 14 and 15 for beam B16. This beam was strengthened by 1.5 mm thick, 100 mm wide and 1100 mm long plate. End anchorage was given to the plate 172

102. Photograph showing the mode of failure for beam B24. This beam was strengthened by 1.5 mm thick, 100 mm wide and 1100 mm long plate. End anchorage was given to the plate..... 174

103. Photograph showing the mode of failure for beam B19. This beam was strengthened by 1.5 mm thick, 100 mm wide and 1100 mm long plate. End anchorage was given to the plate 175

104. Load vs strains 4, 11 and 12 for beam B23. This beam was strengthened by 1100 mm long, 100 mm wide and 1.5 mm thick steel plate. End anchorage was given to the plate 176

105. Load vs plate strains 22, 26 and 30 for beam B23. This beam was strengthened by 1.5 mm thick, 100 mm wide and 1100 mm long plate. End anchorage was given to the plate 178

106. Photograph showing the mode of failure for beam B22. This beam was strengthened by 1.5 mm thick, 100 mm wide and 1100 mm long plate. End anchorage was given to the plate 179

107. Load vs strains 19, 20 and 26 for beam B22. This beam was strengthened by 1.5 mm thick, 100 mm wide and 1100 mm long plate. End anchorage was given to the plate 180

108. Load vs strains 1, 8 and 9 for beam B22. This beam was strengthened by 1.5 mm thick, 100 mm wide and 1100 mm long plate. End anchorage was given to the plate..... 181

109. Photograph showing the mode of failure for beam MF1. This beam was strengthened by 1000 mm long, 100 mm wide and 3.00 mm thick steel plate. No end anchorage was given to the steel plate 183

110. Composite beam consisting of I-beam and concrete slab. The axial force in the slab and the beam is same and is denoted by F..... 195

111. Figure showing the boundary conditions for Newmark

approach. Two extra nodes out side the boundaries are shown 196

112. Cross-sectional dimensions of the composite beam. This beam has been adopted from reference [22] ,..... 199

113. Distribution of slip at the interface for Ks=2180 N/mm/mm. and for a uniformly distributed load of 12 N/mm 200

114. Distribution of slip at the interface for Ks=2180 N/mm/mm and for a central point load of 49.3 kN 201

115. Distribution of slip at interface for Ks=54.5 N/mm/mm and for a uniformly distributed load of 12 N/mm..... 202

116. Distribution of slip at interface for Ks=54.5 N/mm/mm and for a central point load of 49.3 KN 203

117. Element of composite beam of length dx 205

118. Free body diagram of the upper layer of Robert's model. Horizontal equilibrium of the upper layer 208

119. Free body diagram of the upper layer of Robert's model. Vertical equilibrium of the upper layer 210

120. Boundary conditions for program ROB1 215

121. Effect of variation of Ks on the central deflection for composite beam taken from reference [22] ,..... 217

122. A typical epoxy bonded plated beam 221

123. Boundary conditions to modify ROB1 to ROB9 to handle epoxy bonded plated beams..... 222

124. Model for determining peeling stresses at the interface. Considering the plate as the beam on the elastic foundation. Adhesive layer has been considered as an elastic foundation..... 225

125. Dimensions, loading and material properties of the beam taken from reference [21] ,..... 227

126. Shear stress distribution at interface for Ks=20000 N/mm/mm and for a/l=0.75..... 228

127. Peeling stress distribution at interface for Kn = 50000 N/mm/mm and for a/l = 0.75 229

128. Tensile stress distributions along plate for a/l = 0.5 and 0.75 respectively and for Ks = 20000 N/mm/mm 231

129. Effect of shear stiffness of the adhesive on the central deflection for a/l = 0.75 and 0.50 respectively 232

130. Effect of shear stiffness of the adhesive on the maximum tensile stress of the steel plate for a/l = 0.5 and 0.75 respectively 233

131. Shear stress distributions alon plate for a/l = 0.5, a/l = 0.75 and a/l = 0.95 respectively and Ks = 20000 N/mm/mm 234

132. Shear stress distributions along plate for Ks = 5000 N/mm/mm and Ks = 40000 N/mm/mm respectively and for a/l = 0.75 235

133. Shear stress distributions along plate for Ks = 5000 N/mm/mm and Ks = 40000 N/mm/mm respectively and for a/l = 0.50 237

134. Peeling Stress distributions along plate for Kn = 50,000 N/mm/mm and Kn = 100,000 N/mm/mm respectively, and for a/l = 0.50 238

135. Peeling Stress distributions along plate for Kn = 50,000 N/mm/mm and Kn = 100,000 N/mm/mm respectively, and for a/l = 0.75 239

136. Peeling Stress distributions along plate for a/l = 0.50, a/l = 0.75 and a/l = 0.95 respectively and for Kn = 50000 N/mm/mm 240

137. Variation of maximum shear stress at the ends of the plate with respect to shear stiffness of the Glue for a/l = 0.50 and a/l = 0.75 respectively 242

138. Variation of maximum peeling stress at the ends of the plate with respect to normal stiffness of the Glue for a/l = 0.50 and a/l = 0.75 respectively 243

139. Variation of maximum shear stresses at the ends of the plate with respect to the thickness of the plate for a/l = 0.75 244

140. Effect of moving load on the shear stress at the interface 246

141. A typical simply supported beam and the Free-body diagram of the beam to the left of the section A-A 252

142. A typical simply supported beam. Free-body diagram of an element abcd above the neutral axis 255

143. Redistribution of shear resistance after the formation of the inclined cracks 257

144. Variation in shear strength with a/d for rectangular beams. This figure has been taken from reference [36] , ... 260

145. Arch action in deep beams 261

146. Modes of failure in deep beams with a/d less than or equal to 1.00. Adopted from reference [36] , ... 263

147. Shear tension failure in short beams 264

148. Shear compression failures in short beams 265

149. Diagonal tension failure or Tooth cracking failure for intermediate length beams; a/d about 2.5 to 6 266

150. Reinforcement detail of beams of MS-series. A total of four U-stirrups were used, at the supports and at the third points 271

151. Stress strain curve of the bar reinforcement 273

152. Marking of beams and loading SETUP for damaging and final testing respectively 275

153. Load deflection curve of a typical beam to induce shear damage 276

154. Strengthening detail of beams MS6 and MS10 strengthened by Jacket-A 282

155. Strengthening detail of beams MS3 and MS8 strengthened by Jacket-B 283

156. Strengthening detail of beams MS4 and MS9 strengthened by Wings 284

157. Strengthening detail of beams MS2 and MS11 strengthened

by U-strips 285

158. Strengthening detail of beams MS5 and MS7 strengthened by Straight Strips 286

159. Load deflection curve for beam MS6 repaired by Jacket-A 289

160. Load deflection curve for beam MS10 repaired by Jacket-A 290

161. Load deflection curve for beam MS3 repaired by Jacket-B 291

162. Load deflection curve for beam MS8 repaired by Jacket-B 292

163. Load deflection curve for beam MS4 repaired by Wings 293

164. Load deflection curve for beam MS9 repaired by Wings 294

165. Load deflection curve for beam MS2 repaired by U-strips 295

166. Load deflection curve for beam MS11 repaired by U-strips 296

167. Load deflection curve for beam MS5 repaired by Straight Strips 297

168. Load deflection curve for beam MS7 repaired by Straight Strips 298

169. Photograph showing the cracks at failure for the beam MS10 repaired by Jacket-A 302

170. Photograph showing the cracks at failure for the beam MS8 repaired by Jacket-B 304

171. Photograph showing the cracks at failure for the beam MS4 repaired by Wings 305

172. Photograph showing the cracks at failure for the beam MS2 repaired by U-strips 307

173. Photograph showing the cracks at failure for the beam MS5 repaired by Strips 308

174. Stress strain curve of the rebar steel 332

175. Elastic curve of the beam in the constant moment region. This curve has constant curvature 354

THESIS ABSTRACT

NAME OF STUDENT : MUNAWAR HUSSAIN

TITLE OF STUDY : FLEXURE AND SHEAR BEHAVIOUR OF DAMAGED RC BEAMS REPAIRED BY PLATE BONDING

MAJOR FIELD : CIVIL ENGINEERING

DATE OF DEGREE : JULY, 1992

The research regarding plate bonding technique presented here has been divided into flexure and shear parts. The research regarding flexure has been further classified into experimental and theoretical parts. In the flexure experimental part, first of all a large number of RC beams were damaged in flexure by giving 10 mm central deflection. Then these flexure damaged beams were repaired by bonding steel plates of different thicknesses on the bottom faces of the beams. In some of the plated beams end anchorage was given to the plates by anchor bolts. Beams repaired by 1.00 mm and 1.5 mm thick plates reached the theoretically predicted ultimate flexural strengths. Beams repaired by 2.00 mm and 3.00 mm thick plates could not reach the theoretically predicted ultimate flexural strengths. In general ductility was improved by giving end anchorage to the plates. The modes of failure of the beams repaired by 1.5 mm, 2.00 mm and 3.00 mm thick plates with and without end anchorage were due to the separation of the plates at the ends. In the theoretical study a computer program was written based on the partial interaction theory to determine the shear and peeling stresses at the interface in the epoxy bonded plated beams. This program can be used for designing plate size for strengthening RC beams in flexure such that separation of plates does not take place before the yielding of the plates. In the shear part of the research program, first of all, RC beams having insufficient shear reinforcement were damaged in shear under four point loading. Then these shear damaged beams were repaired by bonding jackets, U-strips, straight strips and wings respectively in the shear spans. All the shear repaired beams showed improvement in strength and ductility. However, the improvement in strength and ductility for the beams repaired by Jacket-A (full encasement of the shear span) was maximum.

MASTER OF SCIENCE

KING FAHD UNIVERSITY OF PETROLEUM AND MINERALS

Dhahran, Saudi Arabia

خلاصة الرسالة

اسم الطالب : منور حسين

عنوان الدراسة : سلوك الثني والقص في الكمرات الخرسانية التالفة والمصلحة بالصفائح اللاصقة .

التخصص : هندسة مدنية .

تاريخ الشهادة : يوليو ١٩٩٢م .

قسم البحث المتعلق باصلاح الكمرات الخرسانية بواسطة الصفائح الفولاذية اللاصقة إلى قسمي الثني والقص ، كما تم تصنيف البحث في الثني إلى جزء تجريبي وآخر نظري .

في جزء الثني التجريبي ، لقد تم اتلاف عدد من الكمرات الخرسانية المسلحة بعمل انحناء مركزي قدره ١٠ ميللميتر . وبعدها تم ربط صفائح معدنية مختلفة السماكة على الوجه السفلي لهذه الكمرات بقصد إصلاحها ، وفي بعض الكمرات التي ربط بها صفائح تم تثبيت هذه الصفائح من نهاياتها بالبراغي .

لقد وجد أن الكمرات المصلحة بصفائح سمكها ١ ملليمتر و ١ر٥ ملليمتر قد وصلت إلى القيم النظرية المتوقعة لقوى الثني العظمى . أما الكمرات المصلحة بصفائح سمكها ٢ ملليمتر و ٣ ملليمتر فلم تستطع الوصول للقيم النظرية المتوقعة لقوى الثني العظمى كما وجد أن الليونة تتحسن بشكل عام ، للكمرات التي ثبتت صفائحها ببراغي على الأطراف .

وقد وجد أيضاً أن حالات الإنهيار للكمرات المصلحة بصفائح سمكها ١ر٥ ميللميتر ، ٢ ملليمتر و ٣ ملليمتر - يوجد التثبيت الطرفي أو عدمه - كان بسبب إنفصال الصفائح من أطرافها .

أما في الدراسة النظرية ، فقد كتب برنامج حاسوبي يعتمد على نظرية التفاعل الجزئي ، وذلك لإيجاد إجهاد القص والإجهادات العمودية على السطح ...

ويمكن استعمال هذا البرنامج في إيجاد أبعاد الصفائح التصميمية اللازمة لتقوية كمرات الخرسانة المسلحة عندما تتعرض للثني ، كما يمكن أن يستخدم البرنامج في اختيار هذه الأبعاد التصميمية بحيث لايتم إنفصال الصفيحة عن الكمرة الخرسانية قبل حصول الانهيار التام للصفيحة نفسها وفي الجزء الخاص بالقص من البرنامج ، تم (تلف) الكمرات الخرسانية والتي لاتمتلك تسليحاً كلياً ضد القص بأن أتلفت بإجهادات القص وباستعمال أربع نقاط للتحميل . وبعد ذلك تم إصلاح هذه الكمرات التالفة بطرق مختلفة منها : سواتر ربط ، شرائح شكل حرف U شرائح وأجنحة مستقيمة في منطقة القص .

لقد وجد أن جميع الكمرات المصلحة والتي كان القص سبباً في إتلافها قد أظهرت تحسناً في قوتها وليونتها . كما وجد أن التحسن في القوة والليونة للكمرات التي عولجت وأصلحت باستعمال سواتر A (بحيث كانت تغطي كامل منطقة القص) ، وجد أن التحسن فيها أكبر مايمكن .

درجة الماجستير في العلوم

جامعة الملك فهد للبترول والمعادن

الظهران ، المملكة العربية السعودية

Chapter I

INTRODUCTION

The strengthening and repair of structures or the replacement of structures become necessary when the performance of the structures with respect to ultimate loads and serviceability becomes unsatisfactory. In recent years emphasis is being given to repair or strengthening of all types of structures in preference to demolition or reconstruction because of the economic reasons. Therefore, strengthening and repair of structures have become as important as the designing of new structures. Concrete structures built during the peak period of construction are now showing defects. Cast-in-situ concrete structures are hardly built under ideal conditions. There are various reasons behind the unsatisfactory performance of the structures which follows:-

1. The performance of a structure may be unsatisfactory because of the inferior materials used, unsuitable construction methods, poor workmanship or failure to appreciate hazards associated with a particular structural form or with prevailing weather conditions.
2. Sometimes, concrete mix design is unsuitable which can cause a variety of defects such as severe honey combing and excessive shrinkage cracks. Concrete mixes sometimes satisfy strength requirements but do not satisfy other requirements such as compactibilty and long term durability.

3. Apparent savings in the cost of labour or formwork will produce defects in the buildings.

4. Mistakes in design calculations and improper detailing of reinforcement can cause problems in structures. For example for congested reinforcement, concreting can not be done properly which reduce the strength of the structural members considerably and cracks appear in these structures.

5. Damage due to fire, blasts and earthquakes may reduce the strength of the structures. Due to fire concrete covers are broken which reduce the strength. Earthquakes and blasts apply dynamic loads to the structures because of which improperly designed structures show cracks and reduction in strength.

6. In order to change the function of a strucure from lower service load to a higher service load. For example, for the conversion of an office building to a library building or to a ware house, the building must be strengthened to meet the new functional needs.

7. Corrosion may reduce the area of conventional steel reinforcement and thus the load carrying capacity of the structure reduces. In order to regain the original load carrying capacity strengthening becomes necessary.

Structures with unsatisfactory performance are not acceptable from the point of view of safety as well as public acceptance. Such structures should be either replaced by the new one and in case of structurally defective buildings strengthening operation should be carried out to get the satisfactory performance. The

choice between these two alternatives depends on many important factors, such as material cost, labour cost, time during which the structure may be out of use and disruption of other facilities such as plumbing, electrical and HVAC facilities in the buildings etc. Hence, replacement of structures is very expensive and this is only done when there is no other solution. In the present economic climate, the second alternative has become much more attractive, particularly if a simple and quick strengthening technique is available. In the past many structures have been strengthened by various techniques such as

1. Replacing non-structural toppings by structural toppings of light weight concretes.
2. Providing extra supports to reduce the span lengths.
3. Stapling and guniting the steel plates externally.
4. Using external prestressing.
5. Polymer impregnation.

1.1 PLATE BONDING

With the invention of epoxy adhesives another technique of strengthening of structures has been added to the repair world and because of its various advantages this technique has become very popular.

Plate bonding technique may be defined as the technique in which a steel plate of relatively small thickness, of the order of a few millimeter, is bonded with epoxy glue to the reinforced concrete beams and slabs for improving their structural behaviour and strength. Plated beams show control on cracks and deflection and increased flexural stiffness [30] .

1.1.1 ADVANTAGES OF PLATE BONDING

The following are the most important advantages of the plate bonding technique.

1. The site disruption is minimum in plate bonding as compared to other repair techniques. Site disruption means breaking of structures during repair. For plate bonding only the surface of the structural members is abraded by sand blasting to make the structural members rough for proper adhesion.
2. The sizes of the structural members increase by almost a few millimeters by strengthening them by plate bonding because the plates of about few millimeters are bonded to the structures with epoxy glue and thus the clear height reduces only by a negligible amount. Also the increase in the dead load of the structural members due to repair by plate bonding is very small as compared to other strengthening methods.
3. For the application of the plate bonding technique to strengthen structures minimum scaffolding and shuttering is required.
4. By plate bonding the structures can be strengthened while in operation because during application of this technique no vibration or noise is produced and hence normal activities can go unaffected. This is very important advantage of plate bonding. Some bridges and buildings have been strengthened while under operation.

1.1.2 HISTORICAL BACKGROUND OF PLATE BONDING

In spite of little data available into the performance of this technique, this technique has been used to strengthen many structures in the past. This technique has been used to strengthen both buildings and bridges in Belgium [1] , France [2,3] , Japan [4] , Poland [5] , South Africa [6] , Switzerland [7,8] and in the United Kingdom [9,10,11] .

A brief description of some of the buildings and bridges strengthened by this technique is given in the following paragraphs:-

For the expansion and renovation of Fusslistrasse Telephone Exchange in Zurick [12] , Postal building department after studying various alternatives came to the conclusion that instead of demolition and reconstruction of exchange building, which claimed high cost, the building had been strengthened to meet the new functional needs. The first floor was strengthened by pouring a 12 cm thick layer of lightweight mesh reinforced concrete over the existing 11 cm thick reinforced concrete slab. The shear transmission bond between the two layers was obtained by using araldite adhesive. The second floor was strengthend by bonding steel plates on the soffit of the slab and the joists.

Hottingerstrasse Telephone Exchange in Zurick was constructed in 1914 in which switching rooms were designed for $7kN/m^2$ and secondary rooms were designed for $2kN/m^2$. Later for the expansion of the exchange it was decided to increase the load carrying capacity of the secondary rooms from $2kN/m^2$ to $7kN/m^2$. This objective was achieved by bonding steel plates to the soffit of the

joists and slabs. The steel plates bonded to the joists were also anchored by tie rods to the concrete facade columns. Figure 1 shows the reinforcement of haunched ceiling in the exchange. Figure 2 shows the anchoring detail of beam reinforcement. The exchange remained in operation during strengthening process because reinforcement operation was done dry and without vibration [13] .

In order to increase the load carrying capacity, shopping centre at Spreitenbach, Switzerland [14] was strengthened by this technique. A total of 216 steel plates each of 6 mm thickness, widths varying from 160 mm to 200 mm, and lengths varying from 6600 mm to 7900 mm were used to strengthen the floor above the ground. The repaired slab was not tested after repair. So the percentage improvement in the strength of the repaired slab was not reported. Figure 3 shows the reinforcement of floor above underground garage. Insulation has been cut out in the vicinity of the external reinforcement.

In order to fit the air conditioning system in the Neue Hard Development Building Zurick [14] , 22 triangular openings were made around the periphery of the conventionally reinforced concrete floor. In order to compensate the loss of the steel rods, 28 cranked steel plates of 10 mm thickness, 300 mm widths and 2150 mm lengths were bonded to the soffit of the floor and were covered with fire resisting and heating materials as shown in the Figure 3 .

In Contraves AG Zurick [14] modifications at two locations at the edges of a mushroom slab reduced the load carrying capacity of the slab. It was strengthened by bonding steel plates arranged in a crosswise pattern. A total of 26 steel

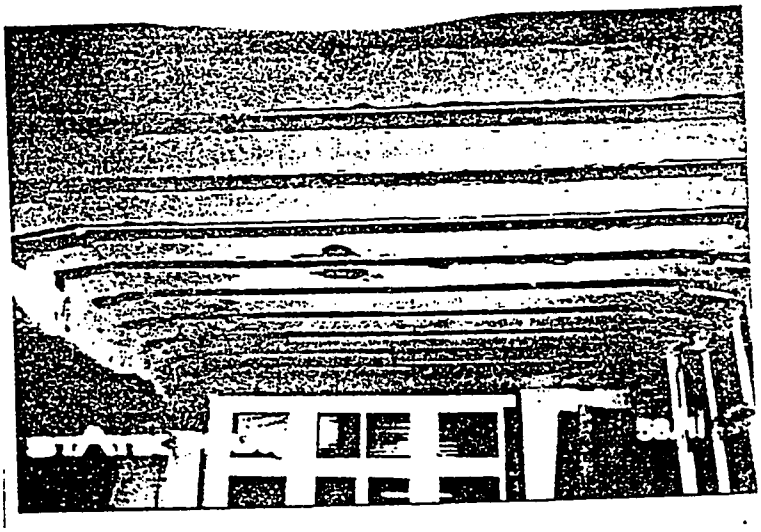

Figure 1: Reinforcement of the haunched ceiling in the Hottingerstrasse telephone exchange, Zurick.

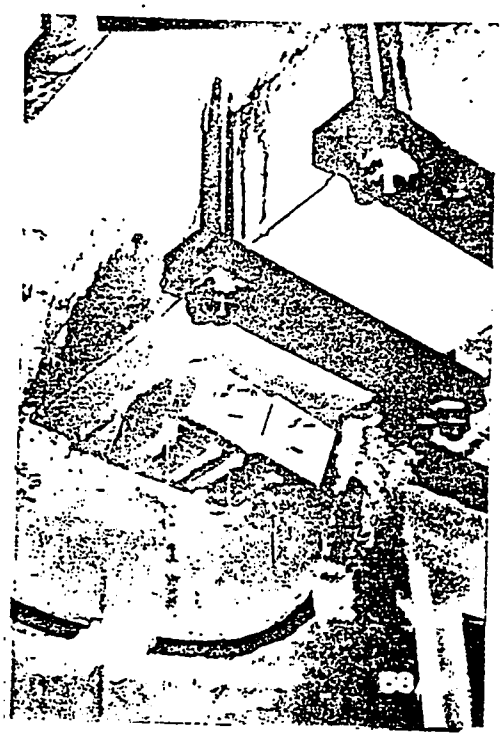

Figure 2: Anchoring detail of a beam reinforcement in the Hottingerstrasse telephone exchange, Zurick.

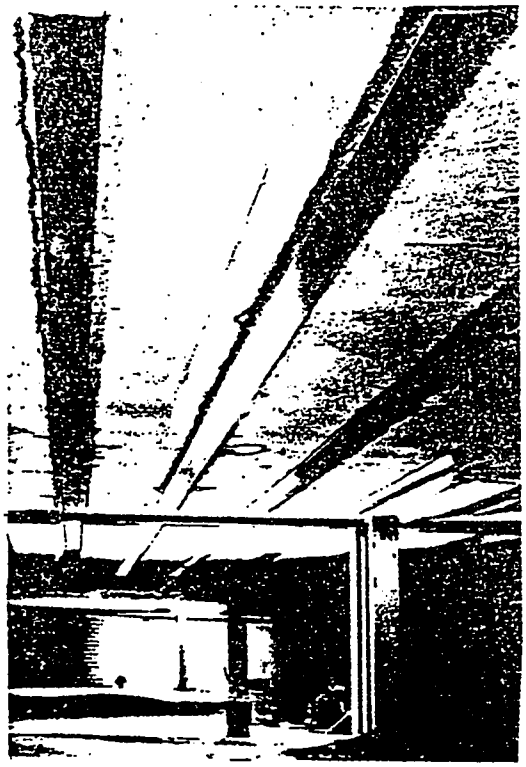

Figure 3: Reinforcement of floor above underground garage in shopping centre at Spreitenbach. Insulation has been cut out in the vicinity of the external reinforcement.

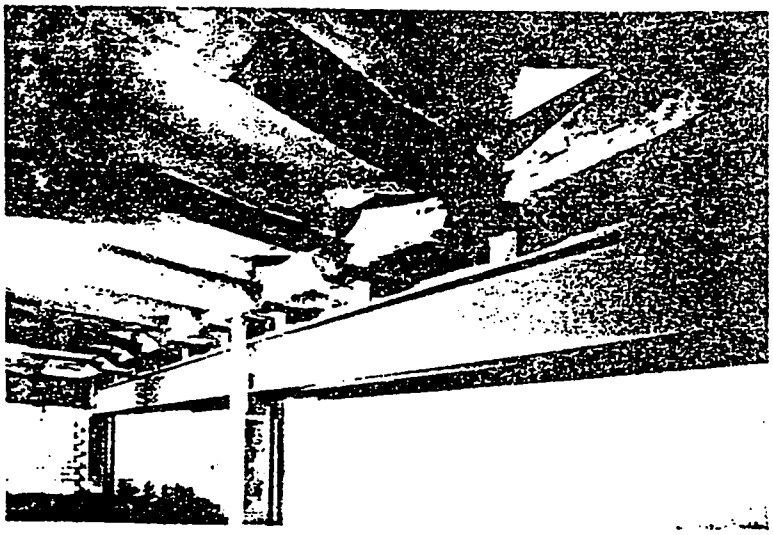

Figure 4: Supplementary reinforcement between the new floor openings in Neue Hard, Zurick. Heat insulation has already been applied.

plates were bonded. The plates of 6 mm thickness, 120 mm widths and 6600 mm lengths were kept in the upper layer and the plates of 12 mm thickness, 120 mm widths and 7300 mm lengths were kept in the bottom layer and were milled to accommodate 6 mm thick plates running in the perpendicular direction as shown in Figure 5

In 1974 ALBA Aluminium Smelter Bahrain [14] was strengthened by plate bonding technique. The appearance of cracks in the prefabricated concrete frames, which support the melting ladles and transmit the load to the soil, revealed that the load assumed in the designing of the frames was much less than the actual applied load. These frames were strengthened by bonding steel plates of 8 mm thickness, 280 mm widths and 2850 mm lengths to the soffits of the beams after injecting epoxy resin in the cracks. A strengthened concrete frame of the Aluminium Smelter is shown in the Figure 6

This technique played a very important role in connecting the Swiss Industries Fair Parking Garage Basle [14] to one of the exhibition halls with the help of an excalator. For this purpose an opening of 1.7 by 3.15 m was made in one of the mesh reinforced concrete walls adjacent to the parking garage. In order to compensate the removal of the reinforcing mesh, a steel frame 15 mm plate thickness was bonded to both sides of the opening to act as shear reinforcement as shown in the Figure 7

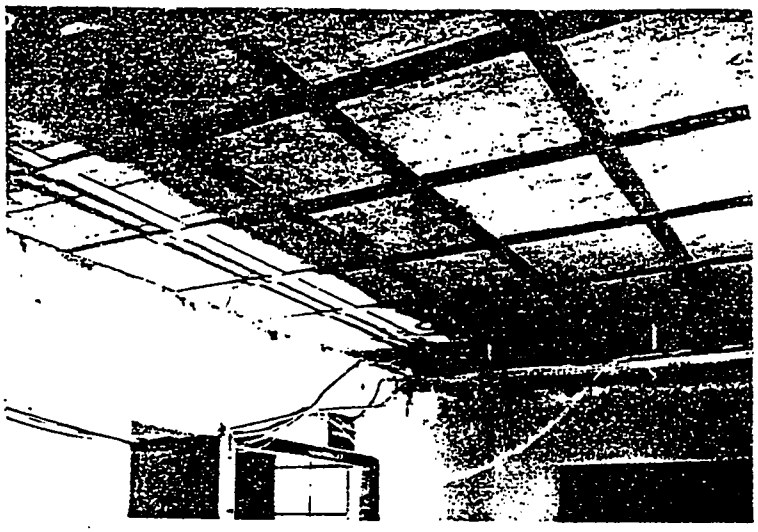

Figure 5: Lattice reinforced mushroom slab in Contraves AG, Zurick.

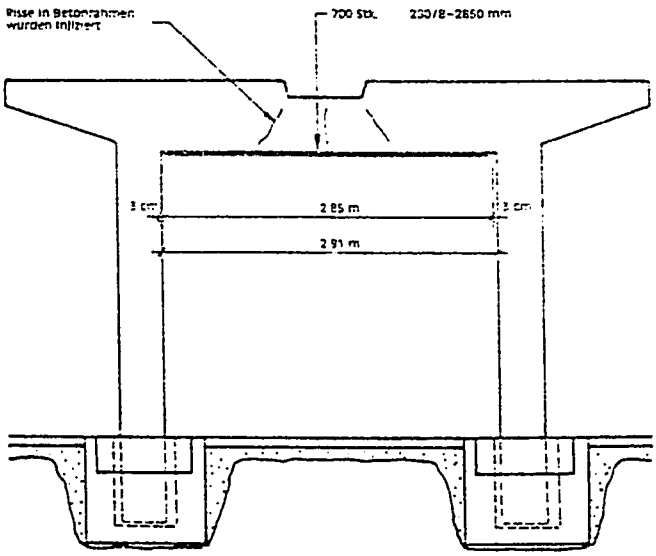

Aluminium smelter, Bahrein. Strengthend concrete frame.

Risse in Betonrahmen	cracks in concrete crossbeam
wurden injiziert	were injected
700 Stk.	700 units

Figure 6: Strengthened concrete frame in Aluminium Smelter Bahrein.

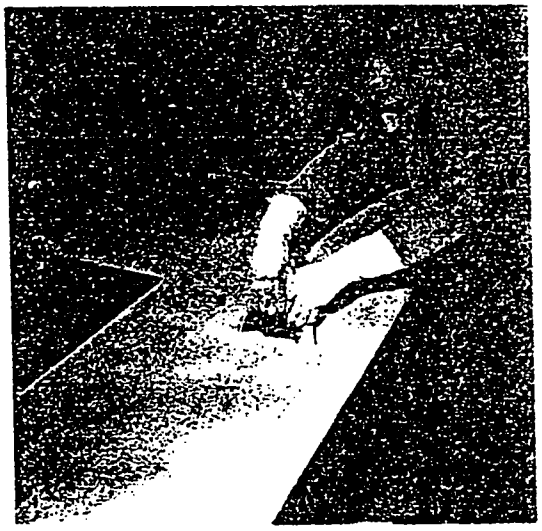

Figure 7: Installation of frame immediately following the application of the adhesive in Swiss industries fair parking garage.

When Selnau Telephone Exchange Zurick [14] was expanded, a 15 m long three storey connection structure between the two exchange buildings was strengthened by external prestressing and by plate bonding. The two supporting beams underneath the passageway were made wider and higher and were prestressed at the midspan. Prestressing operations created tensile stresses in the slab. To resist these tensile stresses steel plates were bonded to the under side of the slabs and some plates were anchored to the main girders by tie rods. Figure 8 show the strengthened prestressed concrete structure at the underside of the passage. Figure 9 shows the reinforcement anchored at sides to absorb lateral tensile loads. Figure 10 shows the prestressed sides girders with strengthened reinforced concrete slab.

In Japan [15] , over 200 bridges have been strengthened by this technique. All of these bridges became under designed because of the sudden increase in the traffic intensity after the completion of the construction of these bridges.

J. P. Sevene [16] reported on the repair and the reinforcement of a bridge of French 'Route Nationale 186' crossing the Saint Denis Canal. Because of the closeness of this bridge to the water it was subjected to severe weathering. In order to regain its original capacity the bridge was strengthened by plate bonding.

Swanley Bridges in Great Britain were strengthened by plate bonding technique [17] . Some bridges of M25-M20 motorway intersection showed cracks shortly after opening to the traffic. The review of the design showed the inade-

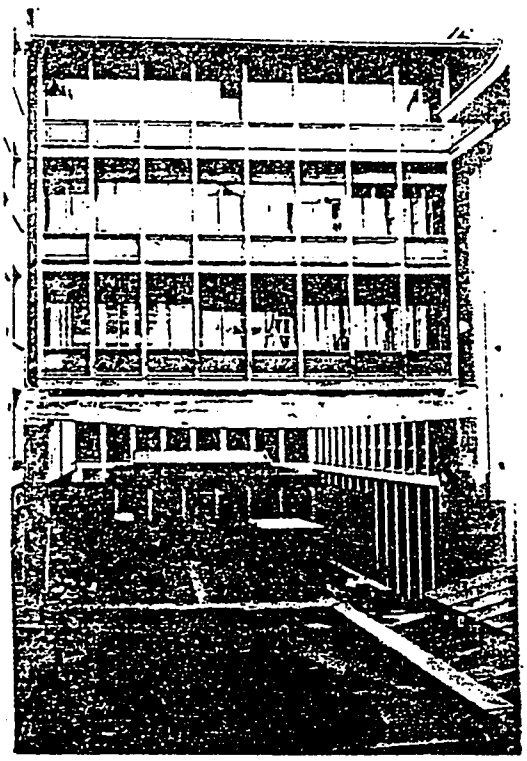

Figure 8: Strengthened prestressed structure at the underside of the passage in Selnau telephone exchange, Zurick.

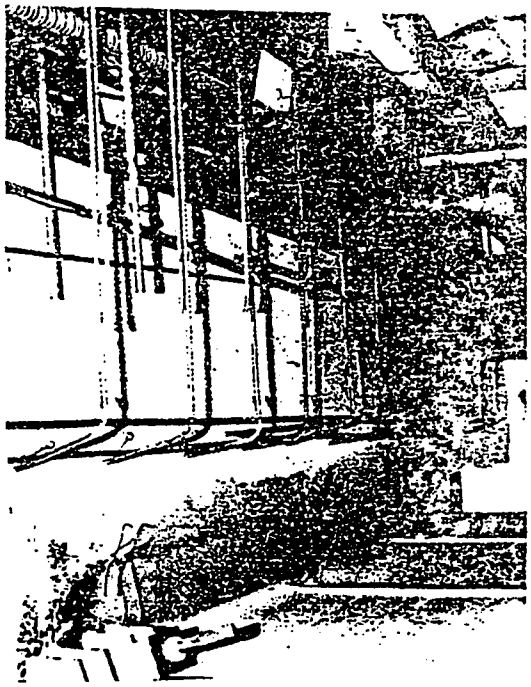

Figure 9: Bonded reinforcement for absorbing lateral tensile loads anchored at sides in Selnau telephone exchange, Zurick.

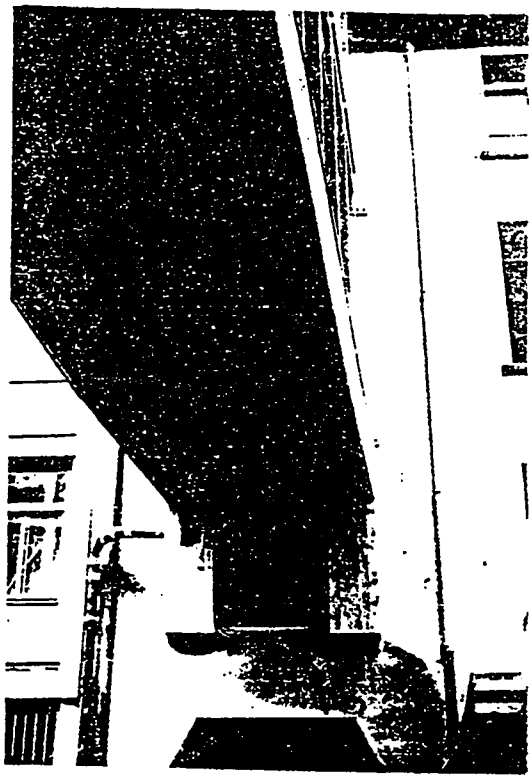

Figure 10: Prestressed side girders with strengthened reinforeced concrete slab as seen from underneath in Selnau telephone exchange, Zurick.

quacy of the reinforcement in one end section. These bridges were strengthened by 6 mm thick, 250 mm wide plates of lengths varying from 3.0 m to 6.0 m. At the end section of the slab three layers of the plates were used. Each strip was 12 m long and a total of 15 strips were distributed across the width. Four steel plates were bonded to one another on the top side of the slab above pier. Strip length was 12 m and a total of 21 strips were used in the entire width. Figure 11 shows the reinforcement of an end span. Figure 12 shows the reinforcement of plate on the underside of the road way. Figure 13 shows the top of the slab above the pier. The sand bags were used to press the plates until the hardening of the adhesive.

Gizenen Bridge, Muotta Valley was also strengthened by plate bonding technique [14] . Strengthening became necessary to withstand the heavy truck load carrying timber in Winter. First the damaged parts of the slabs were repaired by epoxy resin mortar. The joints in the roadway slab were structurally closed and new cross beam was poured at the same time. Main girders were strengthened by bonding 15 mm thick and 200 mm wide plates. Transverse girders were strengthened by 10 mm and 150 mm wide plates. The plates running longitudinally were butted together under suspension ports. The joint was covered with butt strap of same cross-section. Figure 14 shows the testing of the bridge after strengthening by plate bonding. Figure 15 shows the reinforced main girders and cross ties. The butt straps are clearly visible on the outer main girders.

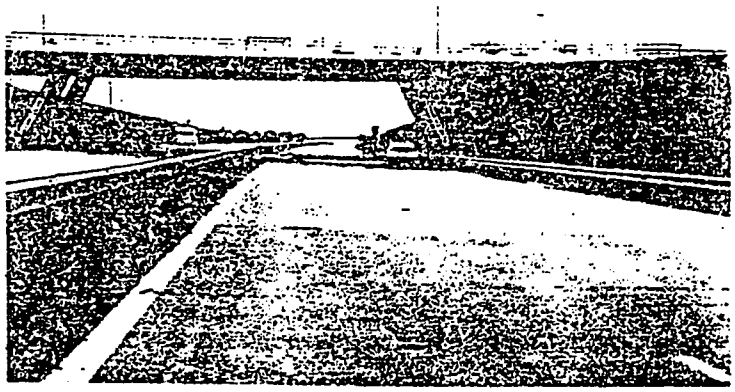

Figure 11: Reinforcement of an end span in Swanley bridges.

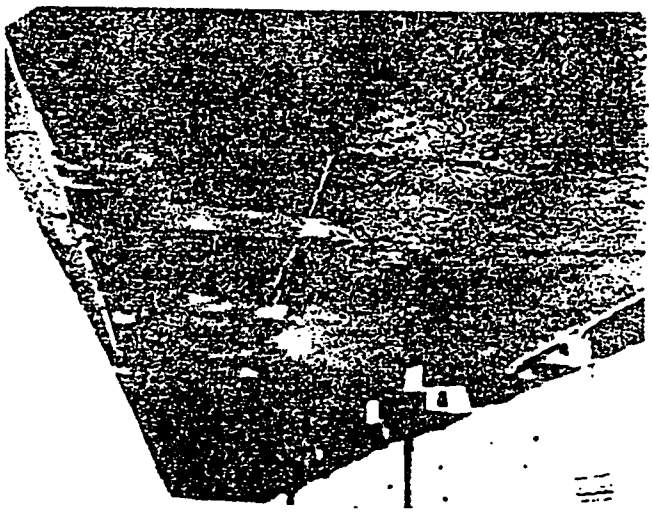

Figure 12: Reinforcement of the plate on the underside of the roadway in Swanley bridges.

Figure 13: Bonding of the plates to the top of the slab above the pier. The sand bags were used to weigh down the plates until the hardening of the adhesive in Swanley bridges.

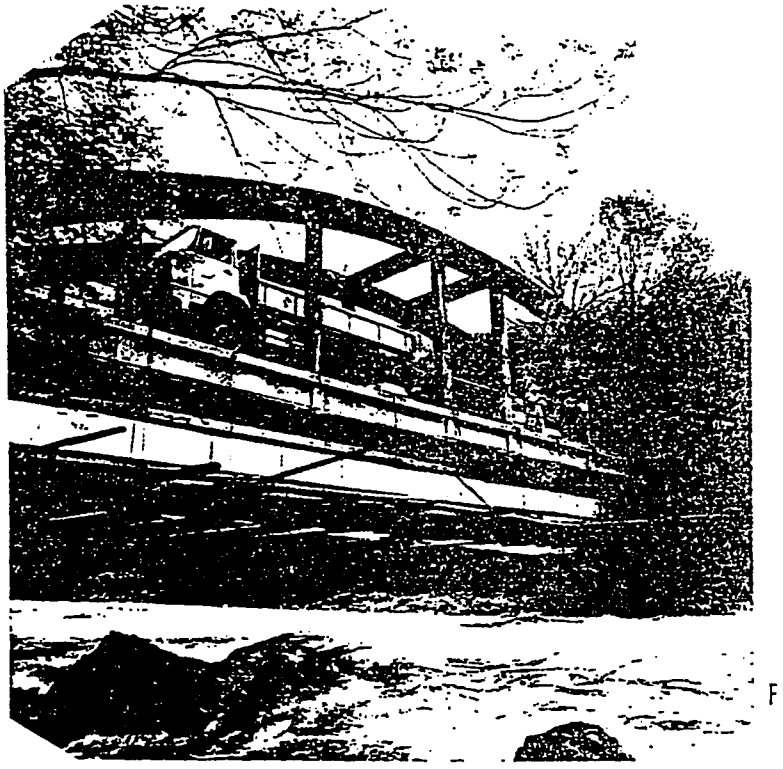

Figure 14: Testing of the Gizenen bridge following the reinforcement of the roadway slab.

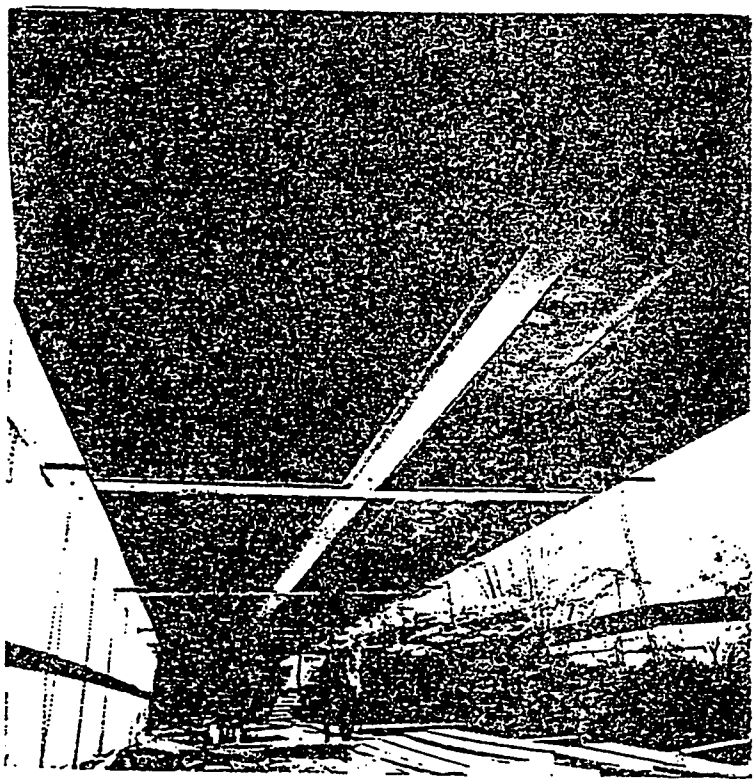

Figure 15: The reinforced main girders and cross-ties of the Gizenen bridge. The butt straps are clearly visible on the outer main girders.

In 1975, in the United Kingdom, a group of four bridges at an interchange on M5 motorway at Quinton were strengthened by plate bonding. [18] . Each bridge consists of a deck of voided slab of variable depth which is continuous over three spans. The centre span of the deck is 27.4 m and side span is 7 m in each of the four bridges. This bridge complex was opened to traffic in 1970. In 1973 design checks showed that these bridges were under designed. Also close inspection of these bridges indicated the presence of cracks on the critical locations on the underside of the decks. Strengthening operation was carried out by plate bonding without closing the bridges for normal traffic while restrictions on heavy traffics were imposed during strengthening operations. A total of 1376 steel plates were bonded to the curved under surfaces of the four bridges at the interchange. The plates were mostly 254 mm wide, 6.5 mm thick and lengths varying upto 3.6 m. At some locations effective thickness of the plates was increased locally by bonding additional steel plates. Two types of adhesives were used from different suppliers. Both adhesives were structural grade two-part epoxy resins. This strengthening operation took six months to complete. Full scale loading tests were carried out on one side span and on half of the centre span of one of the four bridges at the interchange. The load testing was done with three single axle loads successively. Strains and deflections at various locations were measured. It was noticed that the bridges showed impoved behaviour after strengthening with plates. Figure 16 shows the reinforcement of the end sections. Figure 17 shows the procedure for installation of plates. Pressing of plates was done by means of wooden wedges. Figure 18 shows one of the reinforced end spans.

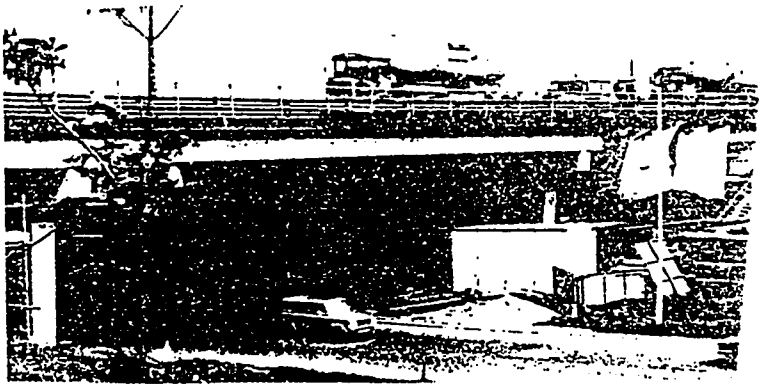

Figure 16: Reinforcement of end sections in Quinton bridges. The steel plates were shotblasted at the site.

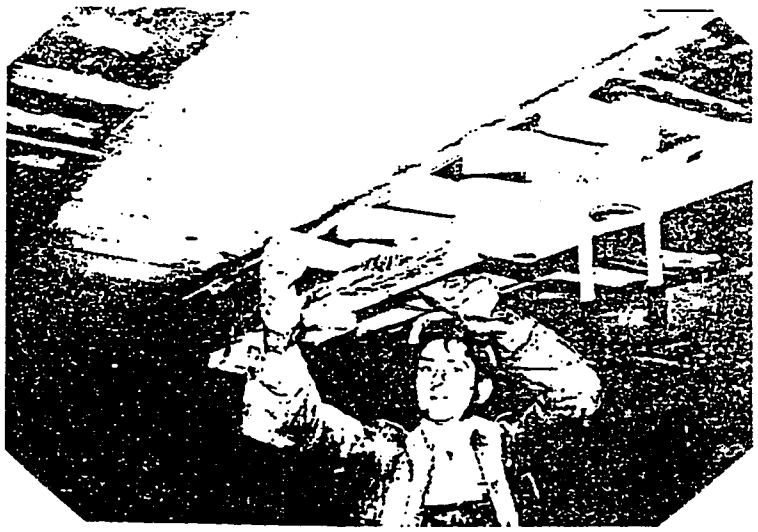

Figure 17: Installation of a plate in Quinton bridges. Pressing is being done by means of wooden wedges.

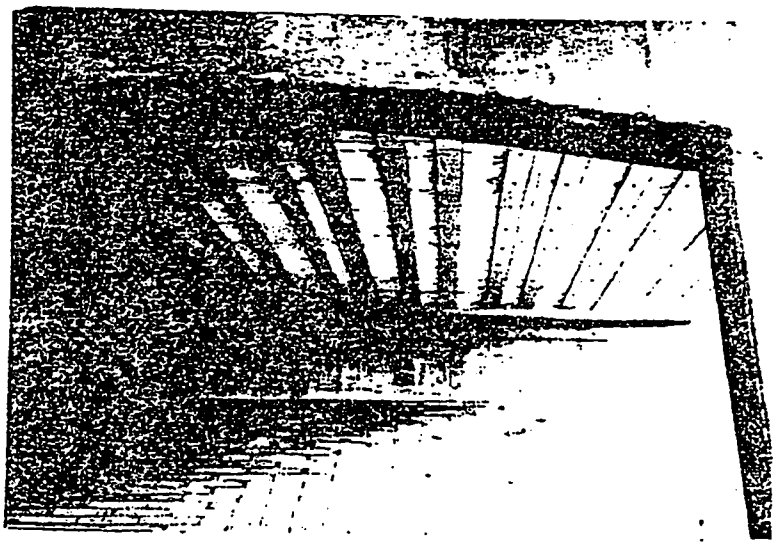

Figure 18: One of the reinforced end spans of the Quinton bridges.

1.2 PROBLEM DEFINITION

1. FLEXURE PART

a. Many researchers have done work to see the performance of the epoxy bonded plated beams. The plated beams, bonded with thin strips of steel on the tension faces of the beams, showed improved behaviour both at the service load and ultimate load levels. But when relatively thicker plates were used separation of the steel plates took place starting from the ends of the plates and the beams failed not only without reaching the theoretically predicted ultimate strengths but also showed lack of ductility. It is recalled that for safety, structural members should have enough ductility to give warning before failure.

The separation of plates at terminate ends of plates takes place due to high concentrations of shear and normal stresses (peeling stresses). In order to overcome this problem of separation of the plates a limited study was performed by R.Jones [19] . He used anchor bolts and angle plates at the terminate ends of the plates. He reported that anchor bolts improved the ductility but the separation of the plate at the ends could not be prevented. Angle plates proved to be the best anchorage system because they improved the ductility and prevented plate separation as well. However, angle plates are not suitable for wider beams and can not be used for slabs. His study was not confirmed by others and did not clearly explain the stress state at the terminate ends of the plate.

b. Various researchers like R. Jones [19] , T. M. Robert [20] and T. M. Robert and Haji-Kazemi [21] have tried to give analytical expressions for predicting shear and normal stresses at the interface of the concrete beams and steel plates. Robert's [20] method is approximate and R. Jones' method [19] , based on simple elastic theory, gives only average values of stresses at interface. T. M. Robert and Haji-kazemi's [21] analytical solution for predicting the shear and normal stresses at the interface is a very complicated expression and is not amenable to hand calculations even for very simple loadings. So there was a need to write a computer program for finding the shear and normal stresses at the interface of the concrete beam and the steel plate.

2. SHEAR PART

Very minimum work has been done to strengthen the concrete beams damaged in shear, by bonding steel plates externally.

1.3 SCOPE OF PRESENT RESEARCH WORK

1. FLEXURE

a. PLATE SEPARATION

In order to overcome the problem of plate separation anchor bolts were used. The variable studied were depth of anchor bolts and layout of anchor bolts when more than one anchor bolts at each end of the plate were used. The complete detail of the anchoring systems used to overcome separation will be given in chapter 3.

b. PREDICTION OF SHEAR AND PEELING STRESSES

A linear finite difference computer program based on partial interaction theory [22] for predicting shear and normal stresses at the interface of the concrete beam and the plate in epoxy bonded plated beams has been written. The curtailment of the plate before the supports of the beam has been done in a unique way.

2. SHEAR

Various types of external shear reinforcements such as jackets, straight strips , U-strips and wings were used to repair RC beams damaged in shear and the improvement in strength and ductility for different types of strengthening arrangements has been compared.

1.4 RESEARCH SIGNIFICANCE

This research has been motivated by the fact that, with the vast increase in the oil revenue, the economy of Saudi Arabia was improved and a lot of buildings and bridges were constructed rapidly. Most of the construction was done by foreign companys who were not familiar with the climatic conditions of the Kingdom and also no local building code was available during the time of construction. After the completion of construction, some structures began to deteriorate because of the climatic conditions and because of the improper design loads taken for the design of these buildings and bridges. For economic reasons many damaged buildings and bridges have to be repaired by plate bonding. These facts motivated to investigate the performance of plate bonding technique.

Also the present work is a part of the continued research in the plate bonding technique all over the world.

Chapter II

LITERATURE SURVEY

(FLEXURE PART)

Investigations into the performance of the plate bonding technique started in 1960s [23-25] . A lot of experimental work has been done to study the performace of this technique. A limited theoretical studies have also been made to determine the shear and peeling stresses at the interface in the epoxy bonded plated beams. In the present chapter, review of the selected experimental and theoretical studies is presented.

2.1 REFERENCE 28

Irwin in 1975 [28] reported the test result of beams strengthened by plate bonding in flexure. He tested two RC beams one with bonded steel plate and one without steel plate. It was found that the crack width in the beam with bonded steel plate was significantly less than that of the beam without steel plate. The failure in the beam with bonded plate took place due to separation of the plate. Then the plate was removed and both beams were loaded upto failure and both beams showed the same moment capacity. However, plated beam showed higher moment capacity during the first cycle of loading, before the separation of the plate. The capacity of the plated beam suddenly dropped down due to the sudden separation of the plate.

2.2 REFERENCE 33

In 1979, A. J. J. Calder [33] reported the test results of unreinforced concrete beams exposed to different environments upto two years. A total of 300 beams of size 508 mm × 102 mm × 102 mm were cast with a compressive strength of 48 N/mm^2 . The steel plates of widths and thicknesses equal to 38 mm and 3 mm respectively, and of the same length as that of the beam were bonded to one face of the beams with glueline thickness of 0.5 mm. Some beams were kept under uncontrolled conditions (Preliminary) and some were kept under controlled laboratory conditions. Some beams were placed at Silverdale, Pilsey and Tinsely sites having different environmental conditions for exposure. Some beams were kept in loaded state and some in unloaded state. It was planned to do testing of the beams placed under different conditions after one, two, five and ten years. But this report by A. J. J Calder, covers only test results of only one and two years of exposure.

Bending tests and observations of the fractured surfaces and shear tests of glues were performed. The results which were obtained upto two years of exposure are summarized below.

1. The corrosion took place at the steel/glue interface in all the specimens which were exposed to natural environments. Because of this corrosion at the steel/resin interface, some reduction in strength took place in the exposed specimens as compared to the controlled laboratory specimens in which corrosion did not take place.
2. It was considered that corrosion in the exposed specimens was due to the migration of moisture from concrete to the steel plate passing

through the glue layer. Microcracking, in the broken pieces of the glue, which were extracted from broken beams, was observed.

3. The analysis of results showed that there were significant differences of results for beams which were exposed to different environments and between loaded and unloaded specimens. No significant difference in the results of beams were found which were tested after one or two years of exposure.
4. The load applied to the beams decreased to about 70 % of the original value after first 8 month of exposure.
5. The stress carrying capacity of the glue reduced significantly after two years of exposure but it was still greater than that of the concrete.
6. A significantly higher area of steel plate was rusted after two years of exposure as compared to one year of exposure.

2.3 REFERENCE 26

In 1980 R. Jones, R. N. Swamy, J. Bloxham and Bouderbalah [26] published the experimental data on the effects of glueline thickness , plate lapping, multiple plates and on the effects of precracking prior to bonding. Their experimental program consisted of three series of beams, that is, series A, series B and series C.

In series A, eight beams of length 710 mm and 150 by 150 mm in cross-section, were used. All the beams were strengthened by 500 mm long, 100 mm wide and 1.00 mm thick steel plates. Two types of glues, A and B were used. All the beams of this series were without longitudinal reinforcement. Beams A1

and A2 had no shear reinforcement. All the other beams of this series had shear reinforcement to prevent shear failure outside the plated length. Table 1 gives the detail of glue layers for these beams.

Table 1: Detail of beams of series A

Beam ID.	Glue Type	Glueline Thick. (mm)	Profile of Glueline
A1	A	4.0	Uniform glue thickness
A2	B	4.5	Uniform glue thickness
A3	A	3.5	Uniform glue thickness
A4	B	5.0	Uniform glue thickness
A5	A	3.8	Tapering glue Thickness
A6	B	4.0	Tapering glue thickness
A7	-	-	Unplated beam
A8	-	-	Unplated beam

The glueline thicknesses given above are the average thickesses at mid-span of the beams.

All the beams were tested simply supported, under centre point loading, over an effective span of 610 mm. The load deflection curves for beams A2, A4, A6 and A8 are shown in the Figure 19 .

From the load-deflection curve of beams of series A, it is clear that the beam A4 with shear reinforcement at support showed better performance than the comparable beam A2 without shear reinforcement. Beam A6 with tapering glueline

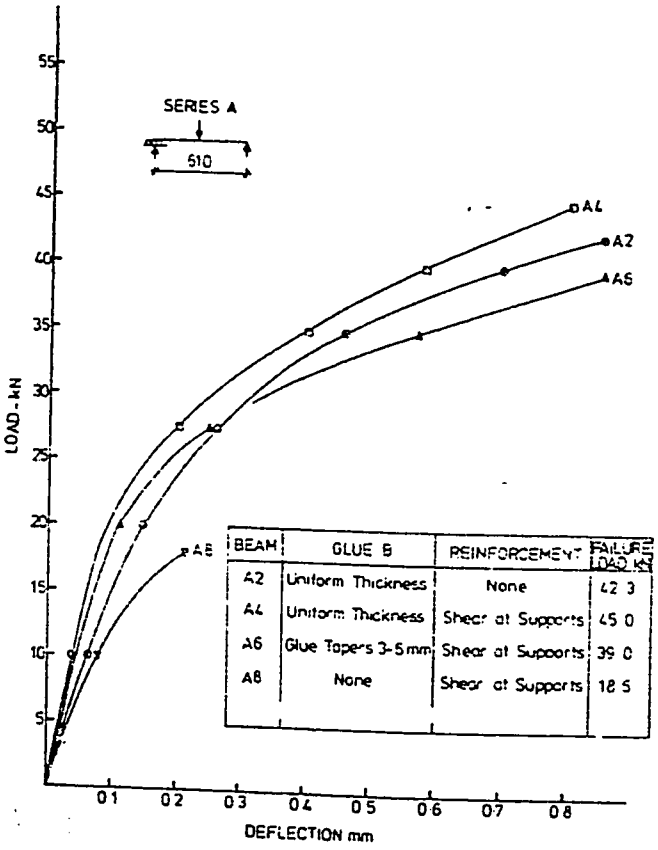

BEAM	GLUE B	REINFORCEMENT	FAILURE LOAD kN
A2	Uniform Thickness	None	42 3
A4	Uniform Thickness	Shear at Supports	45 0
A6	Glue Tapers 3-5mm	Shear at Supports	39 0
A8	None	Shear at Supports	18 5

Figure 19: Load-deflection curves for beams of series A

showed higher stiffness in the beginning than that of the beam A2 with uniform glueline. But at higher loads with cracking in the glue, stiffness for this beam became less than that of the beam A2. Comparing the load-deflection curves for plated beams A2, A4 and A6 with that of plain concrete beam A8 it was observed that bonded steel plates

1. Increase the range of elastic behaviour.
2. Increase the stiffness of the beams.
3. Increase the ultimate flexure capacity.
4. Increase the ductility of the beams.

Series B consisted of ten plain concrete beams of length 1200 mm, and width and depth of 100 mm and 150 mm respectively. With the help of the beams of this series, the effect of uniform glueline thickness, lapping of plates and the provision of notches at the soffit of the beams were studied. The notches were triangular. All the beams of this series had shear reinforcement at the support. The plates used to strengthen these beams were 1000 mm long 75 mm wide and 1 mm thick. Table 2 gives the strengthening details of the beams of series B.

The load-deflection curves of beams of series B were drawn and are shown in the Figure 20 . Load-deflection curves of unplated beams B5 and B8 with and without notches at the bottom are almost same which means that the presence of notches at the bottom in the unplated beams had no adverse effect. Plated beam B10 with notches at the bottom showed marginally better behaviour than plated beam B2 with uniform glue thickness. Also beam B4 with lapped plates showed better performance than beams B2 and B10.

Table 2: Detail of plain concrete test beams of series B

Beam ID.	Average Glue Thickness	Glue Type	Glue Layer Profile
B1	3.5	A	Uniform glue thickness
B2	3.0	B	Uniform glue thickness
B3	5.0	A	Uniform glue, lapped plates
B4	3.0	B	Uniform glue, lapped plates
B5	-	-	Unplated beam
B6	-	-	Unplated beam
B7	-	-	Unplated, notched beam
B8	-	-	Unplated, notched beam
B9	3.5	A	Plated, notched beam
B10	3.0	B	Plated, notched beam

The glueline thickness given is average glueline thickness at mid-span.

Strains were measured over the depth of typical beams for series A and series B. Figure 21 show the strain distribution for beams A2 and B5 respectively. From these diagrams it is clear that the assumptions that plain section remain plain is valid for plated beams. These diagrams also show that the strain distribution remain linear in compression zone over the full elastic range. But in the tension zone it remains linear at low loads but at higher loads they become non-linear due to cracking of the concrete. Movement of the neutral axis towards the compression face with increasing load is also clear from these diagrams.

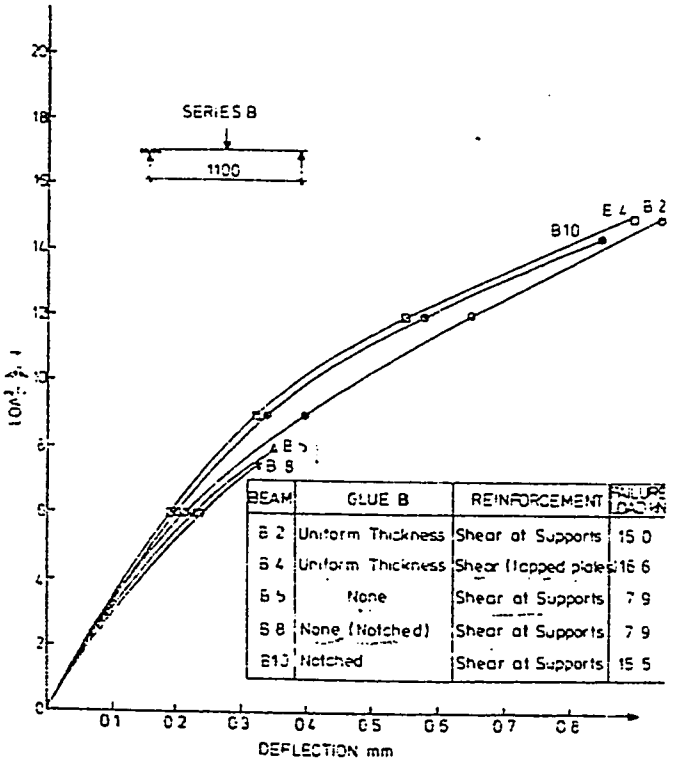

Figure 20: Load-deflection curves of beams of series B

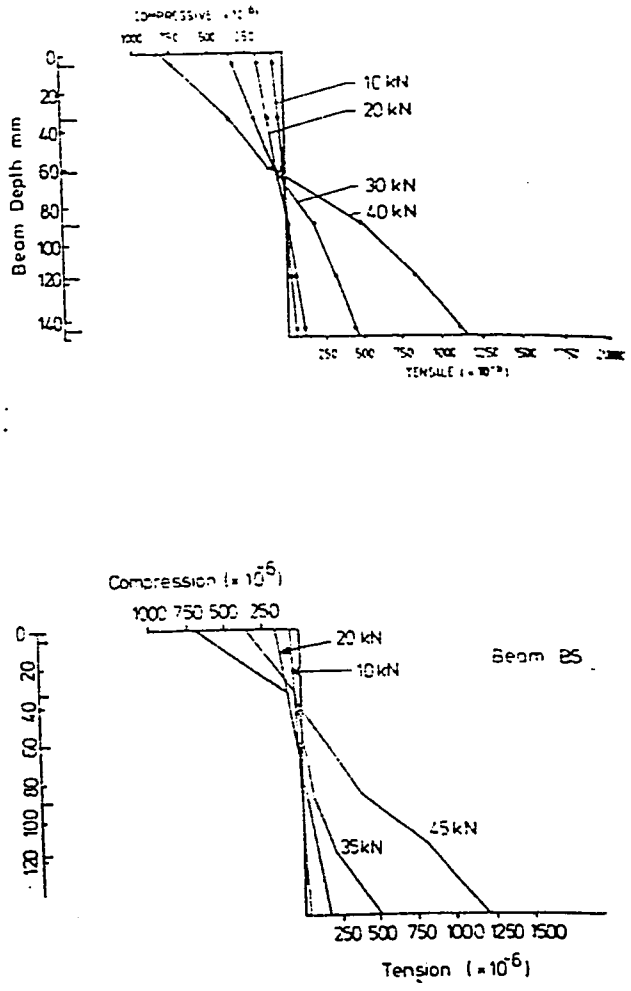

Figure 21: Strain distributions for beams A2 and B5

In series C, a total of sixteen beams were tested. Beams C1 to C8 were designed to determine the effect of glueline thickness from 1.6 to 8 mm. Two beams were tested with one glueline thickness for repeatability. These beams were tested with single point load at the centre. Table 3 shows the strengthening detail of beams C1 to C8. The load-deflection curves for these were drawn. It was found that the stiffness of the beams increases by increasing the thickness of the glueline.

Table 3: Detail of beams of series C from C1 to C8

Beam ID.	Adhesive Thickness	Steel plate area	Plate Detail
	mm	mm	
C1,C2	-	0	unplated
C3,C4	1.6	128	Sinlge plate
C5,C6	4	128	Single plate
C7,C8	8	128	Single plate

Beams C9 to C12 were designed to see the effect of changing the mode of failure by changing the load position. These beams were tested with two point loads. Beams C9 and C10 were kept unplated. Beams C11 and C12 were plated beams. In Beams C9 and C12 a/d ratio was kept equal to 2.8. In beams C10 and C11 a/d ratio was kept equal to 1.9. Unplated beam C9 (a/d = 2.8) failed by crushing of concrete whereas unplated beam C10 (a/d = 1.9) showed flexure

and shear cracking and failed in combined flexure shear mode. Plated beams C11 (a/d = 1.9) and C12 (a/d = 2.8) both failed in shear and showed all the conventional cracking characteristics of shear failures. However plated beam C12 (a/d = 2.8) showed more shear capacity than that of the beam C11 (a/d = 1.9).

Beams C13 to C15 were used to study the effect of plate lapping and multiple plates. These beams were tested under single point load at centre. Beam C16 was cracked prior to bonding. Table 4 shows the strengthening detail of these beams.

Table 4: Detail of beams C13 to C15.

Beam ID.	Adhesive thickness	Plate area	Detail of Plate
C13	1.6	128	Single plate lapped
C14	1.6	192	1-1/2 plates
C15	1.6	256	2 plates
C16	1.6	128	single plate

Figure 22 shows the load deflection curve of these beams. From these curves it is clear that the stiffness of the beams increases with increasing the area of the external reinforcement. Beam with lapped plates show higher stiffness and ultimate load than beam with single plate of the same area. Precracked plated beam show improved strength and stiffness as compared to original beams but these values are maginally less than those of the plated as-cast beams.

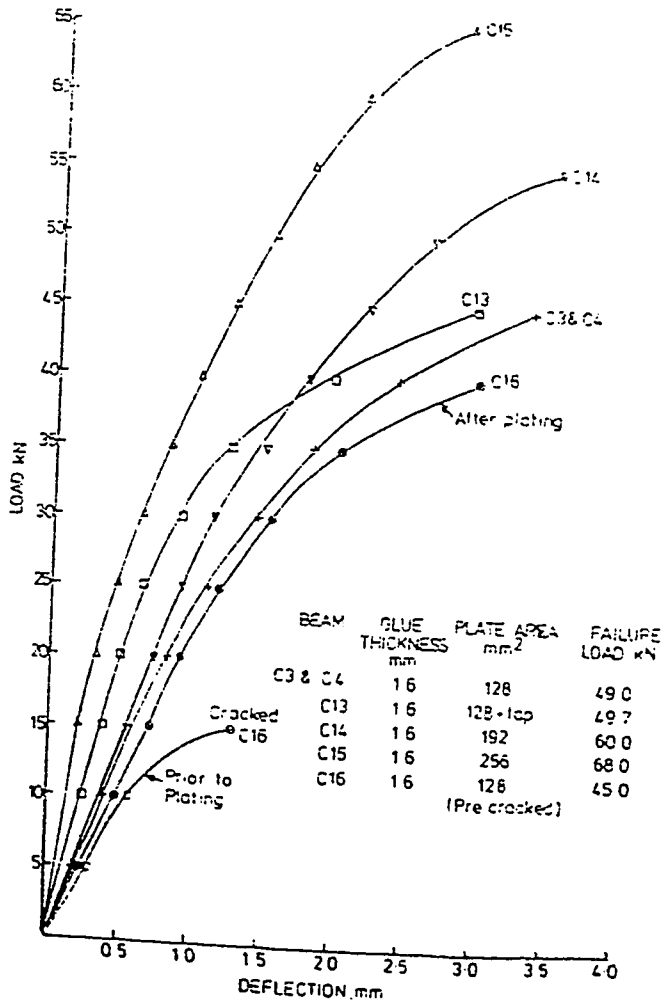

Figure 22: Load-deflection curves for beams C13, C14, C15, C16, C3 and C4

2.4 REFERENCE 27

In 1982, R. Jones, R. N. Swamy and T. H. Ang [27] reported the test results of under and over-reinforced RC beams strengthened by bonding steel plates externally. Eight beams were used in this study. All the beams were of the same dimensions. The beams URB1, URB2 , URB3, URB4 and URB5 were under-reinforced and the beams ORB1, ORB2 and ORB3 were over-reinforced. The beams URB1 and ORB1 were tested as unplated beams. The beams URB2, URB3, URB4 and URB5 were strengthened by 1.5 mm, 3 mm, 5 mm and 10 mm thick plates on the tension faces. The beams ORB2 and ORB3 were strengthened by bonding 5 mm thick plates on the tension and compression faces respectively. The analysis of the plated sections, based on actual stress-strain diagram, showed that by the addition of plates beam URB4 became balanced section and beam URB5 became over-reinforced section. The width of plates in all the beams was 80 mm. The Glueline thickness in all the beams was 3 mm. All the beams were tested simply supported with two point loads applied at the ends of the middle third.

2.4.1 DEFORMATIONAL BEHAVIOUR

Figure 23 shows the load-deflection curves of all the beams used in this study. Load deflection curves of beams URB1, URB2, URB3, URB4 and URB5 were compared. It was seen that the stiffness of the beams increases by increasing the cross-sectional area of the bonded plates. Comparison of the curves of ORB1, ORB2, ORB3 shows that bonding the steel plate on the compression face has less effect on increasing the stiffness than that by bonding the plates on the tension face.

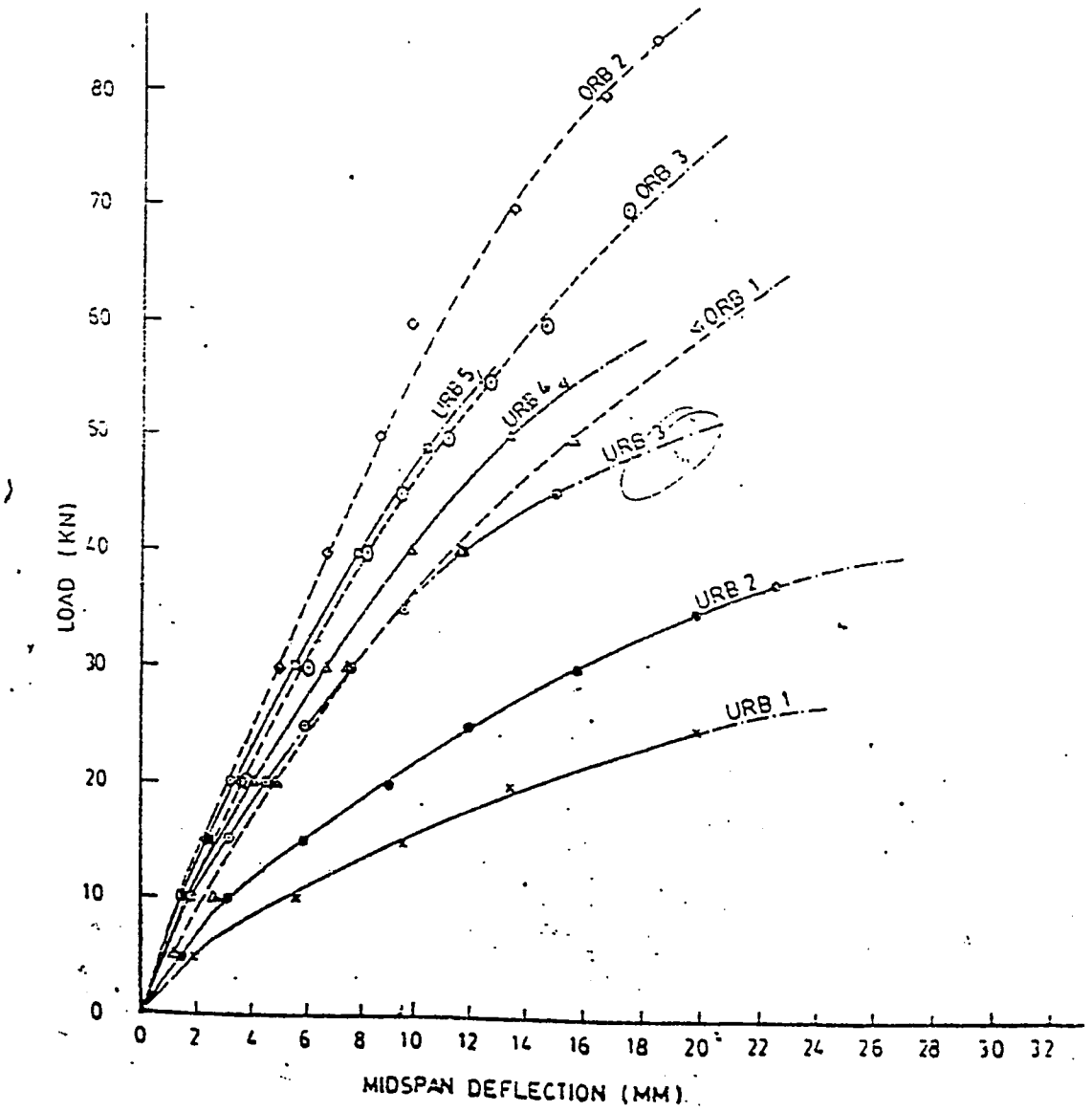

Figure 23: Load deflection curves of beams URB1, URB2, URB3, URB4 and URB5.

2.4.2 COMPOSITE ACTION

For this purpose the results of beam URB2 are selected. This beam failed in pure flexure mode. The maximum experimental moment sustained and theoretical moment calculated assuming full composite action, showed very good agreement. From this it can be concluded that full composite action can be obtained if gluing operation is done properly.

2.4.3 CRACKING

The load vs average crack widths in the middle third of the beam were drawn. It was noticed that the external plating control the cracking. Hence service load increase by the addition of plates. These curves for beams ORB2 and ORB3 were compared and it was found that the addition of plate on compression face has less effect on the control of cracks as compared to bonding the plates on the tension face. Average crack height and spacings were measured in the middle third region. The plating has little effect on the spacing of cracks for beams URB2 to URB4 but crack height reduces as the plate thickness increases. However, the results of beam URB5 were not consistent with the above mentioned behaviour.

2.4.4 EFFECT OF PLATES ON THE COMPRESSION FACE

The bonded plates on the compression face improve the structural behaviour of the beams with respect to original unplated beams. But the improving effect was less as compared to bonding similar plates on the tension face.

2.4.5 EFFECTS OF PLATE THICKNESS

The bonded plates increased the flexural stiffness of the beams with corresponding decreases in deflection and rotation. The increase in the bending stiffness for thicker plates was more as compared to thinner plates. The bonded plates increased the ultimate strengths of the basic beams in all cases. Thicker plates generally had greater effect, but the mode of failure changed from yielding to separation as the plate thickness increased.

2.5 REFERENCE 29

In 1982, M. D. Macdonald [29] reported the test results of seventeen beams on the flexure performance of concrete beams with various bonded external reinforcement. Seventeen beams of length 3.5 mm, width 150 mm and over all depth 250 mm, bonded by external plates were tested under four point loading. The variable studied were different adhesives, plate geometries, a jointed plate, glueline thickness , partial bonding and multilayered plates.

2.5.1 TYPE OF ADHESIVE

This study was done on the plated As-cast beams. Three types of adhesives were used for comparison with same plate size. All the beams with different adhesives behaved in the same manner with respect to load-deflection characteristics. There was a significant effect on the cracking pattern of the type of the adhesive used. With stiff adhesives closely spaced cracks were obtained while with flexible adhesive crack spacing obtained was almost similar as in the As-cast beams. Using stiff adhesive, the load for first visible crack was high. But for the beam with flexible adhesive first crack load was same as that for the As-cast beam. Therefore, stiff glue was recommended for use.

2.5.2 PLATE GEOMETRY

In order to prevent the failure by plate separation b/t ratio was varied for the plates but the area was kept same. This study was done on plated As-cast and plated pre-cracked beams. The behaviour of plated As-cast beams bonded with plates of b/t ratios of 12, 24, 57 and 142 respectively was studied. For the beams bonded with plates of b/t ratios of 12 and 24 failure was by the tearing of concrete at the terminate end of the plate. For beams bonded with plates of b/t ratios of 57 and 142 pure flexure failure was obtained. On this basis b/t ratio for the plates equal to 60 was recommended to avoid failure by the tearing of concrete at the terminate end of the plate.

2.5.3 EFFECT OF PRECRACKING

For this purpose beams bonded with plates of b/t ratios of 24 and 142 were selected. Strengthening of precracked beams was done while under load. With further increase in load the plates came in action. Then load-deflection curves for plated precracked and plated as-cast beams followed almost the same path indicating that there is no adverse effect of precracking on the behaviour of the plated beams. From this it was concluded that this technique can be used to strengthen the precracked structures.

2.5.4 EFFECT OF MULTIPLE PLATES

This study was done on the precracked beams. For this purpose results of test 14 and test 19 were selected. Beam of test 14 was strengthened by a single plate of width and thickness equal to 85 mm and 3.6 mm respectively. Beam 19 was strengthened by three plates of width and thickness equal to 47 mm and 2 mm

respectively. The area of the external reinforcement in both cases was same. The ultimate load obtained for the beam with multiple plates was less as compared to that of the beam with single plate.

2.5.5 EFFECT OF PARTIAL BONDING

For this purpose the results of beam 14 and 18 were compared. In beam 18 plate used was 3500 mm long. The plate was bonded only over a distance of 250 mm at each end. The interior plate length was debonded by using polythene sheeting and grease. The partial bonding had no adverse effect. The gain in strength and stiffness was same as that for the beam with fully bonded plate but the distribution of cracks was like that of the As-cast beam because there was no distribution of strains in the unbonded length. It was also noticed that the steel plate strain in the unbonded length was uniform with plate acting as an unbonded tendon.

2.5.6 EFFECT OF GLUELINE THICKNESS

For this purpose, results of beam 14 and beam 17 were compared. The glueline thickness for beam 17 was higher than that of the beam 14. The load-deflection curve for the beam 17 was a little lower than the load deflection curve for the beam 14. The beam with thick glueline had marginally less stiffness and less ultimate load as compared to those of the beam with thin glueline.

2.5.7 EFFECT OF JOINTED PLATE

Test results of beam 14 and 16 were compared. Beam 16 was strengthened with a jointed plate and beam 14 was strengthened using a single full plate. The load-deflection curves of these beams showed marginal differences from each other, that is, using jointed plates had no adverse effect on the behaviour of the beam.

2.5.8 ULTIMATE LOADS

By the addition of plates average ultimate loading capacity increased by 40 percent both for As-cast and Pre-cracked beams.

2.5.9 EFFECT OF PLATING ON STIFFNESS

Stiffness increased by 190 % for beams which were strengthened without pre-cracking and it increased to 250 % for beams which were strengthened by external plates after cracking upto 0.1 mm crack width, in the constant moment region.

2.6 REFERENCE 34

In 1982, G. O. Lloyd and A. J. J. Calder [34] reported, on the basis of microstructural analysis of concrete/resin interface system using marker solution and electron microscopy, that there exists cracks and pores in the concrete and epoxy layer through which moisture travel and reach the steel plate and cause corrosion in the epoxy bonded plated beams. They also reported that the use of primer on the steel plate is better for resisting corrosion.

2.7 REFERENCE 30

In 1987, R. N. Swamy, R. Jones, J. W. Bloxham [30] presented the test results of 24 epoxy bonded plated beams. All the beams were 155 mm by 255 mm in cross-section and 2500 mm lengths. All the beams were reinforced with three 20 mm dia. bars as the main reinforcement. The shear spans were provided with 6 mm diameter links at a spacing of 75 mm centre to centre. All the beams were tested over simple span of 2300 mm. Variables studied were effect of glued steel plates on the first crack load, cracking behaviour, structural deformations, serviceability loads and ultimate strength of strengthened reinforced concrete beams.

2.7.1 FIRST CRACK LOAD

The theoretical and experimental first crack loads were compared for plated and unplated beams. The ratio of experimental and theoretical first crack loads for unplated beams was 1.12 but for plated beams it increased to 1.38. The increase of the ratio show the restraining effect of glue and plate on the first crack load. It was found from the test results that the first crack load increase with increasing glueline thickness for beams with plate thickness of 1.5 mm. For higher plate thicknesses first crack load show a tendency of decreasing with increasing glueline thickness. However, this increase or decrease of first crack load, with increase in glueline thickness was marginal. Neither the first crack loads nor the service loads were constant. Both of these loads were changing with the thickness of the bonded plates. The ratio of first crack load to service load for the unplated beams was 0.35. This ratio for the beams bonded with 1.5 mm, 3.00 mm and 6.00 mm thick plates was 0.45, 0.37, 0.32 respectively. It was seen that

the first crack load showed marginal change with increasing the area of the steel plate. It was observed that lapping of plates, variable glueline thickness and presence of V-notches had practically no effect on the first crack load.

2.7.2 DEFORMATIONAL BEHAVIOUR

Figure 24 show the load-deflection curves for beams 201, 202, 203, 204 ,205 and 206 respectively. Comparison of the load-deflection curves of beams 203, 204, 206 show that with increasing the plate thickness (other variables constant) stiffness of beams increases. At the bottom face in beam 201 no glue layer was applied. But at the bottom face of beam 202 glue was applied but no plate was bonded. Comparison of the load deflection curves for beams 201 and 202 show the stiffening effect of the glue layer. Beam 202 showed higher stiffness than that of the beam 201. Load-deflection curves of beams 204 and 206 show that beam with multiple plate has marginally higher stiffness. From these curves it is also clear that stiffness of all the beams is different at different load levels. It was also observed that the stiffness of the beams increases with increasing the thickness of the glueline. It was also noticed that the stiffening effect was much more influential in reducing the rebar strain and plate strain than on reducing the deflection. This has significance because the rebar strain control the cracking in the concrete and steel plates provide restraining medium to crack initiation.

2.7.3 COMPOSITE ACTION

The strain measurements in all the beams showed yielding of the plates in case of 1.5 mm and 3 mm thick plates. Upon unloading the plastically deformed plates warped away from the concrete. It was seen that the failure took place in the concrete but not in the glue/concrete interface or plate/glue interface.

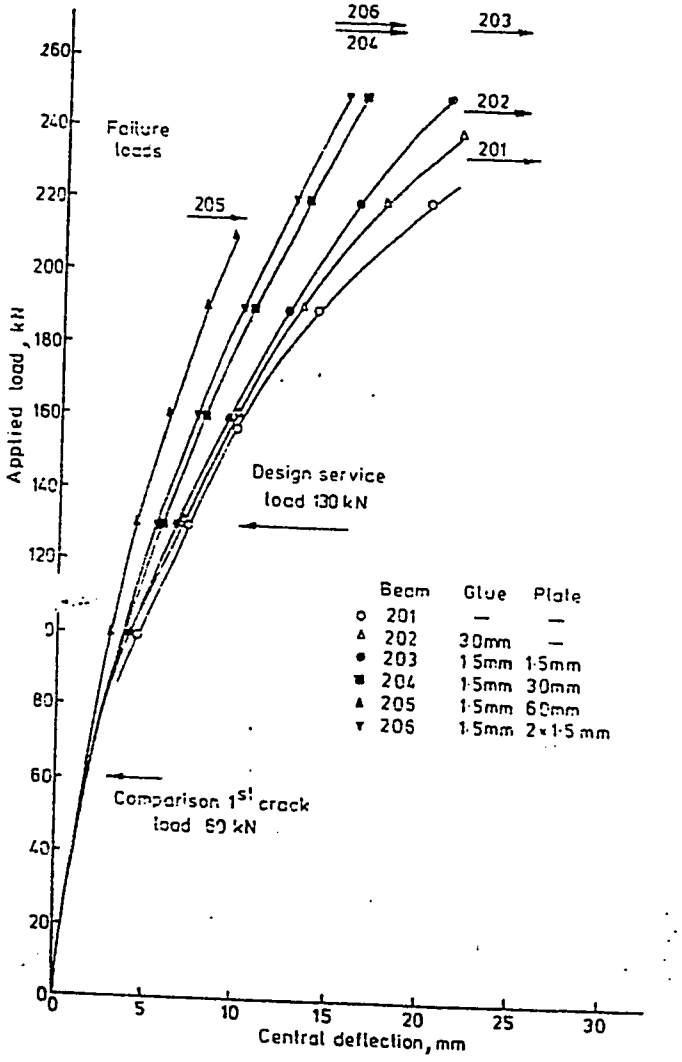

Figure 24: Load-deflection curves for beams 201, 202, 203, 204, 205 and 206 respectively.

2.7.4 SERVICEABILITY

The externally bonded plates substantially reduce the deflections and rotations, steel bar strain and cracking. The load carrying capacity at the serviceabilty limit state increases with increasing the plate thickness. Effect of precracking on the serviceabilty loads was studied. It was found that the serviceabilty loads increase with increasing the plate thickness for the precracked beams.

2.7.5 ULTIMATE LOADS

The experimental ultimate loads for plated and unplated beams were compared. The beams with 1.5 mm, 3.00 mm thick plates showed higher ultimate loads as compared to that of the unplated beams. But beams with 6 mm thick plates gave less ultimate load as compared to that of the beams with 1.5 mm and 3 mm thick plates because of premature failure due to plate separation. The ratio of ultimate load to service load for unplated beam was 2.32. This ratio decreased by increasing the plate thickness. Lapping of plates also lowered this ratio. Precracking of beams had no adverse effect on this ratio.

2.7.6 MODES OF FAILURE

Beams with 1.5 mm thick plates (b/t=83.3) showed pure flexure failure. Beams with 3 mm thick plates (b/t=40.3) showed a combination of shear/bond failure. However, flexure was predominent because failure occurred due to separation after yielding of plates and rebars. However, with 6 mm plates failure took place due to separation of plates. It was recommended tentatively that in order to obtain the pure flexure failure the following conditions should be met

1. The ratio of width of plate to the depth of plate should be kept equal to 50
2. The ratio of depth of neutral axis to the effective depth of beam should be kept equal to 0.4

2.8 REFERENCE 19

In 1988, R. Jones, R. N. Swamy, A. Charif [19] presented a theoretical study based on simple elastic theory to determine average bond stresses anywhere along the external reinforcing plate at the interface level. Figure 25 shows an element of a beam away from the plate cut-off. The bond stress at the glue/ plate interface is given by the following expression :-

$$f_{bp} = \frac{VA_p y_p \alpha_p}{I_T b_p} \qquad (1)$$

Where

V is the shear force.

A_p is the cross-sectional area of the bonded plate.

y_p is the distance from the neutral axis to the mid-plane of the plate.

α_p is the modular ratio $E_{plate}/E_{conc.}$

I_T is the transformed second moment of area.

b_p is the width of the bonded plate. It was shown that the bond stress at glue/ plate interface and glue/concrete interface is almost same. The bond stress in the end region taking into account the effect of plate cut-off was also found. Figure 26 shows the end region of a plated beam defining the variables L and $\bar{x}$. The average bond stress over the length $\bar{x}$ is given by

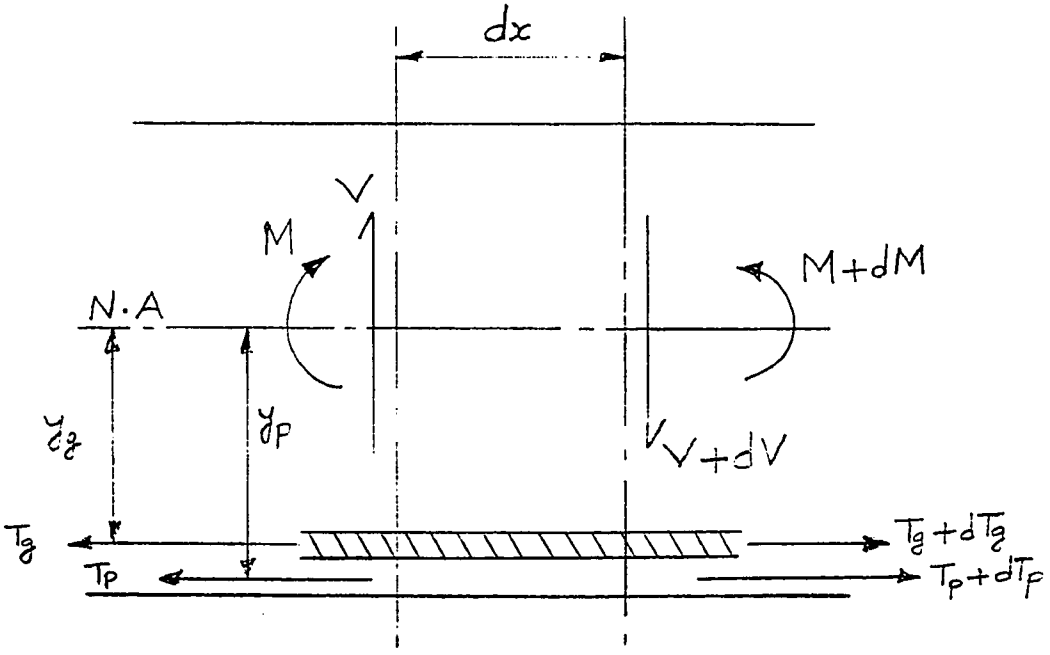

Figure 25: Element of a typical plated beam.

$$f_{bp} = [1 + \frac{L}{\bar{x}}] \frac{V y_p A_p \alpha_p}{I_T b_p} \qquad (2)$$

The lengths L and $\bar{x}$ are of the same order of magnitude. This equation show that at the end of the plate the bond stresses are high as compared to the interior region. Also tapering of plates at the end and using multiple plates with curtailment, will not reduce the average bond stress because in such a case, at failure the value of V will become high and values of $\bar{x}$, A_p and I_T will decrease.

Similarly an expression for peeling force at the interface was derived. For the simple case where the average bond stresses are constant in the anchorage zone and the peeling force reduces to a single point load at the end of the plate of magnitude M_{xy} which for glue/concrete interface is given by the following expression:-

$$M_{xy} = V y_p \alpha_p A_p (t_g + \frac{t_p}{2}) [1 + \frac{L}{\bar{x}}] \qquad (3)$$

Where

t_g is the thickness of the glue.

t_p is the thickness of the bonded plate. The other terms in the above equation have already been explained. This equation suggests that the peeling forces can be reduced by reducing A_p , t_g , t_p and L and by increasing $\bar{x}$. It was suggested that glues with lower elastic modulus gives higher values of $\bar{x}$. However, the research on this aspect is being done at Sheiffield and Dundee Universities.

In order to investigate the problem of sudden failure by plate separation, seven beams of size 155 mm × 255 mm × 2500 mm were tested over a simple

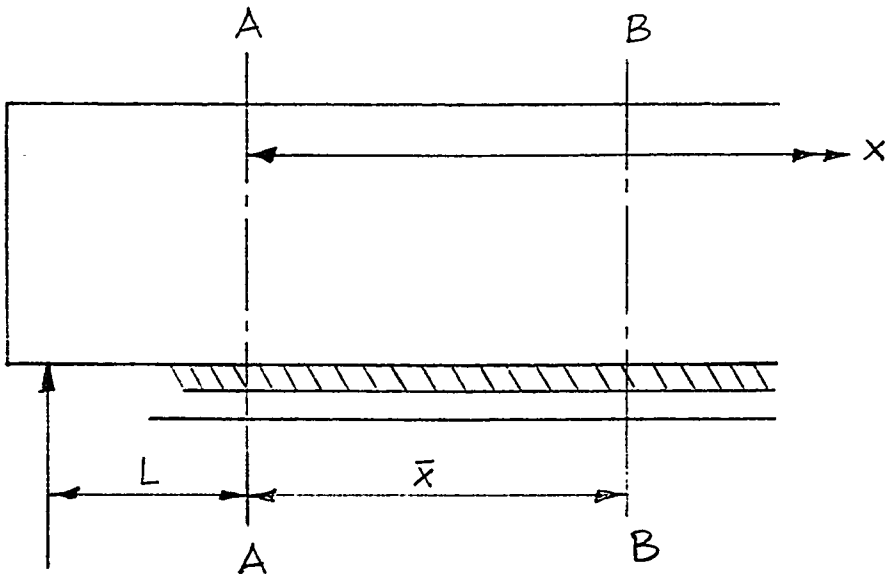

Figure 26: End region of a Plated beam

span of 2300 mm with loading applied at 3rd points. These beams were designated as F31, F32, F33, F34, F35, F36 and F37. The glueline thickness was 1.5 mm and the width of plates was 125 mm. Table 5 gives the summary of the strengthening detail of these beams.

Table 5: Summary of strengthening detail of beams

Beam No.	Strengthening Detail
F31	One 6 mm plate
F32	Two 3 mm plates curtailed
F33	One 6 mm plate tapered
F34	As F31 + Bolts
F35	As F32 + Bolts at End and at Curtailment
F36	As F31 + One short and one long anchor Plates
F37	As F31 + Short end Anchor Plates

The complete strengthening and anchorage detail of all the beams is shown in Figure 27 and Figure 28 .

The external reinforcement was designed in such a way that the theoretical ultimate strength for all the plated beams was equal to 283 kN. Figure 29 shows the load deflection curves for all the beams.

The failure of the beams F31, F32, F33 took place in tearing mode at loads 182, 208, 191 kN respectively. Beams F34, F35 gave composite behaviour upto 200

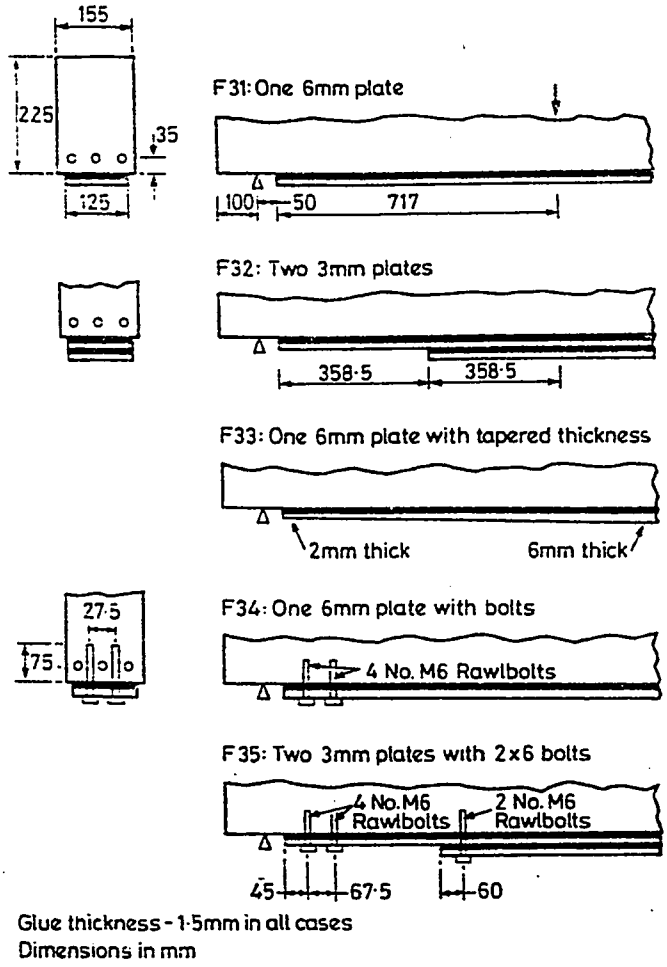

Figure 27: Strengthening detail of beams F31, F32, F33, F34 and F35

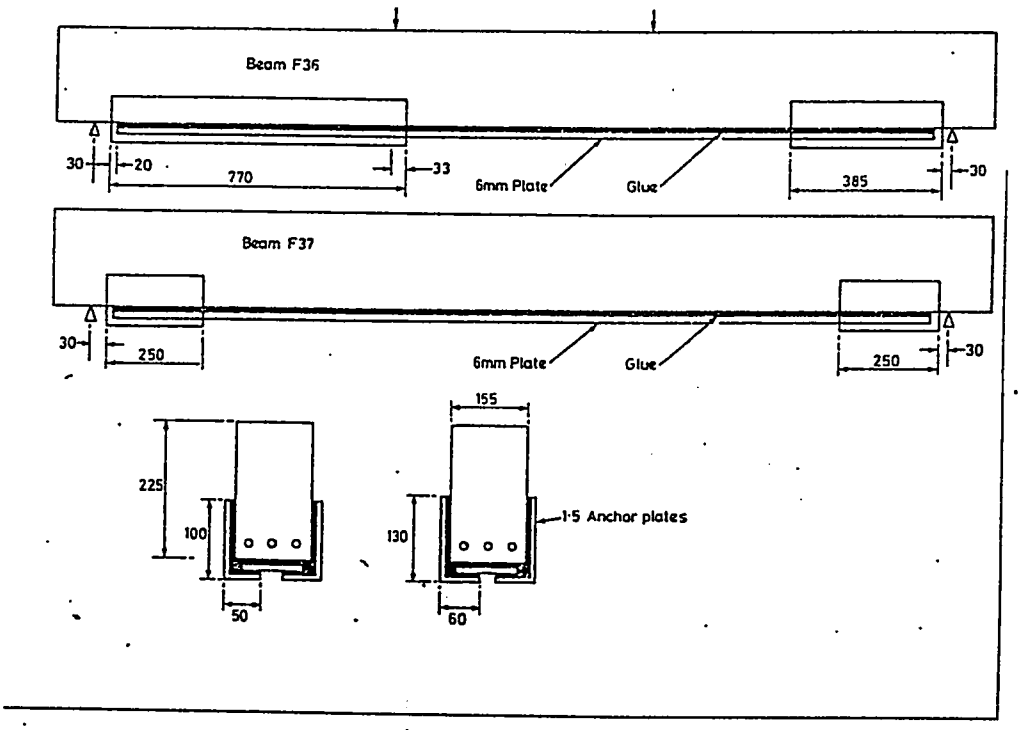

Figure 28: Strengthening detail of beams F36 and F37

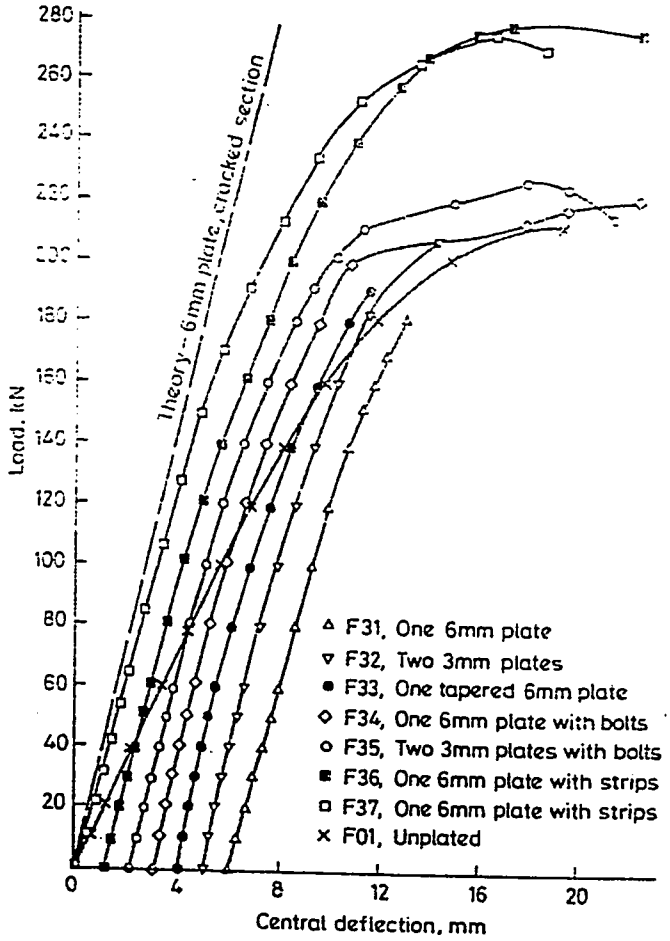

Figure 29: Load-deflection curves for beams F31, F32, F33, F34, F35, F36 and F37 respectively.

kN, 210 kN respectively. Then debonding took place at the end of the plates at these loads. Tearing action took place away from the bolts and ultimately the failure was by the crushing of the concrete, without yielding of the steel plate. The L-shaped anchor plates were the most effective anchoring system used in beams F36, F37. These beams reached full theoretical ultimate capacities. From the test results following conclusion were drawn:-

1. Curtailed multiple plates and tapered plates did not help in changing the mode of failure from the tearing mode to pure flexure failure as shown by the analysis and by the test results.
2. With anchor bolts ductility was improved but tearing of the concrete could not be prevented. However, flexure failure was obtained.
3. With angle plates not only the ductility was improved but also there was no tearing of concrete at the terminate ends of the plates.
4. Very high shear stresses are produced at the terminate end of the plate with a limiting value equal to $\sqrt{2} \times$ tensile splitting strength of the concrete

2.9 REFERENCE 31

In 1989, R. N. Swamy, R. Jones, A. Charif [31] published the test results of nine rectangular beams to show that the plate bonding technique can be used to strengthen the precracked beams in the loaded and unloaded states. All the beams were identical with respect to dimensions, internal reinforcement and material properties of both concrete and steel. These beams were divided into three series. Each series was consisted of three beams. Series I beams (F01,

F02, F11) were used as control beams. Beam F01 was tested without plate and adhesive and F02 was tested with 3 mm adhesive layer at the tension face and F11 was tested after bonding 1.5 mm thick plate with glueline thickness of 1.5 mm. Series II beams (F12, F13 and F14) were loaded upto 30 %, 50 %, 70 % respectivly of the maximum experimental load of the control beam F01 and then were repaired in the unloaded state. All the beams were tested after curing of glue. Series III beams (F22, F23 and F24) were also loaded to 30 %, 50 % and 70 % of the maximum experimental load of control beam F01 and were strengthened by bonding steel plates of 1.5 mm with glueline thickness of 1.5 mm in loaded state. These beams were kept under load for two weeks to allow the epoxy adhesive to cure. No anchorage arrangement was used. All the beams failed in flexural crushing and no separation of the plates was observed. Figure 30 and Figure 31 show the load-deflection curves of beams of series II and series III respectively.

1. The load-deflection curves for all the three series of beams were drawn. Comparison of the load deflection curves of the plated beams showed that this technique can be used to strengthen the structures which are pre-cracked. Comparison of the load-deflection curves of beams of series II and beam F11 showed that all the beams showed almost identical behaviour. Load-deflection curves of beams of series III and F11 were compared and it was noticed that beam F11 had only slightly higher ultimate loads but almost same stiffness as that of the beams of series III. Series III beams gave more deflection because of the creeping effect due to sustained loading of two weeks. So, it was concluded that this

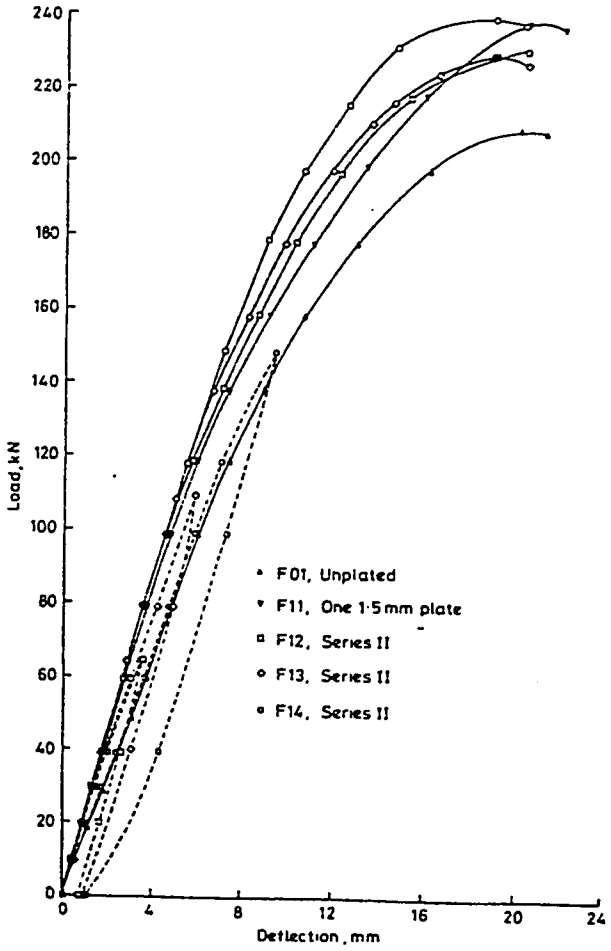

Figure 30: Load-deflection curves of beams of series II (F12, F13 and F14). These beams were strengthened after unloading.

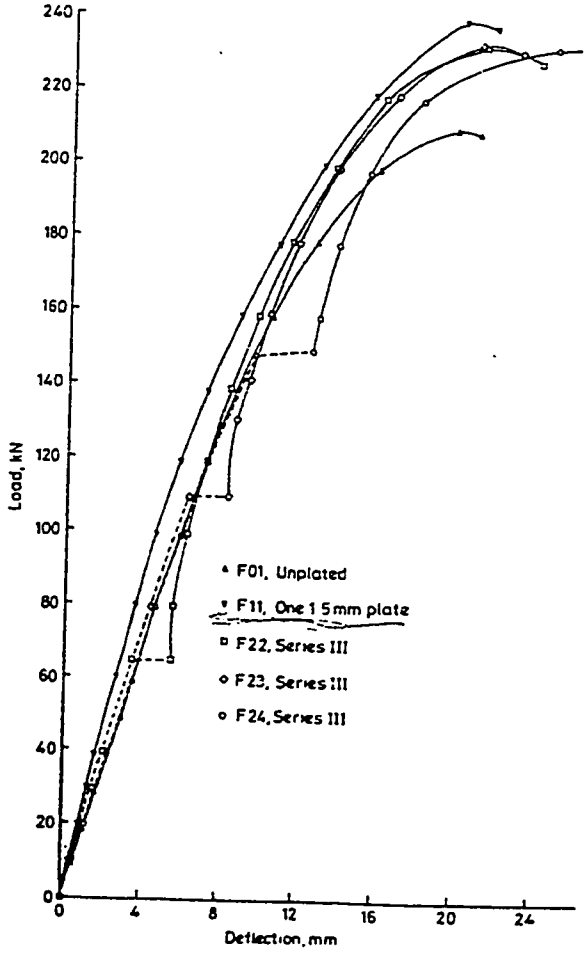

Figure 31: Load-deflection curves of beams of series III (F22, F23 and F24). These beams were strengthened in loaded state.

technique can be used to strengthen the damaged structures while under load.

2. Strain distributions over the depth of the concrete beams for all the three series of beams at crack load, service load and ultimate loads were drawn and it was noticed that the strain distribution diagram maintain reasonable linearity upto ultimate load justifying the assumption that plane section remain plane on which all elastic and failure models depend, that is, basic laws of mechanics can be applied to plated concrete beams. But the selection of appropriate glue is very important for this assumption to hold.

3. Load vs mean crack width at the level of the main steel were drawn for beams F01, F02, F11, F14 and F24. It was noticed that the bonded plates control crack width effectively in structurally damaged RC beams strengthened in the loaded and unloaded state.

2.10 REFERENCE 20

In 1989, T. M. Roberts [20] provided a simple, approximate procedure for predicting the shear and normal stress concentrations in the adhesive layer of the plated reinforced concrete beams. Robert performed the analysis in three stages. During the first stage stresses were determined assuming full composite action between reinforced concrete beam and epoxy bonded steel plate. During the second and third stages the analysis was modified to take into account the actual boundary conditions at the end of the steel plate. The complete solution was obtained by superposition. The solutions for shear and normal stress were sim-

plified and the simplified expressions for shear and normal stresses at the end of the plate are given below.

The shear stress at the ends of the plate at interface is given by the following expression.

$$\tau_0 = [F_0 + (\frac{K_s}{E_p b_p d_p})^{1/2} M_0] \frac{b_p d_p}{I b_a} (h_p - h) \quad (4)$$

The normal stress at the ends of the plate is given by the following expression.

$$\sigma_0 = \tau_0 d_p (\frac{K_n}{4 E_p I_p})^{1/4} \quad (5)$$

Where F_0 is the global shear force in the beam at the terminate end of the plate. E_p is the elastic modulus of the steel plate. M_0 is the global bending moment at the terminate end of the plate. I is the moment of inertia of fully composite transformed steel section. K_s is the shear stiffness of the glue per unit length, K_n is the normal stiffness of the glue per unit length The other terms in the equations (4) and (5) are explained with the help of Figure 32

Where b_p and d_p denotes the width and depth of steel plate. Similarly, b_c and d_c denote width and depth of concrete beam. b_a, is the width of the glue layer. h_s and h_p are the effective depths of conventional reinforcement and the external plate reinforcement. A_s is the area of the conventional steel reinforcement. The equations (4) and (5) under estimates the shear and normal stresses upto 30 %. It was suggested, therefore, that wherever M_0 appears in the solution, it should be replaced by M^* which is the value of the global bending moment evaluated at

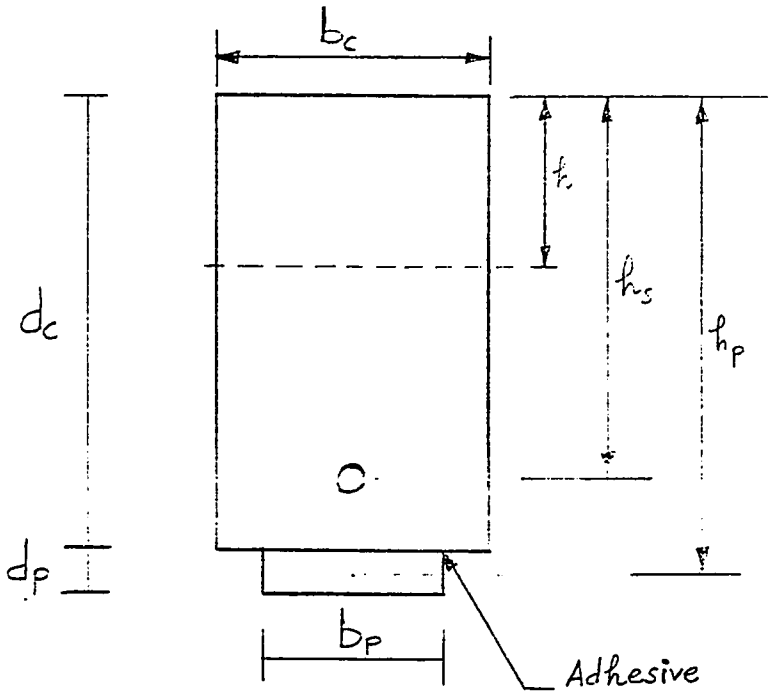

Figure 32: Cross-sectional view of a plated beam.

a distance $x = \frac{(d_c + d_p)}{2}$ from the end of the steel plate. This modification resulted in satisfactory correlation with the solutions based on the partial interaction theory.

2.11 REFERENCE 32

In 1990 Sadaatmanesh and Ehsan [32] reported the test results of five beams. One beam was kept unplated and is called control beam. All the beams were of the size 3.5 in. × 6 in. × 66 in. Four of these beams were bonded with GFRP plates of width and thickness of 3 inch and 1/4 inch respectively. These four beams were designated as A, B, C and D. In these four beams different epoxies were used for bonding. The epoxy glue used for beam A was very flexible. The epoxy glue used for beam B was stiffer than that for beam A. The epoxy glue used for beam C was stiffer than that for beam B. The epoxy glue used for beam D was stiffer than that for beam C. All the beams were tested simply supported over a clear span of 60 inches with two loads symmetrically placed about the mid-span. The test results of these beams are discussed here briefly.

2.11.1 DEFORMATIONAL BEHAVIOUR

Load-deflection curves for all the beams were drawn and their behaviour was studied.

1. Beam A showed marginally higher initial stiffness as compared to control beam. Because the epoxy was very flexible to transfer shear between plate and concrete beam, therefore, no improvement in ultimate strength was obtained.

2. The increase in the stiffness of the beam B was more than that of beam A. Large shear cracks appeared and failure was imminent so the beam was unloaded and C-clamps were used to increase the shear strength. The beam was reloaded till failure. The failure took place due to separation of plate at the bondline because in the first cycle of loading bondline was damaged due to shear cracks.

3. C-clamps were used to prevent premature shear failure. Beam C showed more stiffness than that of the control beam. Epoxy C performed very well and no bond failure occurred throughout the entire range of loading. Failure occurred due to tearing of concrete above the bondline.

4. This beam was strengthened by using the most rigid epoxy among the four. In this case the failure occurred after cracking of concrete in tension due to separation of plate with a shatter sound. The failure was at bondline, that is, in the epoxy layer.

It was concluded that

1. GFRP plates can increase the strength of concrete beams provided the plates are bonded to the concrete beam with a suitable glue.

2. The selection of epoxy, in strengthening the beams successfully , is very important. The epoxy should have sufficient strength and stiffness to transfer the shear force between the plate and the concrete beam. It should be tough enough to prevent bondline failure due to the cracking of concrete as was observed in the beam D.

Chapter III

EXPERIMENTAL PROGRAM

(FLEXURE PART)

3.1 PREPARATION OF BEAMS

The experimental program consisted of two series of beams and named as Series-B and Series-MF beams. The beams of both series were designed such that they would fail in flexure under four point loading in the loading set up which will be explained later. The shear strength of these beams was more than the flexure strength. The beams of both series were 150 by 150 mm in cross-section and 1250 mm in length. However, there were some differences in the reinforcement and in the material properties of the beams of the two series.

3.1.1 BEAMS OF SERIES-B

The casting of these beams was done in the yards of Al-Moraba contracting and construction company. Cylinders of 150 mm dia. and of 300 mm length were also cast for finding the strength of the concrete. The curing of the beams and cylinders was done for 28 days under gunny bags by sprinkinlg water over them intermittantly. The average cylinder strength of concrete for these beams was found to be 31 MPa. These beams were reinforced with two 10 mm dia. steel bars at the bottom as longitudinal reinforcement. U-Stirrups of 6 mm dia. bars were also provided at 60 mm centre to centre throughout the length of the

beams. The clear cover from all sides to the stirrups was 30 mm. Figure 33 shows the reinforcement detail of beams of series B.

The yield strength of the rebars was 414 MPa. However, actual stress strain curve was used for calculating the ultimate flexural strength of the beams. The elastic modulus of the rebar steel is 200,000 MPa.

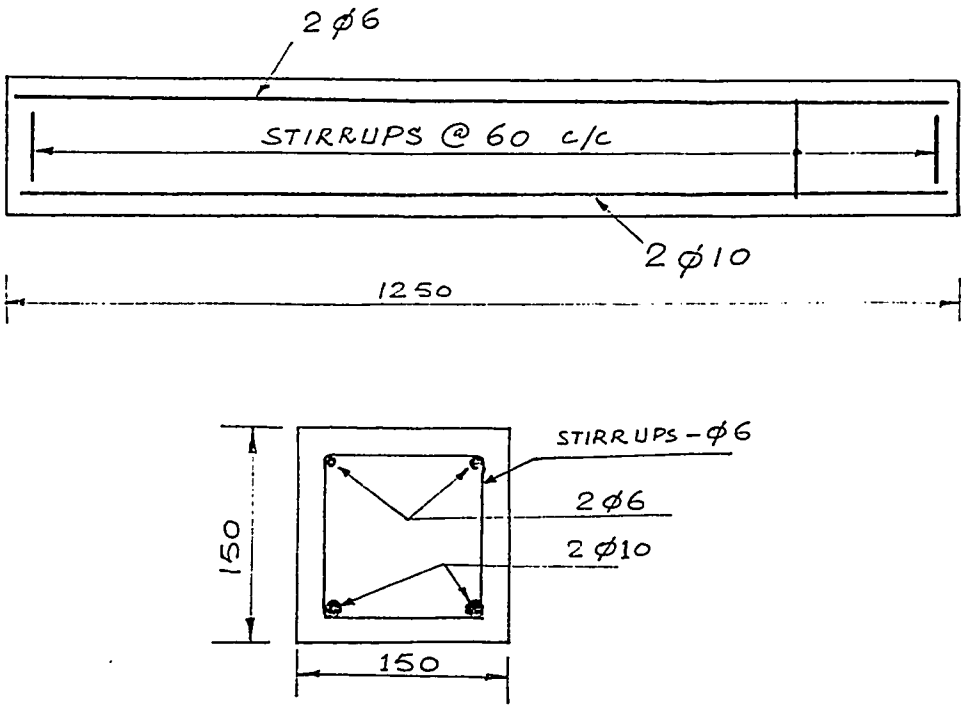

Figure 33: Reinforcement detail of beams of Series-B

3.1.2 BEAMS OF SERIES-MF

The casting of these beams was done in the Ferrocement laboratory of KFUPM. Cylinders of 150 mm dia. and of 300 mm length were also cast for finding the cylinder strength of the concrete. Curing of Beams and Cylinders was done for 28 days under gunny bags by sprinkling water over them intermittantly. The average cylinder strength of the concrete was found to be equal to 39.5 MPa. Two 12 mm dia. bars were provided at the bottom as main steel. The 6 mm dia. U-stirrups were provided at 60 mm centre to centre throughout the length of the beams. The clear cover to the main steel was 30 mm. Figure 34

The yield strength of the rebar steel was 414 MPa. However, actual stress strain curve of the rebar steel was used for finding the ultimate flexural strength of the beams. The elastic modulus of the rebar steel was 200,000 MPa.

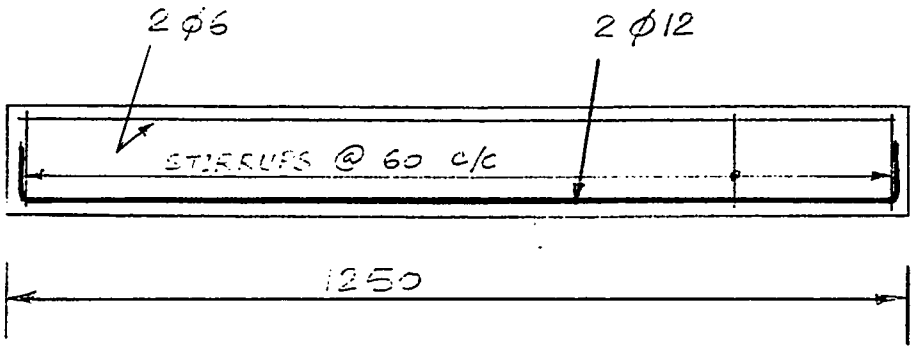

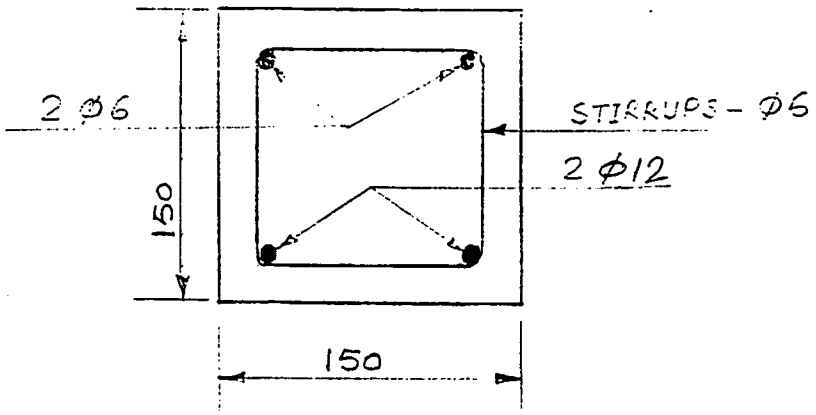

Figure 34: Reinforcement detail of beams of MF-series.

3.2 DAMAGING OF BEAMS

For this purpose all the beams of both series were marked at supports, at mid-span and at third points to facilitate the placing of supports, distribution beam and LVDTs (Linear Variable Differential Transformer). The beams were damaged under four point loading. Two point loads were applied at the ends of the middle third and reactions were set at 25 mm from the ends of the beam. Figure 35 shows the marking of beams and detail of loading setup. For loading 25 tons capacity INSTRON machine was used. The beams were loaded upto 10 mm central deflection and then the load was gradually released. The rate of loading and unloading was kept 1 mm per minute. The crack widths were measured at the level of main steel at various load levels. The load vs central deflection curve for damaging a typical beam of Series-B is given in the Figure 36 . Similarly the beams of MF-series were also damaged. Table 6 shows the maximum load obtained during damaging process and the residual deflections after unloading for beams of both series. From residual deflection, the level of damage given to the beams can be assessed.

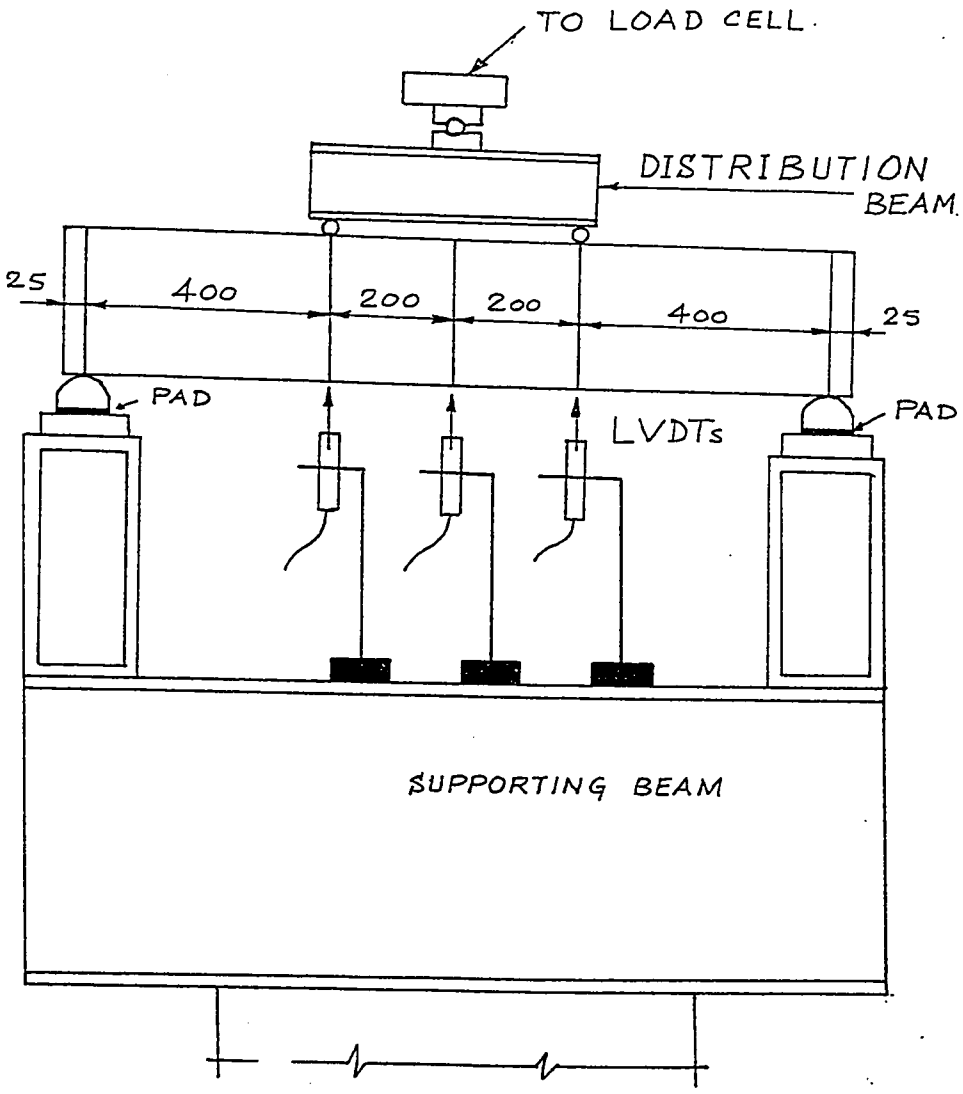

Figure 35: Beam Marking and Loading Setup. 25 Tons INSTRON machine was used for loading

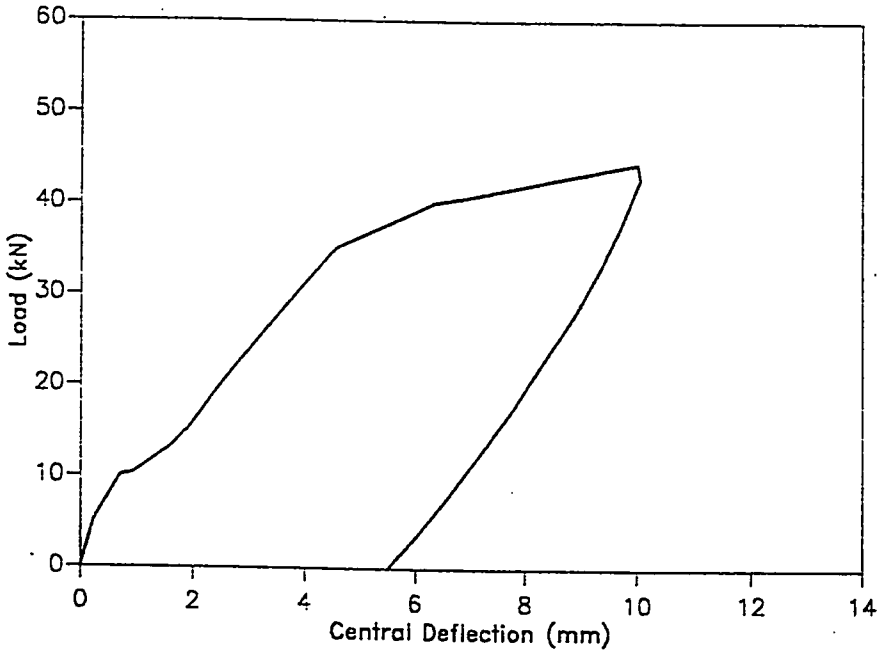

Figure 36: Load vs central deflection. The loading was done upto 10 mm central deflection and then the load was gradually removed.

Table 6: Table showing the extent of damage in flexure

Beam ID.	Maximum Load (kN)	Residual Deflection (mm)
B1	44.370	5.495
B2	46.053	5.434
B3	43.099	5.343
B4	45.192	5.353
B5	44.980	5.768
B6	46.296	5.495
B7	45.035	5.363
B8	42.824	5.485
B9	40.186	5.439
B10	43.922	5.576
B11	45.187	5.267
B12	46.630	5.388
B13	46.015	5.575
B14	44.601	5.474
B15	48.837	5.454
B16	41.694	5.479
B17	48.710	5.540
B18	47.203	5.550
B19	45.474	5.485
B20	44.396	5.292
B21	46.429	5.366
B22	46.938	5.424
B23	46.949	5.302
B24	47.405	5.449
B25	45.529	5.343
MF1	42.427	3.496
MF2	44.974	4.519

3.3 STRENGTHENING OPERATION

After damaging, as mentioned in the previous section, the beams were strengthened by bonding steel plates on the tension faces of the beams. The plates were of mild steel and the yield strength of the steel plates was 269 MPa. The elastic

modulus of the plates was 200000 MPa. In some beams the plates were anchored and in some beams the plates were not anchored. The strengthening of the beams consisted of the following steps:-

1. SAND BLASTING

   Concrete beams and the steel plates were roughened by sand blasting, for proper bonding. In concrete beams sand blasting was done until the exposure of the aggregate. Sand blasting was done only at the bottom faces of the beams.

2. CLEANING

   Sand blasted concrete beams and steel plates were blown with air to make them free from dust. After that steel plates were also cleaned with acid to make them free from grease/oil etc.

3. MIXING OF GLUE

   The adhesive was two part epoxy glue. The two parts were mixed in the ratio (1:2). Hand mixing was done with the help of a stirrer. The mixing was done until the two parts were fully mixed and the paste became homogeneous.

4. BONDING

   The glue was applied at the appropriate places of concrete beams and steel plates with brushes. The glue was spread such that all the area to be bonded was fully wet with the glue. Steel spacers were spread evenly on the freshly glued surface to maintain glueline thickness. The steel plates, already applied with the glue, were laid on the glued concrete beams within appropriate marks. The plates were pressed with the help

of clamps and the excessive glue squeezed out which was cleaned with the help of brushes. The clamps were removed after the curing of the glue. The testing was done after not less than seven days of the gluing operation. The glueline thickness of 1.5 mm was maintained for all the beams. However, the glueline thickness was less accurate for the beams bonded with thinner plates because of the warping of the plates due to sand blasting.

In some beams anchorage to the steel plates was given by bolts. Bolts were installed after curing of the glue under the plates according to the procedure given in the following box.

> The holes were drilled in the beams. The holes were cleaned with tap water and then beams were left in laboratory for some time for drying the holes completely. The procedure for mixing the glue has already been described. The holes were filled with the glue. Glue was also applied on the bolts. Then the bolts were inserted in the holes and pressed. The excessive glue which came out of the hole, was cleaned with brushes. The testing was done after curing of the glue in the holes.

3.4 STRENGTHENING DETAIL OF BEAMS

Table 7 gives the summary of the strengthening detail of the beam. For detail of end anchorage see the corresponding figures showing the strengthening detail of the beams.

Figure 37 through figure 50 give the complete strengthening detail of the beams.

Table 7: Summary of strengthening detail of beams.

Beam ID.	Plate Thick.	layout of anchor bolts	Embed. Length of Bolts	Diameter of anchor Bolts
	(mm)		(mm)	(mm)
B6,B7	unplated	-	-	-
B5,B25	1.00	-	-	-
B10,B17	1.50	-	-	-
B11,B13	1.50	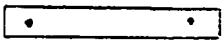	75	12
B14,B16	1.50	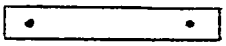	110	12
B21,B24	1.50	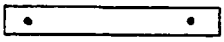	150	12
B19,B23	1.50	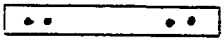	75	12
B15,B22	1.50	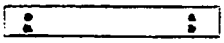	75	12
B8	2.00	-	-	-
B4	2.00	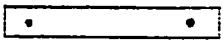	90	12
B1	3.00	-	-	-
B3,B18	1.50	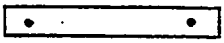	75	12
MF1	3.00	-	-	-
MF2,MF4	3.00	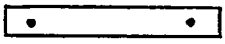	90	15
MF3	2.00	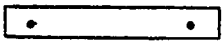	90	15

In beams B3 and B18 the plates were not bonded to the concrete beams. Only end anchorage was given to the plates.

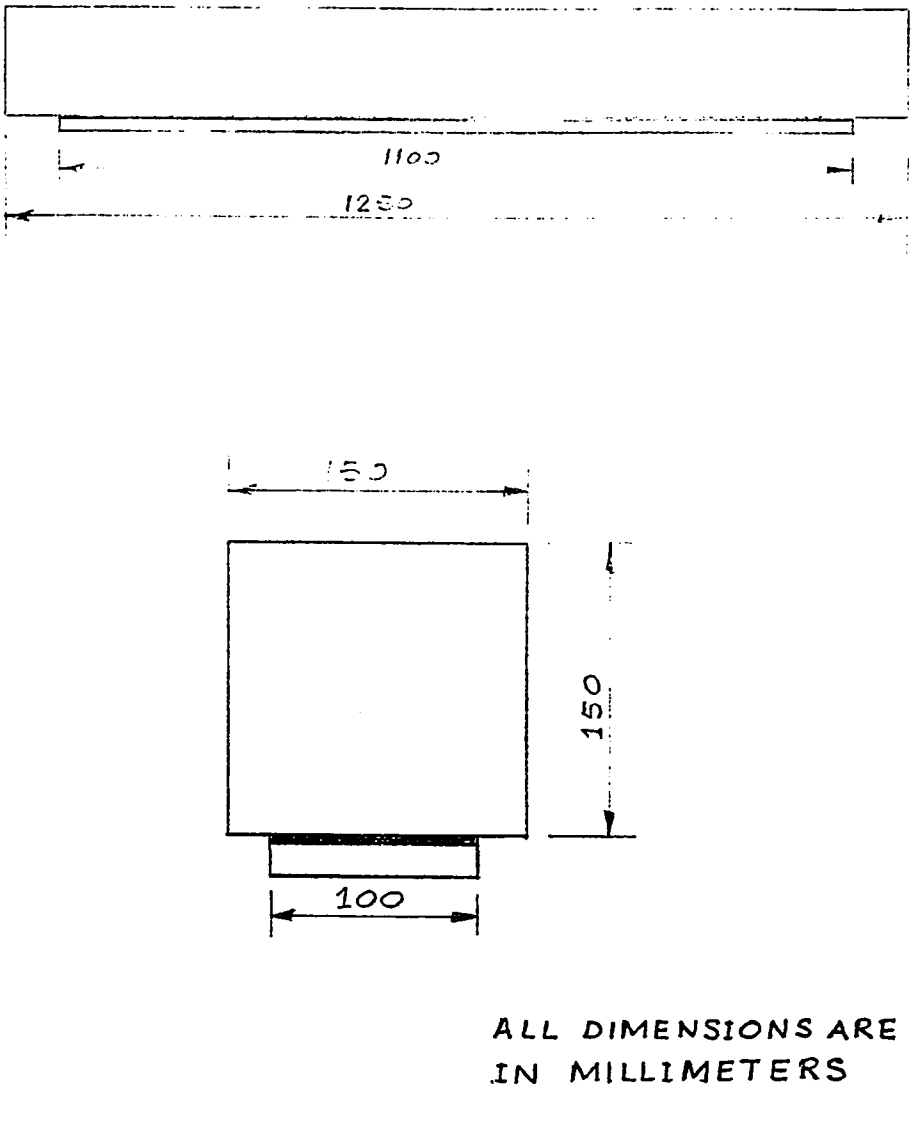

Figure 37: Strengthening detail of beams B5 and B25. These beams were bonded with 1100 mm long, 100 mm wide and 1.00 mm thick steel plates. No end anchorage was given to the steel plates.

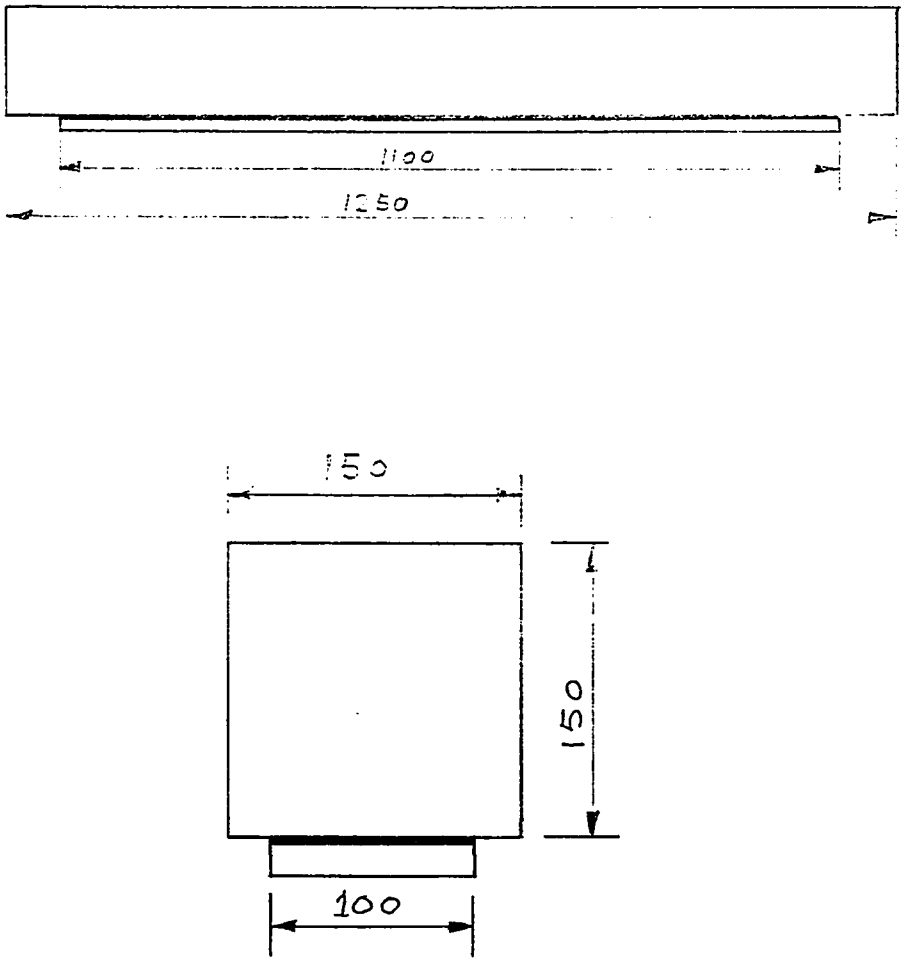

Figure 38: Strengthening detail of beams B10 and B17. These beams were bonded with 1100 mm long, 100 mm wide and 1.5 mm thick steel plates. No end anchorage was given to the plates.

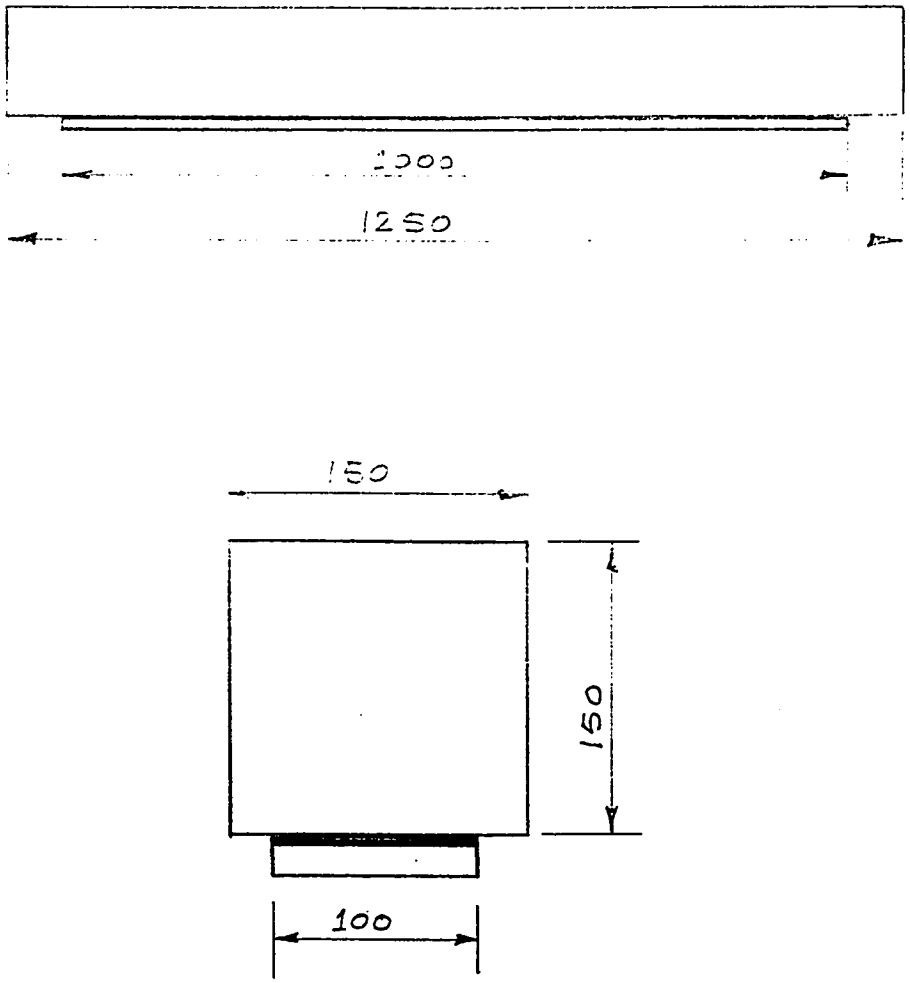

Figure 39: Strengthening detail of beam B8. This beam was bonded with 1000 mm long, 100 mm wide and 2 mm thick steel plate. No end anchorage was given to the steel plate.

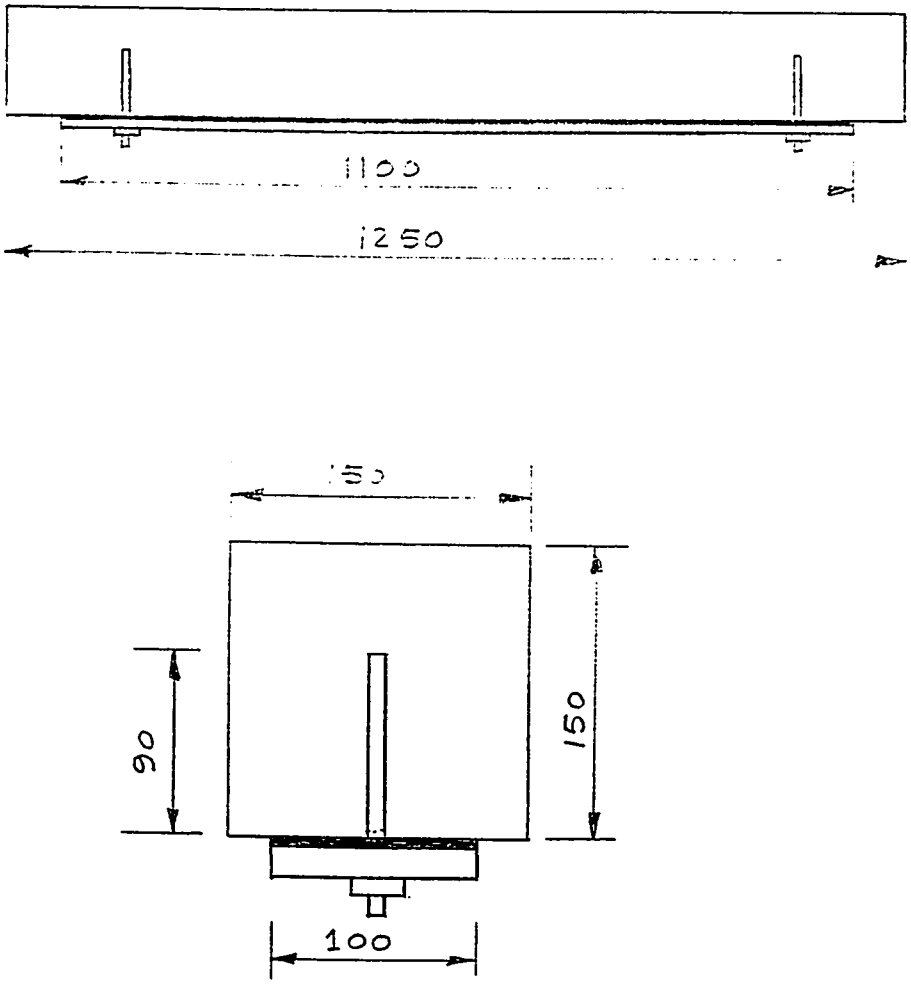

Figure 40: Strengthening detail of beam B4. This beam was bonded with 1100 mm long, 100 mm wide and 2 mm thick steel plate. End anchorage was given to the steel plate by bolts.

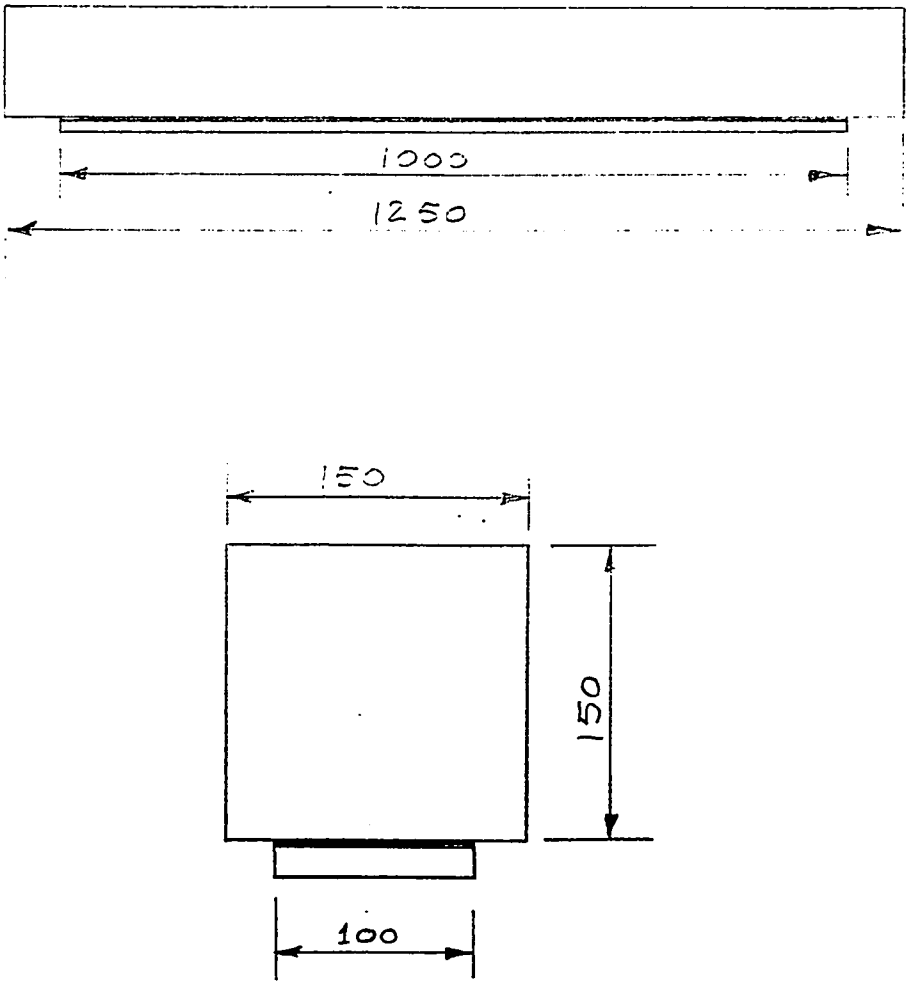

Figure 41: Strengthening detail of beam B1. This beam was bonded with 1000 mm long, 100 mm wide and 3 mm thick steel plate. No end anchorage was given to the steel plate.

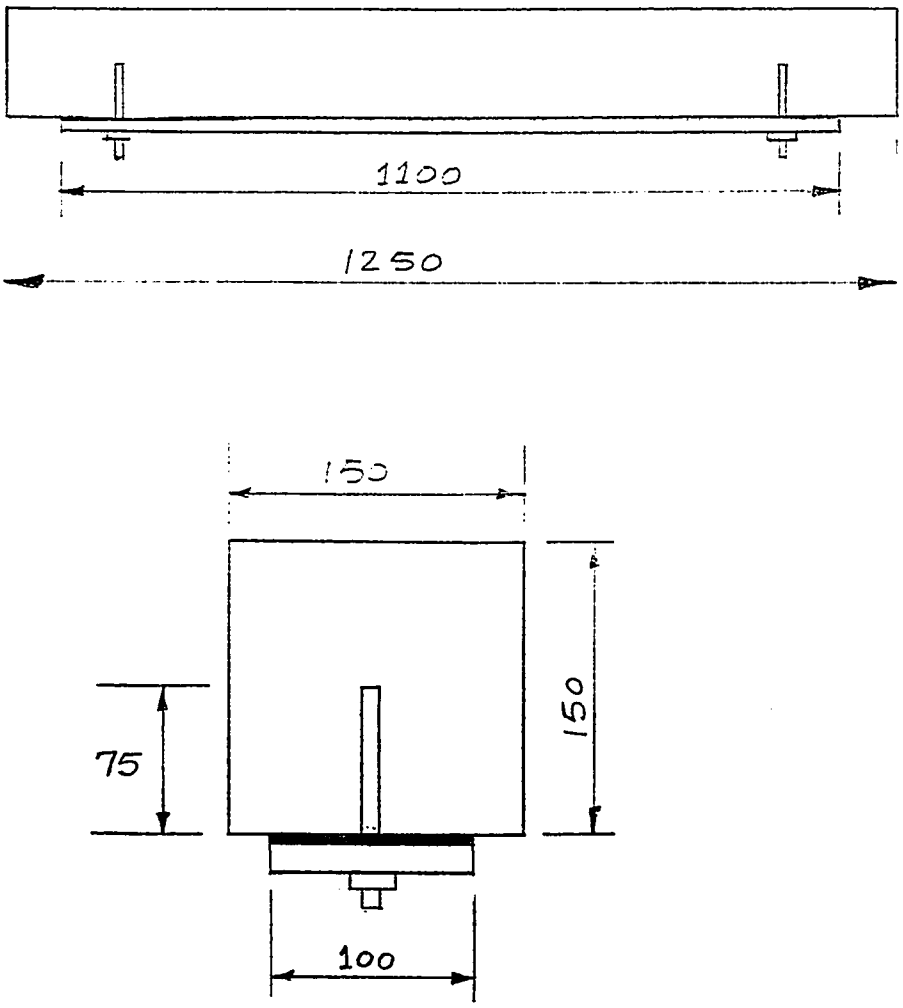

Figure 42: Strengthening detail of beams B11 and B13. These beams were bonded with 1100 mm long, 100 mm wide and 1.5 mm thick steel plates. End anchorage was given to the plates.

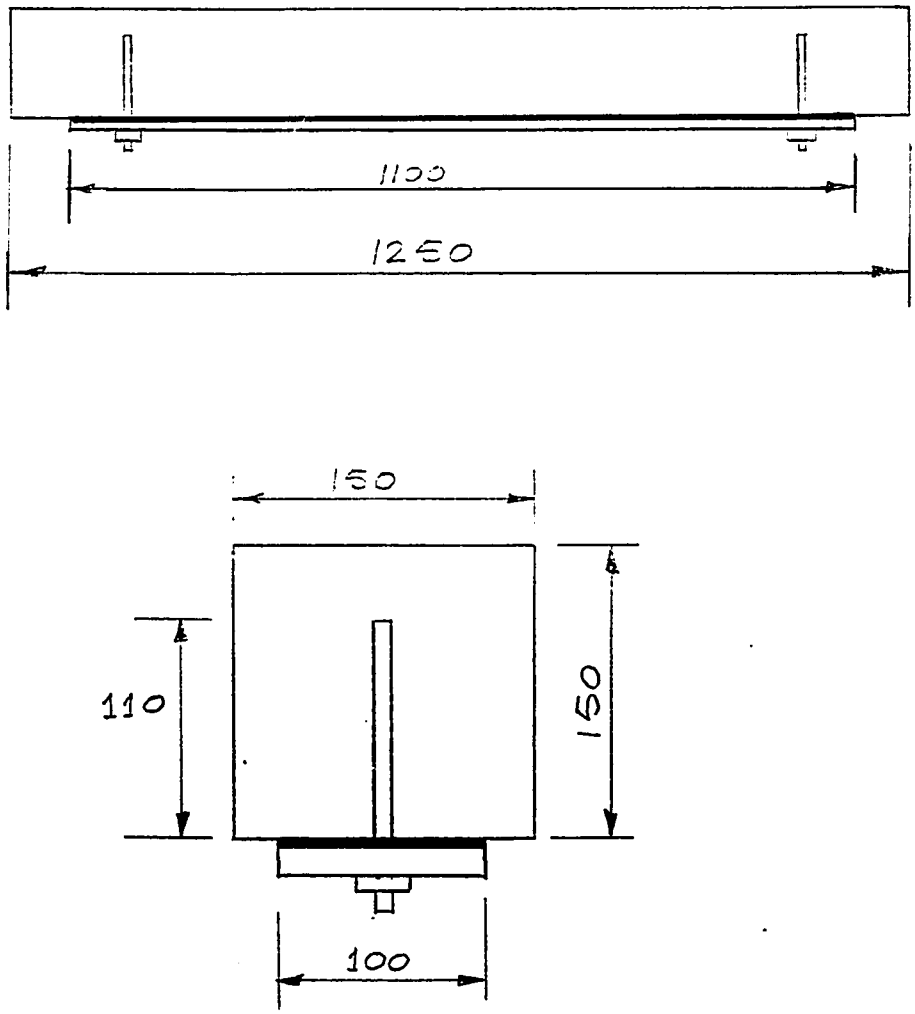

Figure 43: Strengthening detail of beams B14 and B16. These beams were bonded with 1100 mm long, 100 mm wide and 1.5 mm thick steel plates. End anchorage was given to the steel plates.

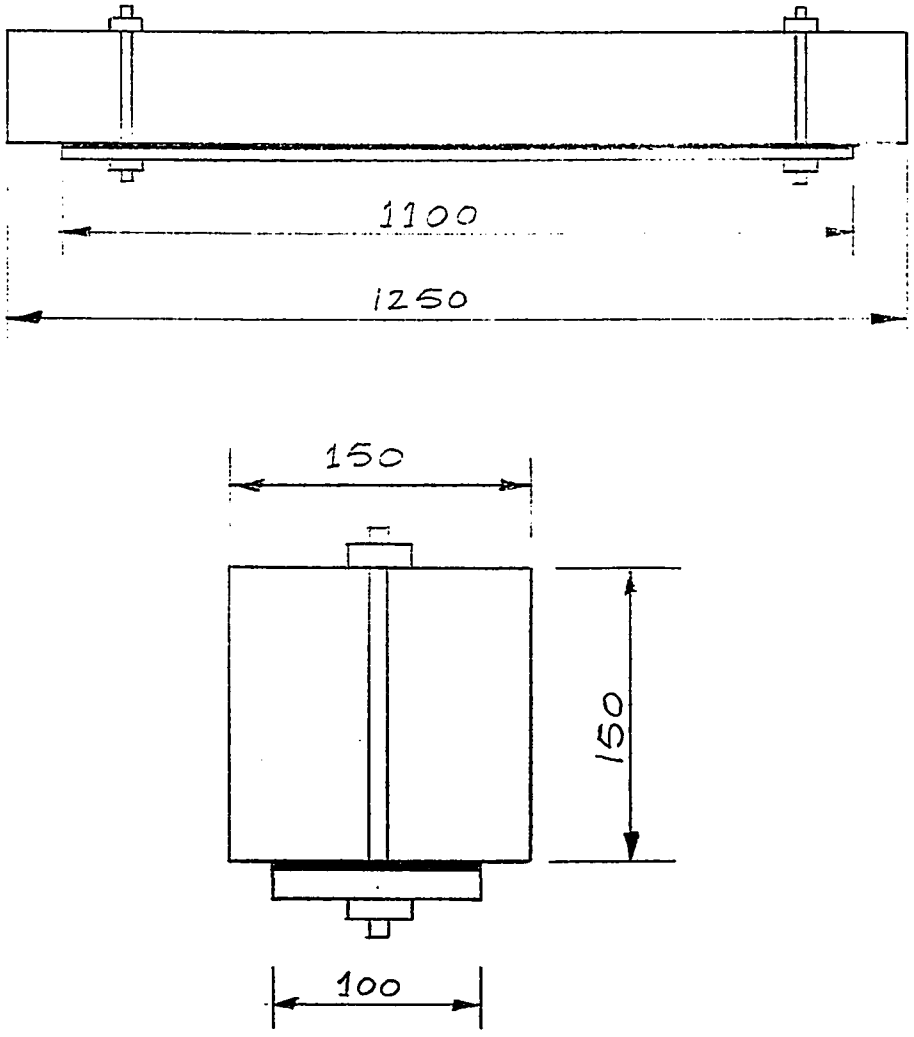

Figure 44: Strengthening detail of beams B21 and B24. These beams were bonded with 1100 mm long, 100 mm wide and 1.5 mm thick steel plates. End anchorage was given to the steel plates.

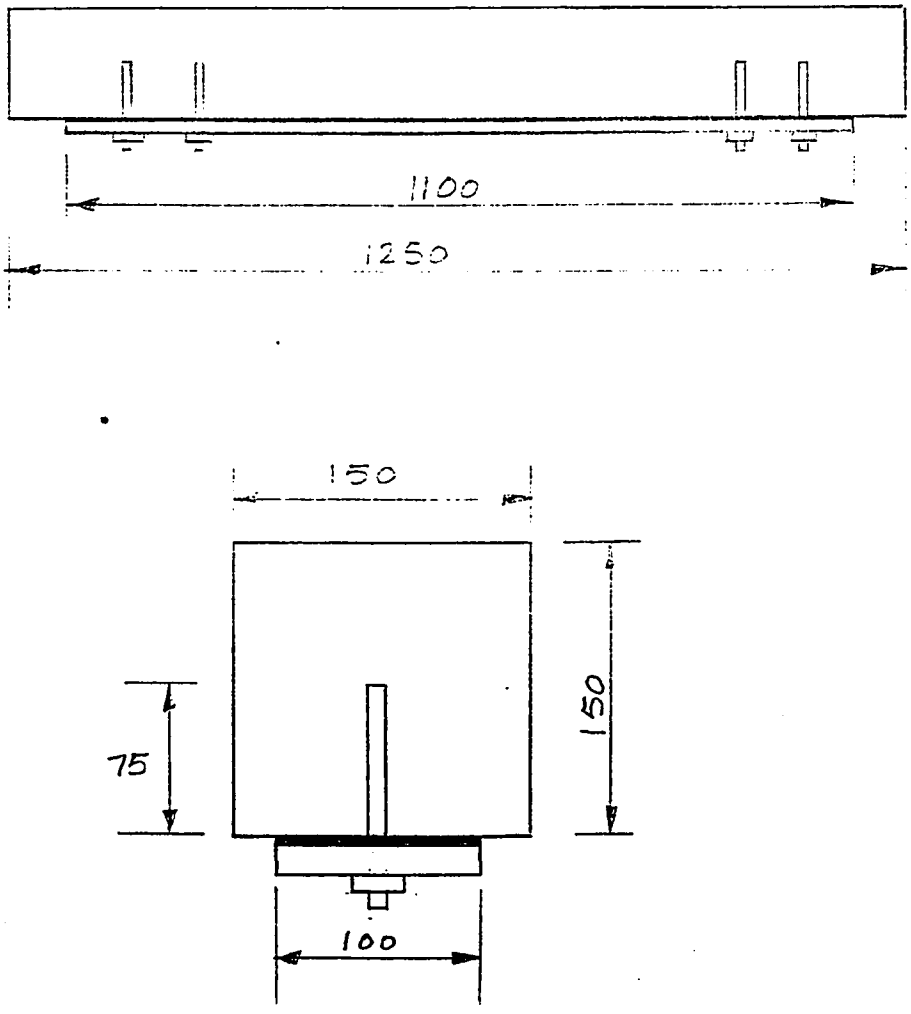

Figure 45: Strengthening detail of beams B19 and B23. These beams were bonded with 1100 mm long, 100 mm wide and 1.5 mm thick steel plates. End anchorage was given to the steel plates.

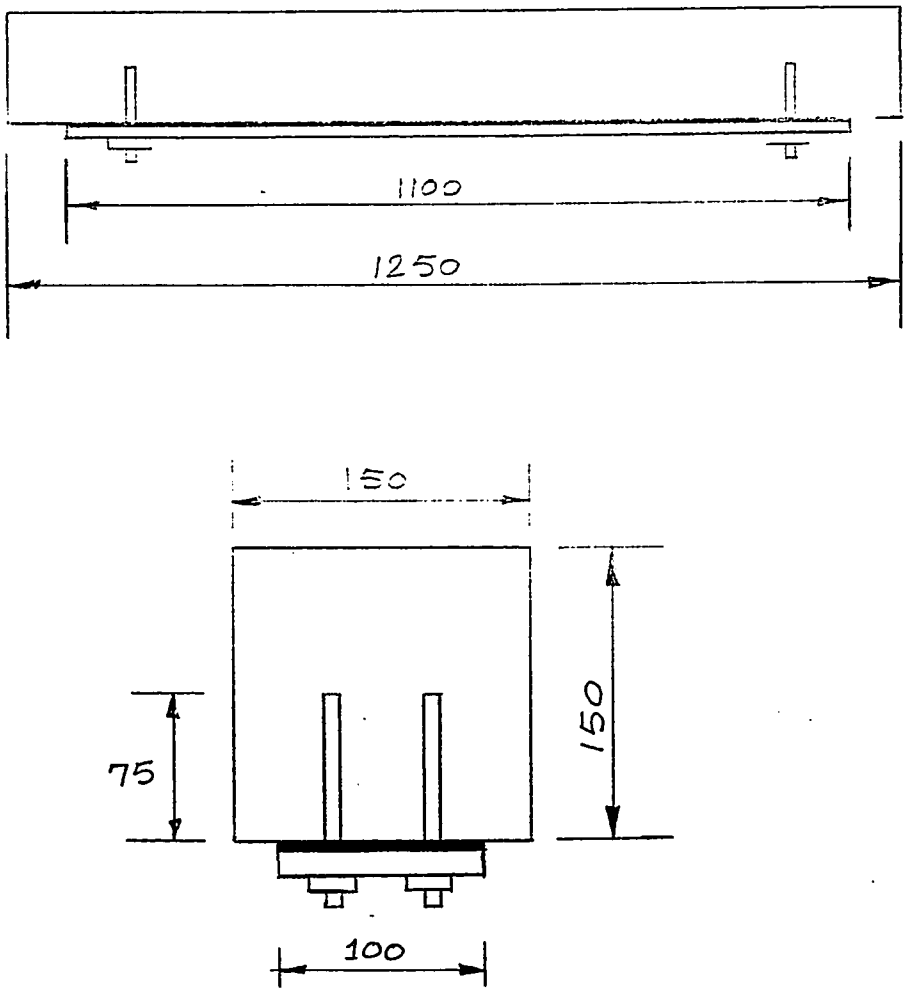

Figure 46: Strengthening detail of beams B15 and B22. These beams were bonded with 1100 mm long, 100 mm wide and 1.5 mm thick steel plates. End anchorage was given to the steel plates.

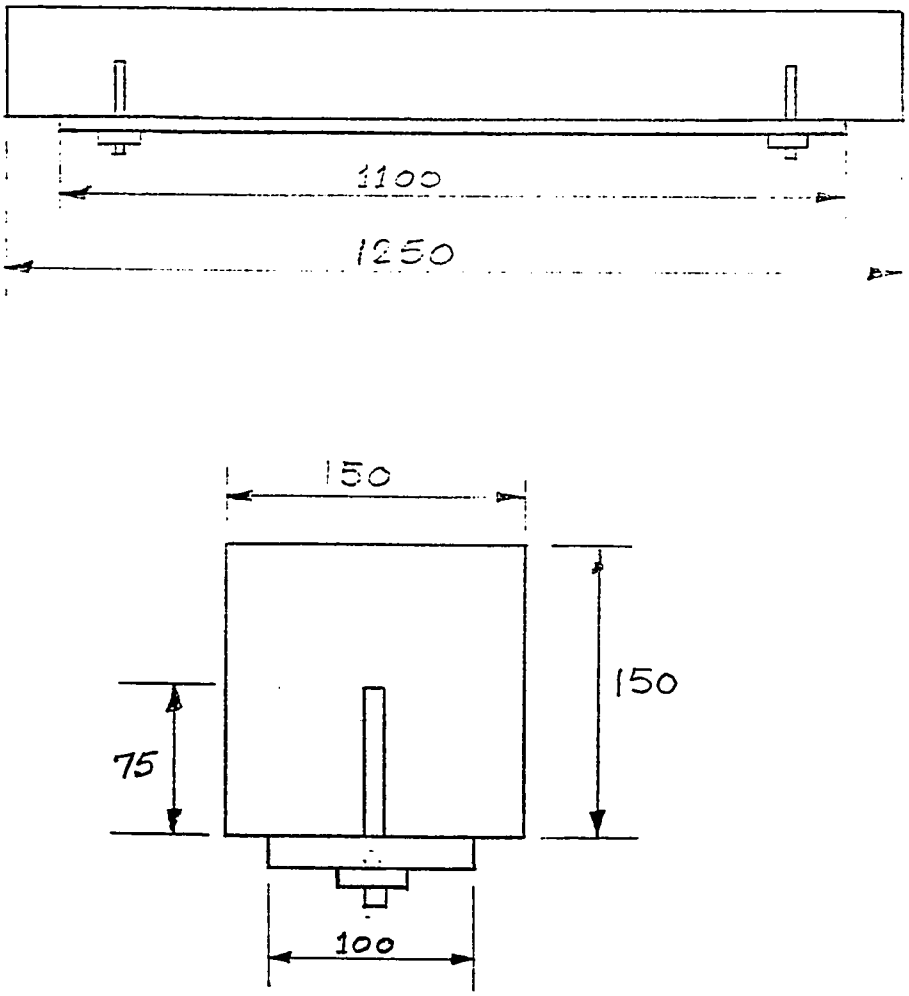

Figure 47: Strengthening detail of beams B3 and B18. These beams were strengthened with 1100 mm long, 100 mm wide and 1.5 mm thick steel plates. The plates were anchored by bolts at ends. These plates were not bonded to the beams.

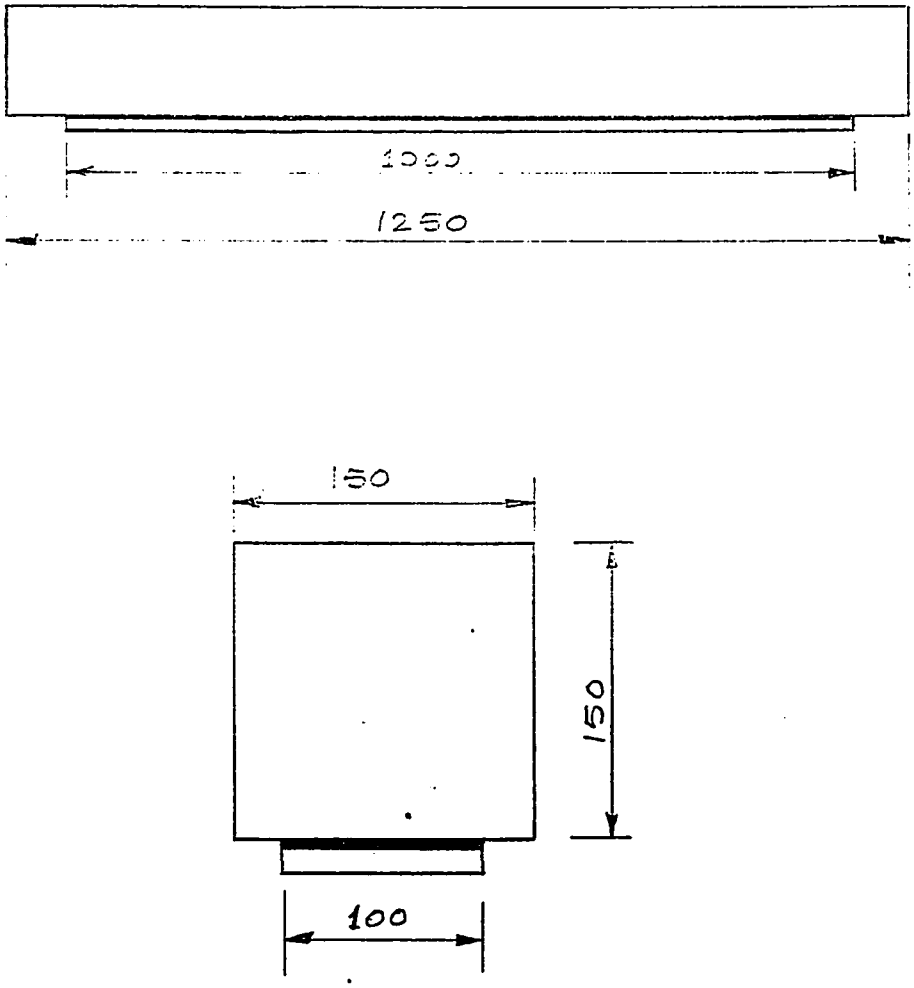

Figure 48: Strengthening detail of beam MF1. This beam was bonded with 1000 mm wide, 100 mm wide and 3 mm thick steel plate. No end anchorage was given to the steel plate.

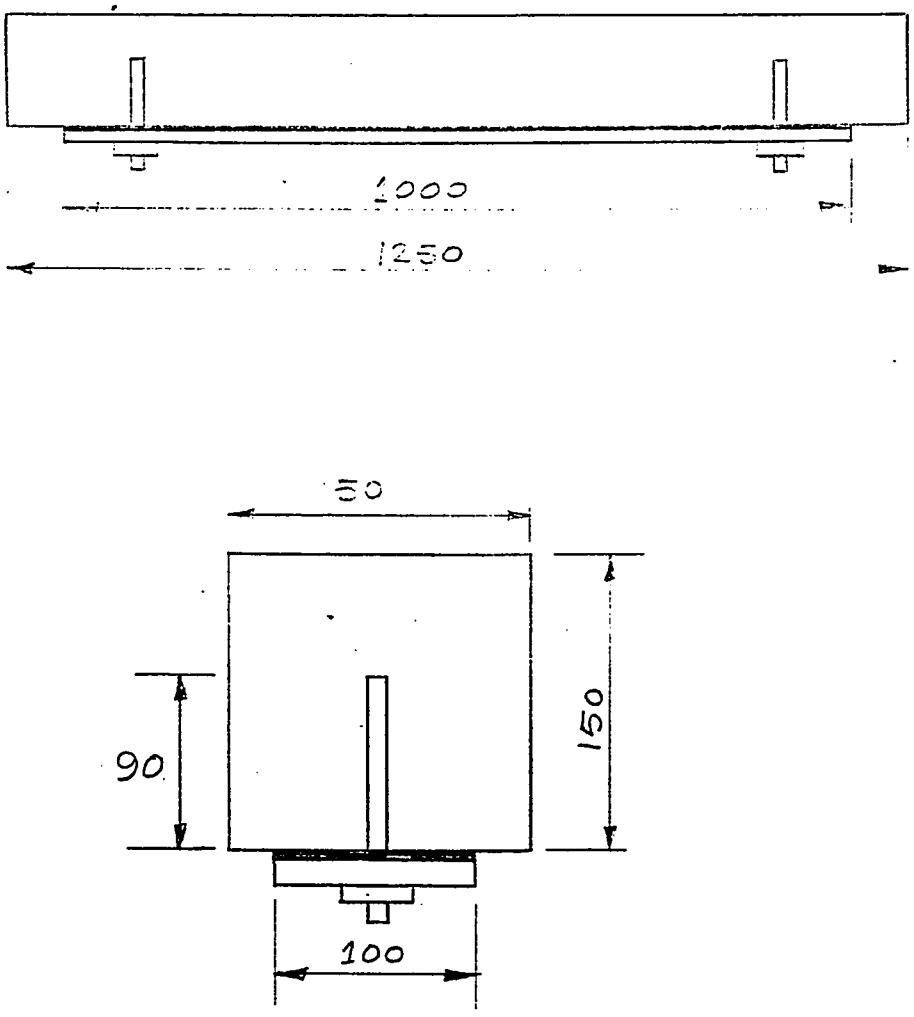

Figure 49: Strengthening detail of beams MF2 and MF4. These beams were bonded with 1000 mm long, 100 mm wide and 3 mm thick steel plates. End anchorage was given to the steel plates.

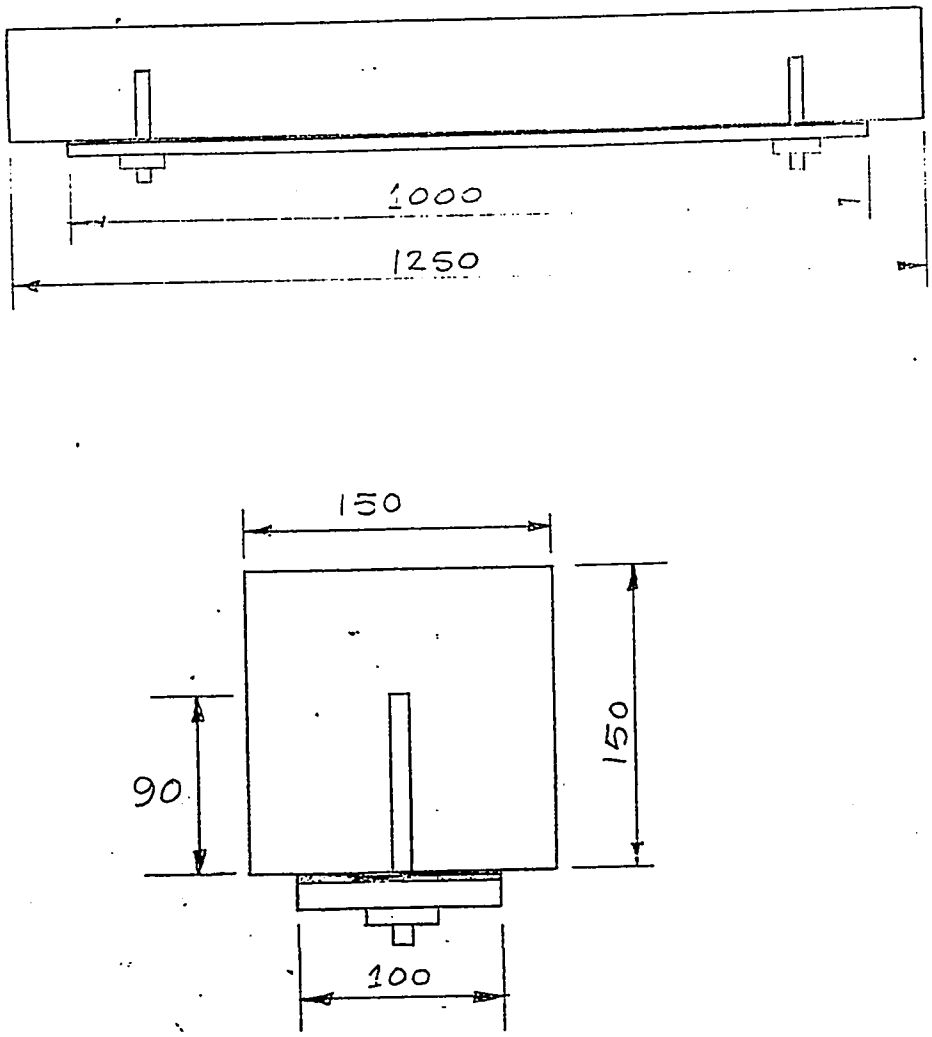

Figure 50: Strengthening detail of beam MF3. This beam was bonded with 1000 mm long, 100 mm wide and 2 mm thick steel plate. End anchorage was given to the steel plate.

3.5 INSTRUMENTATION DETAIL

The instrumentation of all the beams was different. Strain gages were installed according to the requirement on the beams and the bonded plates. In addition to the strain gages on the steel plates and the concrete beams, strain gages were also installed on the anchor bolts and on the internal reinforcement in some beams.

3.6 TESTING OF THE REPAIRED BEAMS

Final testing was done after curing of glue and installation of strain gages at the appropriate locations for measuring strains as discussed in the previous section. The same loading setup was used as that for original loading. The testing was done under four point loading. The loads were applied at the ends of the middle third of the beams and reactions were set at 25 mm from the ends of the beams. The loading was done at the rate of 1 mm per minute. The crack widths were measured at the level of the main reinforcement at various load levels for some beams. All the beams were loaded upto failure. The beam is said to be failed when the load sustained by beam start decreasing. All the calculations regarding, modulus of toughness are based on this criterion of failure.

Chapter IV

PRESENTATION OF TEST RESULTS AND DISCUSSION

(FLEXURE PART)

4.1 DEFORMATIONAL BEHAVIOUR

Figure 51 through Figure 73 show the load delection curves of all the beams. Each figure shows two cycles of loading. The first cycle represents loading of the original beam and the second cycle represents the loading of the repaired beam except for beams B6 and B7. Beams B6 and B7 were reloaded upto ultimate without strengthening.

Table 8 shows the ultimate loads, modulus of toughness and modes of failure of all the beams. The modes of failures will be explained at the end of this chapter. In the second cycle of loading, the beams were loaded upto ultimate. Modulus of toughness is the area under the load deflection curve upto failure. In this table, only the area under the load deflection curve for the second cycle of loading is given. Modulus of toughness represents the energy absorbed by the beams upto failure.

Table 9 gives the flexural rigidity (EI) of all the beams. The slope of the moment curvature diagram is equal to the flexural rigidity of the beams. The moment curvature diagrams for all the beams were drawn. The slope of the moment curvature diagram was changing with increasing load. So the values given in the table are the slopes of the secant line starting from origin and crossing the

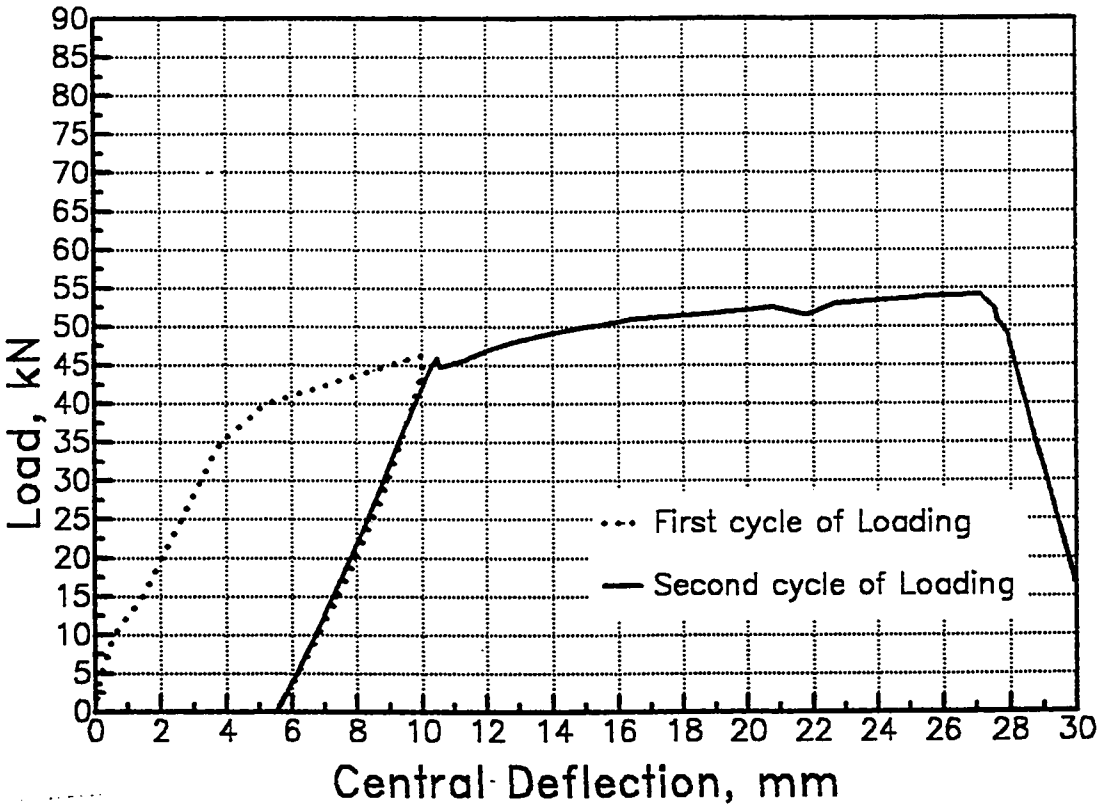

Figure 51: Load vs central deflection for beam B6. This beam was reloaded without strengthening.

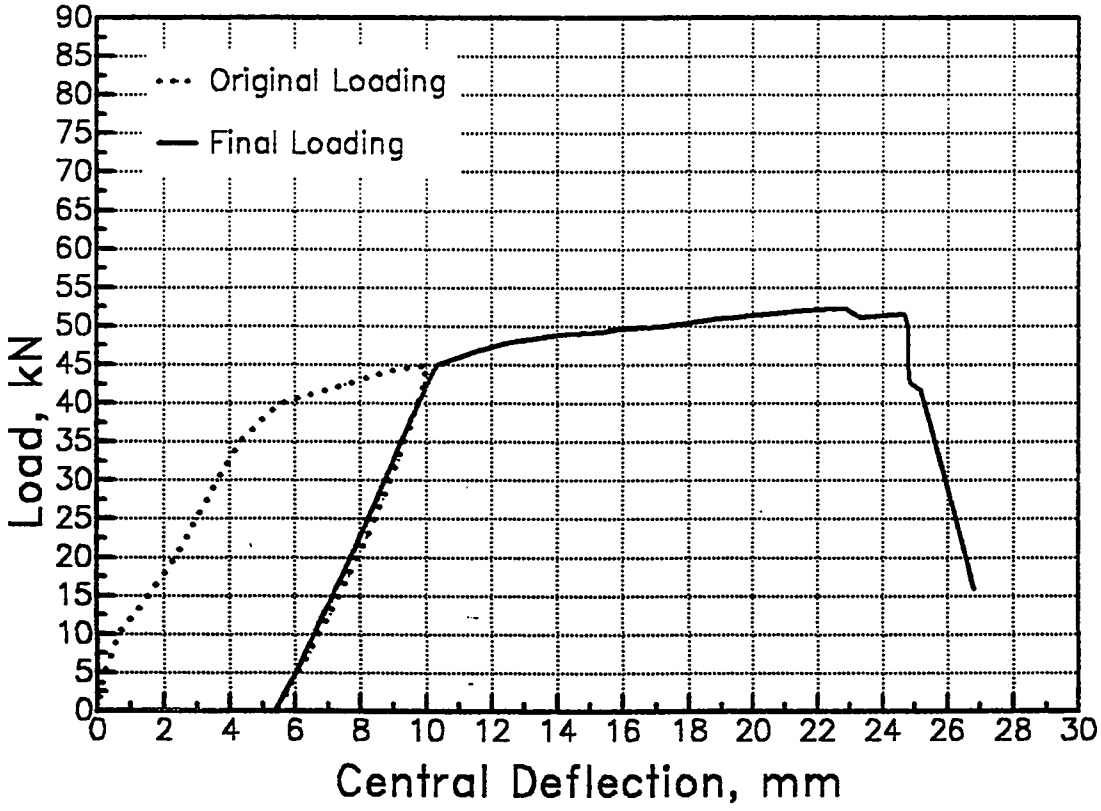

Figure 52: Load vs central deflection for beam B7. This beam was reloaded without strengthening.

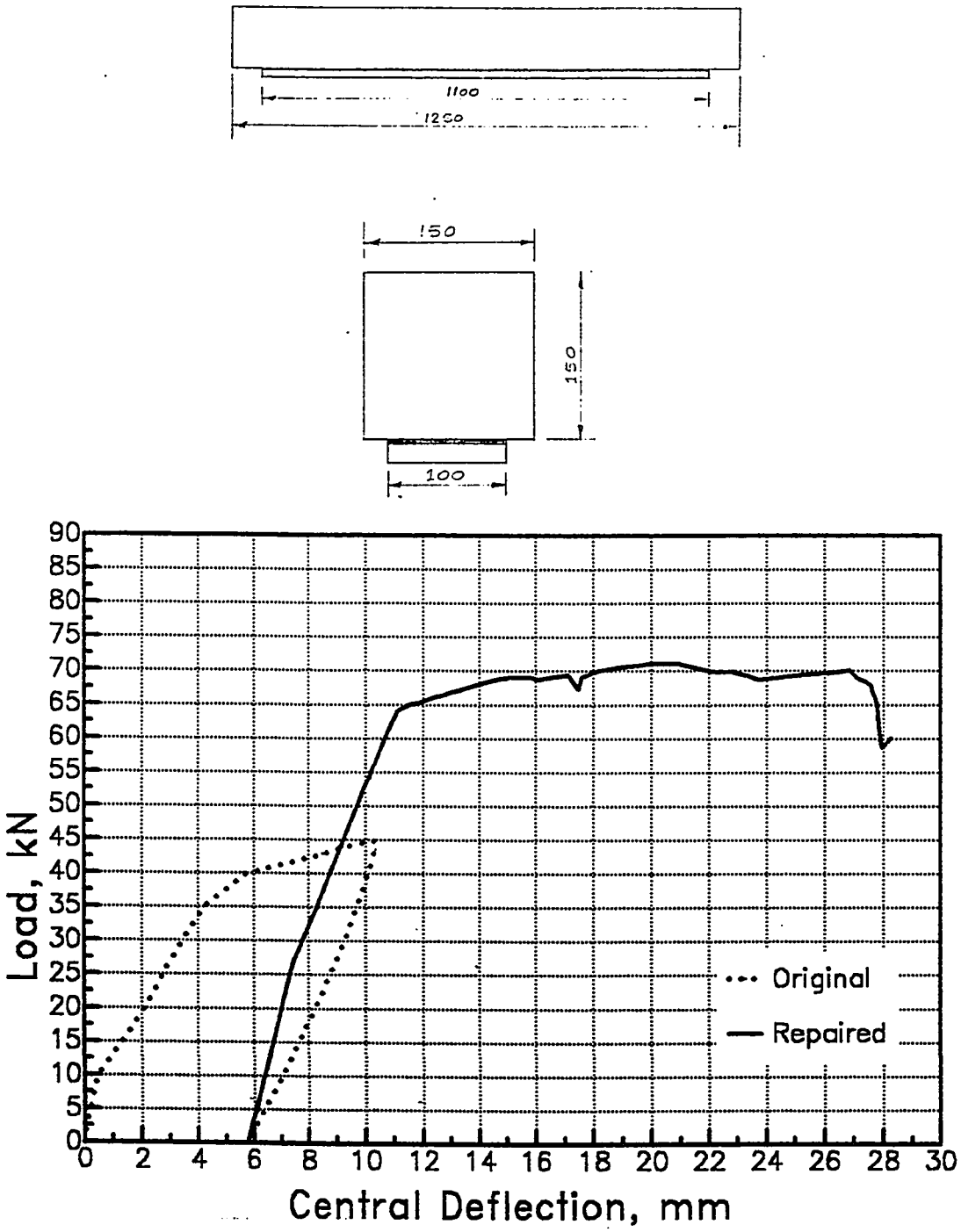

Figure 53: Load vs central deflection for beam B5. This beam was strengthened with 1100 mm long, 100 mm wide and 1.00 mm thick steel plate. No end anchorage was given to the plate.

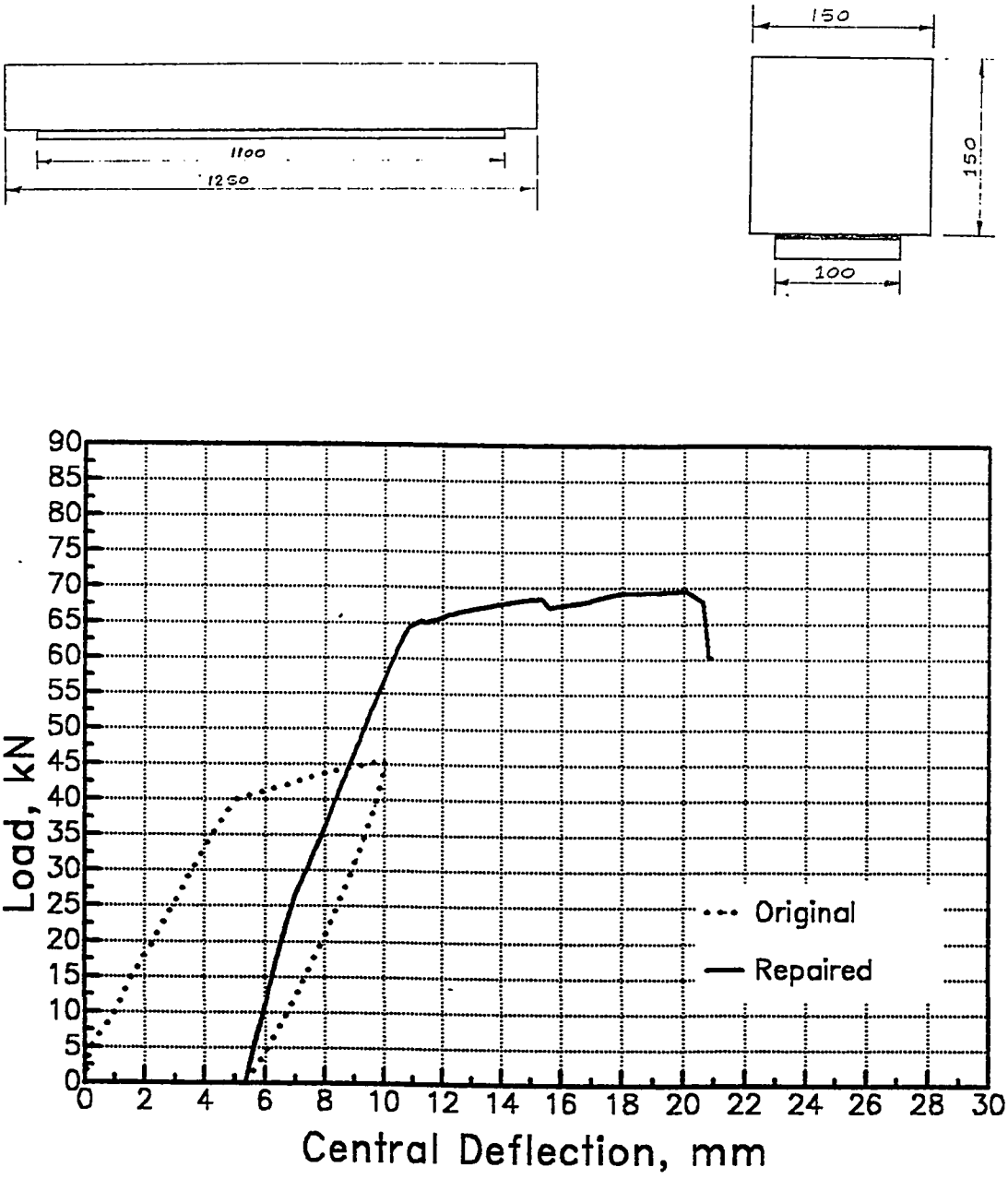

Figure 54: Load vs central deflection for beam B25. This beam was strengthened with 1100 mm long, 100 mm wide and 1.00 thick steel plate. No end anchorage was given to the plate.

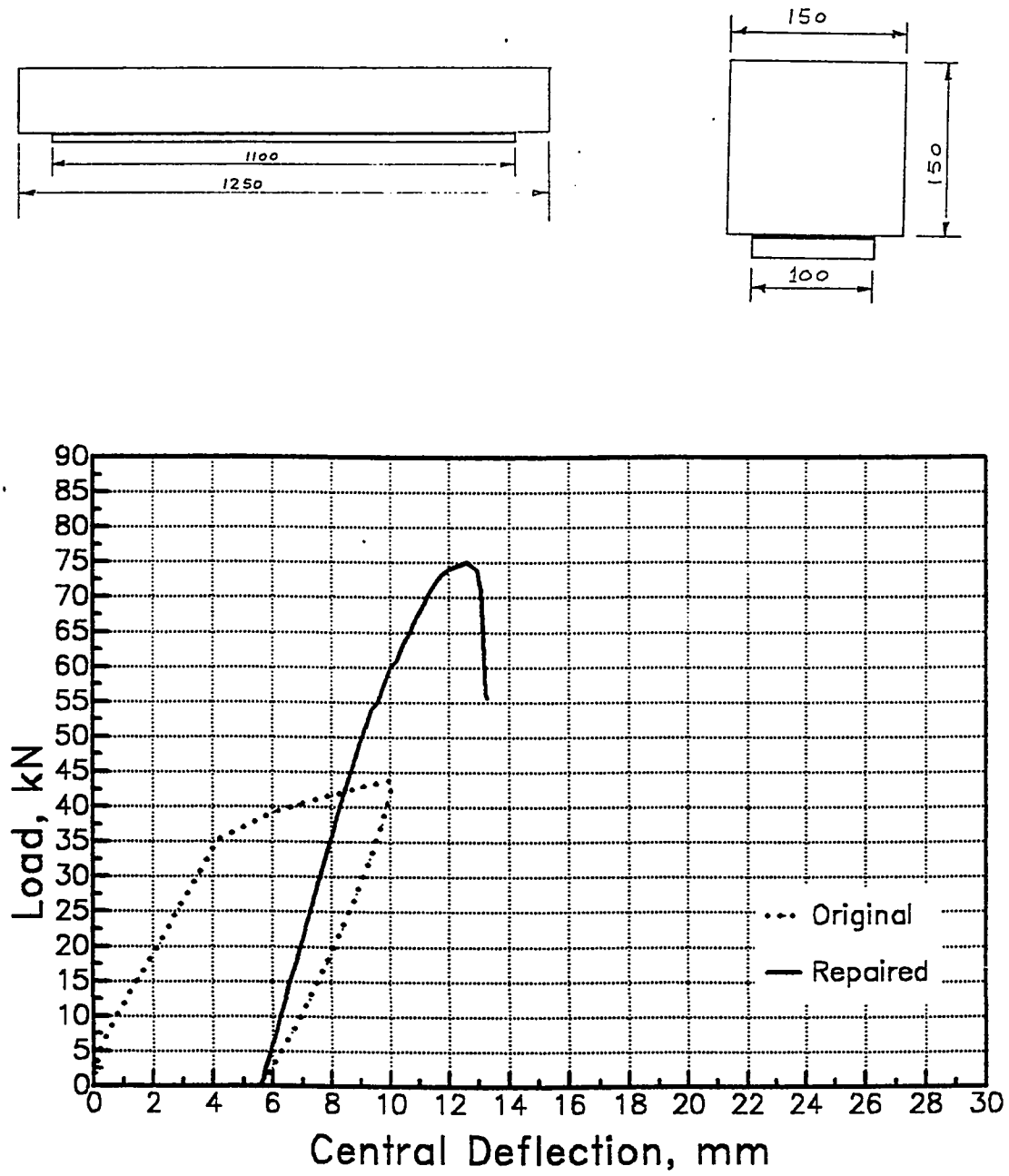

Figure 55: Load vs central deflection for beam B10. This beam was bonded with 1100 mm long, 100 mm wide and 1.50 mm thick steel plate. No end anchorage was given to the plate.

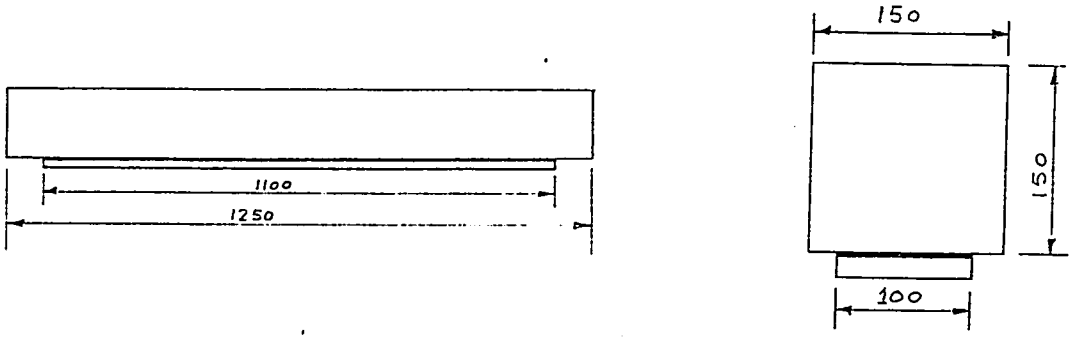

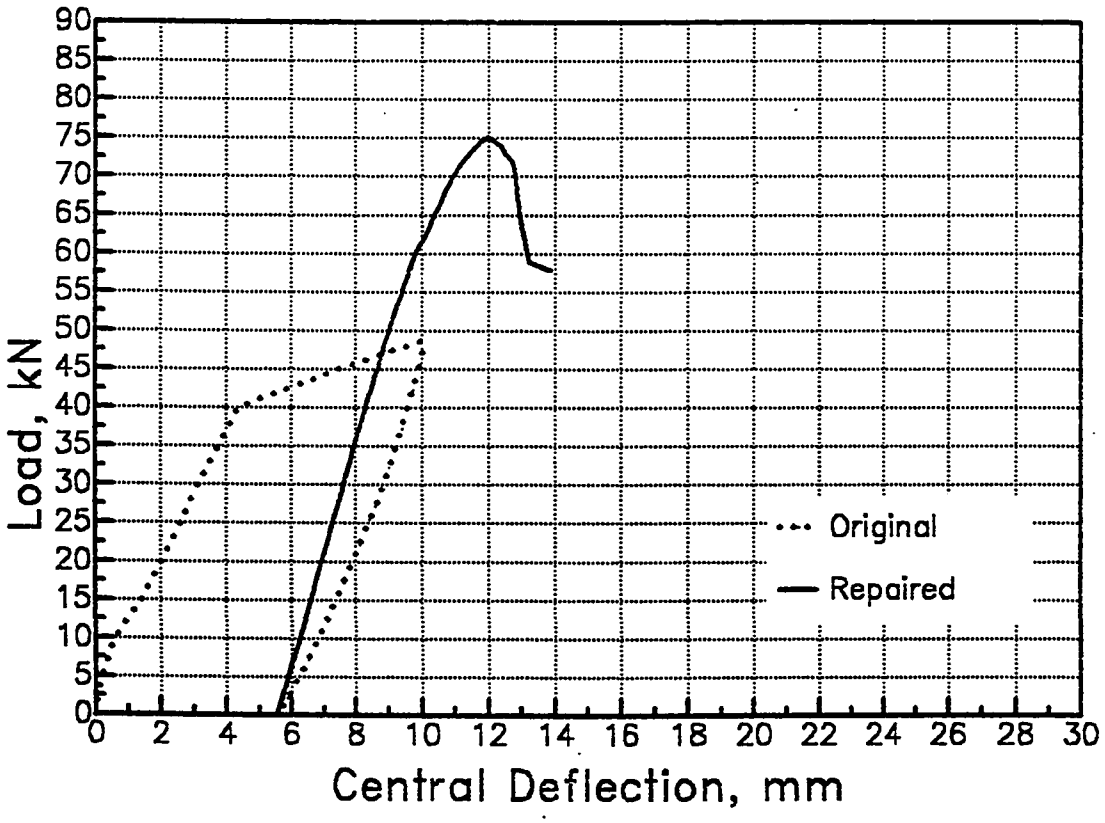

Figure 56: Load vs central deflection for beam B17. This beam was bonded with 1100 mm long, 100 mm wide and 1.50 mm thick steel plate. No end anchorage was given to the plate.

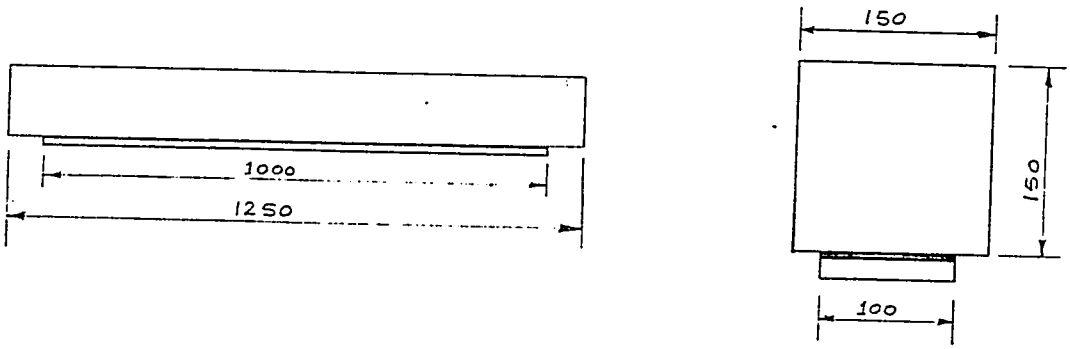

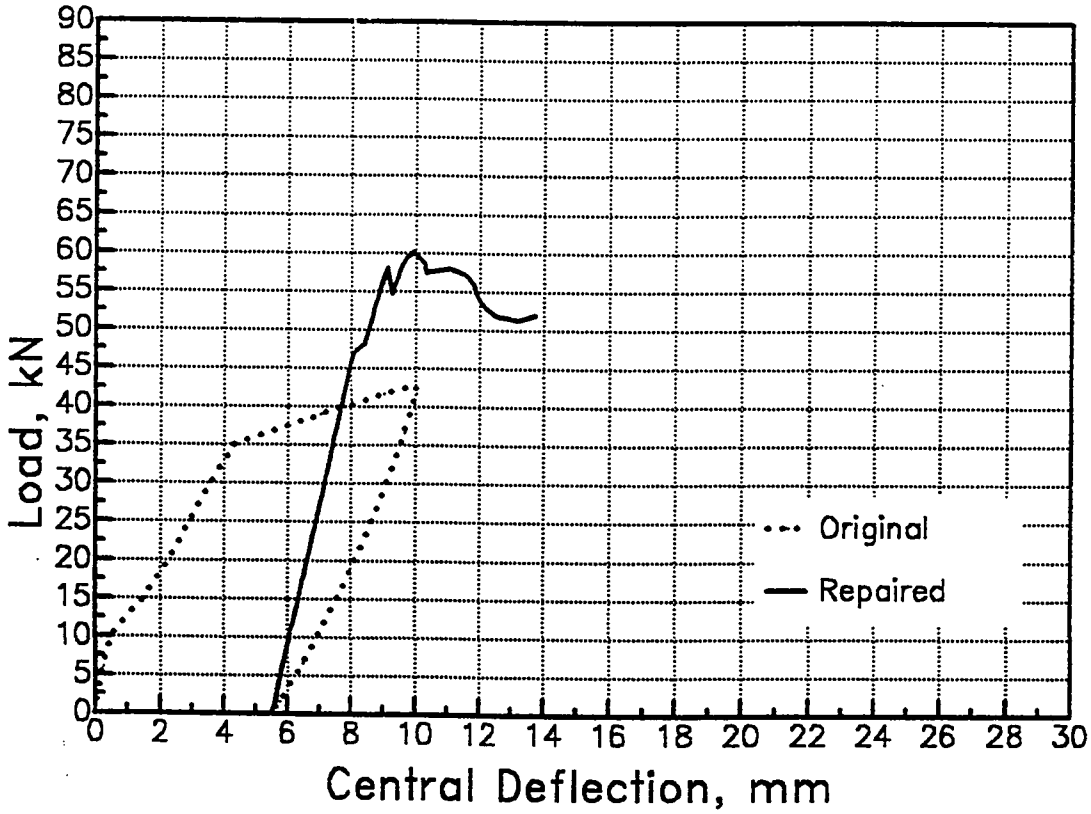

Figure 57: Load vs central deflection for beam B8. This beam was bonded with 1000 mm long, 100 mm wide and 2.00 mm thick steel plate. No end anchorage was given to the plate.

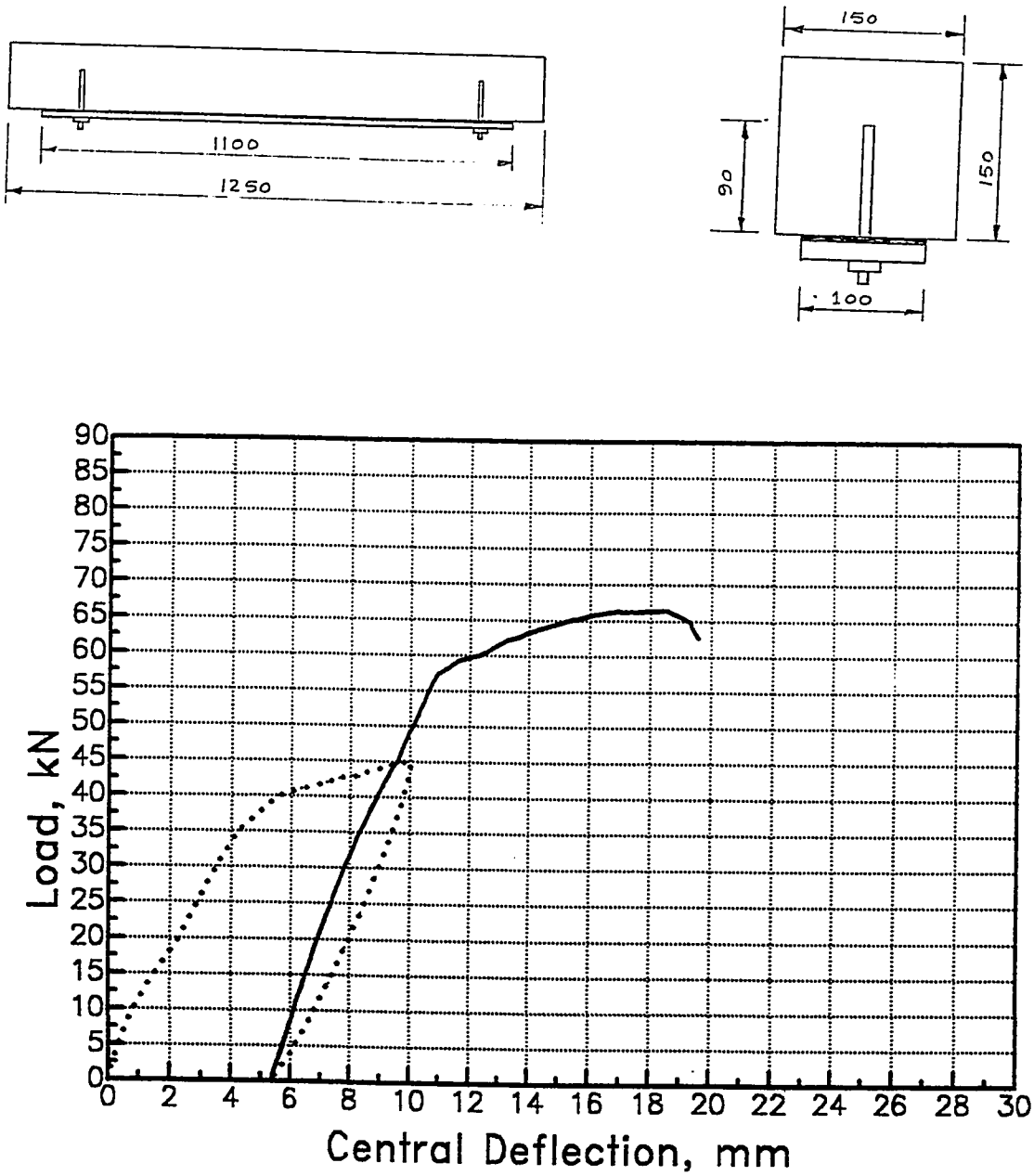

Figure 58: Load vs central deflection for beam B4. This beam was bonded with 1100 mm long, 100 mm wide and 2.00 mm thick steel plate. End anchorage was given to the plate.

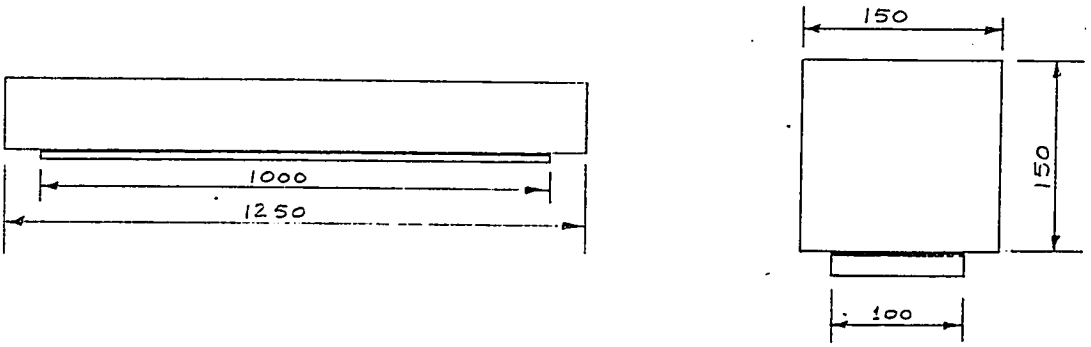

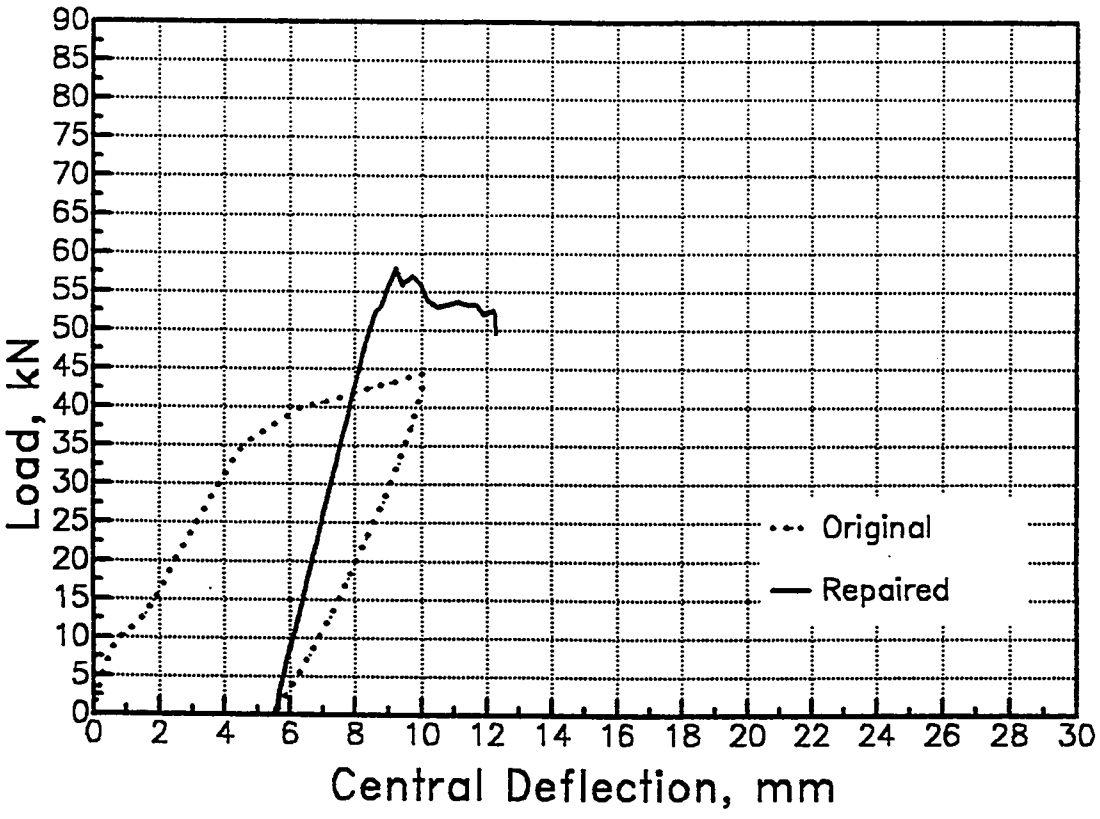

Figure 59: Load vs central deflection for beam B1. This beam was bonded with 1000 mm long, 100 mm wide and 3.00 mm thick steel plate. No end anchorage was given to the plate.

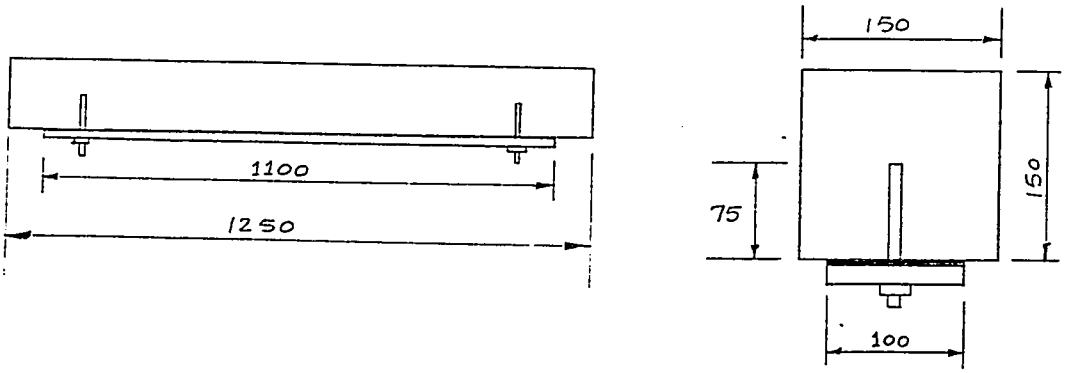

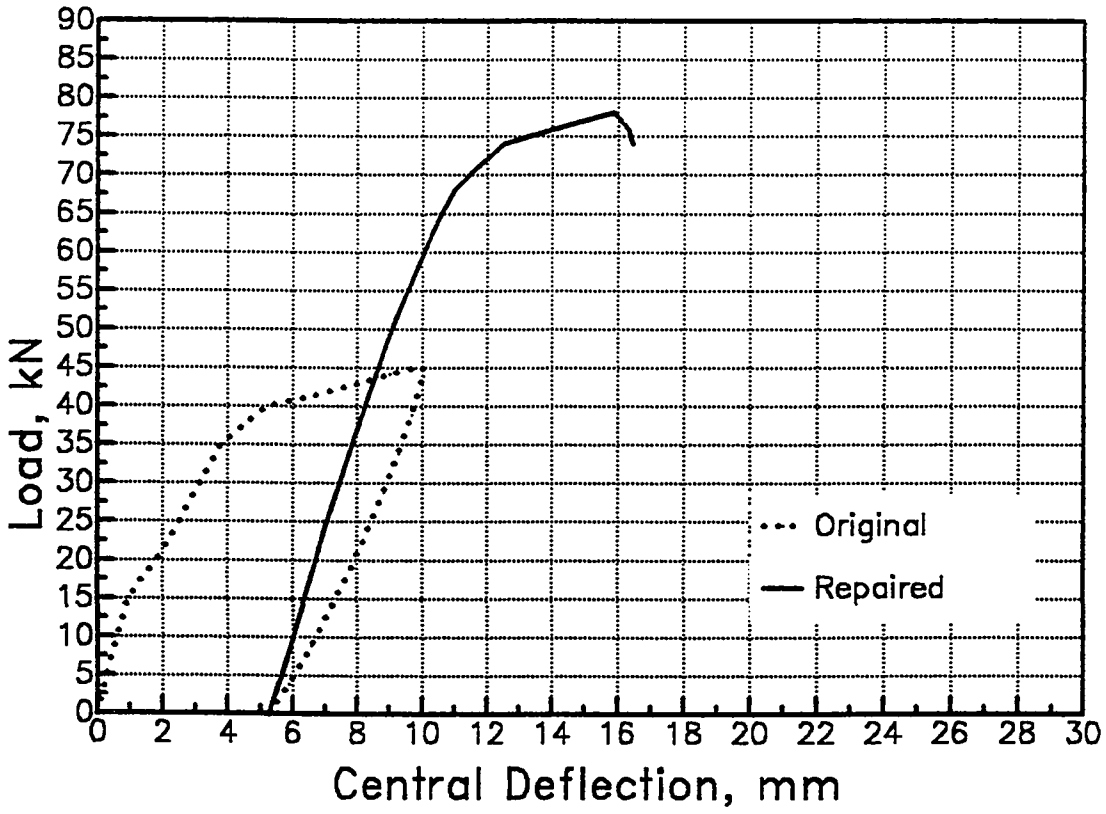

Figure 60: Load vs central deflection for beam B11. This beam was bonded with 1100 mm long, 100 mm wide and 1.50 mm thick steel plate. End anchorage was given to the plate.

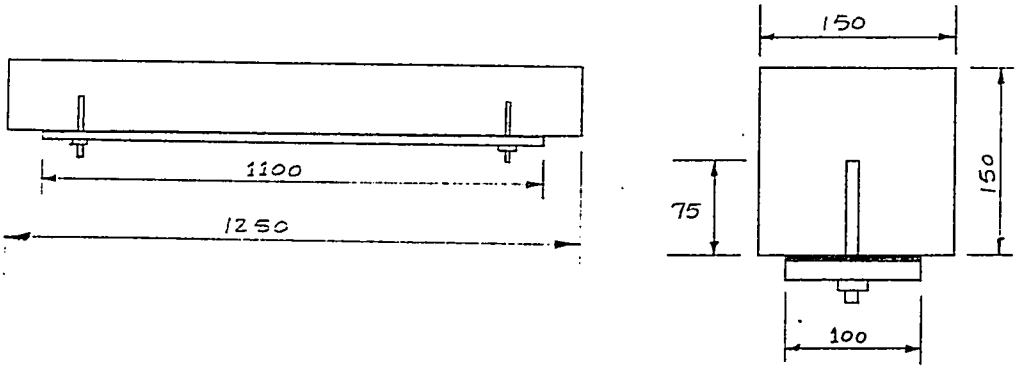

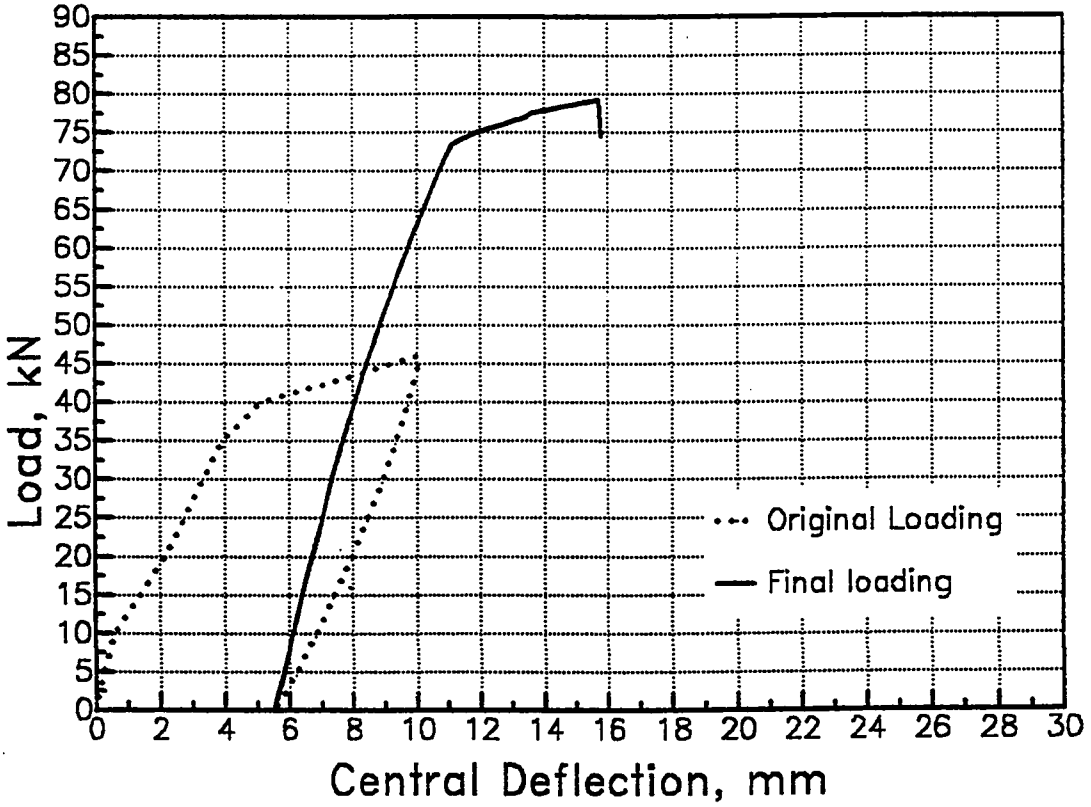

Figure 61: Load vs central deflection for beam B13. This beam was bonded with 1100 mm long, 100 mm wide and 1.50 mm thick steel plate. End anchorage was given to the plate.

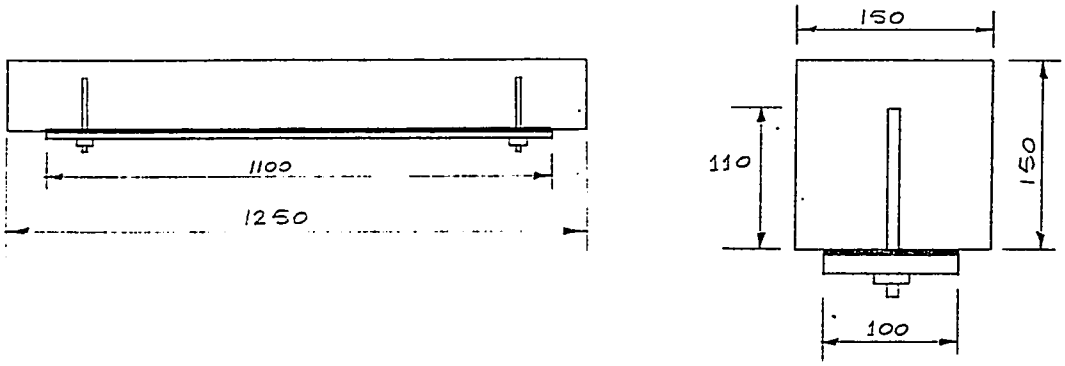

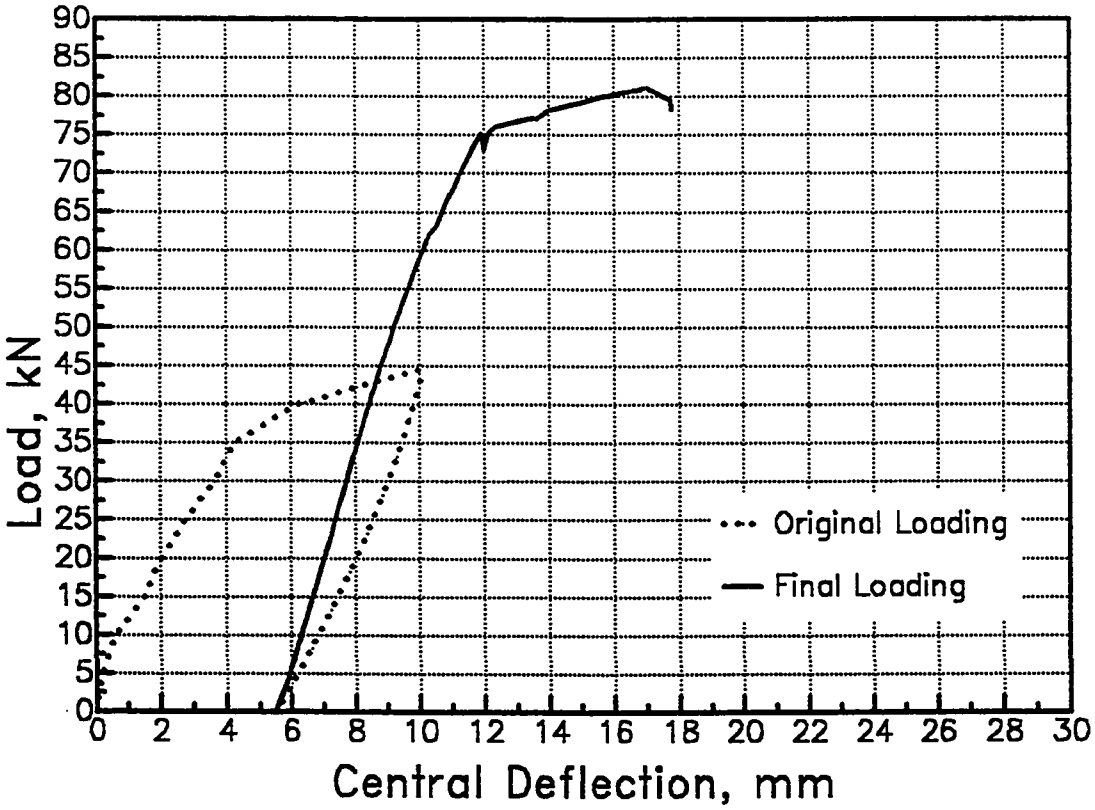

Figure 62: Load vs central deflection for beam B14. This beam was bonded with 1100 mm long, 100 mm wide and 1.50 mm thick steel plate. End anchorage was given to the plate.

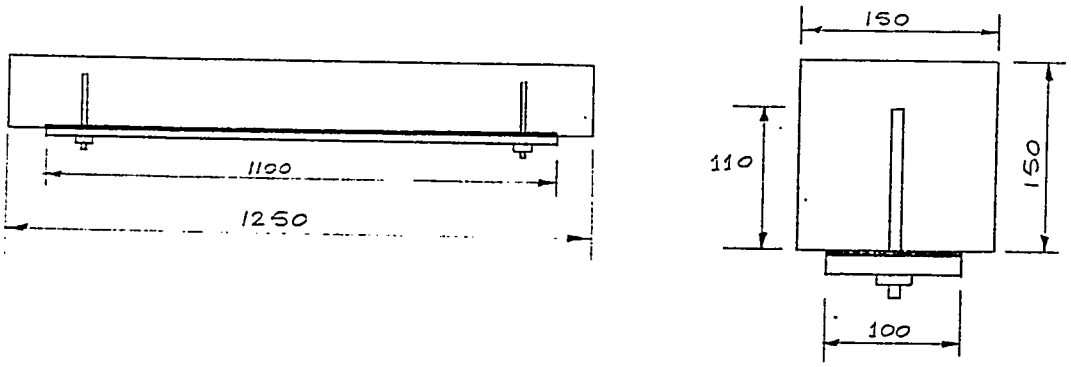

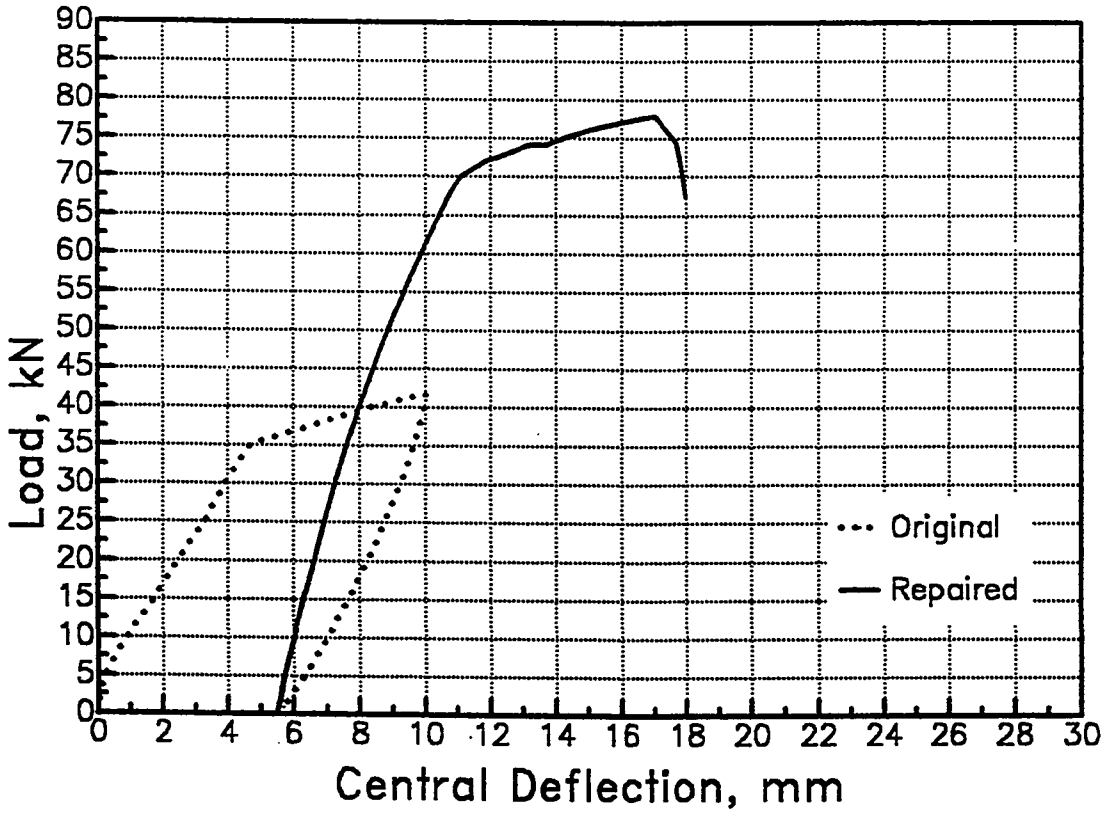

Figure 63: Load vs central deflection for beam B16. This beam was bonded with 1100 mm long, 100 mm wide and 1.50 mm thick steel plate. End anchorage was given to the plate.

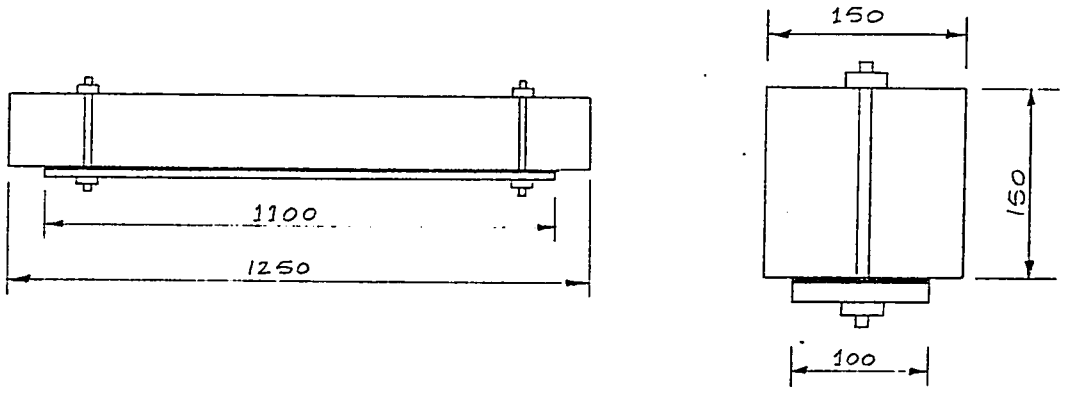

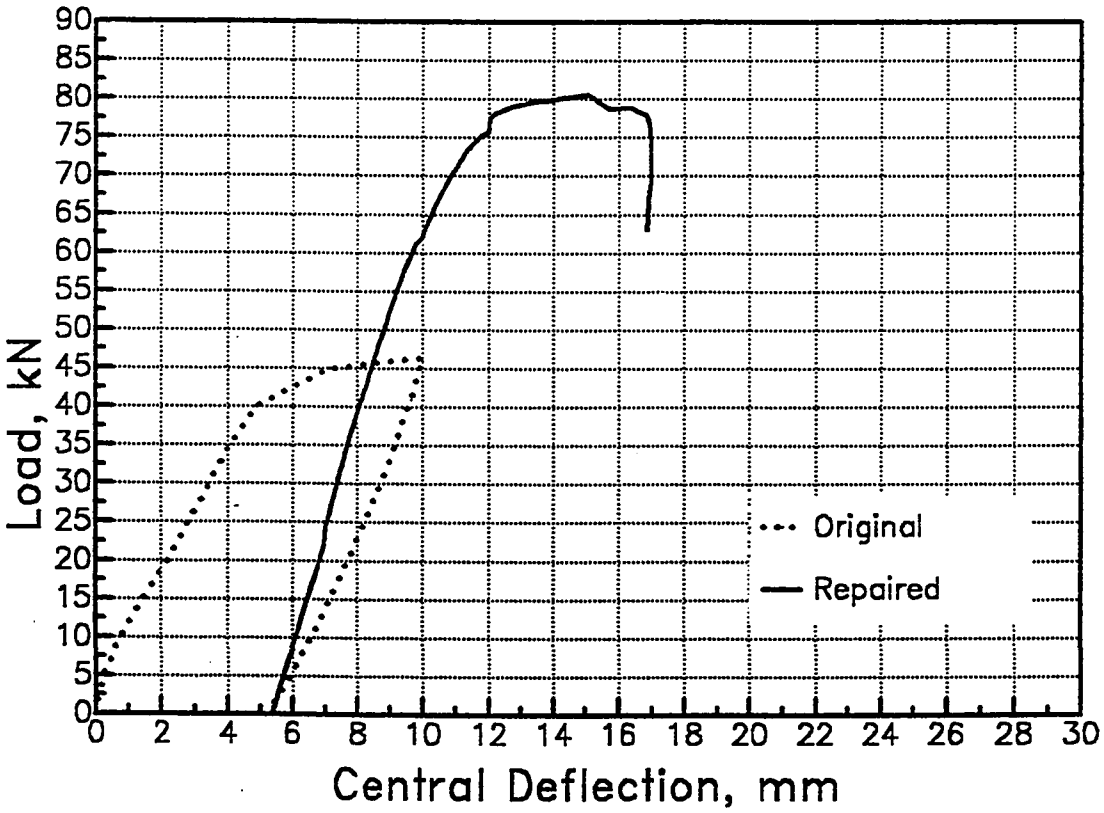

Figure 64: Load vs central deflection for beam B21. This beam was bonded with 1100 mm long, 100 mm wide and 1.50 mm thick steel plate. End anchorage was given to the plate.

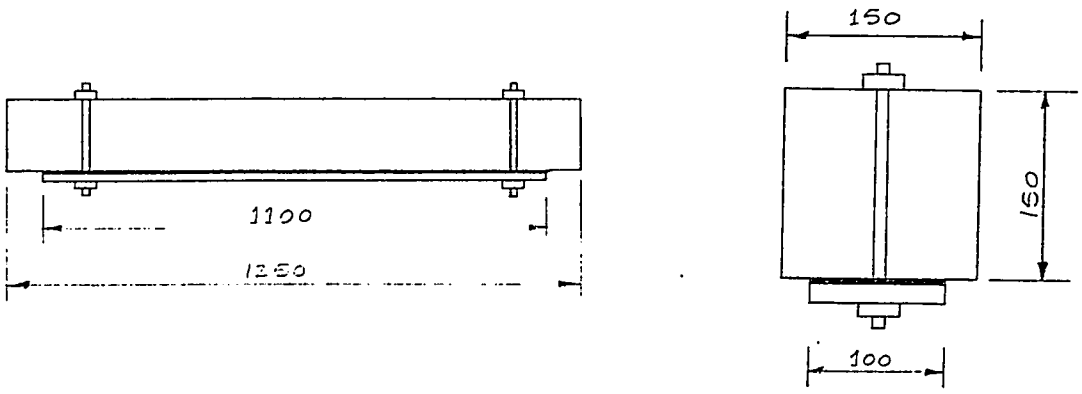

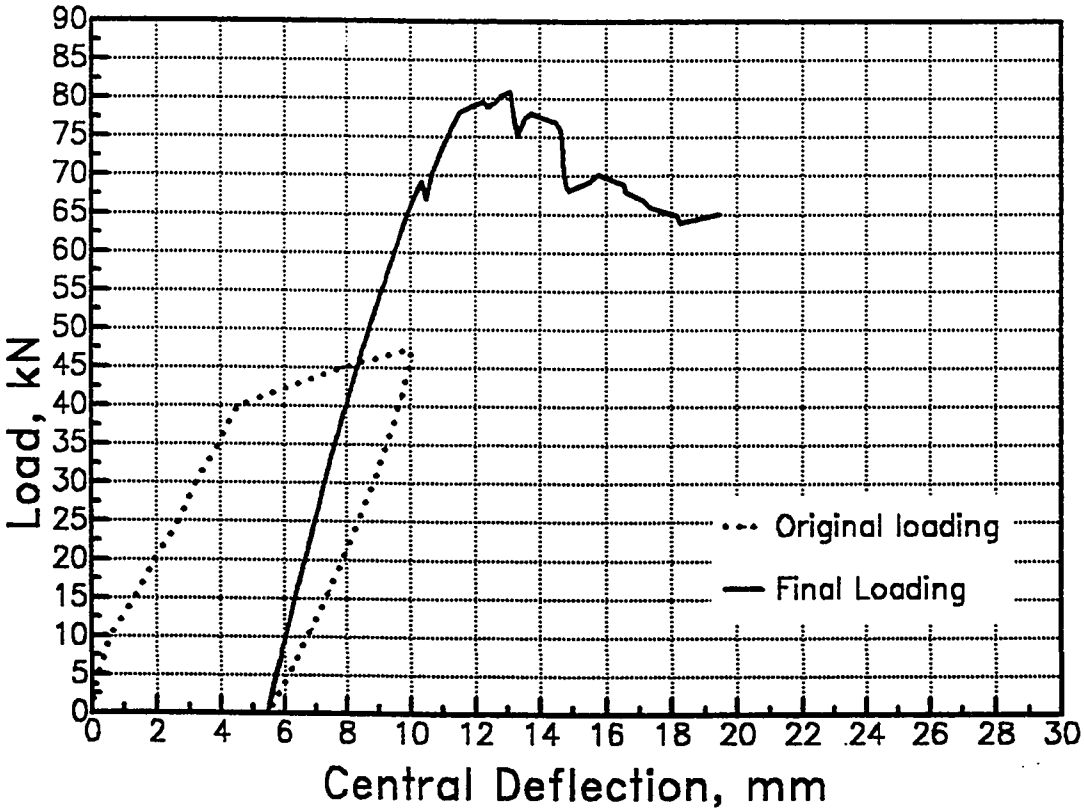

Figure 65: Load vs central deflection for beam B24. This beam was bonded with 1100 mm long, 100 mm wide and 1.50 mm thick steel plate. End anchorage was given to the plate.

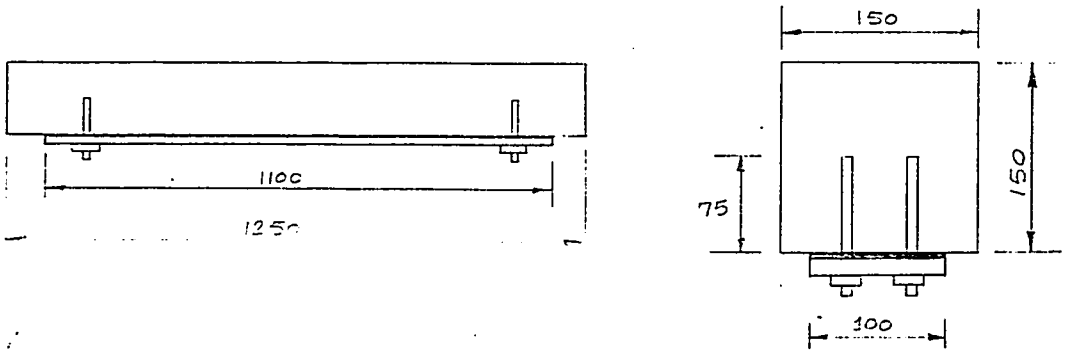

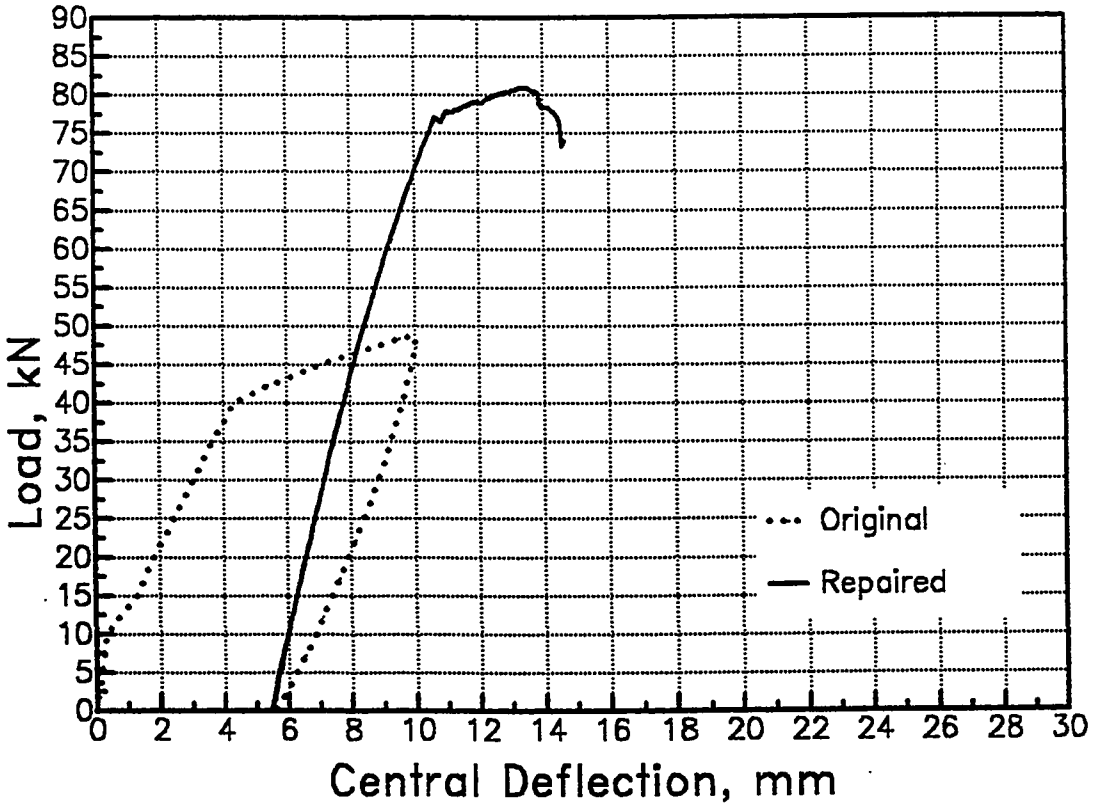

Figure 66: Load vs central deflection for beam B15. This beam was bonded with 1100 mm long, 100 mm wide and 1.50 mm thick steel plate. End anchorage was given to the plate.

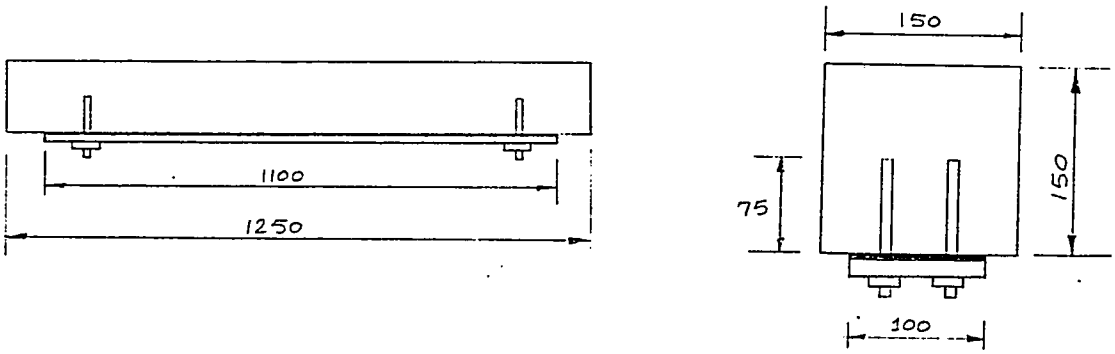

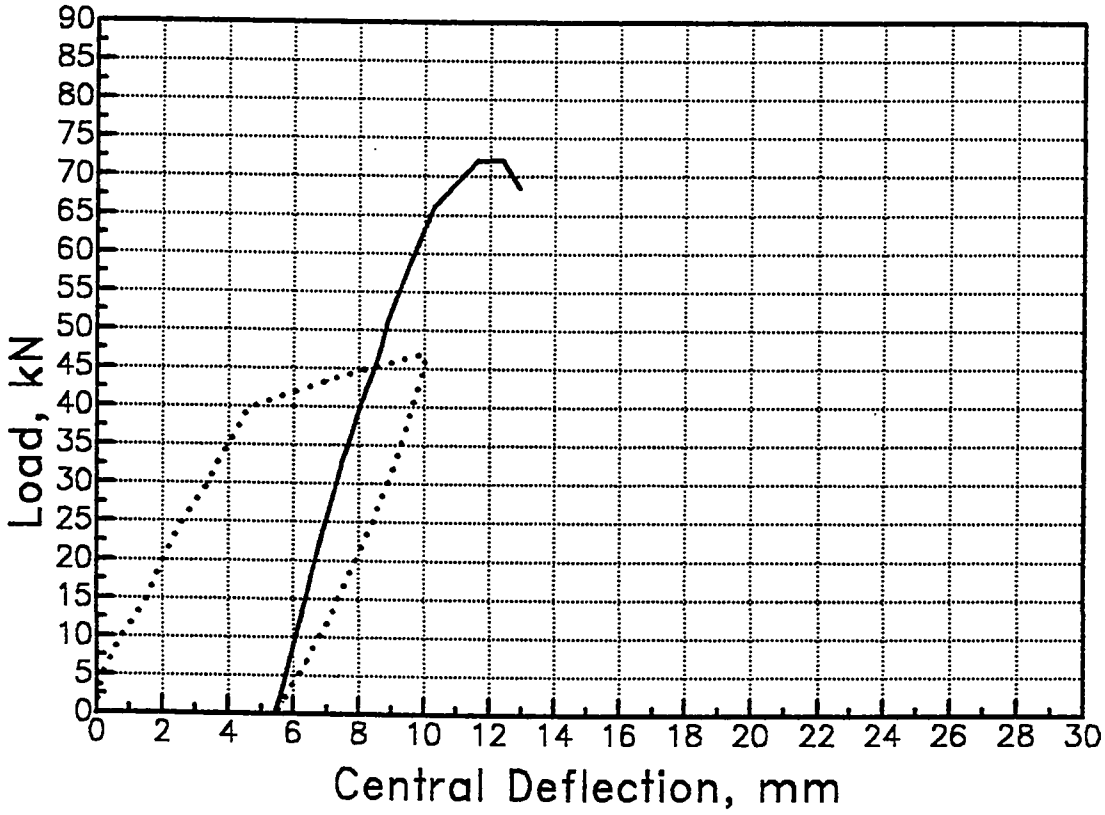

Figure 67: Load vs central deflection for beam B22. This beam was bonded with 1100 mm long, 100 mm wide and 1.50 mm thick steel plate. End anchorage was given to the plate.

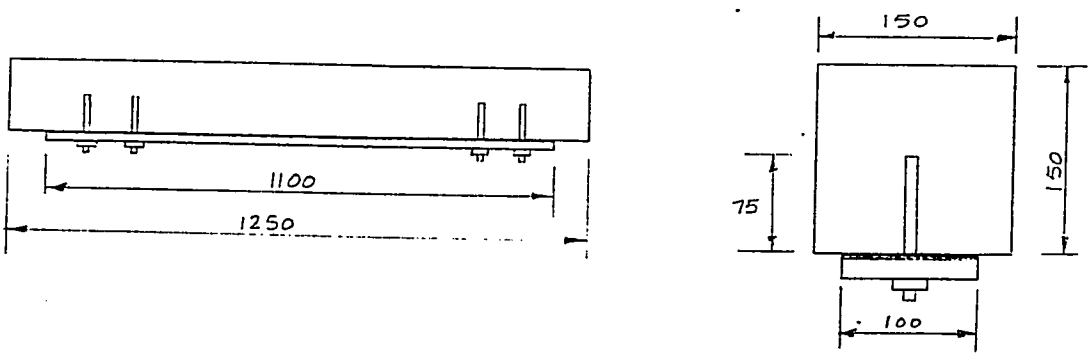

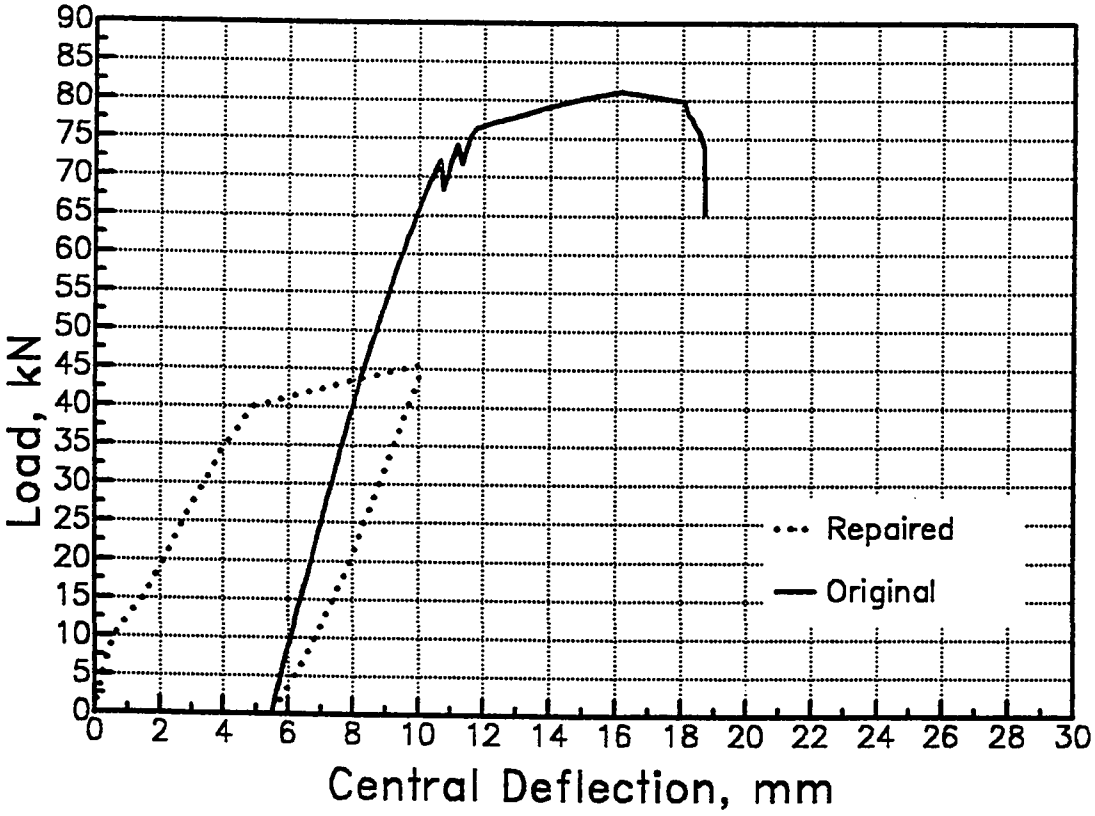

Figure 68: Load vs central deflection for beam B19. This beam was bonded with 1100 mm long, 100 mm wide and 1.50 mm thick steel plate. End anchorage was given to the plate.

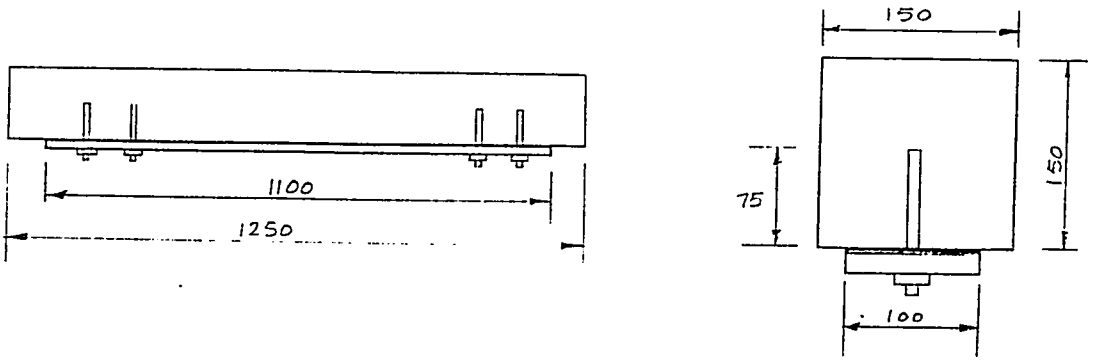

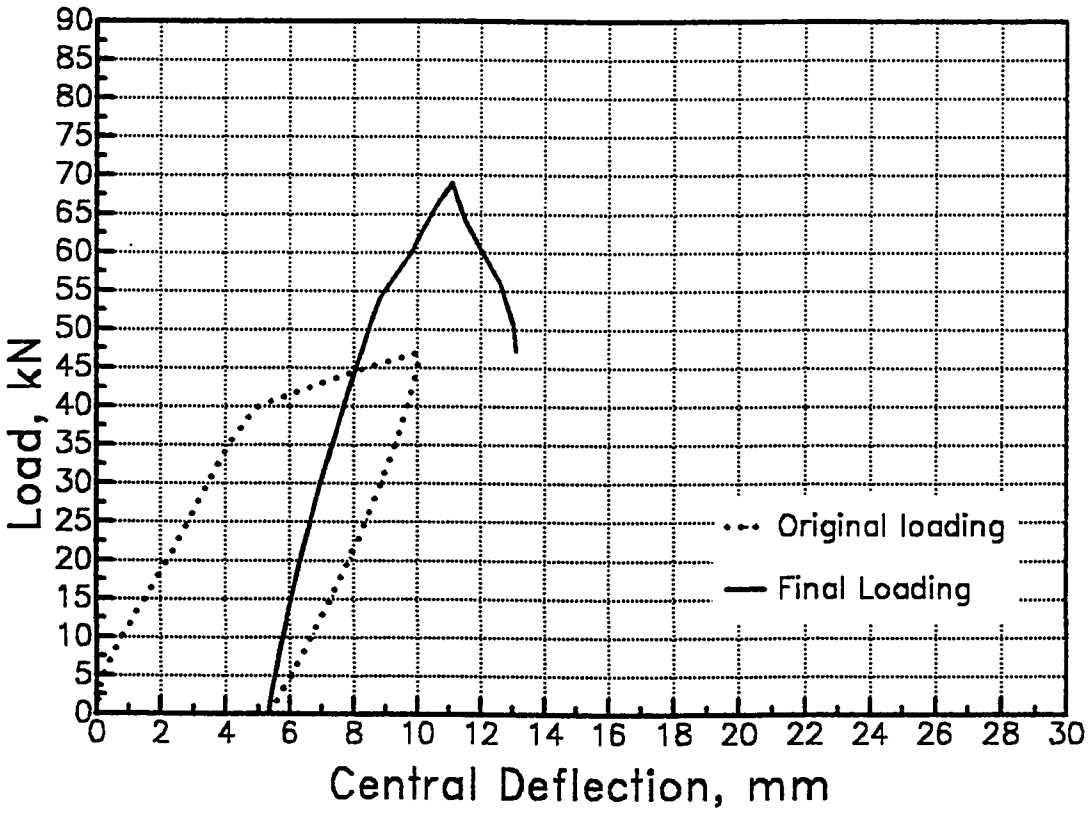

Figure 69: Load vs central deflection for beam B23. This beam was bonded with 1100 mm long, 100 mm wide and 1.50 mm thick steel plate. End anchorage was given to the plate.

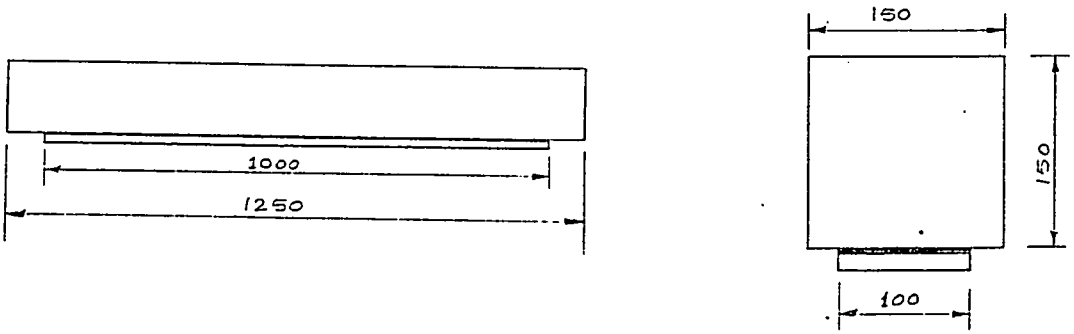

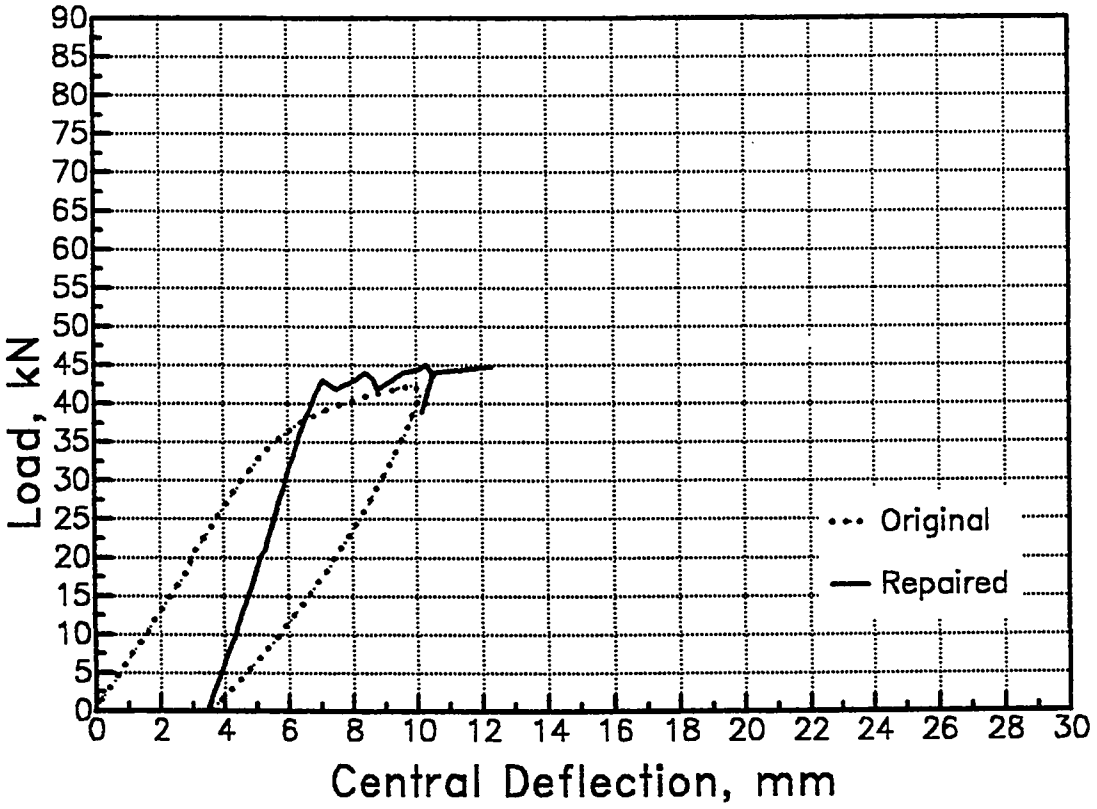

Figure 70: Load vs central deflection for beam MF1. This beam was bonded with 1000 mm long, 100 mm wide and 3.0 mm thick steel plate. No end anchorage was given to the plate.

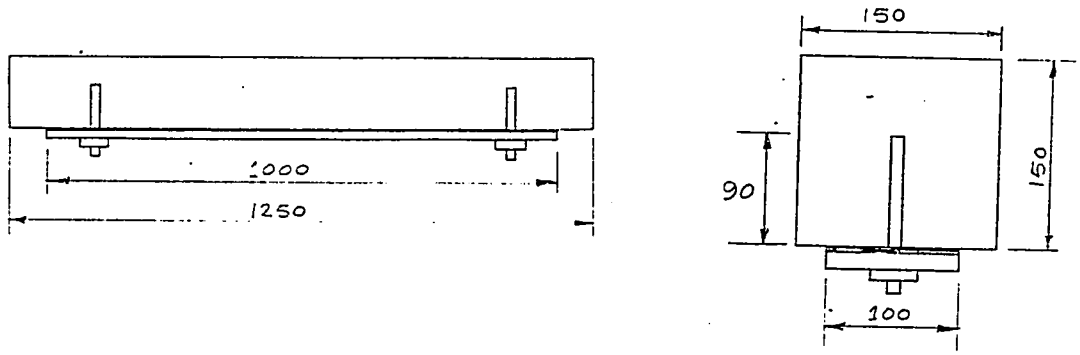

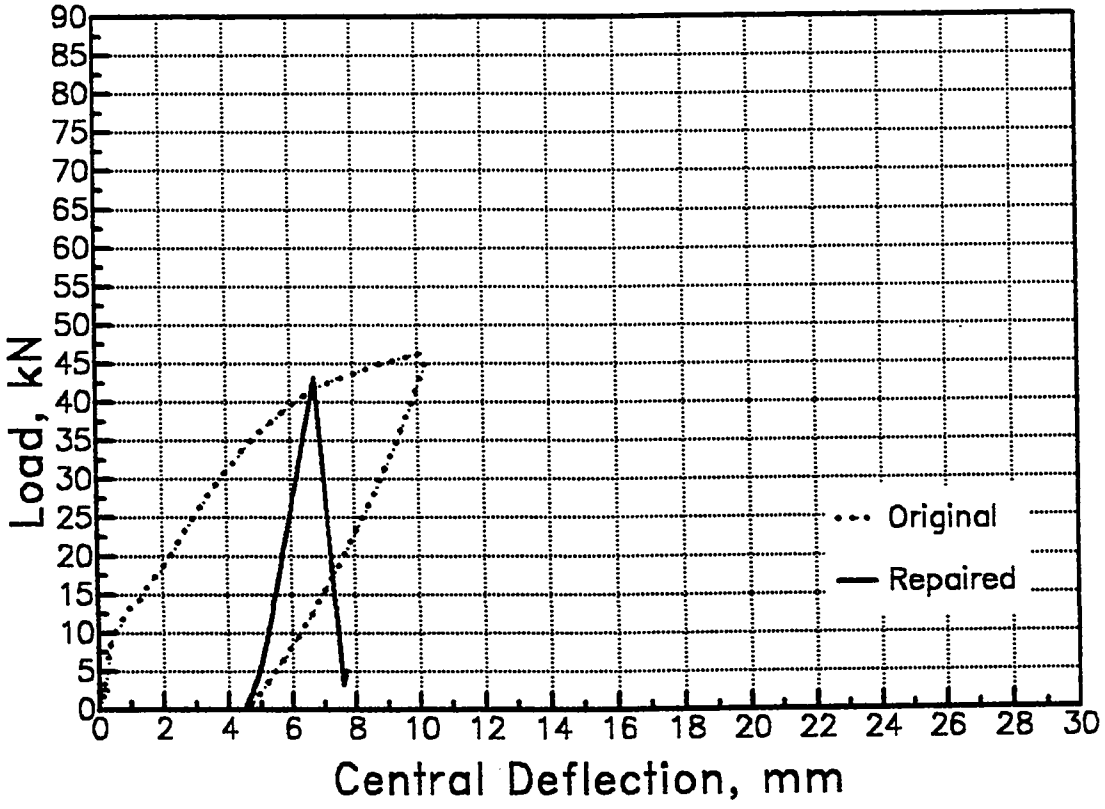

Figure 71: Load vs central deflection for beam MF2. This beam was bonded with 1000 mm long, 100 mm wide and 3.0 mm thick steel plate. End anchorage was given to the plate.

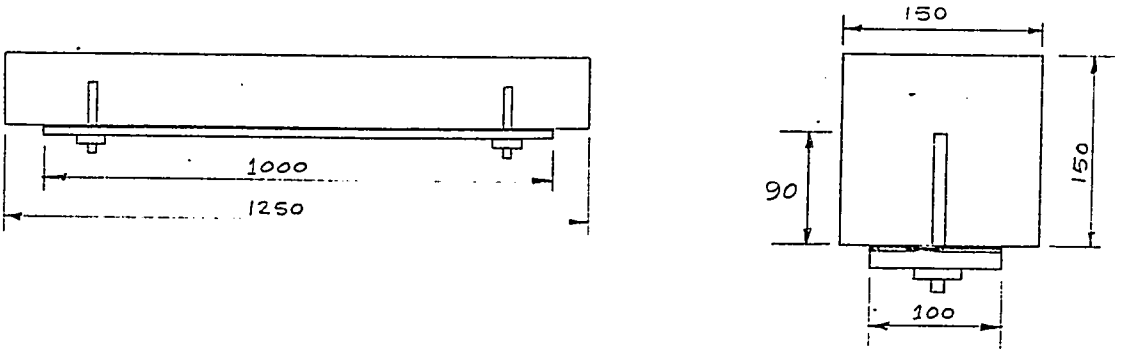

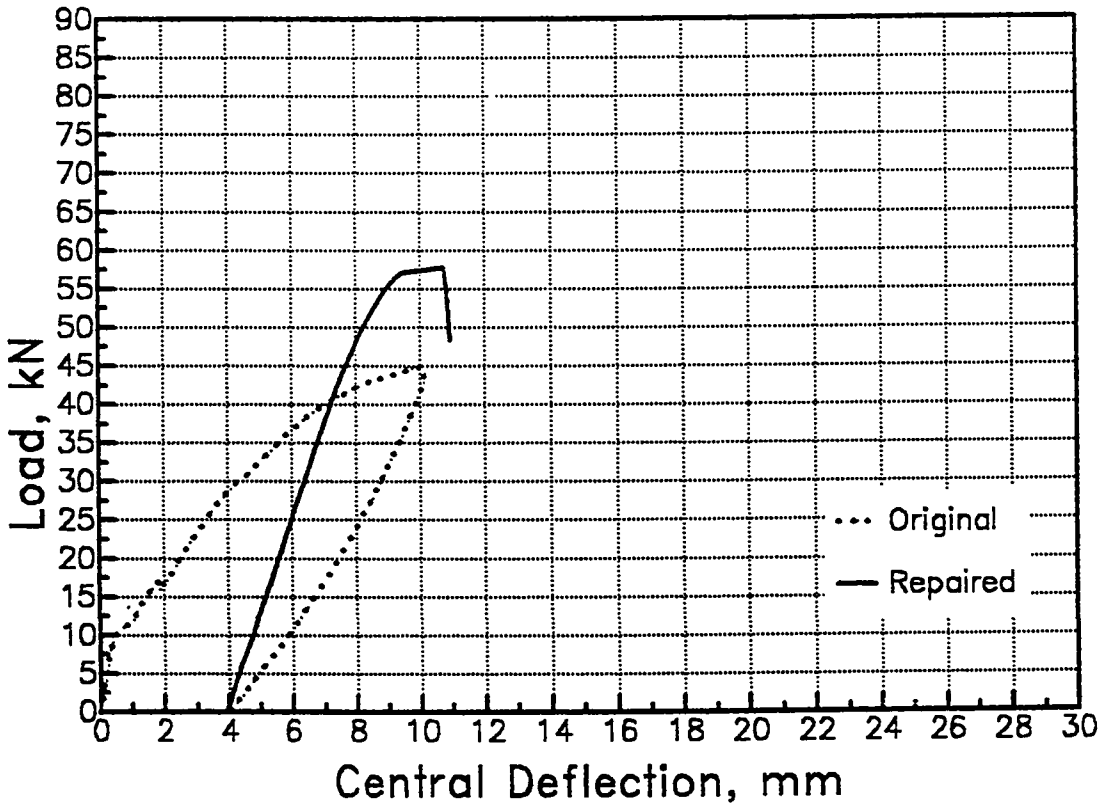

Figure 72: Load vs central deflection for beam MF4. This beam was bonded with 1000 mm long, 100 mm wide and 3.0 mm thick steel plate. End anchorage was given to the plate.

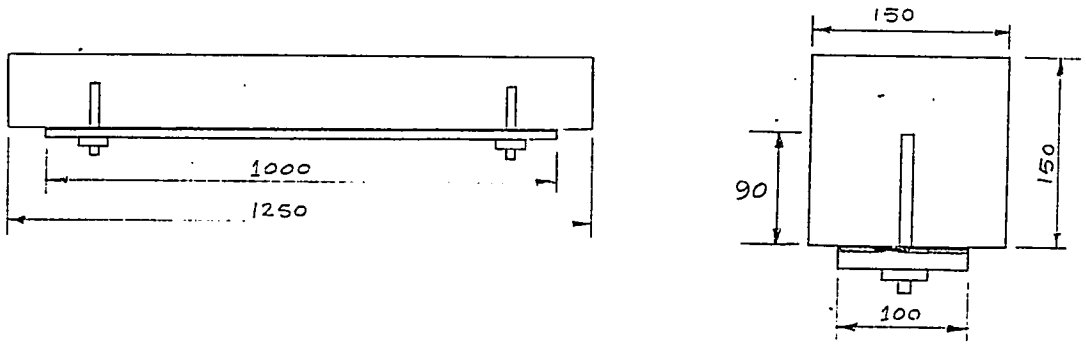

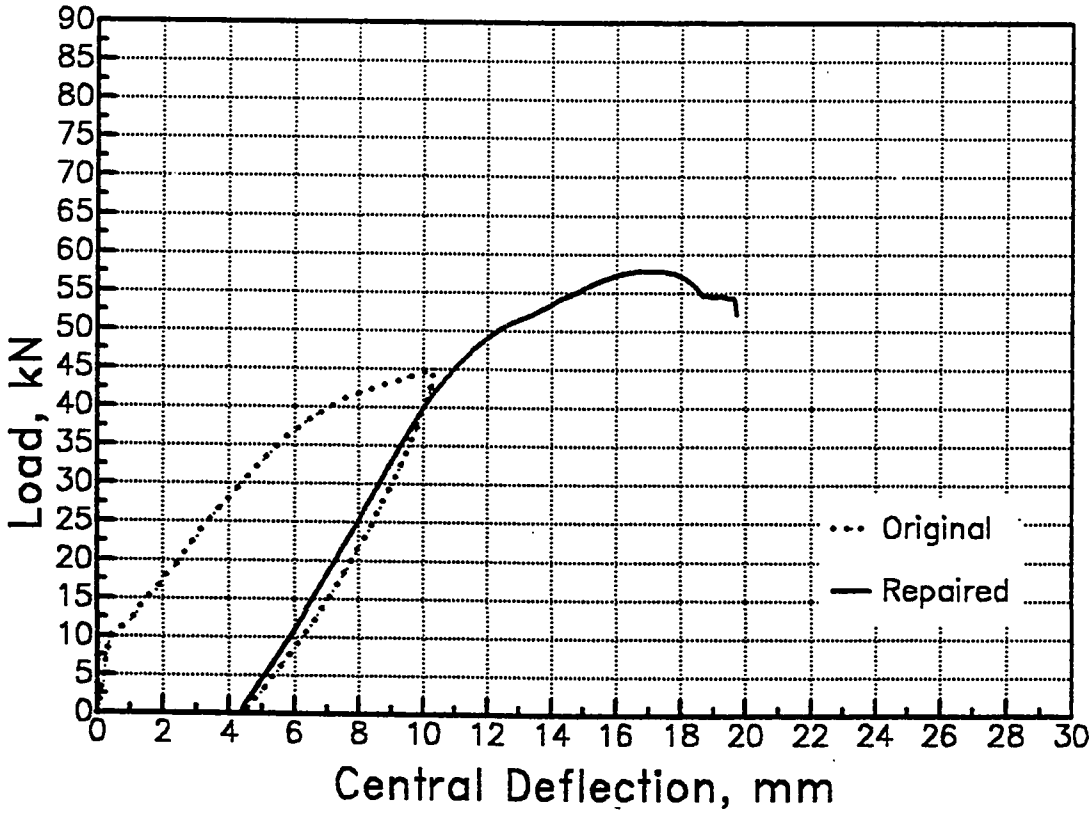

Figure 73: Load vs central deflection for beam MF3. This beam was bonded with 1000 mm long, 100 mm wide and 2.0 mm thick steel plate. End anchorage was given to the plate.

Table 8: Ultimate loads, modulus of toughness and modes of failure

Beam ID.	Plate Thick. (mm)	End Anch.	Ult. Load (kN)	Modulus of Tough. (kN.mm)	Mode of Failure
B6	-	-	54.00	954	Flexure
B7	-	-	52.00	818	=
B5	1.00	No	71.00	1250	=
B25	1.00	No	69.54	872	=
B10	1.50	No	75.00	325	Part. Flex.
B17	1.50	No	75.10	273	=
B8	2.00	No	60.00	178	Separation
B4	2.00		66.33	633	Flexure
B1	3.00	No	58.00	102	Separation
B11	1.50	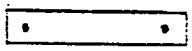	78.05	551	Part. Flex.
B13	1.50		79.18	597	=
B14	1.50	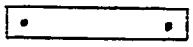	80.85	732	=
B16	1.50		77.86	734	=
B21	1.50	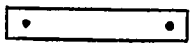	80.57	686	=
B24	1.50		80.79	483	=
B19	1.50	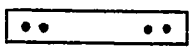	76.97	818	=
B23	1.50		69.05	237	=
B15	1.50	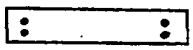	80.85	489	=
B22	1.50		71.97	308	=
MF3	2.00	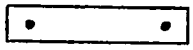	57.82	536	Separation
MF1	3.00	No	45.00	75	=
MF2	3.00	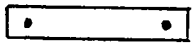	43.12	48	=
MF4	3.00		57.76	237	=
B3	1.50	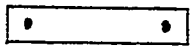	58.00	938	Flexure
B18	1.50		68.94	*	=

moment-curvature curve corresponding to a moment of 6×10^6 N.mm

Table 9: Flexural rigidities of the beams.

Beam ID.	Plate Thickness (mm)	End Anchorage	Flexural Rigidity (EI) N.mm * 10^{11}
B6	-	Unplated	4.28
B7	-	=	4.28
B5	1.00	No	5.00
B25	1.00	=	5.45
B10	1.50	=	5.45
B17	1.50	=	6.00
B8	2.00	=	7.69
B1	3.00	No	7.70
B11	1.50	Yes	5.45
B13	1.50	=	6.66
B14	1.50	=	6.00
B16	1.50	=	6.00
B21	1.50	=	6.67
B24	1.50	=	6.67
B19	1.50	=	6.66
B23	1.50	=	7.50
B15	1.50	=	6.66
B22	1.50	=	7.22
MF1	3.00	No	5.00
MF2	3.00	Yes	11.00
MF4	3.00	Yes	14.90

4.2 ULTIMATE STRAINS

Table 10 shows the ultimate loads, ultimate concrete compression strains at mid-span, ultimate plate strains at mid-span and modes of failure of all the beams. The beams B6 and B7 were reloaded without strengthening. The concrete compression strains given in the table correspond to the second cycle of loading for these beams. In these beams full flexure failure was obtained due to the crushing of the concrete at the mid-span. The ultimate concrete strains of 2870 micron and 2350 micron are less than 3000 micron. The reason why at lower concrete strains crushing failure occurred in these beams is that during the first cycle of loading the beams were strained and there were residual strains at mid-span in these beams. The residual concrete strains were equal to about 1000 micron in these beams. Taking residual strain into account we can say that the crushing of concrete in beam B6 occurred at 3870 micron and in beam B7 it occurred at 3350 micron. The same reason applies to all other beams which failed by the crushing of the concrete at mid-span at concrete strains lower than 3000 microns. As a matter of fact in all the beams there was residual concrete strain at mid-span due to original loading for damaging the beams.

This table also shows that in beams strengthened with 1.00 mm and 1.5 mm thick plates, the steel plates were yielding at failure. In beams B11 and B16, strain gages were also installed on the internal reinforcement at mid-span. It was observed that the internal reinforcement was yielding at failure in these beams. From this we infer that in ali the beams strengthened with 1.00 and 1.5 mm thick steel plates, the internal reinforcements was yielding at failure.

In beams strengthened with 2.00 mm and 3.00 mm thick plates neither the external nor the internal reinforcement were yielding at failure except beam B4. Beam B4 was strengthened with 2.00 mm thick steel plate. End anchorage was given to the plate. This beam failed due to the flexural crushing of the concrete at mid-span. The steel plate in this beam was not yielding at failure. Before the flexural crushing slip of the plate was observed at the interface. Steel plate could not contribute fully to the strength of the beam. However, the load deflection curve of this beam indicate that the internal steel was yielding at failure. The ultimate concrete strain at mid-span is 1582 micron. If we add residual strain of 1000 micron to it, it will become 2582 micron which is close but less than 3000 micron, although crushing failure was obtained in this beam. This discrepancy can be explained with the fact that some times the strain gages do not give good results.

In beams B3 and B18, the plates were not bonded to the concrete beams by adhesives. Only end anchorage was given to the plates by anchor bolts. The external plates could not contribute fully to the strengths of these beams because there were sags in the plate. The sag of plate in beam B18 was less than that in beam B3. Therefore, the ultimate load and the ultimate plate strain at mid-span for beam B18 are higher than those for beam B3.

Table 10: ULtimate strains at mid-span of beams

Beam ID.	Plate Thick. (mm)	End Anch.	Ult. Load (kN)	Plate Strain (micron)	Conc. Comp. (micron)	Mode of Failure
B6	-	-	54.08	-	2870	Flexure
B7	-	-	52.22		2350	=
B5	1.00	No	71.00	11782	2228	Flexure
B25	1.00	No	69.54	9184	1652	=
B10	1.50	No	75.00	2419	1414	Part.Flex.
B17	1.50	No	75.10	2399	-	=
B8	2.00	No	60.00	1268	915	Separation
B4	2.00	Yes	66.33	583	1582	Flexure
B1	3.00	No	58.00	729	760	Separation
B11	1.50	Yes	78.05	6267	-	Part.Flex
B13	1.50	Yes	79.18	2899	1388	=
B14	1.50	Yes	80.85	5017	-	=
B16	1.50	Yes	77.86	4822	-	=
B21	1.50	Yes	80.57	4863	-	=
B24	1.50	Yes	80.79	4689	-	=
B19	1.50	Yes	76.97	11529	-	=
B23	1.50	Yes	69.05	3388	-	=
B15	1.50	Yes	80.85	6105	-	=
B22	1.50	Yes	71.97	3014	-	=
MF3	2.00	Yes	57.82	282	1600	=
MF1	3.00	No	45.00	393	1723	Separation
MF2	3.00	Yes	43.12	710	475	=
MF4	3.00	Yes	57.76	779	904	=
B3	1.50	Yes	58.00	301	2271	Flexure
B18	1.50	Yes	68.94	719	-	=

4.3 EFFECT OF PLATE THICKNESS ON ULTIMATE LOADS

Table 11 shows the average ultimate loads for the beams having same types of repair arrangements. For comparison, theoretical ultimate loads have also been given. The theoretical ultimate loads were calculated based on the actual stress strain curves of the steels assuming full composite action between the steel plates and the concrete beams. The calculations for theoretical ultimate loads for beams of series-B and series-MF are given in the appendix A and appendix B respectively. This table shows, that the strengthening of the beams improve the ultimate strength of the beams provided the plate thickness is within limits.

Beams B6 and B7 were reloaded upto failure without strengthening. Pure flexure failure was obtained in both of these beams. For these beams, the theoretical and experimental ultimate loads were almost equal.

Beams B5 and B25 were strengthened with 1.00 mm thick unachored plates. Pure flexure failure was obtained in both of these beams. Very good agreement exists between the experimental and theoretical ultimate loads for these beams.

Beams B10 and B17 were strengthened with 1.5 mm thick unachored plates. These beams failed due to the separation of the plates after the yielding of the steel plates. These beams gave very less ductility. However, the experimental and theoretical ultimate loads for these beams were almost equal.

In order to improve the ductility of beams bonded with 1.5 mm thick plates different types of bolt anchor arrangements were used at the ends of the plates. In all the beams with different types of anchorages, the ultimate loads obtained were almost same. So, no distinction has been made between the beams bonded with 1.5 mm thick plates having different types of anchorage arrangements.

AABs stands for beams B11, B13, B14, B16, B21, B24, B19 and B15 respectively. It is clear from this table that average ultimate load was improved by giving end anchorage to the plate for the beams which were strengthened by 1.5 mm thick plates.

Beam B8 was strengthened with 2.00 mm thick plate. In this beam no end anchorage was given to the plate. For this beam the experimental ultimate load is less than the theoretical ultimate load. This beam failed prematurely due to the separation of the plate giving less ultimate load and less ductility. The separation took place before the yielding of the steel plate and the rebar steel.

Beam B4 was strengthended with 2.00 mm thick steel plate. End anchorage was given to steel plate by bolts. For this beam the experimental ultimate load is less than the theoretical ultimate load. Although the end anchorage was provided to the steel plate even though the plate could not be fully utilized. The steel plate was not yielding at failure in this beam. The slip of the steel plate at the anchorage was also observed.

Beam B1 was strengthened with 3.00 mm thick plate. No end anchorage was given to the plate in this beam. This beam failed prematurely due to the separation of the plate starting at the end of the plate showing less ductility. The experimental ultimate load for this beam is less than the theoretical ultimate load calculated assuming full composite action between the steel plate and the concrete beam.

Beam MF3 was strengthened with 2.00 thick anchored plate. This beam failed without reaching the full flexural capacity calculated based on the actual stress strain curve of the steel assuming full composite action between the steel plate and the concrete beam.

Beam MF1 was strengthened with 3.00 mm thick plate. No end anchorage was given to plate in this beam. This beam failed prematurely due to the separation of the plate showing less ductility. The experimetal ultimate load is less than the theoretical ultimate load for this beam.

Beam MF2 was strengthened with 3.00 mm thick plate. End anchorage was given to the plate by bolts. At each end of the plate one anchor bolt was used in this beam. The diameter and depth of penetration of the anchor bolts was 15 mm and 90 mm respectively. This beam failed in brittle manner due to the sudden appearance of the diagonal crack starting from the end of the plate. This diagonal crack was steeper than that in beam MF1 without anchor bolts. The drop in load was sudden. The crack appeared with sound. This beam could not reach the theoretical ultimate flexure capacity, although end anchorage was given to the plate.

Beam MF4 was strengthened with 3.00 mm thick anchored steel plate. The beam failed without reaching the full flexural capacity calculated based on the actual stress strain curves of the steels assuming full composite action between the steel plate and the concrete beam.

Table 11: Average ultimate loads and modulus of toughness

Beam ID.	Plate Thick. (mm)	Anch-orage	Theo. Load (kN)	Exp. Load (kN)	Mod. of Tough. (KN.mm)	Mode of Failure
B6,B7	-	-	52.23	53.00	886	Flex.
B5,B25	1.00	No	69.00	70.27	1061	Flex.
B10,B17	1.50	No	76.50	75.04	299	Part.Flex.
AABs	1.50	Yes	76.50	79.42	636	=
B8	2.00	No	83.80	60.00	178	Separation
B4	2.00	Yes	83.80	66.33	633	Flexure
B1	3.00	No	98.00	58.00	102	Separation
MF3	2.00	Yes	106.13	57.82	536	Separation
MF1	3.00	No	120.20	45.00	75	Separation
MF2,MF4	3.00	Yes	120.20	50.44	143	Separation

Note: AABs stands for beams B11, B13, B14, B16, B21, B24, B15 and B19 respectively.

4.4 EFFECT OF PLATE THICKNESS ON THE DUCTILITY

Table 11 gives the average values of the modulus of toughness of the beams used in this study having same types of repairs. The modulus of toughness is a measure of ductility. It is recalled that in ordinary reinforced concrete beams, by increasing the area of the main reinforcement ductility decreases. This table shows that the modulus of toughness for the unplated beams is less than that of the beams plated with 1.00 mm thick plates. The average modulus of toughness

for the plated beams having 1.00 mm plate thickness is 1061 kN.mm. This table shows that as the plate thickness is increased from 1.00 mm to 1.5 mm, the modulus of toughness decreases from 1061 to 299 kN.mm. This tremendous decrease in the ductility is due to the fact that when the plate thickness was increased from 1.00 mm to 1.5 mm, the mode of failure of the beams was changed from pure flexure to premature failure due to the separation of the plates. The ductility of the beams bonded with 1.5 mm thick plates was improved by giving end anchorage to the plates. Different anchorages were used. However, the improvement in ductility in all cases was almost same. So average values of modulus of toughness for the beams bonded with 1.5 mm thick plates with end anchorages are written in front of AABs in this table. AABs stands for beams B11, B13, B14, B16, B21, B24, B15 and B19 respectively. Beams B22 and B23 are not included in this average because these beams did not gave good results due to improper repair.

This table also shows that as the plate thickness is further increased, the ductility decreases. For example, in case of beam B8 bonded with 2.00 mm thick plate, the modulus of toughness is 178 kN.mm. This beam failed due to the separation of the plate.

For beam B1 bonded with 3.00 mm thick plate the modulus of toughness is 102 kN.mm. The failure in this beam was also due to the separation of the plate.

The beam MF1 was strengthened with 3.00 mm thick steel plate. No end anchorage was given to the steel plate in this beam. In this beam, the failure was also due to the separation of the plate. The modulus of toughness for this beam is 75 kN.mm.

Beams MF2 and MF4 were strengthened with 3.0 mm thick steel plates. End anchorage was given to the plates in these beams by anchor bolts. The average modulus of toughness for these beams is 143 kN.mm.

Beam MF3 was strengthened with 2.00 mm thick steel plate. End anchorage was given to the steel plate by anchor bolts. The modulus of toughness for this beam is 536 kN.mm.

4.5 EFFECT OF PLATE THICKNESS ON STIFFNESS

Table 9 on page 126 shows the flexural rigidities of all the plated and unplated beams. The procedure for finding the flexural rigidities has already been described. From this table it is clear that the flexural rigidities of the plated beams are higher than that of the unplated beams. Table 12 shows the average values of flexural rigidities for the beams having same types of repairs. From this table it can be inferred that with increasing the plate thickness flexural rigidity increases. This table also shows that the anchoring of plates affect the stiffness. By giving end anchorage to the bonded plates the stiffness of beams increased.

Table 12: Average values of flexural rigidities

Beam IDs.	End Anch.	Plate Thick. (mm)	Flexural Rigidity (EI) N.mm * 10^{11}
B6,B7	No	No	4.28
B5,B25	No	1.00	5.23
B10,B17	No	1.50	5.73
B8	No	2.00	7.69
B1	No	3.00	7.70
AABs	Yes	1.50	6.55
MF1	No	3.00	5.00
MF2,MF4	Yes	3.00	12.95

AABs stands for the beams B11, B13, B14, B16, B21, B24, B15, B22, B19, B23. respectively.

4.6 SHEAR STRESSES AT THE INTERFACE

Due to slip at the interface between the steel plate and the concrete beam, shear stresses exist at the interface. Shear stresses at the interface are related to the strain gradient in the plate by the following expression:-

$$\tau = E t \frac{d\varepsilon}{dx}$$

Where E is the elastic modulus of the steel plate and t is the thickness of the steel plate. $\frac{d\varepsilon}{dx}$ represents strain gradient in the plate. Figure 74 shows the

strain distribution along the plate at various load levels for beam B25. This figure shows that the strain gradient at the end of the plate is higher and it decreases towards the mid-span. Also this figure shows that the strain gradient increases with the increase of load. Because at the end of the plate strain gradient is higher so higher shear stresses at interface occur at the ends of the plates as compared to interior portion of the plate.

Figure 75 shows the strain distribution along plate for beam B10 at various loads. As the load increases the strain gradient along the plate also increases. At higher loads close to the ultimate load the strain at the end of the plate drops to zero due to the separation of the plate. After separation the bonded length of the plate becomes less and due to that, strain gradient at the end of the bonded portion of the plate has become higher as compared to the strain gradient at the end of the plate if there had been no separation. This means that with increasing the distance between the support and the end of the plate, shear stress increases provided the other conditions are same.

Figure 76 shows the strain distributions along plate for beam B17 at various loads. On the left hand side there is a drop in plate strain due to separation.

Figure 77 shows the strain distributions along plate at various load levels for beam B8. The separation effect on the strain in plate is very clear on the right hand side of the diagram.

Figure 78 shows the strain distributions along plate at various load levels for beam B1. The separation effect on the strain in the plate is very clear on the left hand side of the diagram.

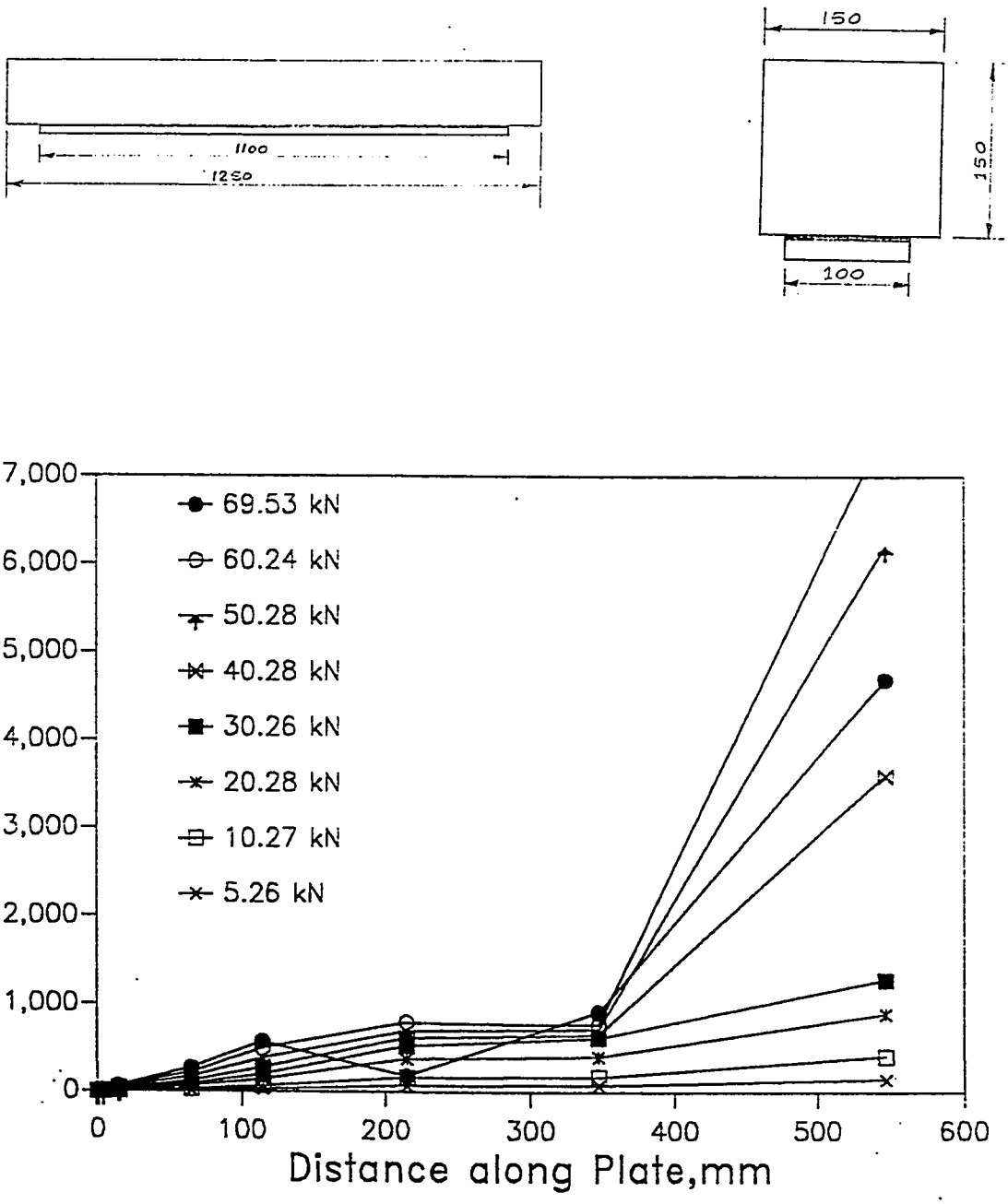

Figure 74: Strain distributions along plate for beam B25. This beam was bonded with 1.00 mm thick, 100 mm wide and 1100 mm long plate. No end anchorage was provided to the plate.

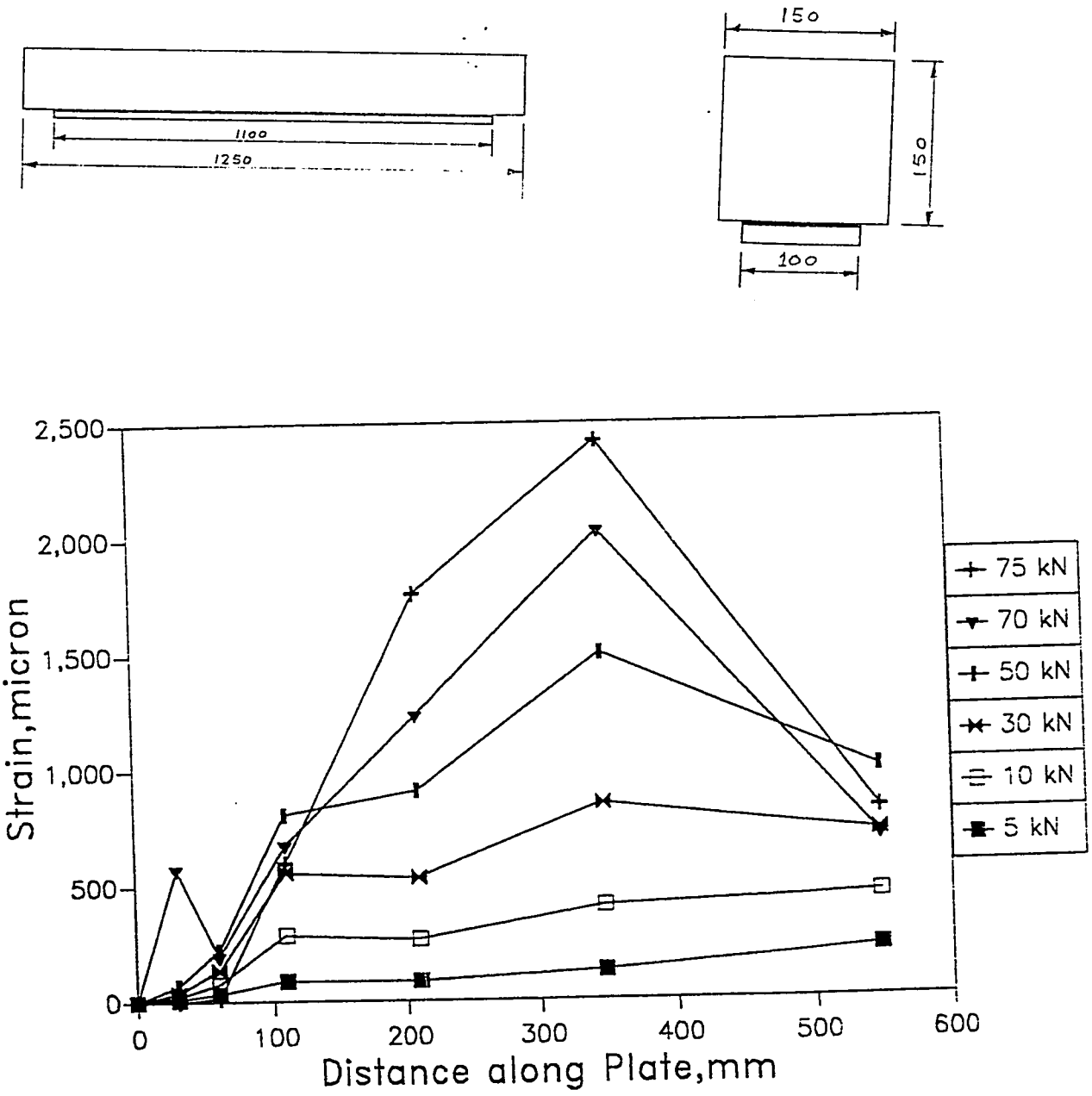

Figure 75: Strain distributions along plate for beam B10. This beam was bonded with 1.5 mm thick, 100 mm wide and 1100 mm long plate. No end anchorage was given to the plate.

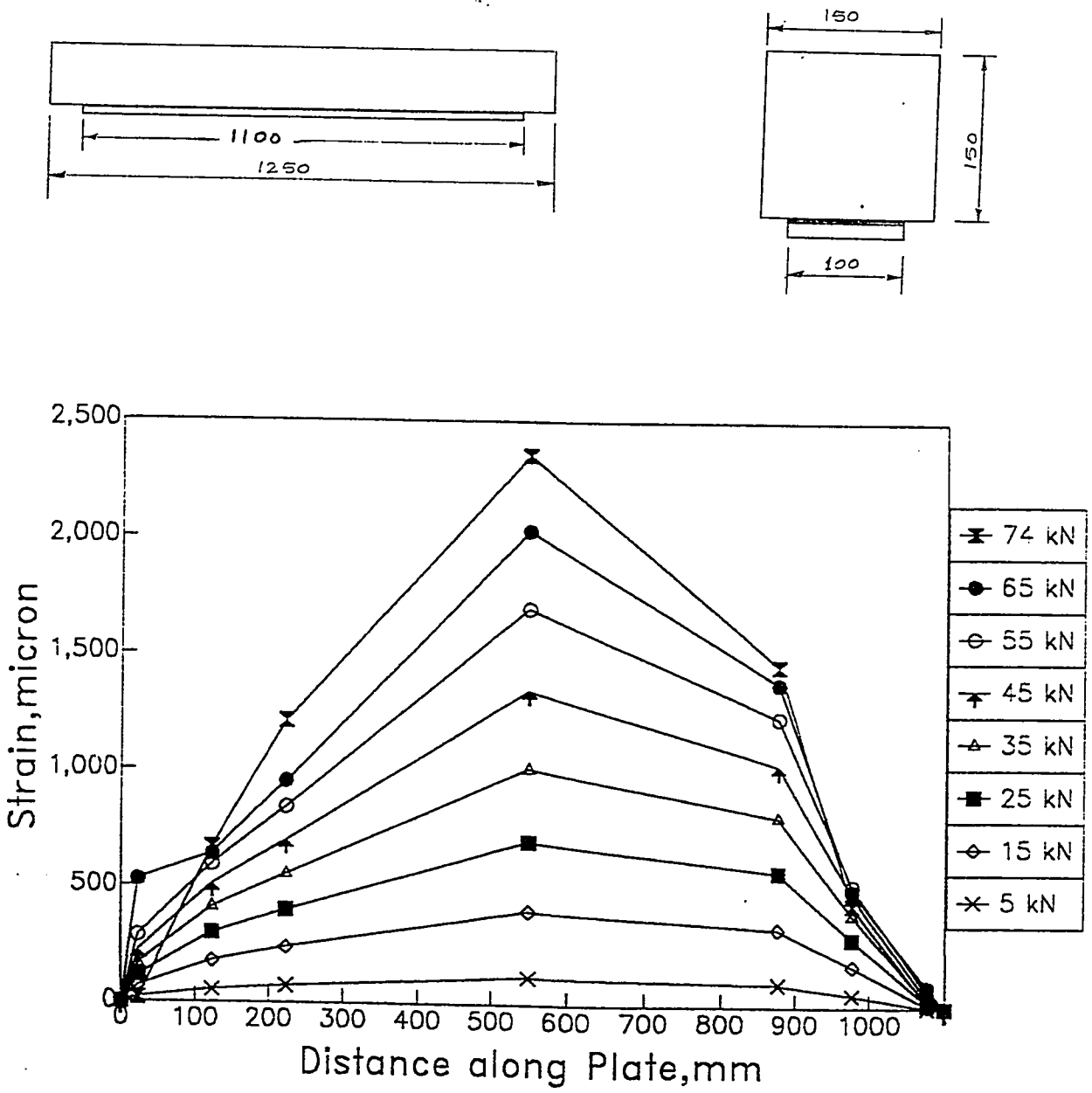

Figure 76: Strain distributions along plate for beam B17. This beam was strengthened by 1.5 mm thick, 100 mm wide and 1100 mm long steel plate. No end anchorage was given to the plate.

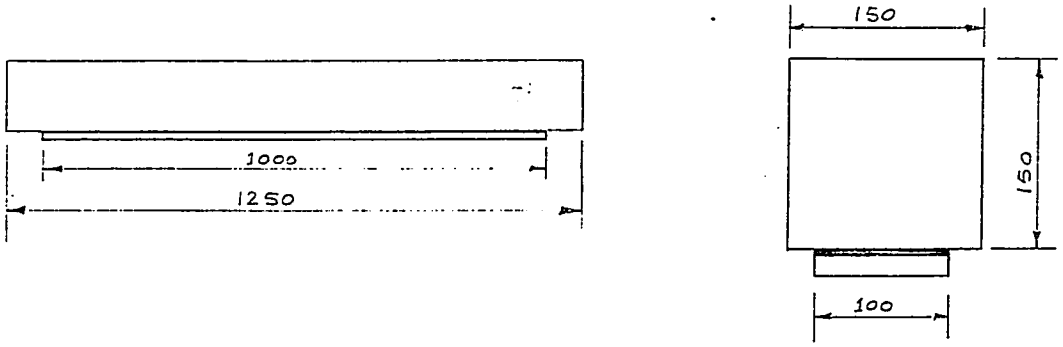

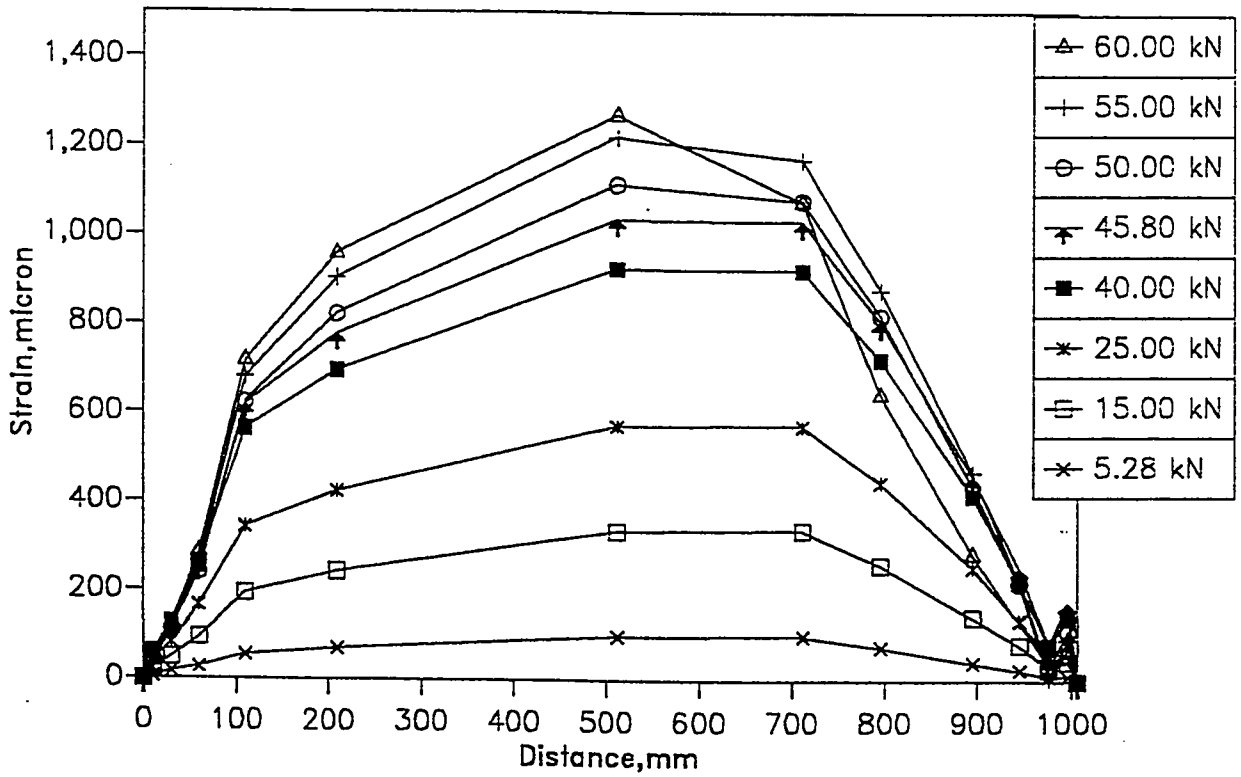

Figure 77: Strain distributions along plate for beam B8. This beam was strengthened by 2.00 mm thick, 100 mm wide and 1000 mm long plate. No end anchorage was given to the plate.

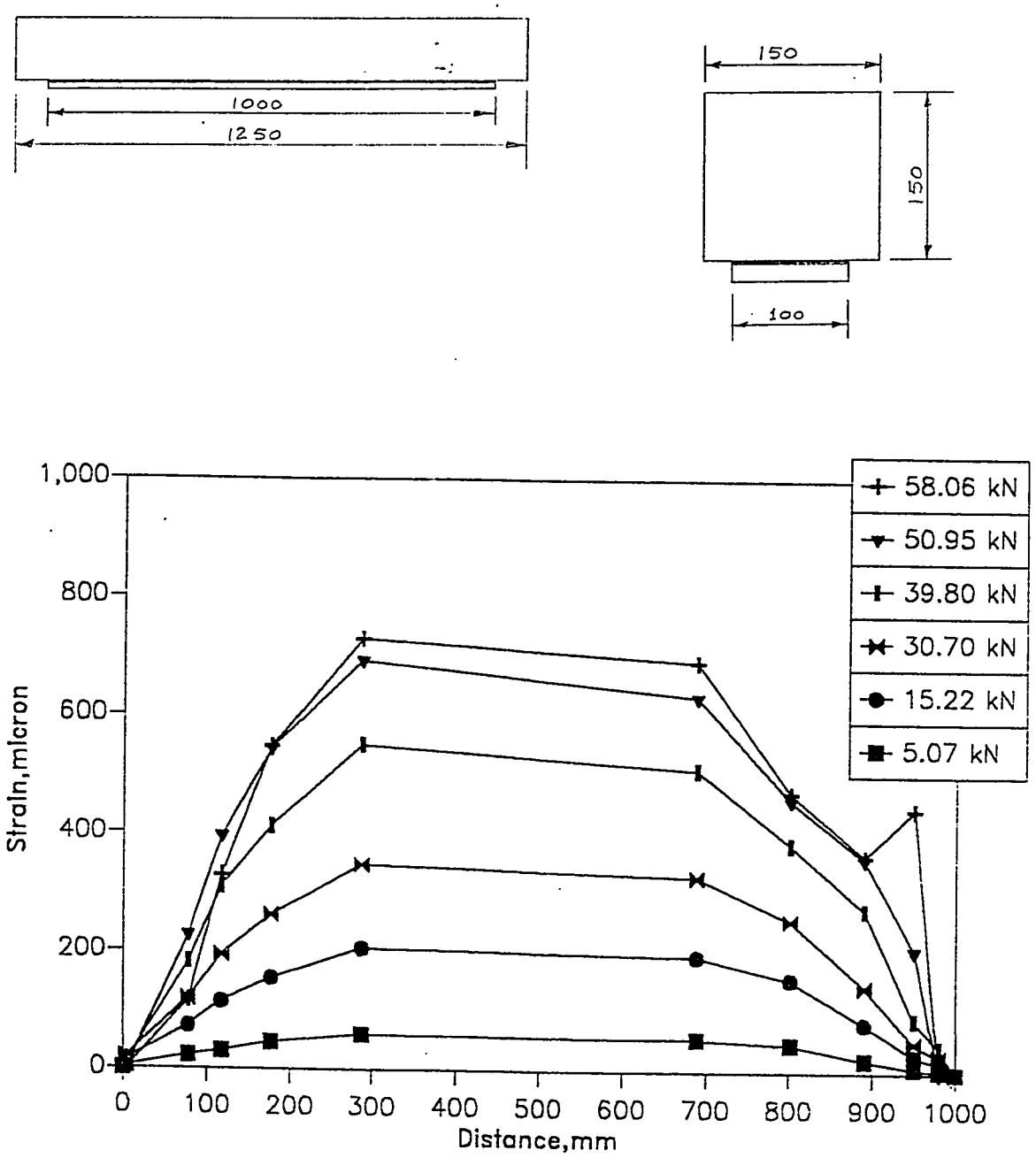

Figure 78: Strain distributions along plate for beam B1. This beam was strengthened by 3.00 mm thick, 100 mm wide and 1000 mm long plate. No end anchorage was given to the plate.

Figure 79 shows the strain distributions along plate at various load levels for beam B11. In this beam plate was anchored at both ends. With the increase of load strain gradient increases. Some gages show inproportionaley high strain, because of the cracking of the concrete beam. There is no drop in the plate strain at the ends that was observed in beams with unachored plates. Diagonal cracks appeared starting from the end of the plate but those cracks did not affect the strain distribution.

Figure 80 shows the strain distributions along plate at various load levels for beam B16. In this beam plate was anchored at both ends. With increasing load strain gradient increases. Some gages show inproportionateley high strain, because of the cracking of the concrete beam. There is no drop in strain that was observed in beams with unachored plates due to separation. Diagonal cracks appeared starting from the end of the plate but those cracks did not affect the strain distribution.

Figure 81 shows the strain distributions along plate for beam B23 at various load levels. On the left hand side of this diagram, the strain drops at 69.05 kN load. This is because of bond failure due to slip of plate at anchorage in this beam and the beam did not reach the full ultimate flexural capacity.

Figure 82 shows strain distributions along plate at various load levels for beam B22. At right hand side of the plate, there is drop in strain at 71.00 kN load. This drop in strain was due to the sudden appearance of the diagonal cracks. This beam could not reach the full flexural capacity.

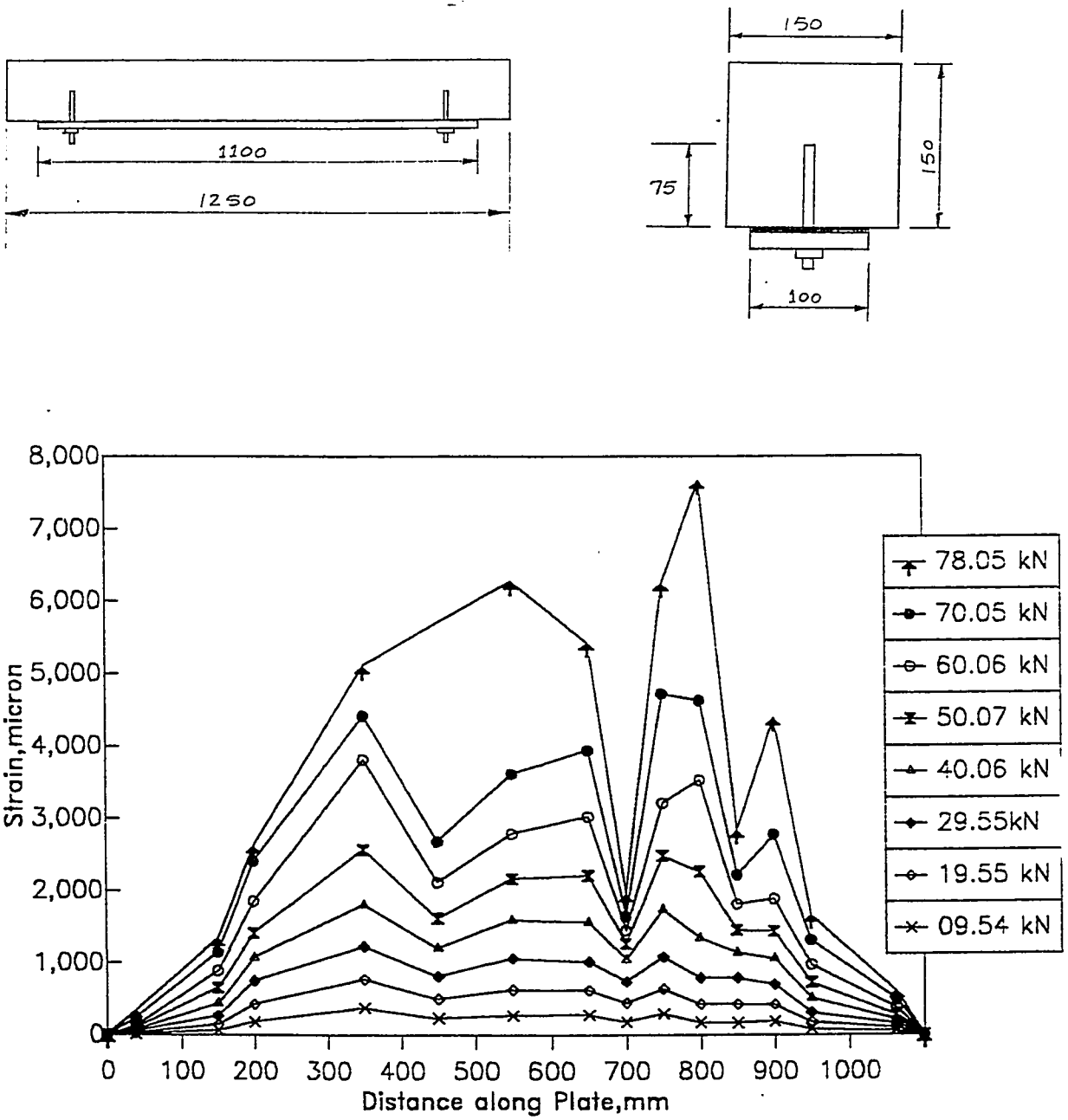

Figure 79: Strain distributions along plate for beam B11. This beam was strengthened by 1.5 mm thick, 100 mm wide and 1100 mm long plate. End anchorage was given to the plate.

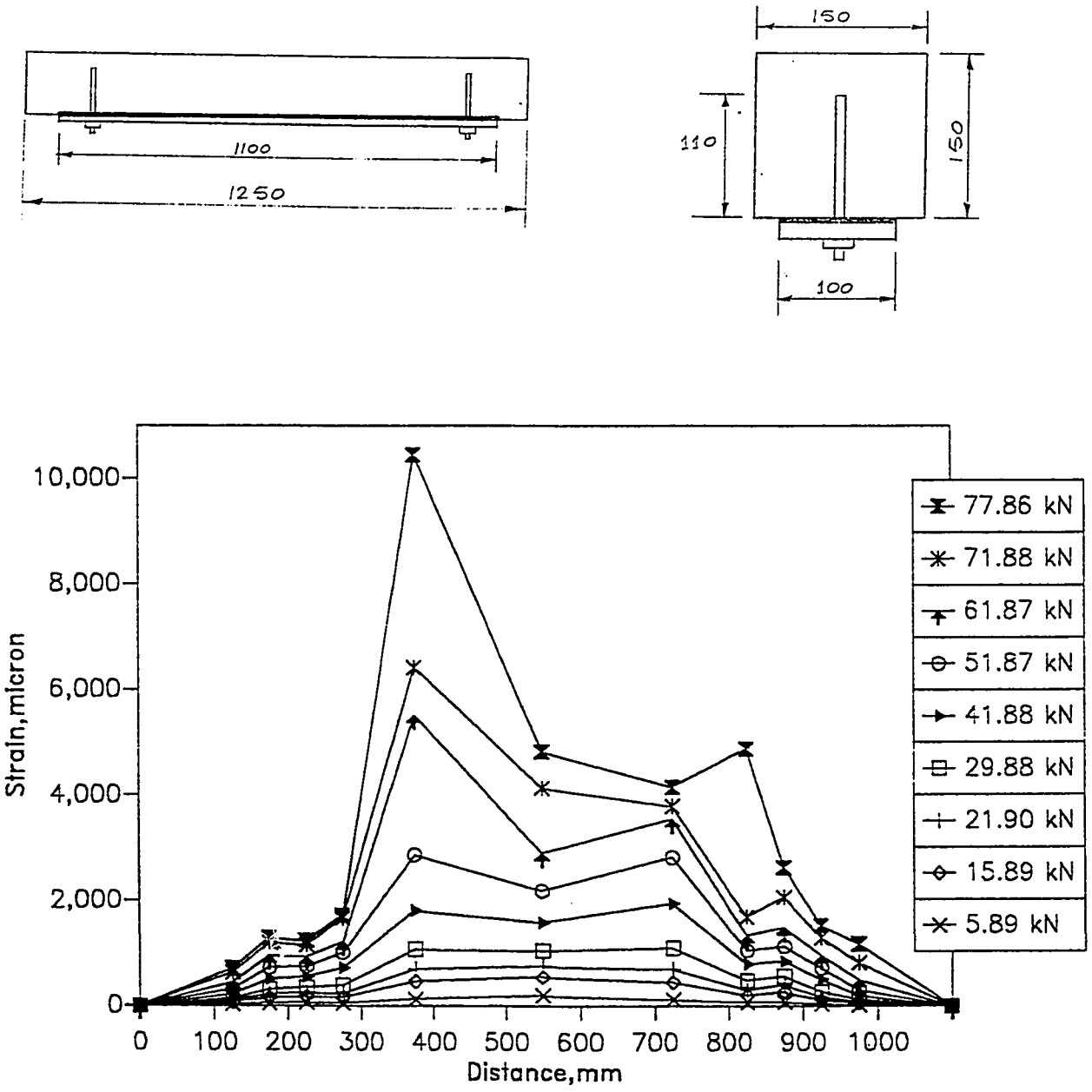

Figure 80: Strain distributions along plate for beam B16. This beam was strengthened by 1.5 mm thick, 100 mm wide and 1100 mm long plate. End anchorage was given to the plate.

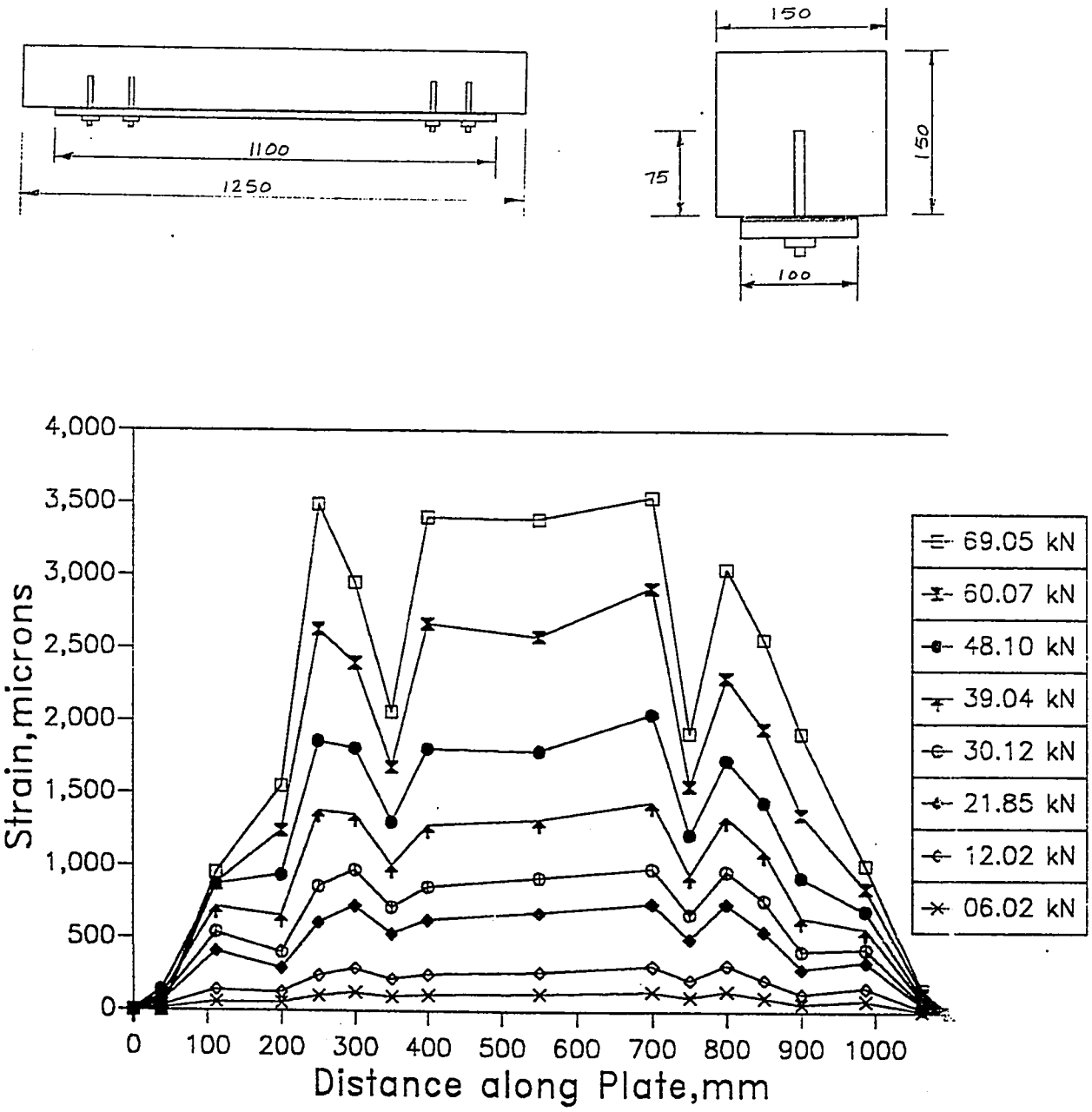

Figure 81: Strain distributions along plate for beam B23. This beam was strengthened by 1.5 mm thick, 100 mm wide and 1100 mm long plate. End anchorage was given to the plate.

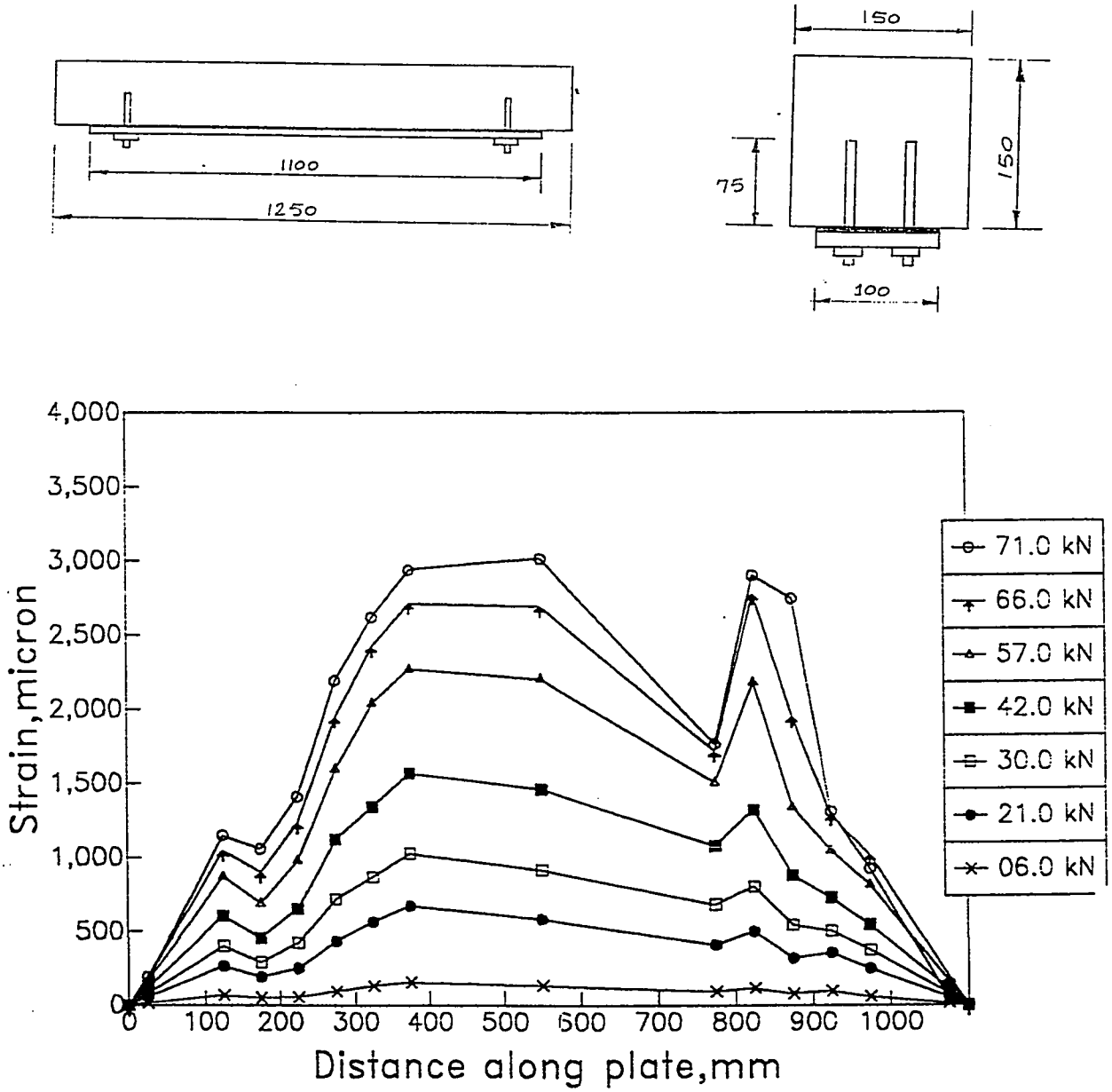

Figure 82: Strain distributions along plate for beam B22. This beam was strengthened by 1.5 mm thick, 100 mm wide and 1100 mm long plate. End anchorage was given to the plate.

4.7 EXTERNAL STRENGTHENING WITHOUT GLUE BUT ANCHOR BOLTS

Beams B3 and B18 were strengthened by 1.5 mm thick, 100 mm wide and 1100 mm long plates. In both of these beams only end anchorage was given to the plates by 75 mm anchor bolts. In these beams the plates were not bonded to the concrete beams. Figure 83 shows the load-deflection curves for beams B3, B11 and B17 respectivley. These curves represent the second cycle of loading, that is, these are the load deflection curves of the repaired beams. In beam B3 full flexure failure was obtained. However, the ultimate load for this beam was less than the corresponding ultimate loads for beams B11 and B17 respectively. The reason for obtaining less load for this beam is the presence of sag in the plate. The steel plate between the anchor bolts was not fully tight. The strain at the centre of the plate for beam B3 was much less than the corresponding mid-span plate strains of beams B11 and B17 respectively. If there had been no sag in the plate then the same flexure capacity could have been obtained as that of beam B11, that is, if the inner portion of the plate would have been filled with a non-adhesive filler. With the presence of the filler the full plate strain could have been obtained for beam B3. Similar testing was done by Madonald [29] . In his testing bonding of the plate was done at the ends only and the inner portion was filled with non-adhesive grease which resembles to our beam B3 with anchor bolts only. In this beam he obtained the same flexure capacity as in the beams with fully bonded plates but in the beam with partial bonding, crack width was high as compared to the beams with fully bonded plates.

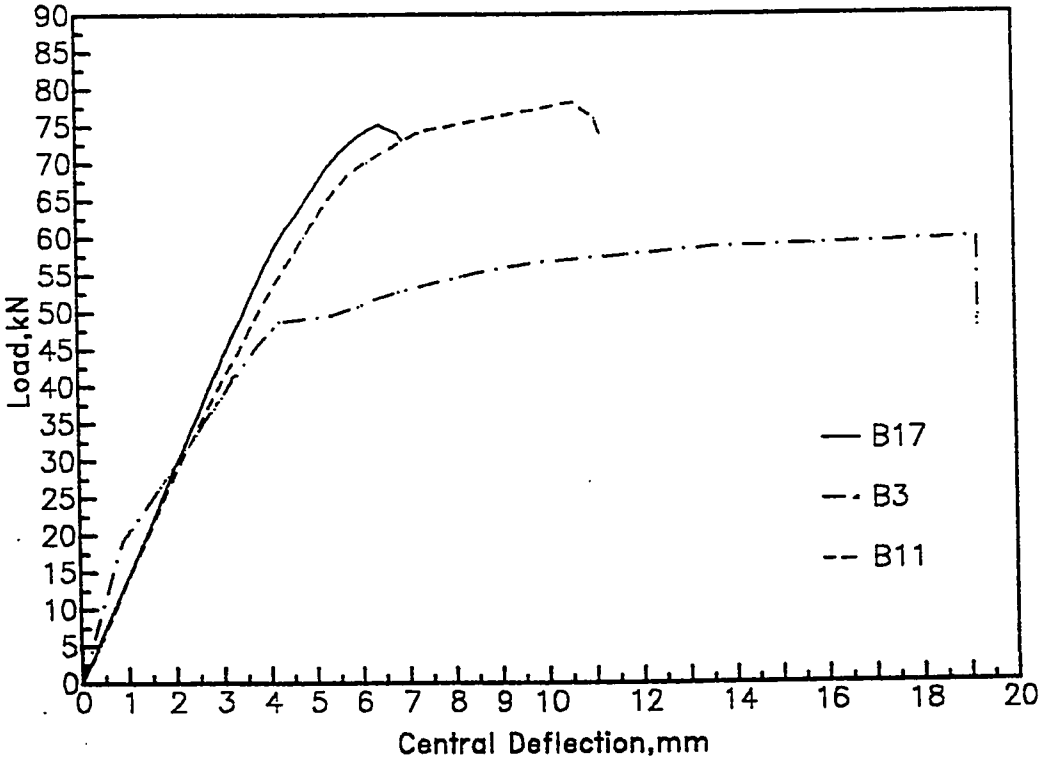

Figure 83: Load-deflection curves for beams B3, B11 and B17 respectivley. These beams were strengthened by 1.5 mm thick, 100 mm wide and 1100 mm long plates. In beam B3 plate was not bonded to the concrete beam. In beams B3 and B11 plates were anchored.

4.8 MODES OF FAILURE

In epoxy bonded plated beams pure flexure failure can be obtained if the plate thickness is small. Researchers like Macdonald [29] and Swamy [30] have suggested that b/t ratios for steel plates should be less than 60 and 50 respectively for getting pure flexure failure. In our case, pure flexure failure was obtained in beams B5 and B25 bonded with 1.00 mm thick steel plates and for these beams b/t ratio was 100. In beams B10 and B17 b/t ratios for the plates were 66.66. In these beams failure occurred by the separation of plates after the yielding of the plates.

In this section modes of failure for all the beams will be discussed.

1. BEAMS B6 AND B7

   Both of these were tested without strengthening. In both of these beams pure flexure failure was obtained.

2. BEAM B5 AND B25

   These beam were strengthened by 1.00 mm thick, 100 mm wide and 1100 mm long plates. No end anchorage was given to the plates in these beam. In both of these beams pure flexure failure was obtained. At failure steel plates were yielding in both of these beams.

   Figure 84 shows the mode of failure of beam B25. In this beam pure flexure failure was obtained.

   Figure 85 shows the load vs strains 5, 6 and 7 for the beam B25. The drop in strains takes place due to the failure of the beam in the flexure mode.

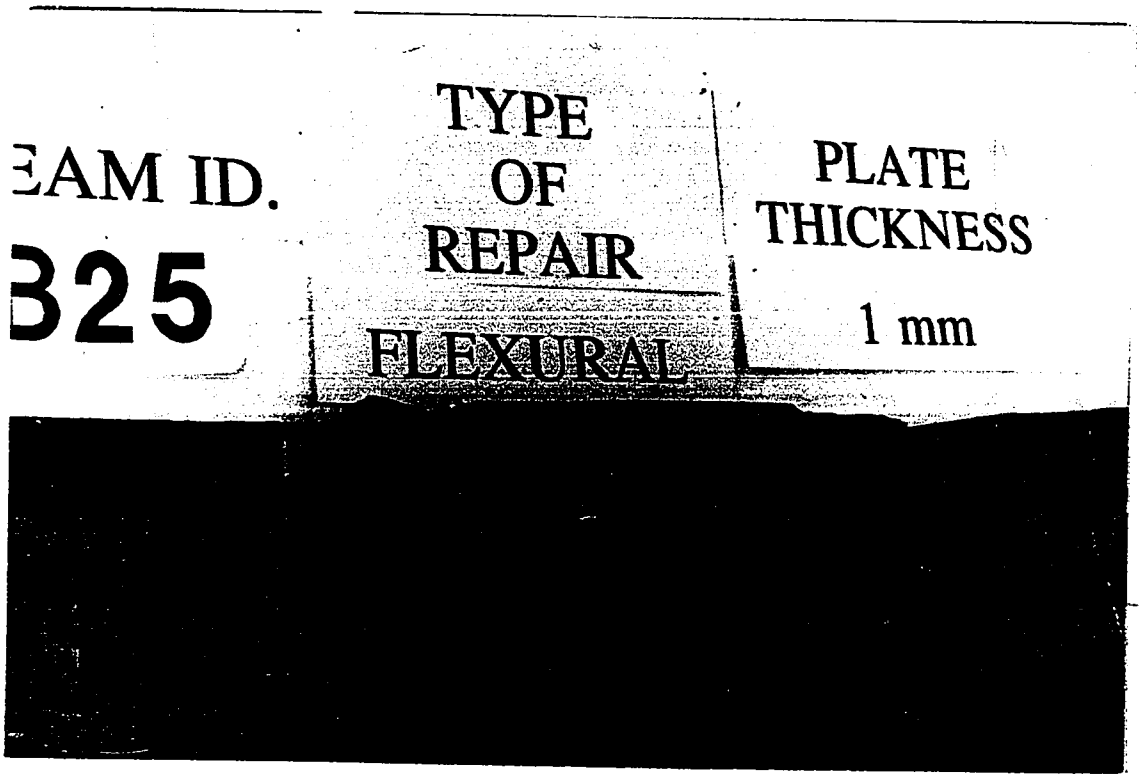

Figure 84: Photograph showing the mode of failure for beam B25. This beam was strengthened by 1.00 mm thick, 100 mm wide and 1100 mm long plate. No end anchorage was given to the plate.

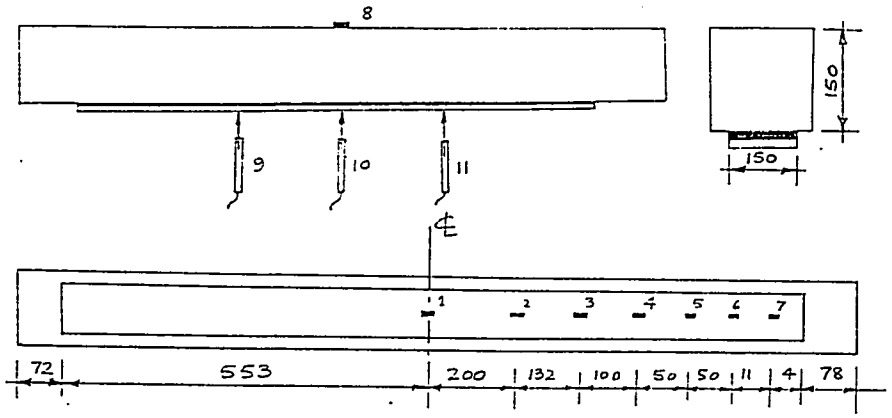

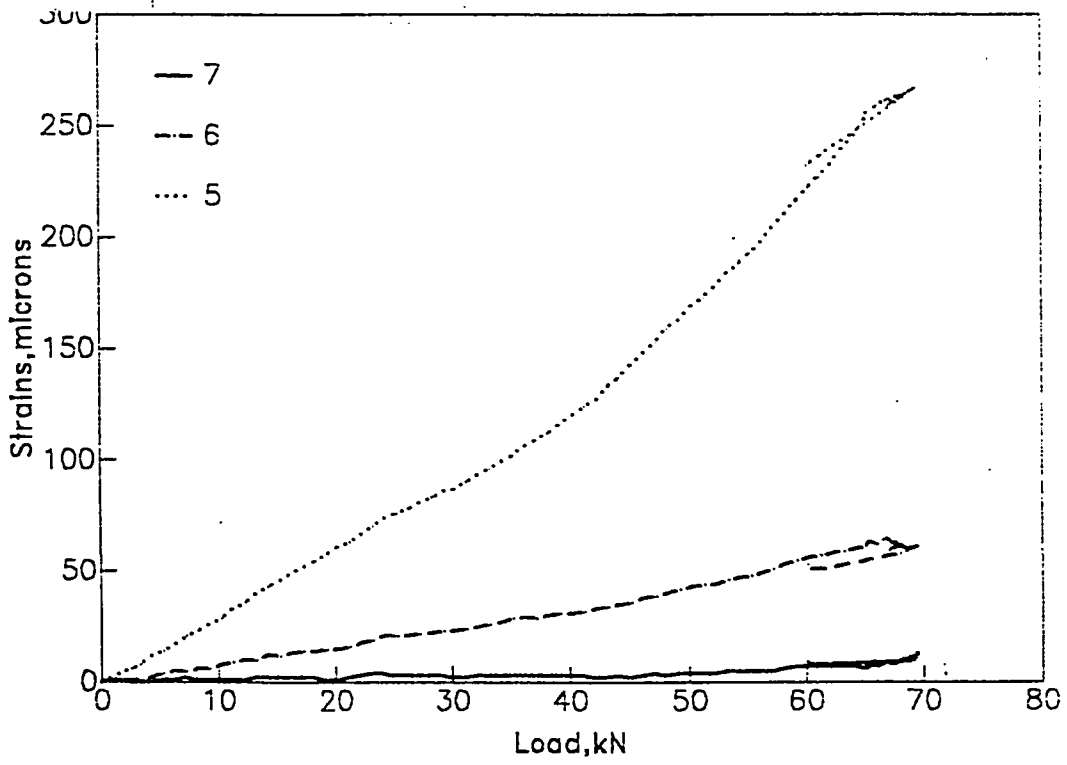

Figure 85: Load vs strains 5, 6 and 7 for beam B25. This beam was strengthened by 1.00 mm thick, 100 mm wide and 1100 mm long plate. No end anchorage was given to the plate.

Figure 86 shows plate strains 5, 6 and 7 vs central deflection for beam B25. This figure shows that after about 4.6 mm central deflection the increase in strain with deflection becomes minimum. The drop in these strains takes place when the beam fails in flexure mode.

3. BEAMS B10 AND B17

These beams were strengthened by 1.5 mm thick, 100 mm wide and 1100 mm long steel plates.

a. In beam B10 the failure occurred due to the separation of the plate. The plate separated at the end over a small length at the glueline and then diagonal crack appeared in the concrete. With the appearance of diagonal cracks, the strains 2, 3 and 4 drop as shown in the Figure 87 . During the testing of this beam diagonal crack was observed at 62 kN load.

Figure 88 shows the mode of failure of beam B10.

b. Beam B17 also failed prematurely due to the separation of the plate after the yielding of the plate. In this beam diagonal crack starting from the end of the plate was observed at 59.10 kN load. Separation of the plate at the end of the plate was observed at 75 kN load and then propagated towards the centre. The separation of the plate took place upto the point load. This separation was above the glueline. Separation of the plate was on the side on which gages 1, 2 and 3 were installed. Figure 89 shows load vs strains 1, 2 and 3 for beam B17.

Figure 90 shows load vs strains 5, 6 and 7 for beam B17.

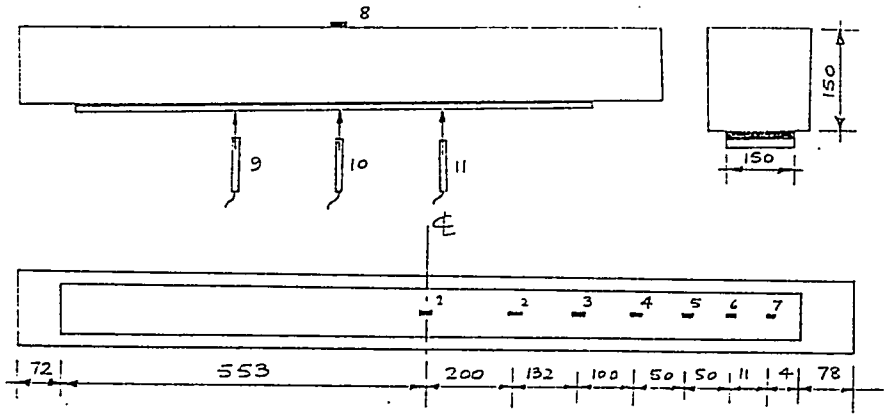

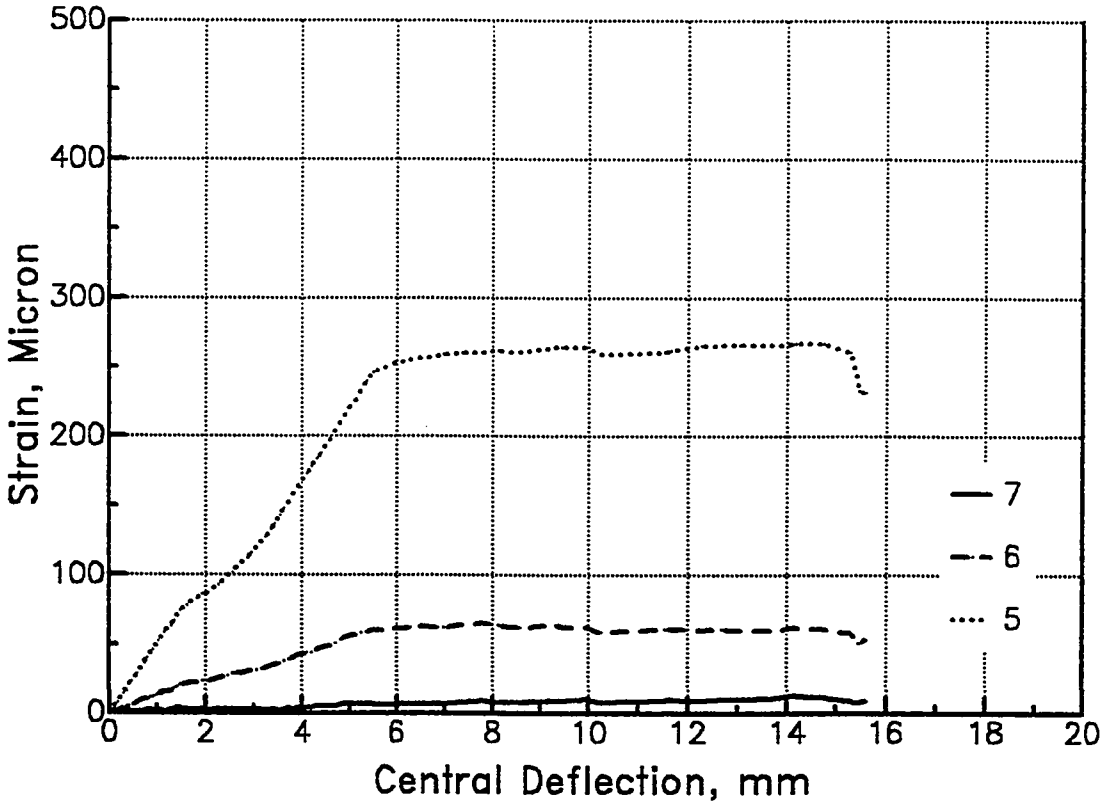

Figure 86: Strains 5, 6 and 7 vs central deflection for beam B25. This beam was strengthened by 1.00 mm thick, 100 mm wide and 1100 long plate. No end anchorage was given to the plate.

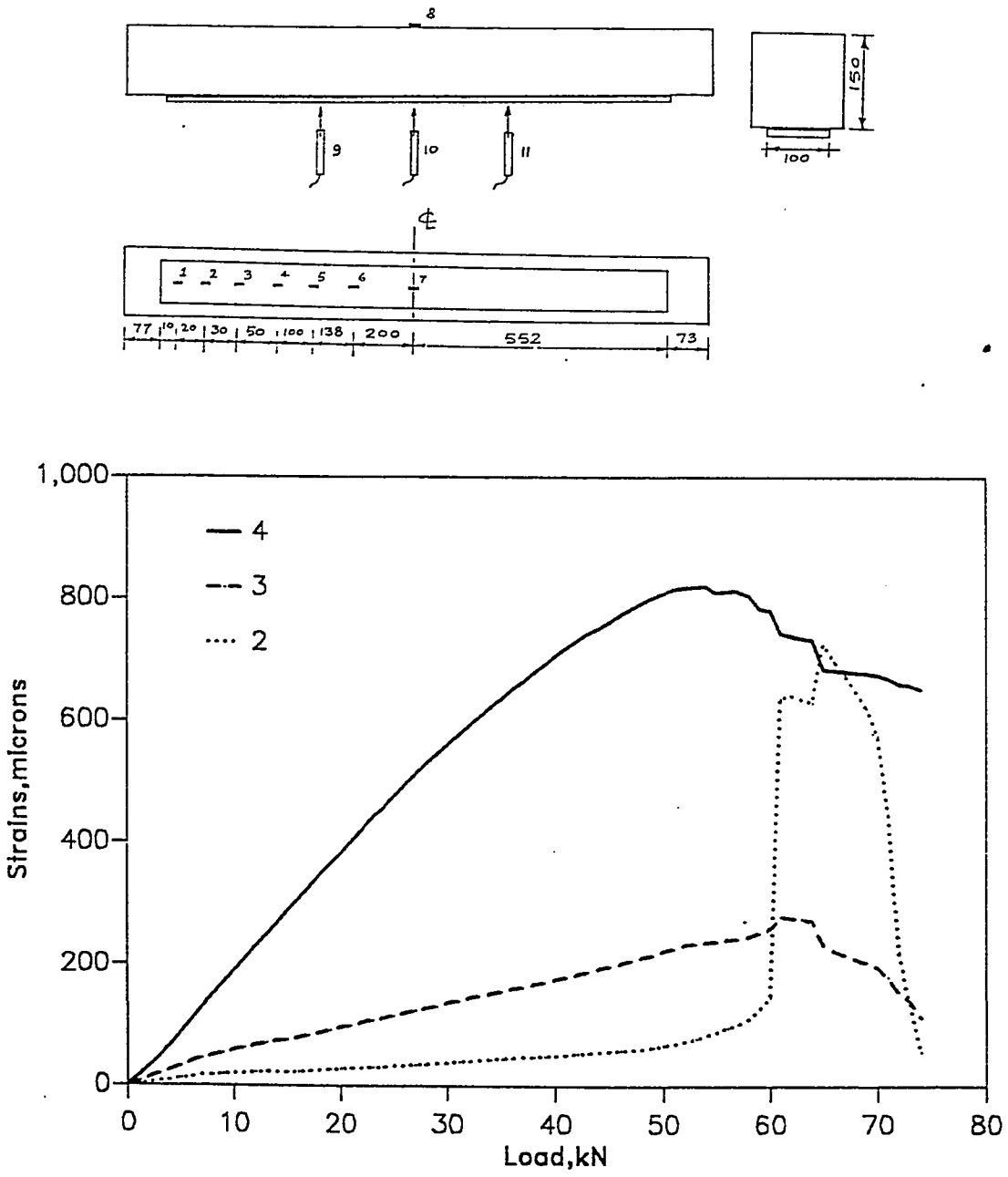

Figure 87: Load vs strains 2, 3 and 4 for beam B10. This beam was strengthened by 1.5 mm thick, 100 mm wide and 1100 mm long plates. No end anchorage was given to the plate.

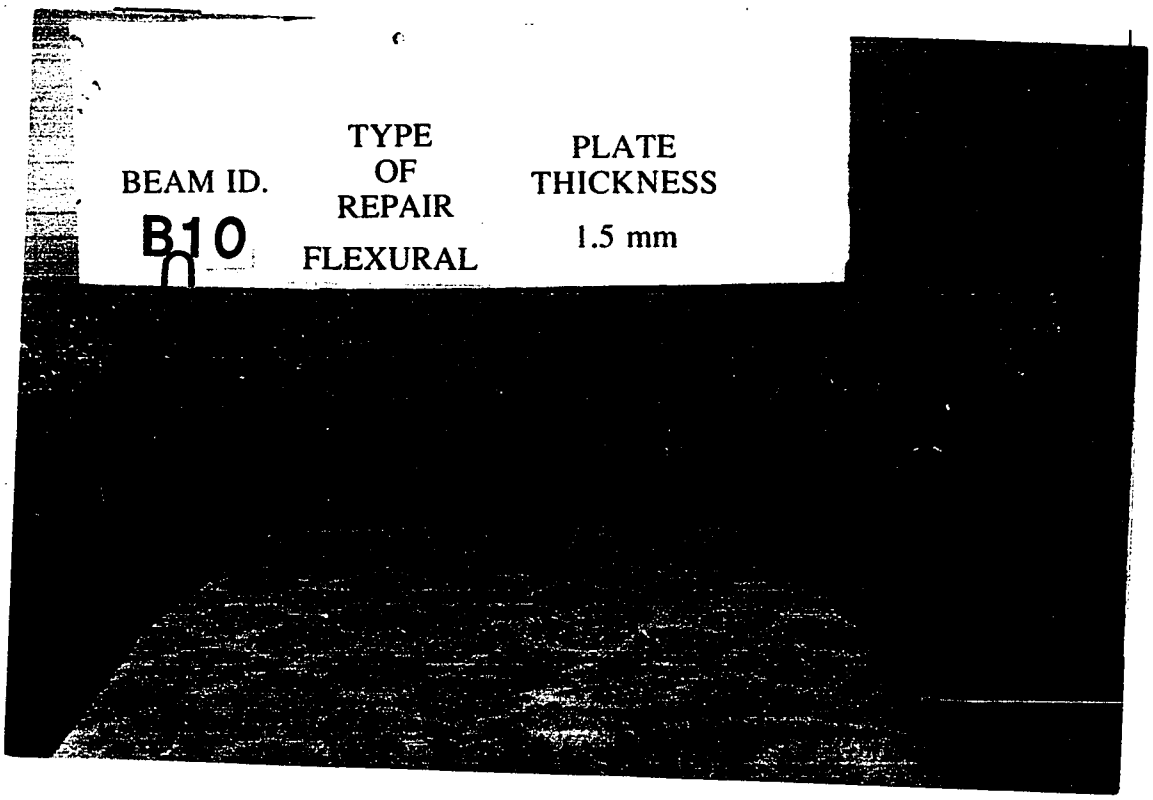

Figure 88: Photograph showing the mode of failure for B10. This beam was strengthened by 1.5 mm thick, 100 mm wide and 1100 mm long plate. No end anchorage was given to the plate.

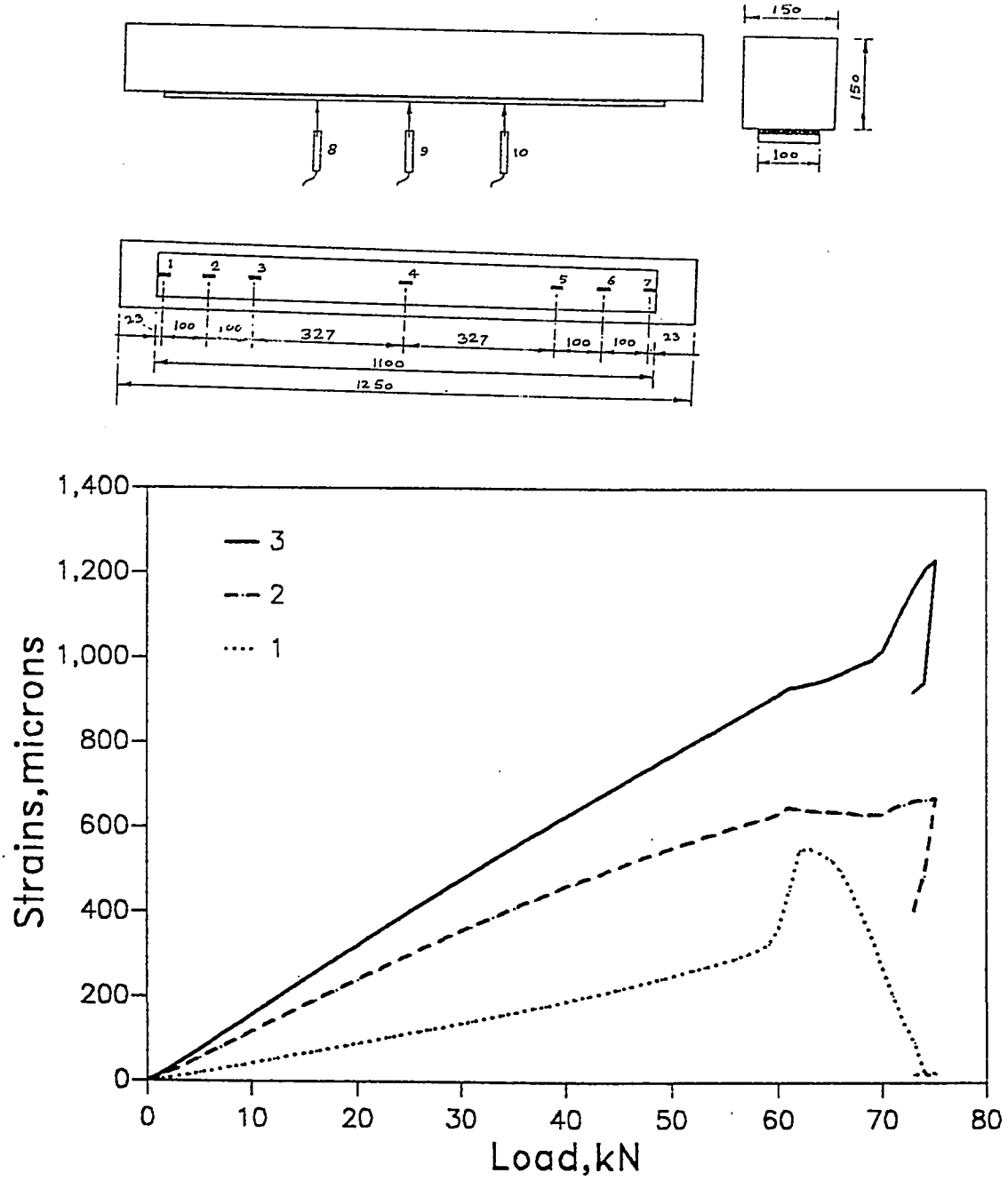

Figure 89: Load vs strains 1, 2 and 3 for beam B17. This beam was strengthened by 1.5 mm thick, 100 mm wide and 1100 mm long plate. No end anchorage was given to the plate.

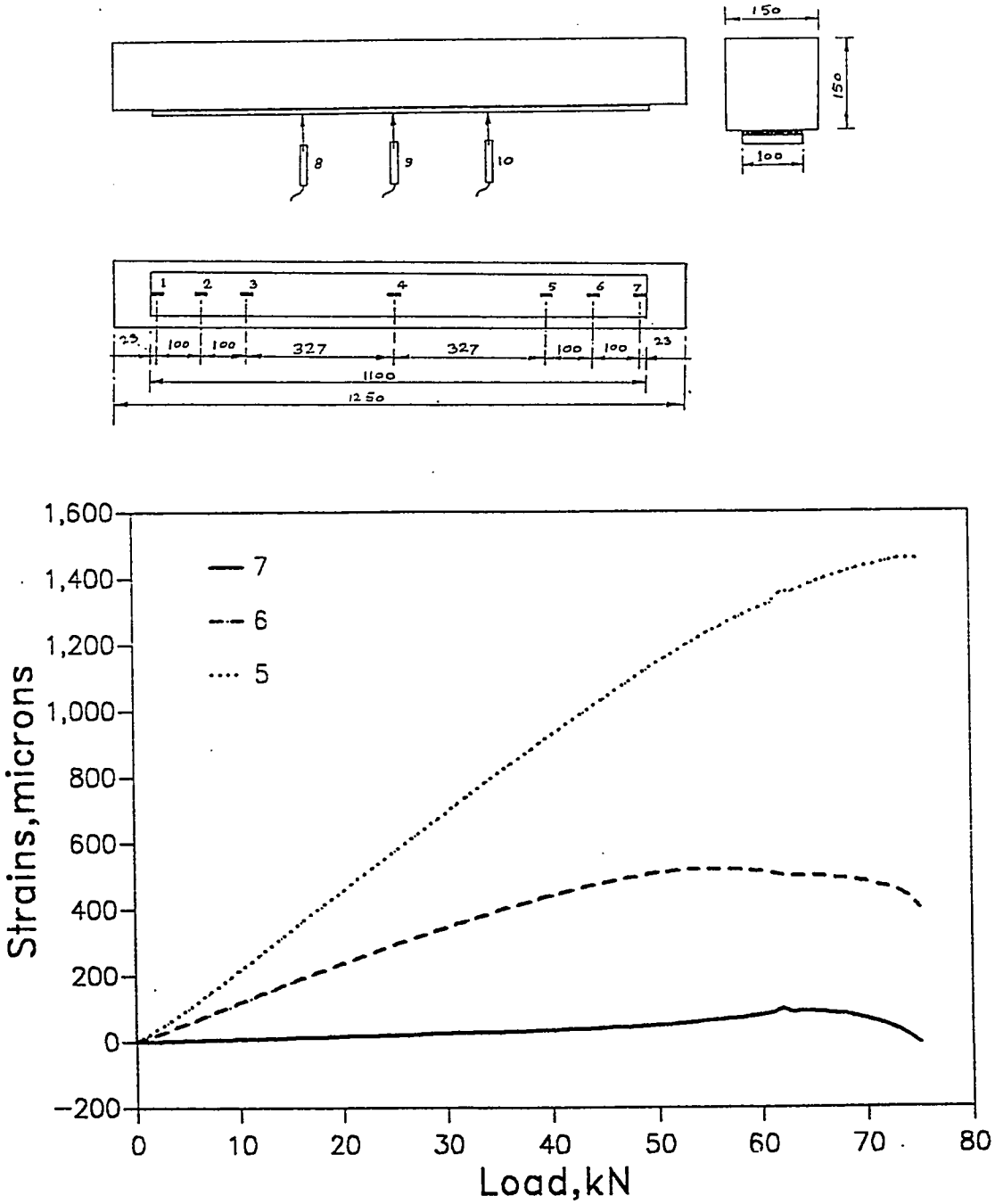

Figure 90: Load vs strains 5, 6 and 7 for beam B17. This beam was strengthened by 1.5 mm thick, 100 mm wide and 1100 mm long plate. No end anchorage was given to the plate.

4. BEAM B8

This beam was strengthened by 2.00 mm thick, 100 mm wide and 1000 mm long steel plate. In this beam failure took place due to the separation of the plate. The separation was not at the glueline. The separation of the plate was due to the tearing of the concrete above the glueline. In this beam the plate was not symmetrically bonded. On right hand side the distance between the centre of the beam and the end of the plate was 494 mm and on the left hand side the distance between the centre of the beam and the end of the plate was 512 mm. Due to this unsymmetry of the plate, the separation of the plate was expected at the right end of the plate. According to the expectation the separation of the plate took place at the right end of the plate. Strain gages 11, 12 and 13 were installed on the right end of the plate and strain gages 1, 2 and 4 were installed on the left hand end of the plate. Figure 91 shows the load vs plate strains 11, 12 and 13. The separation of the plate took place on this side. The drop in the strains 11, 12 and 13 at about 48 kN load is due to the separation of the plate.

Figure 92 shows the load vs plate strains 1, 2 and 3 for this beam. This figure shows a drop in strains 1, 2 and 3 at about 43 kN load. Drop in strains 1, 2 and 3 is mild as compared to the drop in strains on the other end of plate. This drop in strains 1, 2 and 3 is due to the local separation of the plate at the glueline.

Figure 93 shows the mode of failure for beam B8.

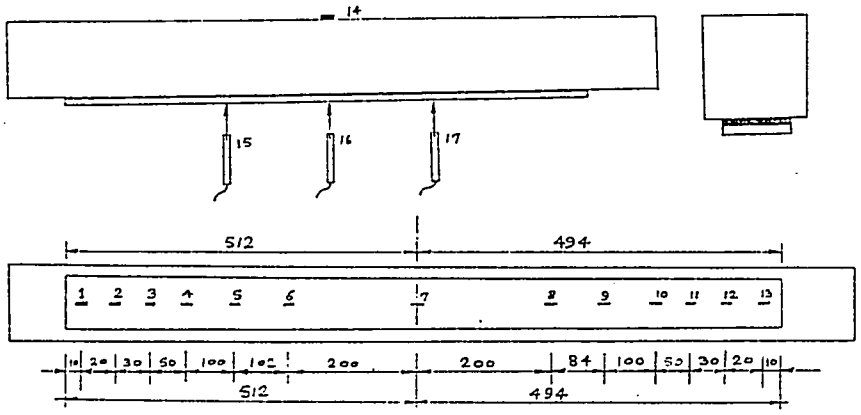

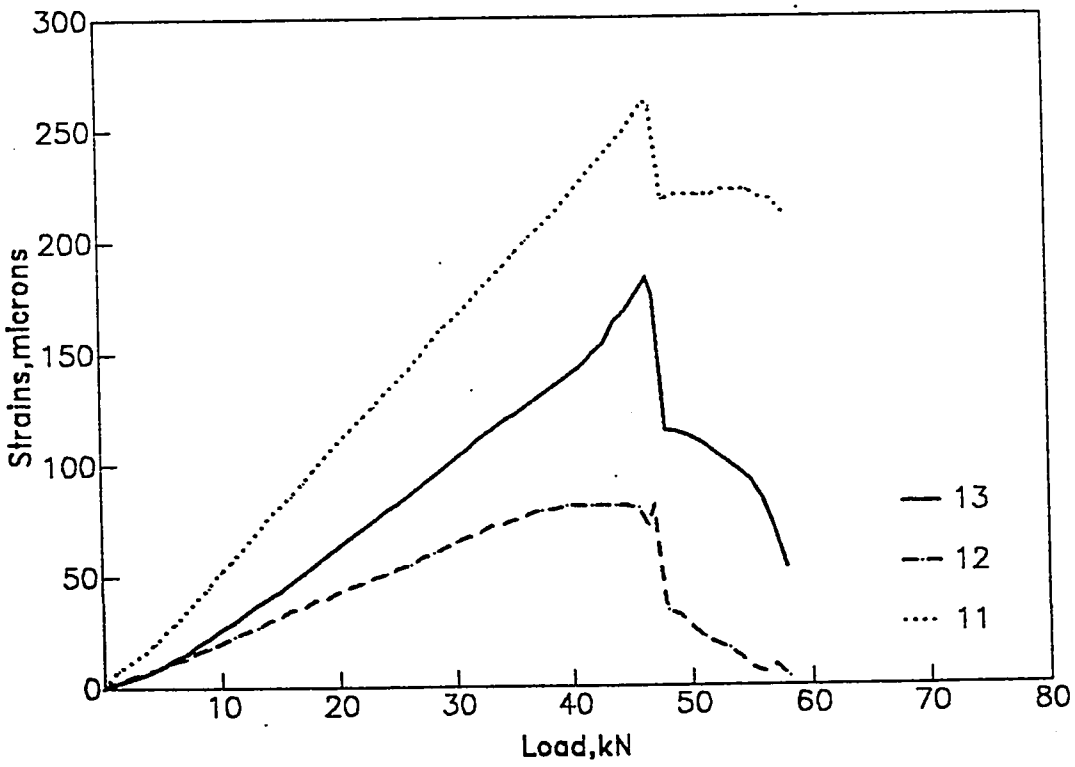

Figure 91: Load vs strains 11, 12 and 13 for B8. This beam was strengthened by 2.00 mm thick, 100 mm wide and 1000 mm long plate. No end anchorage was given to the plate.

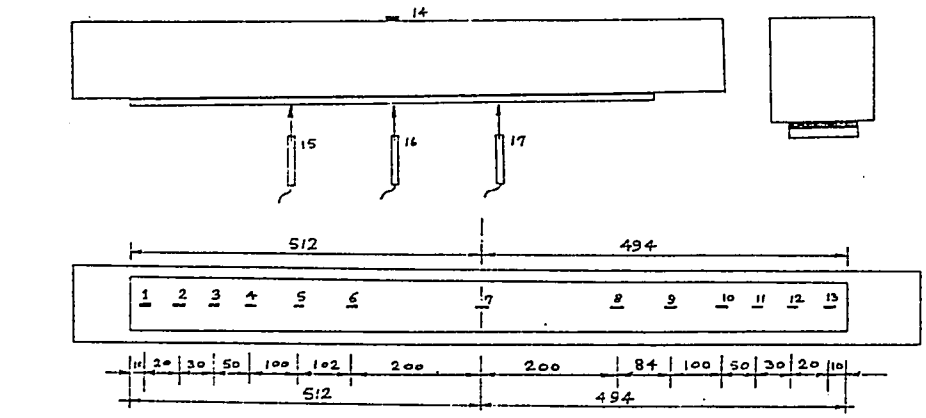

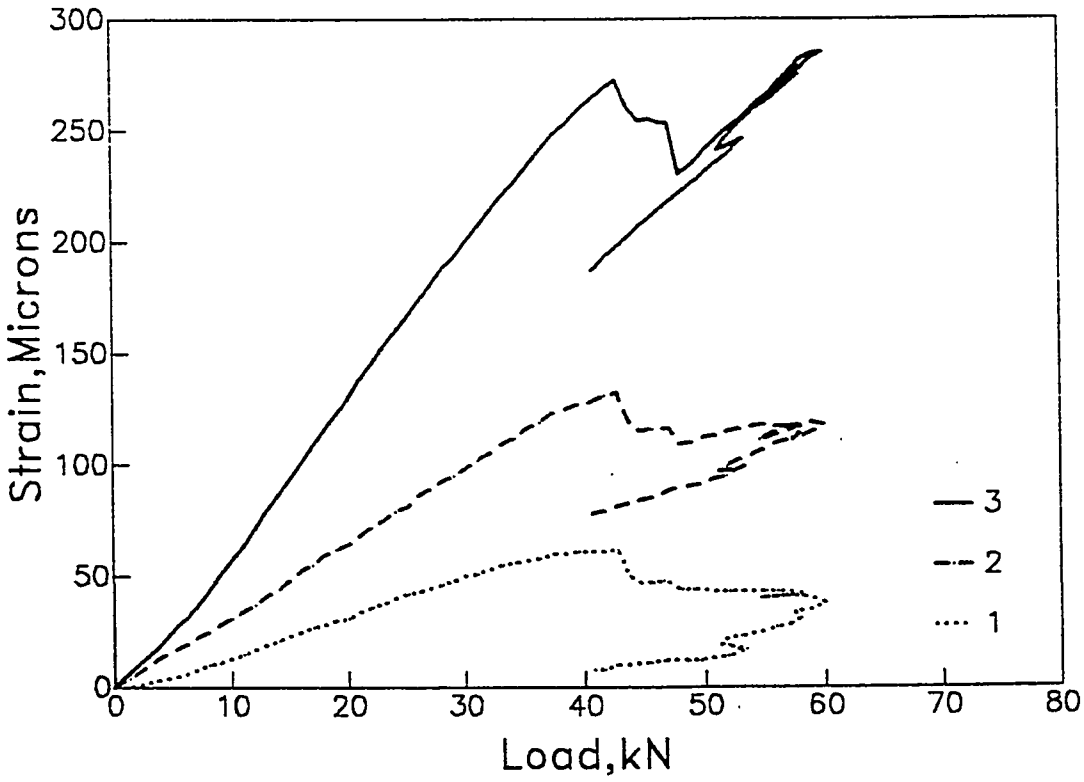

Figure 92: Load vs strains 1, 2 and 3 for B8. This beam was strengthened by 2.00 mm thick, 100 mm wide and 1000 mm long plate. No end anchorage was given to the plate.

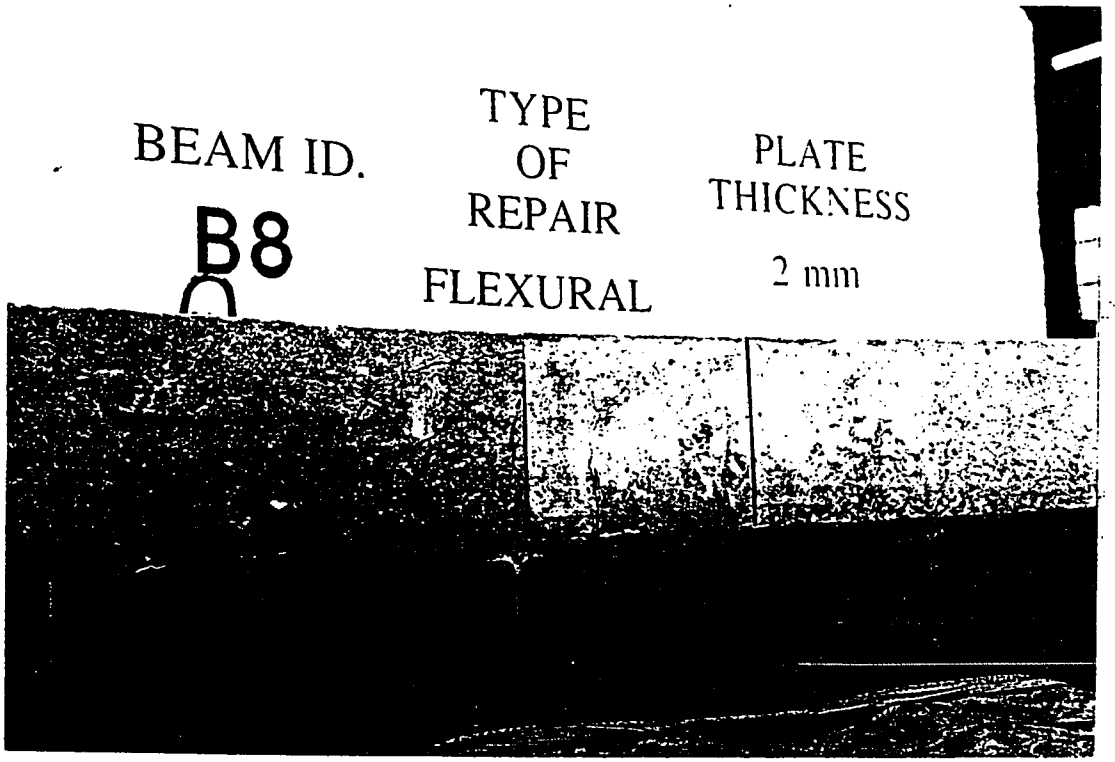

Figure 93: Photograpth showing the mode of failure of beam B8. This beam was strengthened by 2.00 mm thick, 100 mm wide and 1000 mm long plate. No end anchorage was given to the plate.

5. BEAM B4

This beam was strengthened with 2.00 mm thick, 100 mm wide and 1100 mm long steel plate. End anchorage was given to the plate. The beam failed by flexural crushing of the concrete at the mid-span. The experimental ultimate load for this beam was less than the theoretical ultimate load calculated based on the actual stress strain curves of the steels assuming full composite action of the steel plate with the concrete beam. Although the plate was anchored at both ends, the plate could not be strained upto yield strain during the loading of the beam. Slip occurred at the interface. The steel plate could not contribute fully to the strength of the beam.

6. BEAM B1

This beam was strengthened by 3.00 mm thick, 100 mm wide and 1000 mm long plate. The steel plate was not bonded symmetrically with respect to the centre of the beam. The failure took place due to the tearing of the concrete above the glueline on the end on which the distance between the support and the plate was more. Figure 94 shows the mode of failure for beam B1.

Figure 95 shows load vs strains 1, 3 and 4 for beam B1. The drop in strains 3 and 4 at about 53 kN load is due to separation of the plate. The drop in strain 1 at about 30 kN load may be due to the peeling stresses which try to bend the plate away from the concrete beam.

Figure 96 shows load vs plate strains 13, 14 and 15 for beam B1. On this side of the beam no separation of the plate was observed.

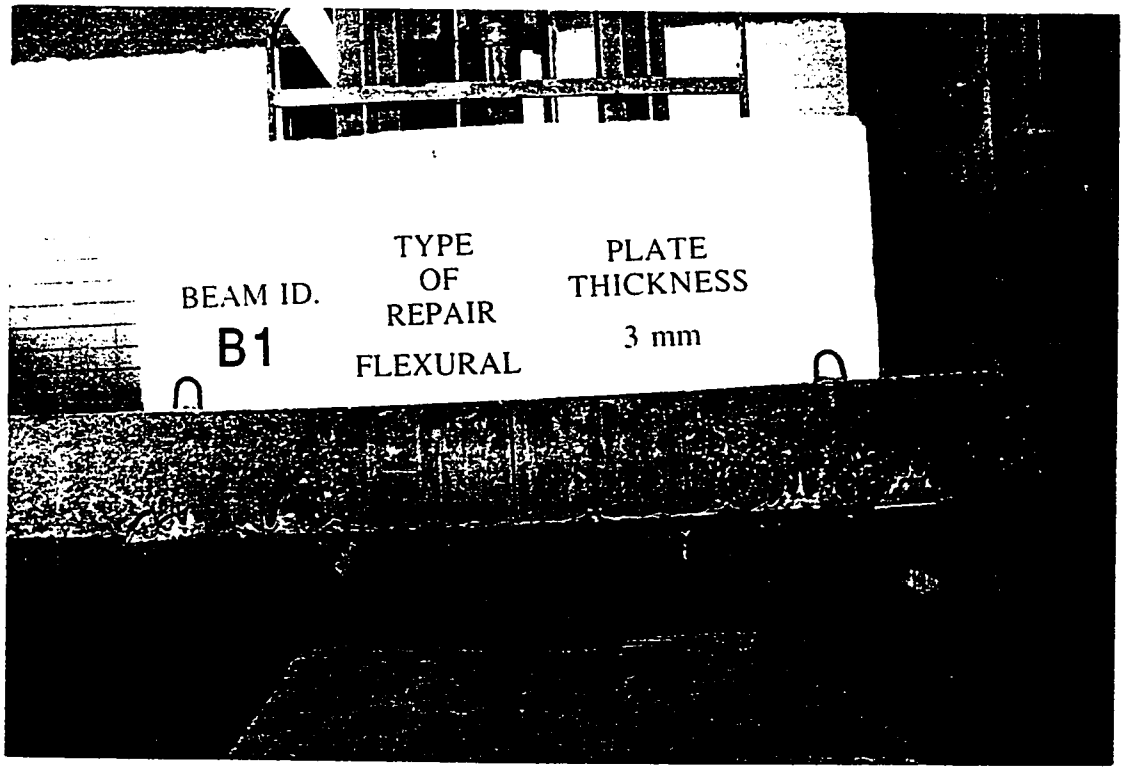

Figure 94: Photograph showing the mode of failure for beam B1. This beam was strengthened by 3.00 mm thick, 100 mm wide and 1000 mm long plate. No end anchorage was given to the plate.

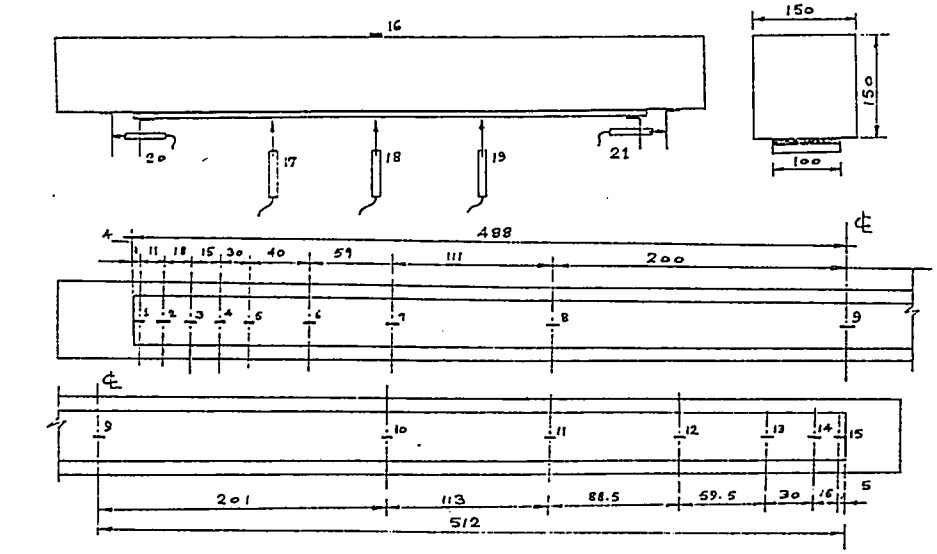

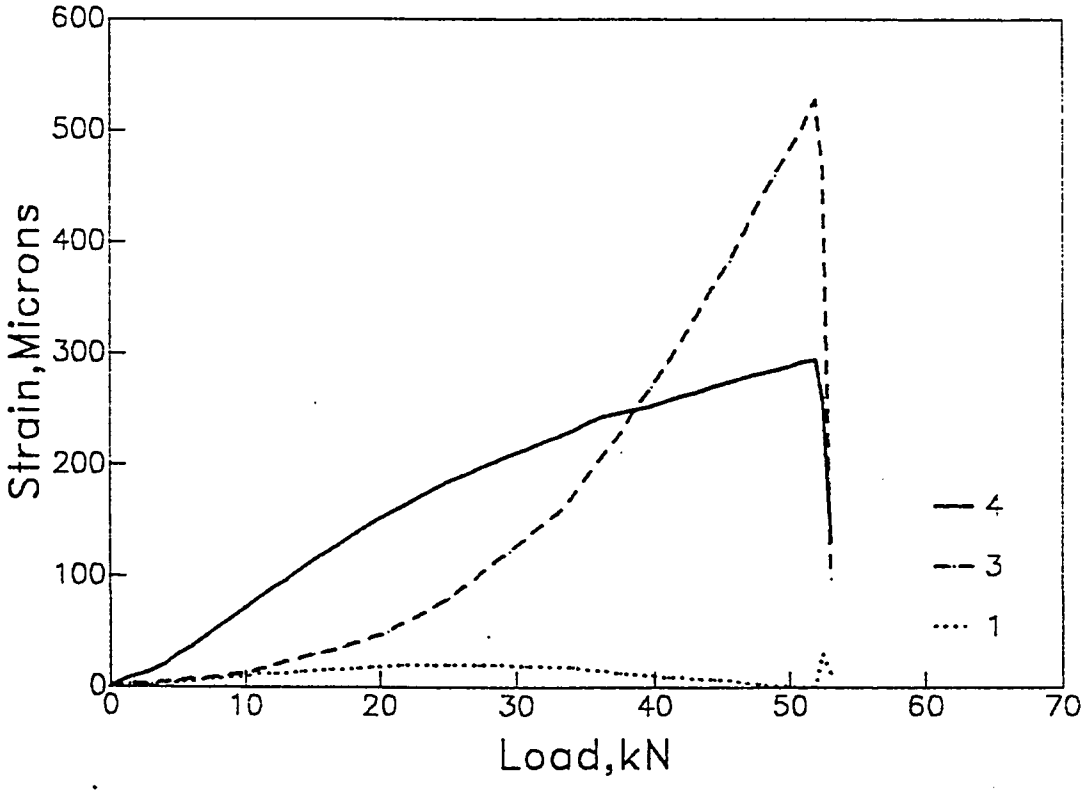

Figure 95: Load vs strains 1, 3 and 4 for beam B1. This beam was strengthended by 3.00 mm thick, 100 mm wide and 1000 mm long plate. No end anchorage was given to the plate.

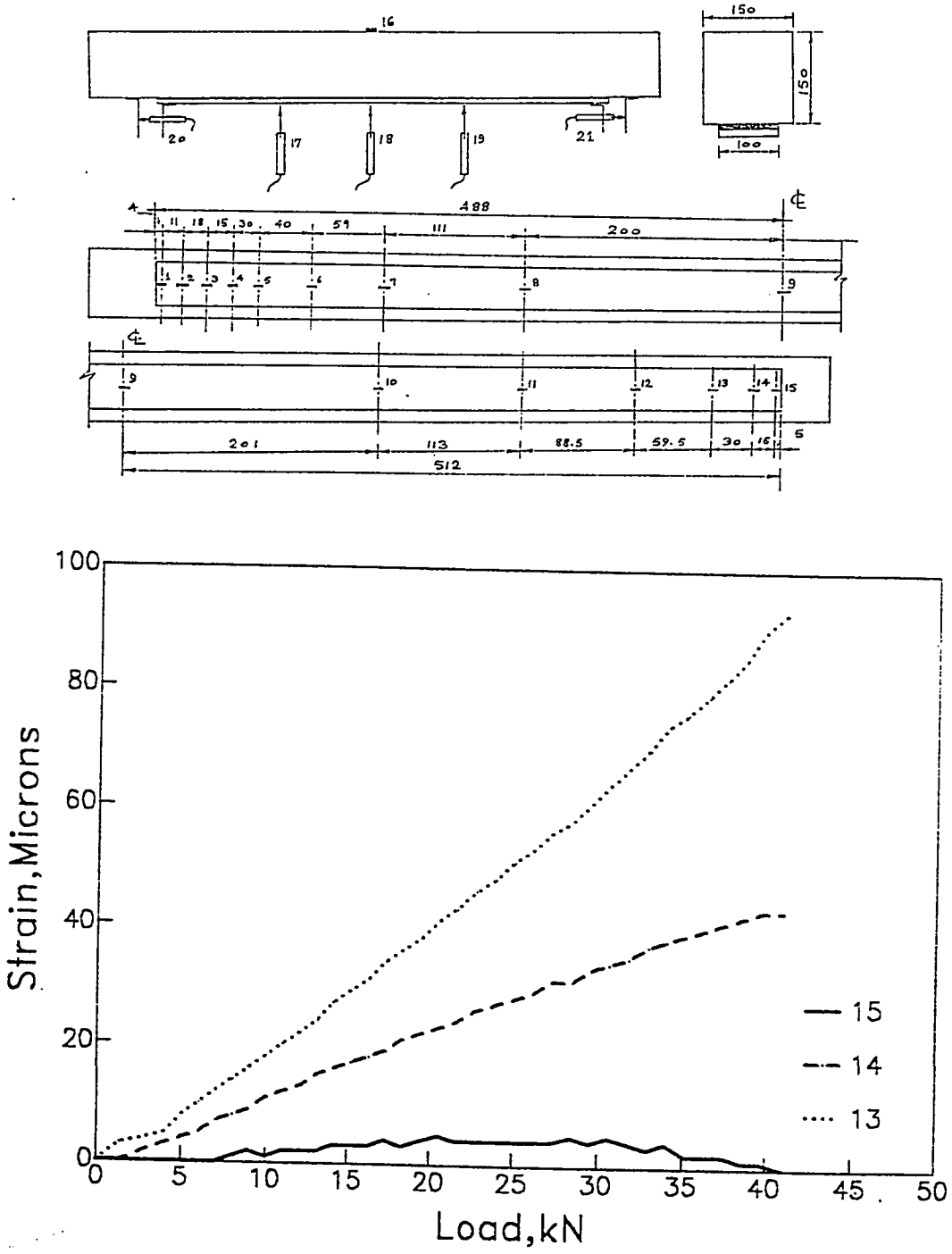

Figure 96: Load vs strains 13, 14 and 15 for beam B1. This beam was strengthended by 3.00 mm thick, 100 mm wide and 1000 mm long plate. No end anchorage was given to the plate.

7. BEAMS B11 AND B13

Both of these beams were strengthened by 1.5 mm thick, 100 mm wide and 1100 mm long plates. End anchorage was given to the plates. The modes of failures of these beams are explained below.

a. In beam B11 the failure was due to the appearance of the diagonal crack. With subsequent loading the crack started to open up and the load started to decrease. Figure 97 shows load vs strains 9, 10 and 13 for beam B11.

Figure 98 shows load vs strains 19, 20 and 23 for beam B11.

b. In beam B13 same type of failure occurred as in beam B11.

8. BEAMS B14 AND B16

Both of these beams were strengthened by 1.5 mm thick, 100 mm wide and 1100 mm long plates. End anchorage was given to the plates in both of these beams.

a. In beam B14, first the diagonal crack starting from the end of the plate appeared and with subsequent loading the beam went in the compression failure as shown in the Figure 99

b. In beam B16, failure took place due to the appearance of the diagonal cracks at both ends of the plate. With subsequent loading the cracks tried to open up further. Figure 100 shows the load vs plate strains 6, 7 and 8. Drop in the strains and load takes place simultaneuosly.

Figure 101 shows load vs strains 13, 14 and 15 for beam B16. Drop in these strains and loads takes place simultaneously.

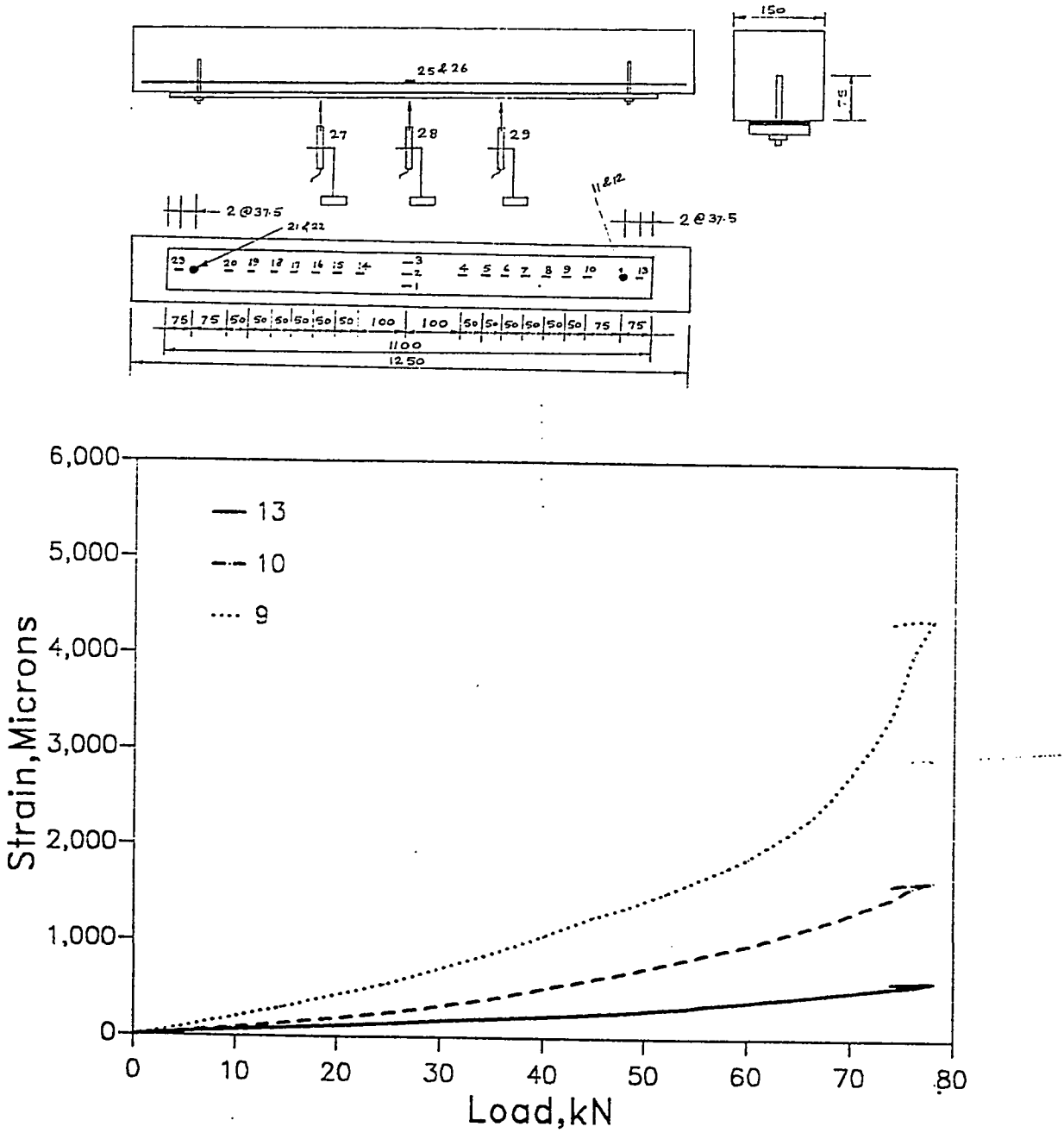

Figure 97: Load vs strains 9, 10 and 13 for beam B11. This beam was strengthened by 1.5 mm thick, 100 mm wide and 1100 mm long plate. End anchorage was given to the plate.

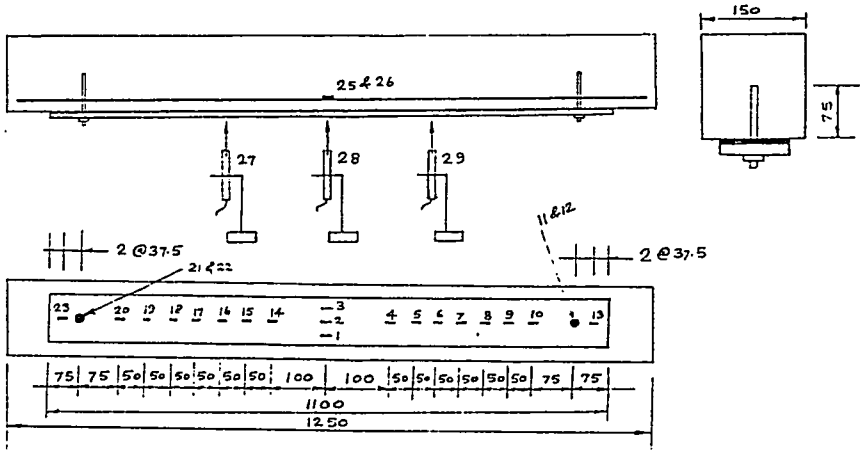

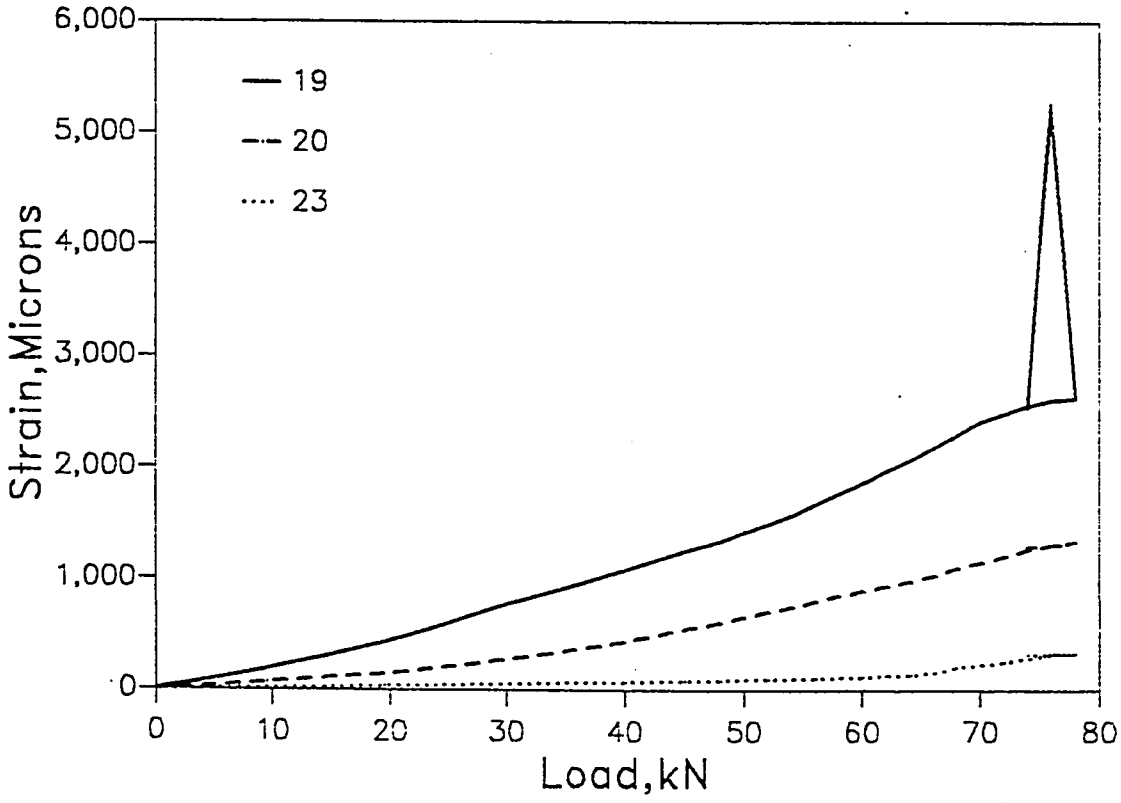

Figure 98: Load vs strains 19, 20 and 23 for beam B11. This beam was strengthened by 1.5 mm thick, 100 mm wide and 1100 mm long plate. End anchorage was given to the plate.

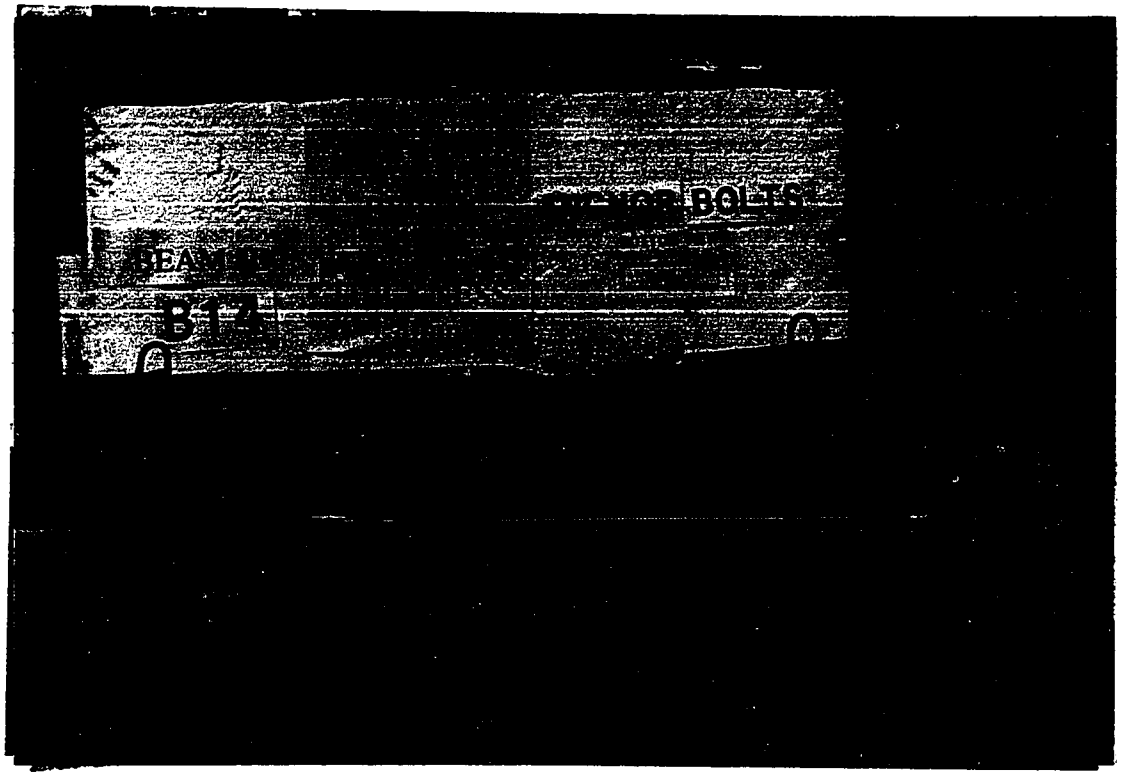

Figure 99: Photograph showing the mode of failure for beam B14. This beam was strengthened by 1.5 mm thick, 100 mm wide and 1100 mm long plate. End anchorage was given to the plate.

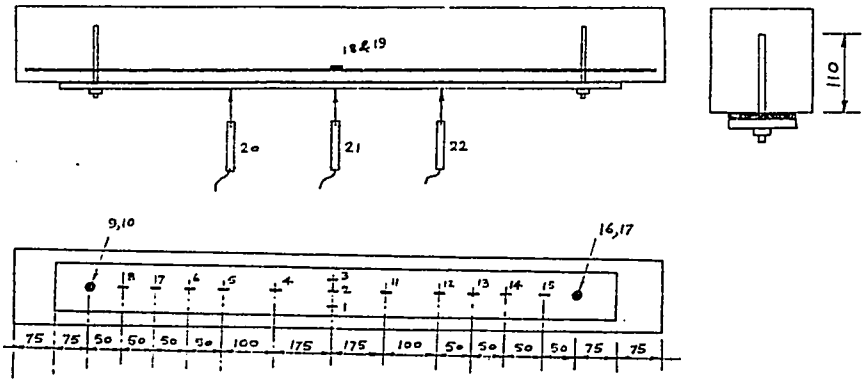

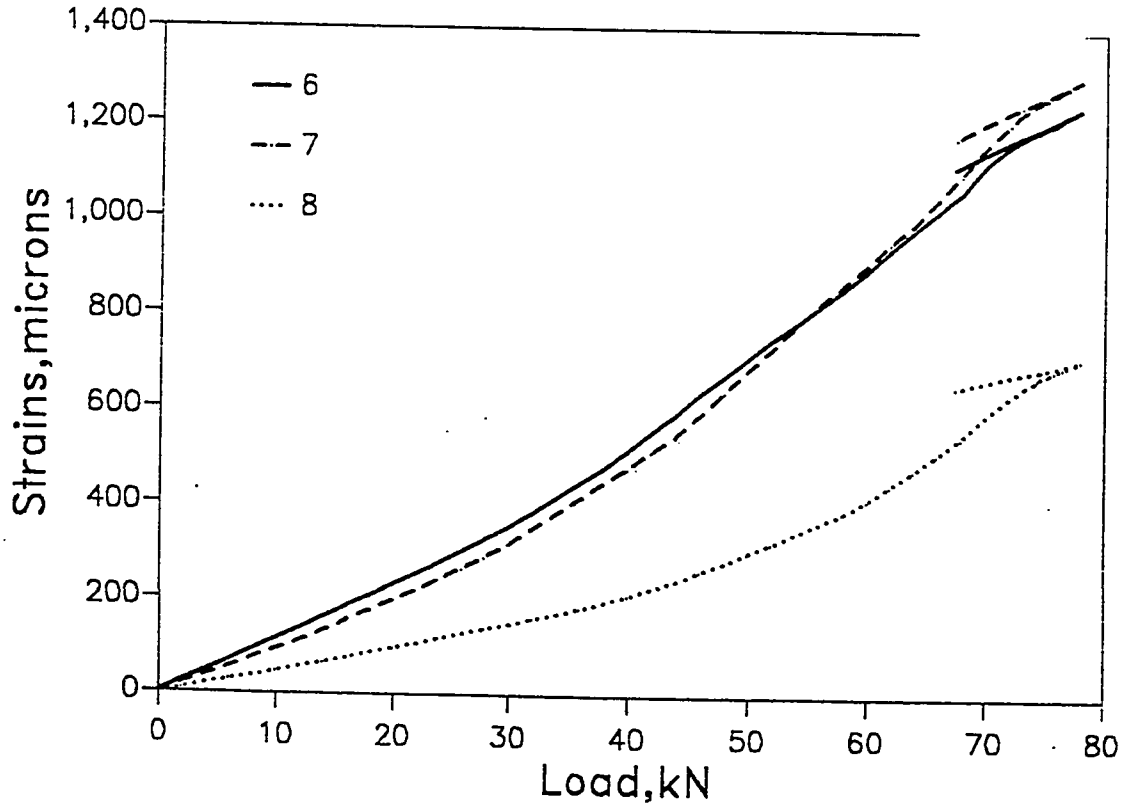

Figure 100: Load vs strains 6, 7 and 8 for beam B16. This beam was strengthened by 1.5 mm thick, 100 mm wide and 1100 mm long plate. End anchorage was given to the plate.

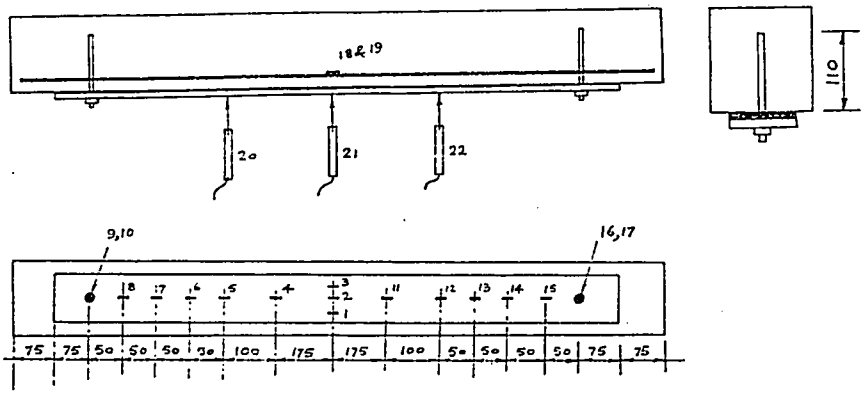

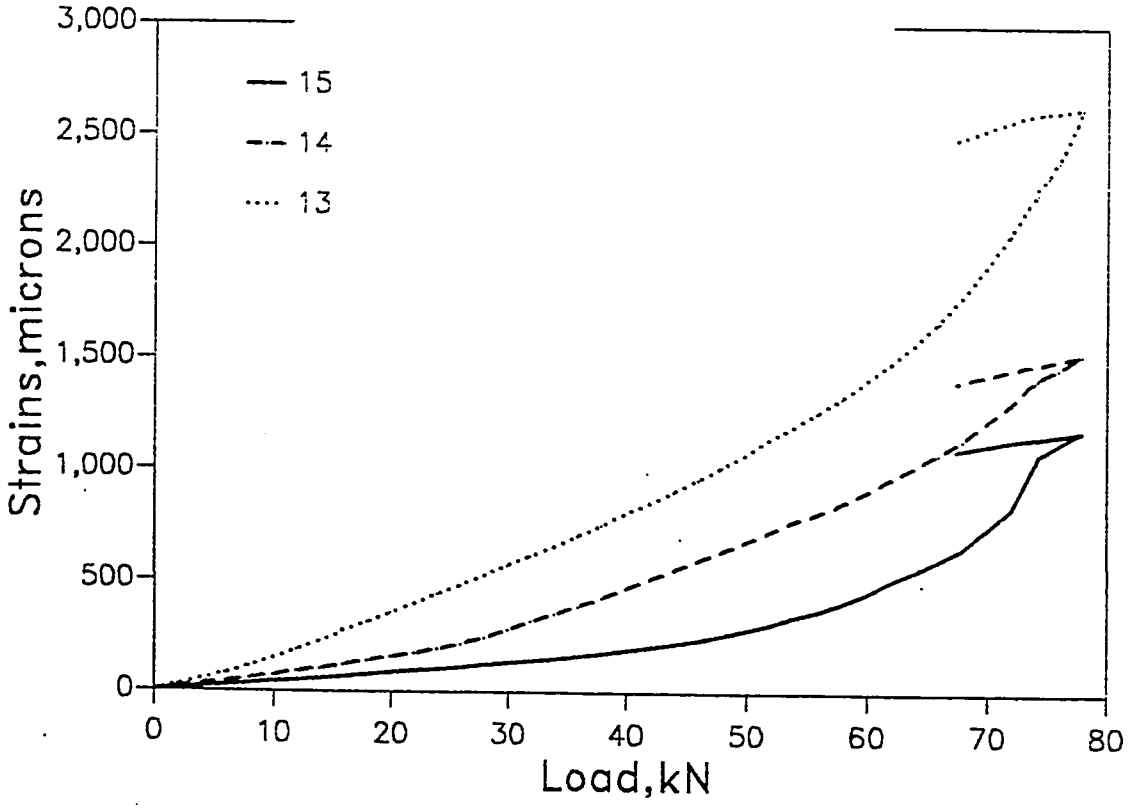

Figure 101: Load vs strains 13, 14 and 15 for beam B16. This beam was strengthened by 1.5 mm thick, 100 mm wide and 1100 mm long plate. End anchorage was given to the plate.

9. BEAMS B21 AND B24

These beams were strengthened by 1.5 mm thick plates, 100 mm wide and 1100 mm long plate. End anchorage to the plates were given by 150 mm bolts at each end of the plates.

a. In beam B21 the failure took place due to the appearance of digaonal crack at the end of the plate. With subsequent loading, the crack started to open up and decrease in load took place. Figure 102 shows the mode of failure for beam B24.

b. In beam B24 same type of failure occurred as in beam B21.

10. BEAMS B19 AND B23

These beams were strengthened by 1.5 mm thick, 100 mm wide and 1100 mm long plates. End anchorage was given to the plates in both of these beams.

a. In beam B19 the failure took place by the appearance of the diagonal crack at the end of the plate. With subsequent loading the diagonal crack opened up and the load started to decrease as shown in the Figure 103

b. Beam B23 failed by the failure of the bond and also diagonal crack appeared at the end of the plate. This beam could not reach the full flexural capacity. Figure 104 shows load vs strains 4, 11 and 12 for beam B23. The drop in the strains 4, 11 and 12 at about 57 kN load is due to the slippage of the plate. Figure 105 shows load vs strains 22, 26 and 30 for beam B23. The drop in the strains 22, 26 and 30 and load takes place

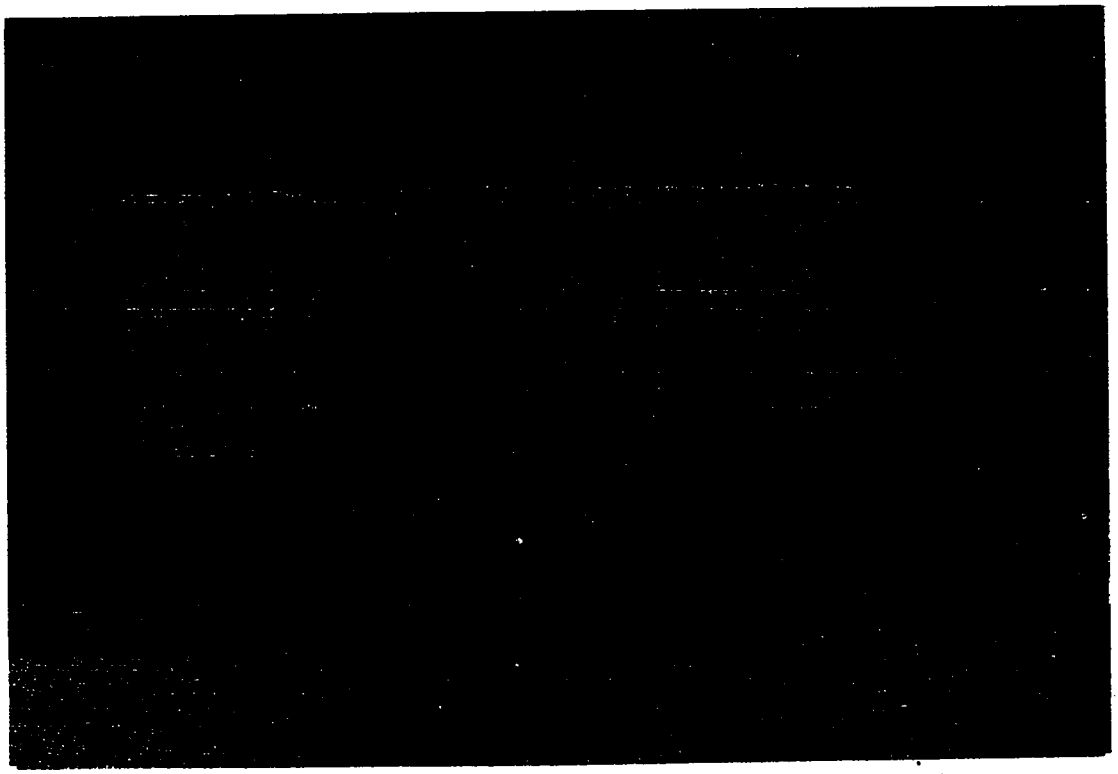

Figure 102: Photograph showing the mode of failure for beam B24. This beam was strengthened by 1.5 mm thick, 100 mm wide and 1100 mm long plate. End anchorage was given to the plate.

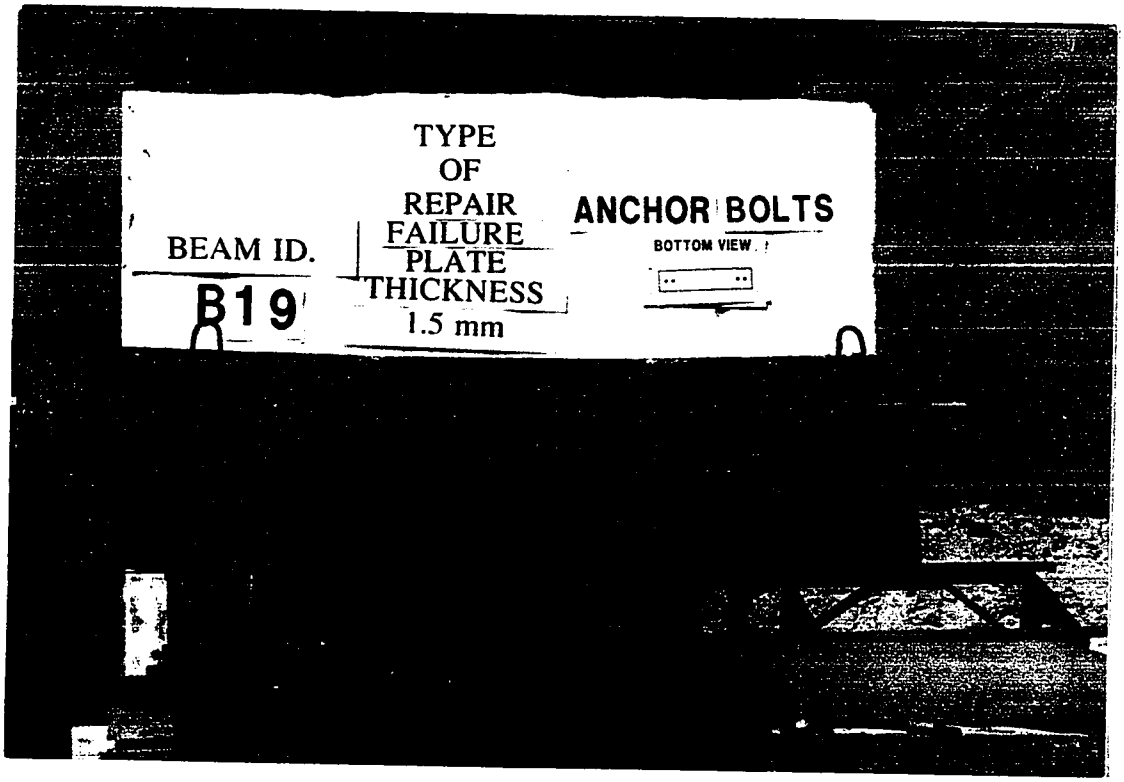

Figure 103: Photograph showing the mode of failure for beam B19. This beam was strengthened by 1.5 mm thick, 100 mm wide and 1100 mm long plate. End anchorage was given to the plate.

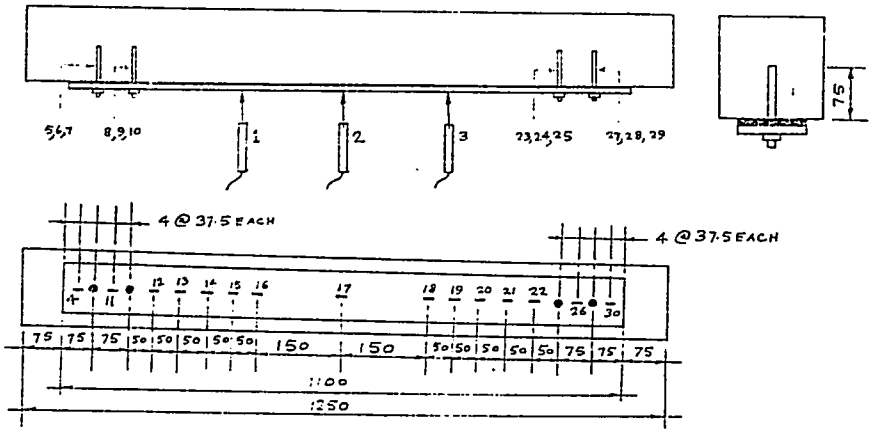

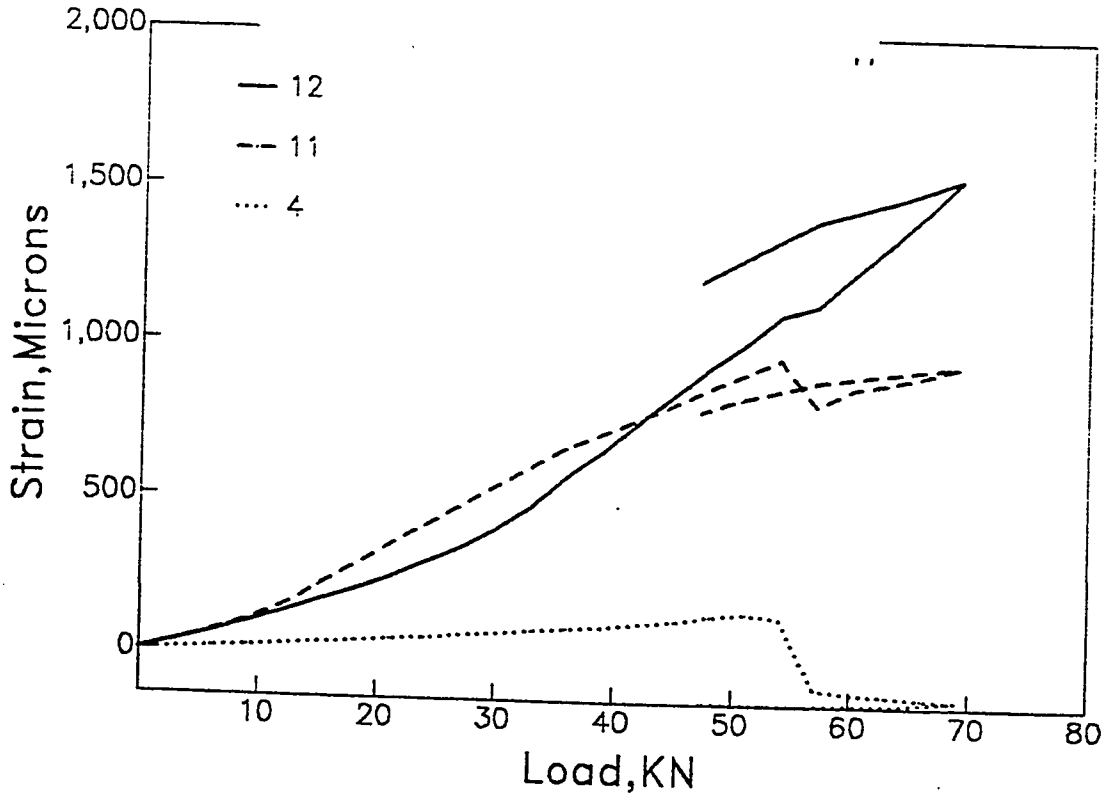

Figure 104: Load vs plate strains 4, 11 and 12 for beam B23. This beam was strengthened by 1.5 mm thick, 100 mm wide and 1100 mm long plate. End anchorage was given to the plate.

simultaneously. It means that on this side no slippage of the plate took place.

11. BEAMS B15 AND B22

Both of these beams were strengthened by 1.5 mm thick, 100 mm wide and 1100 mm long plates. End anchorage was given to the plates in both of these beams.

a. In beam B15 at 77 kN a diagonal crack appeared at one end of the plate. But the beam was still capable of taking loads and with subsequent loading the beam went in pure flexure failure. However, for finding the modulus of toughness, the first drop in the load has been considered as the failure of the beam.

b. In beam B22 failure took place due to the appearance of the diagonal cracks at both ends of the plates. The first diagonal crack appeared at one end of the beam with noise. At about 70 kN load, the crack appeared on the other side of the beam with noise. This beam could reach a maximum load of 71 kN. This beam could not reach the full flexural capacity. Figure 106 shows the mode of failure for beam B22.

Figure 107 shows the load vs strains 19, 20 and 26 for beam B22.

Figure 108 shows the load vs strains 1, 8 and 9 for beam B22.

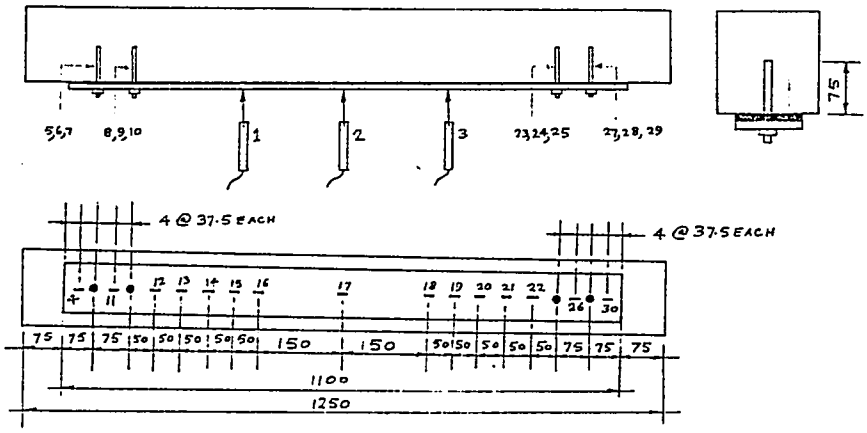

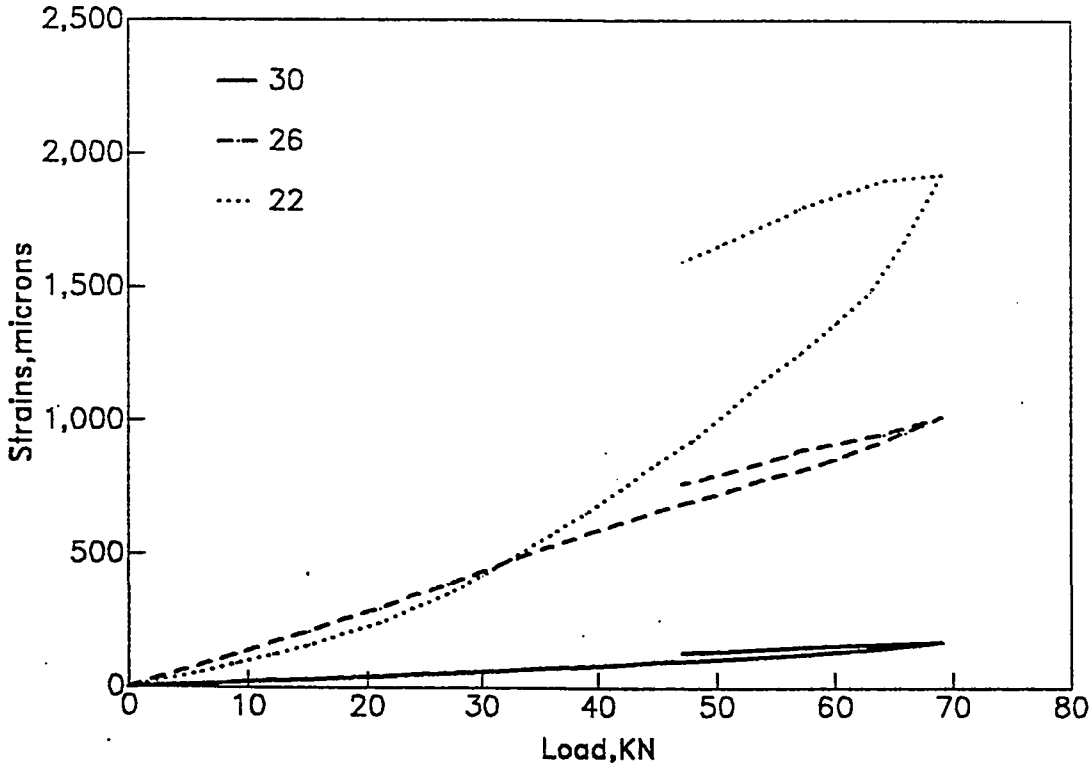

Figure 105: Load vs plate strains 22, 26 and 30 for beam B23. This beam was strengthened by 1.5 mm thick, 100 mm wide and 1100 mm long plate. End anchorage was given to the plate.

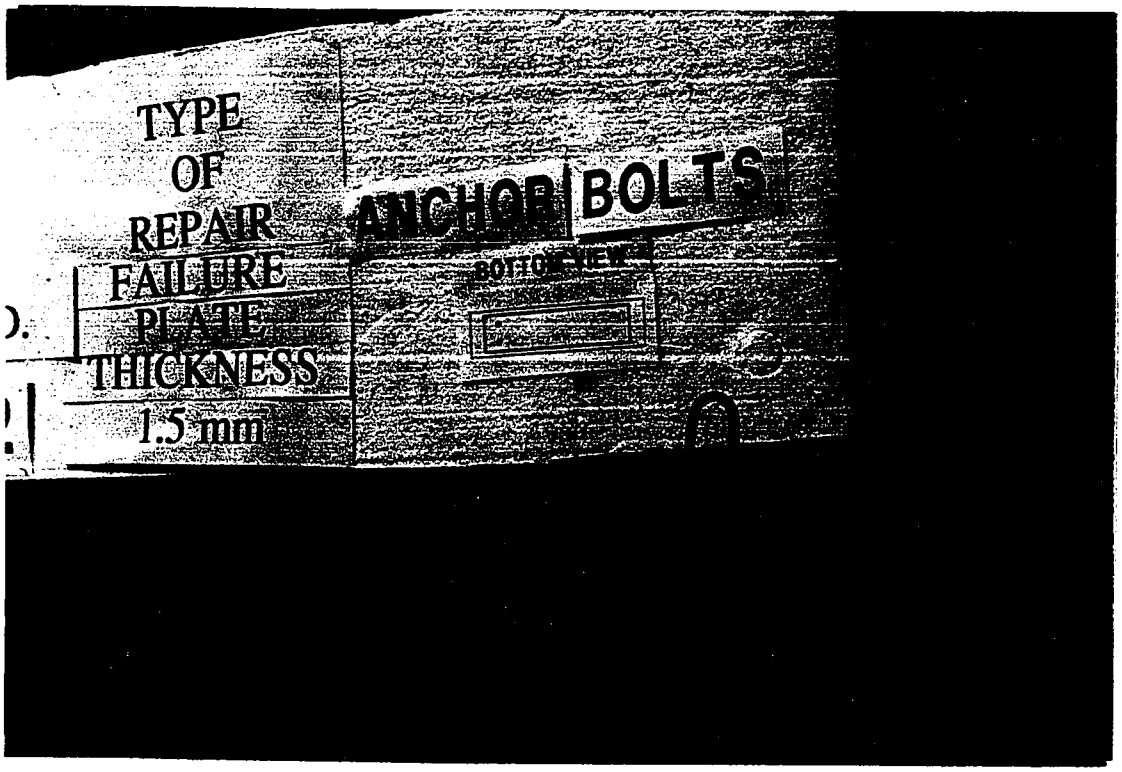

Figure 106: Photograph showing the mode of failure for beam B22. This beam was strengthened by 1.5 mm thick, 100 mm wide and 1100 mm long plate. End anchorage was given to the plate.

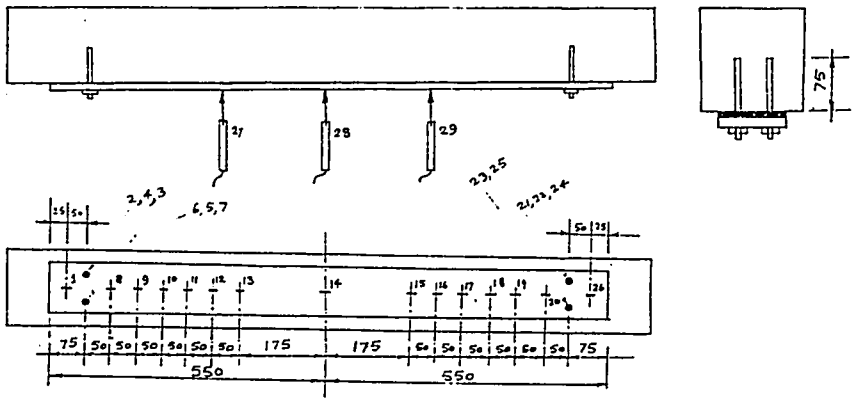

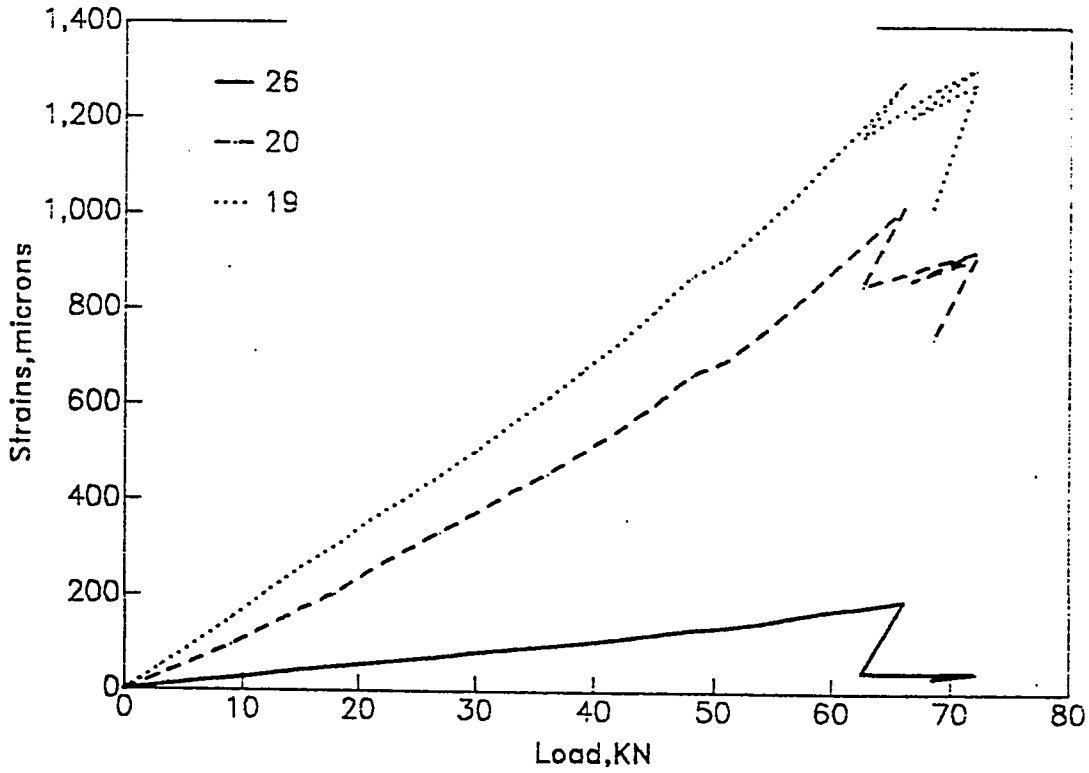

Figure 107: Load vs strains 19, 20 and 26 for beam B22. This beam was strengthened by 1.5 mm thick, 100 mm wide and 1100 mm long plate. End anchorage was given to the plate.

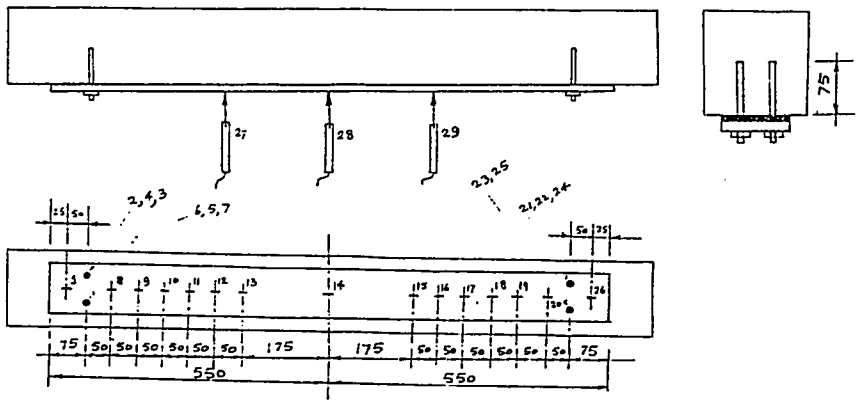

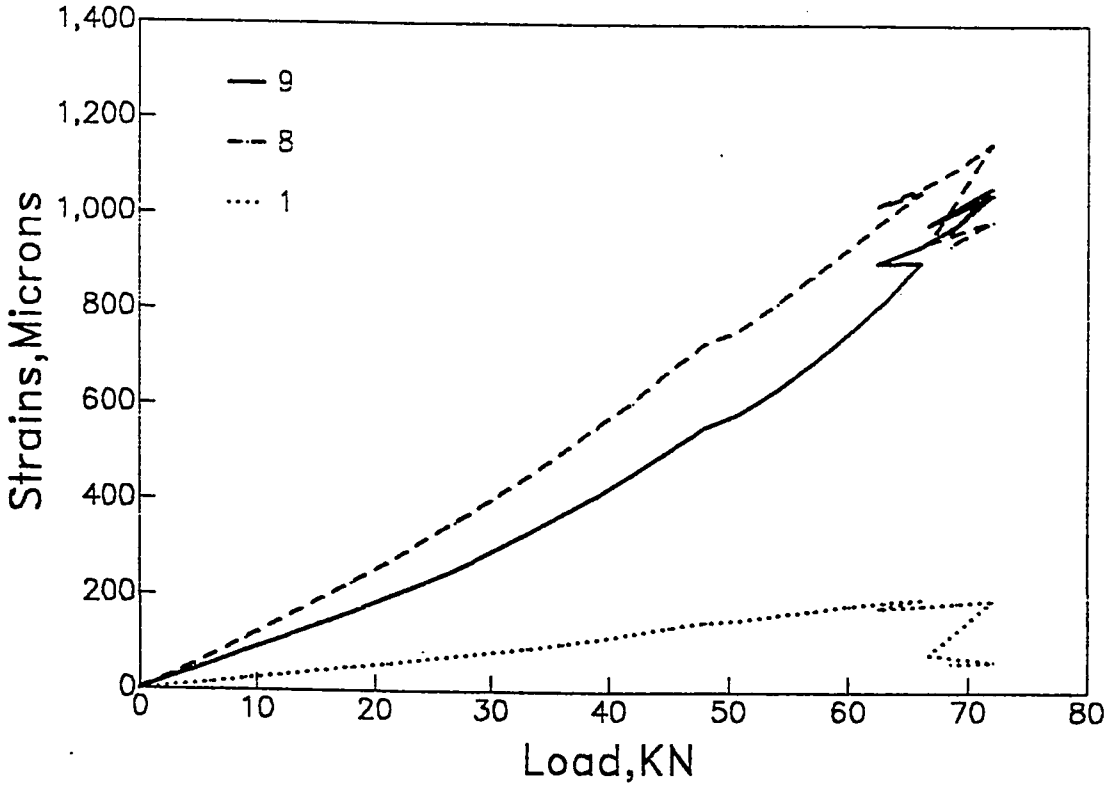

Figure 108: Load vs strains 1, 8 and 9 for beam B22. This beam was strengthened by 1.5 mm thick, 100 mm wide and 1100 mm long plate. End anchorage was given to the plate.

12. BEAMS B3 AND B18

In both of these beams pure flexure failure was obtained. Both of these beams behaved in the same way as if these were not strengthened by the plate. Because of sag in the plates, the plates could not contribute fully to the strength of the beam. In beam B18 the maximum strain in the plate was more than that of the beam B3. Correspondingly, the maximum load sustained by the beam B18 was more than that of the beam B3.

13. BEAM MF1

The failure in this beam occurred by the separation of the plate due to the tearing of the concrete above the glueline. This beam was strengthened by 1000 mm long, 100 mm wide and 3 mm thick steel plate. This beam could not reach its theoretical ultimate capacity calculated based on the actual stress strain curves of the steels, assuming full composite action between the steel plate and the concrete beam. It is recalled that the separation of the plate takes place due to the concentration of the shear and the peeling stresses at the end of the plate. Figure 109 shows the mode of failure for beam MF1.

14. BEAMS MF2 AND MF4

These beams were strengthened by 1000 mm long, 100 mm wide and 3 mm thick steel plates. End anchorage was given to the plates by bolts of 15 mm diameter and embedment length of 90 mm. At each end of the plates only one bolt was installed for anchorage.

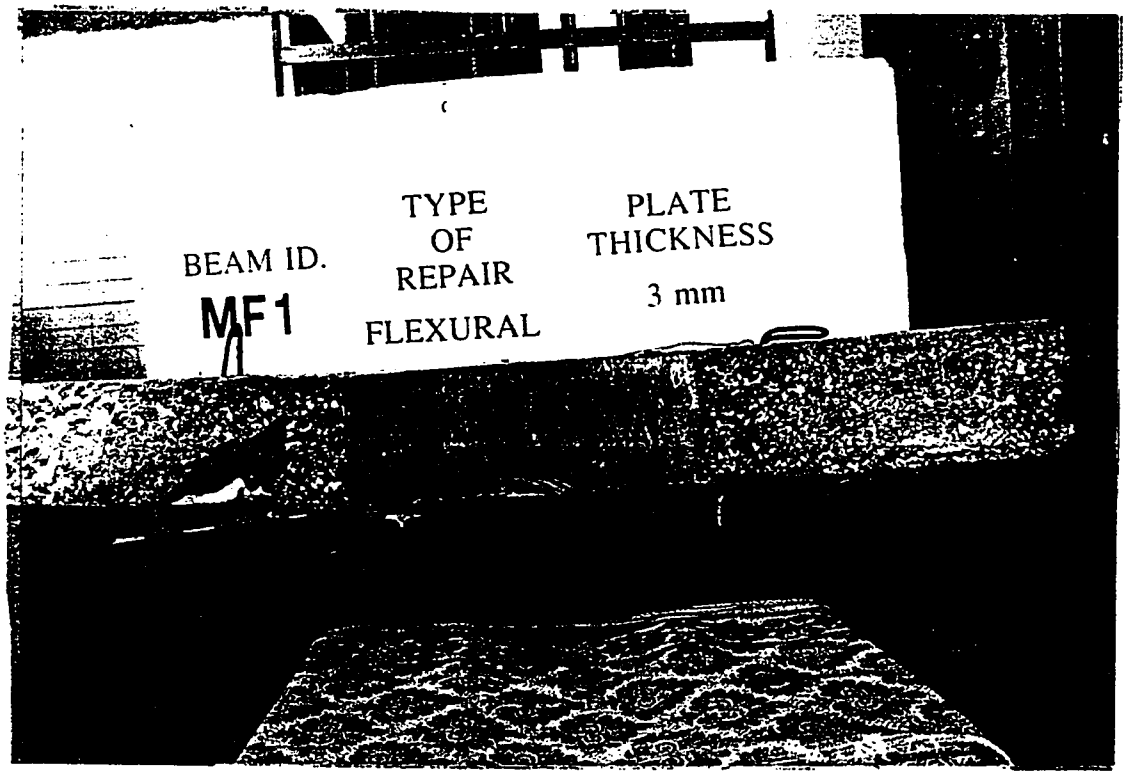

Figure 109: Photograph showing the mode of failure for beam MF1. The beam was stengthened by 1000 mm long, 100 mm wide and 3 mm thick steel plate. No end anchorage was given to the steel plate.

a. Beam MF2 failed prematurely by the appearance of the diagonal crack at the end of the plate. This beam could not reach the ultimate flexural capacity calculated based on the actual stress strain curves of the steels assuming full composite action of the steel plate with the concrete beam. The appearance of the diagonal crack was sudden and also the modulus of toughness for this beam was very less.

b. Beam MF4 failed without reaching the full ultimate flexural capacity calculated based on the actual stress strain curves of the steels assuming full composite action between the steel plate and the concrete beam. The beam failed by the appearance of the diagonal cracks in the shear spans. At one end of the beam the diagonal crack appeared starting from the end of the steel plate. At the other end of the beam the diagonal crack appeared starting from the inner side of the anchor bolt.

15. BEAM MF3

This beam was bonded with 1000 mm long, 100 mm wide and 2.00 mm thick steel plate. End anchorage was given to the plate by 15 mm diameter anchor bolts. The embedment length of the anchor bolts was 90 mm. At each end of the plate only one anchor bolt was used. The beam failed by the appearance of the diagonal cracks in the shear spans. The diagonal cracks started from the inner side of the anchor bolts and reached the ends of the middle third of the beams under the loading

point. When the diagonal crack reached the loading points there was some local crushing of the concrete.

Chapter V

PREDICTION OF SHEAR AND PEELING STRESSES AT INTERFACE IN FLEXURE STRENGTHENED BEAMS

5.1 INTRODUCTION

Various researchers like T. M. Robert [20] , T. M. Robert and Haji-Kazemi [21] , R. Jones [19] have given analytical solutions for finding the distribution of stresses at interface in the epoxy bonded plated beams up to linear elastic range. Robert's approximate solution [20] is amenable to hand calculations, nevertheless, it does not always satisfy the condition that with increasing plate thickness shear stress at interface increases. Secondly, it underestimate the shear stresses and the peeling stresses. Robert and Haji-Kazemi's [21] analytical solution for finding the stress concentrations at the interface in plated beams is a complicated expression and is not amenable to hand calculations and is limited for simple loadings. In order to obtain quick solutions for shear and normal stresses at the interface in plated beams for general loading, the need of a computer program can not be disregarded. Here a finite difference computer program based on the Robert's [22] model has been developed to determine shear and peeling stresses at the interface of the epoxy bonded plated beams. T. M. Robert [22] developed this model to study the influence of slip in composite beams with partial interaction. Prior to Robert [22] , Newmark [48] studied the influence of slip in composite beams with incomplete interaction. In Newmark analysis the equilibrium

and compatibility equations for an element of a composite beam were reduced to a single second order differential equation in terms of axial force in the concrete slab and I-beam.

Two programs were written to determine the slip at the interface of the composite beams. A brief introduction of these programs follows:-

1. PROGRAM NEW1

   This program was based on the Newmark approach [48] .

2. PROGRAM ROB1

   This program was based on the Roberts Model [22]

The purpose of writing the program NEW1 was to verify the results of program ROB1. Because the boundary conditions in case of program NEW1 were very simple and for program ROB1, boundary conditions were not so clear. By comparing the results of these two programs, we confirmed that the boundary conditions now being used in the program ROB1 are correct. Both of these program give similar result although based on different approaches.

The program ROB1 was later modified to program ROB9 to determine shear stresses at the interface of the epoxy bonded plated beams. This modification will be described in detail later in this chapter. This modification has been proposed by us. The procedure to modify Roberts Model [22] to handle epoxy bonded plated beams is new and has been tried for the first time and it gives very consistent results with those of other approaches. Haji-Kazeme [21] also used Roberts model [22] and gave analytical solution to determine the shear stresses at the interface of the epoxy bonded plated beams. The limitations of his approach have already been described. Our approach is different from Haji-Kazeme's [21] analytical approach.

5.2 PROGRAM NEW1

This program is based on the Newmark Approach [48]

5.2.1 ASSUMPTIONS

This analysis for slip has been done with reference to a composite beam consisting of a steel I-section and concrete slab. However, the solution so obtained is general and is applicable to any composite beam consisting of two layers of any material. In this analysis, the material and geometrical non-linearities have not been taken into account. This analysis for slip is based on the following assumptions.

1. The shear connection between the slab and the I-beam (Steel Beam) is assumed to be continuous along the length of the beam.
2. The amount of slip permitted by the shear connection is directly proportional to the load transmitted.
3. The distribution of strains throughout the depth of the slab and the I-beam is linear.
4. The I- beam and the slab are assumed to deflect equal amounts at all points along their length at all times.

The notations used in the analysis for slip in the composite beam consisting of concrete slab and the I-beam are described below. In these notations subscript 's' is for slab and the subscript 'b' is for the beam.

A_s and A_b are the cross-sectional areas of the slab and the beam respectively. c_s is the distance from the centroid of the slab to the interface and c_b is the distance from the centriod of the I-beam to the interface.

$$c_1 = \frac{k}{s}\frac{\overline{EI}}{\overline{EA}\Sigma EI} \tag{6}$$

$$c_2 = \frac{k}{s}\frac{z}{\Sigma EI} \tag{7}$$

$$C = \frac{s}{k}\frac{\pi^2 \overline{EA}\Sigma EI}{L^2 \overline{EI}} \tag{8}$$

Where E_s and E_b are the modulli of elasticity of the slab and the beam

$$\Sigma EI = E_s I_s + E_b I_b \tag{9}$$

$$\overline{EI} = \Sigma EI + \overline{EA}z^2 \tag{10}$$

$$\overline{EI} = \Sigma EI + \overline{EA}z^2 \tag{11}$$

$$\frac{1}{\overline{EA}} = \frac{1}{E_s A_s} + \frac{1}{E_b A_b} \tag{12}$$

F is the force acting at the centroid of the slab and the beam. I_s and I_b are the moments of inertias of the slab and I-beam respectively. L is the span length of the beam. k is the modulus of the shear connector. M is the external moment. M_s and M_b are the moments resisted by the slab and the I-beam respectively. q is the horizontal force per unit length of the beam at the junction of the I-beam and the slab. Q is the load on the shear connector. s is the spacing of the shear connector. z is the distance between the centroidal axes of the beam and the slab. ε_s and ε_b are the strains in the slab and the I-beam. γ represents the slip at the interface of the composite beam.

5.2.2 ANALYSIS

For analysis reference should be made to Figure 110 . This figure shows a composite T-beam consisting of I-beam and the concrete slab. However, the derivations obtained based on this composite beam will be general and will be applicable to any composite beam consisting of two layers whose elastic modulli are known.

When the composite beam is subjected to loads acting vertically downward, the lower extreme fibers of the slab elongate and the upper extreme fibers of the beam contract. The shear connectors counter act these actions by exerting forces which produce compression in the slab and tension in the I-beam. These forces act at the location of the shear connector, but on each element they may be replaced by a couple and the force acting at the centroid of the element. These couples when added algebraically to the moments that would exist in the I-beam and the slab due to external moment, if there were no shear connectors, give the resultant internal forces and the moments acting at any section of the slab and the I-beam. Where M_s is the moment resisted by the slab and M_b is the moment resisted by the I-beam of the composite beam.

Force acting at the centriod of the slab and that of the I-beam is of same magnitude. This force has been denoted by F. No subscript has been used for this force. Force acting at the centroid of the slab is compressive and the force acting at the centroid of the I-beam is tensile provided the beam is subjected to loads acting vertically downward. It is to be noted that this force comes into existence due to the shear connection of the slab and the I-beam. This force will vanish if the shear connection between the slab and I-beam is broken. The mag-

nitude of this force F depends on the magnitude of the shear connection between the slab and the I-beam. The relative movement between the slab and the I-beam is called slip and is denoted by γ . It has been assumed that the amount of slip permitted by the shear connection is proportional to the load transmitted by the shear connection. So the slip at the interface can be written as

$$\gamma = \frac{Q}{k} = \frac{qs}{k} \tag{13}$$

Where Q is the load transmitted by one shear connector. k is the modulus of the shear connector and this is equal to the ratio of the load transmitted by the shear connector to the slip permitted by the shear connector. The load per unit length q is equal to the change in the force per unit length of the beam. Therefore, slip at the interface becomes

$$\gamma = \frac{s}{k}\frac{dF}{dx} \tag{14}$$

The rate of change of slip per unit length of the beam is given by

$$\frac{d\gamma}{dx} = \frac{s}{k}\frac{d^2F}{dx^2} \tag{15}$$

According to the first assumption $\frac{s}{k}$ is constant

The rate of change of slip along the length of the beam can also be written in terms of the strain at the bottom face of the slab and the top face of the I-beam.

$$\frac{d\gamma}{dx} = \varepsilon_b - \varepsilon_s \tag{16}$$

As the distribution of strains throughout the depth of the slab and the I-beam are assumed to be linear it follows that:

$$\varepsilon_s = -\frac{F}{E_s A_s} + \frac{M_s c_s}{E_s I_s} \tag{17}$$

$$\varepsilon_b = \frac{F}{E_b A_b} - \frac{M_b c_b}{E_b I_b} \tag{18}$$

Equating the Right hand sides of equations (15) and (16) and substituting the values of ε_s and ε_b from equations (17) and (18) we get

$$\frac{s}{k}\frac{d^2F}{dx^2} = F\left(\frac{1}{E_s A_s} + \frac{1}{E_b A_b}\right) - \left(\frac{M_s c_s}{E_s I_s} + \frac{M_b c_b}{E_b I_b}\right) \tag{19}$$

The unknown moments M_s and M_b may be written in terms of the known external moment M and the unknown force F as follows:-

$$M = M_s + M_b + Fz \tag{20}$$

The assumption that the slab and the I- beam deflect equal amounts at all points require that the angle changes along the length for the slab and I-beam remain equal, that is, curvature of the I-beam and slab remain same at all points of the composite beam. This condition may be expressed as follows:

$$\frac{M_s}{E_s I_s} = \frac{M_b}{E_b I_b} = \frac{M - Fz}{E_s I_s + E_b I_b} \tag{21}$$

From the equation (21) we can find the expressions for moments resisted by slabs and the I-beams respectively which follows:

$$M_s = \frac{(M-Fz)E_sI_s}{E_sI_s + E_bI_b} \tag{22}$$

and

$$M_b = \frac{(M-Fz)E_bI_b}{E_sI_s + E_bI_b} \tag{23}$$

Substituting M_s and M_b in equation (19) and then by simplification we get the following second order differential equation in terms of F.

$$\frac{d^2F}{dx^2} - \frac{k}{s}\frac{\overline{EI}}{\overline{EA}\Sigma EI}F = -\frac{k}{s}\frac{z}{\Sigma EI}M \tag{24}$$

Where

$$\Sigma EI = E_sI_s + E_bI_b \tag{25}$$

$$\overline{EI} = \Sigma EI + \overline{EA}z^2 \tag{26}$$

$$\frac{1}{\overline{EA}} = \frac{1}{E_sA_s} + \frac{1}{E_bA_b} \tag{27}$$

The equation (24) is a second order differential equation in terms of axial force F. This equation can be solved by finite difference. Two boundary conditions are needed to solve this equation. A computer program has been written to solve this equation and is named as program NEW1. Listing of the program NEW1 and a sample data file are given in the appendix E.

5.2.3 BOUNDARY CONDITIONS

Two boundary conditions are required to solve equation (24) by finite difference because the equation is a second order differential equation. At each boundary, in simply supported composite beam, the axial force acting at the centroid of each layer is zero. For using in the finite difference program NEW1 , the boundary conditions, as mentioned above, are written with reference to Figure 111 which follows:-

$$F_2 = 0 \tag{28}$$

$$F_{n-1} = 0 \tag{29}$$

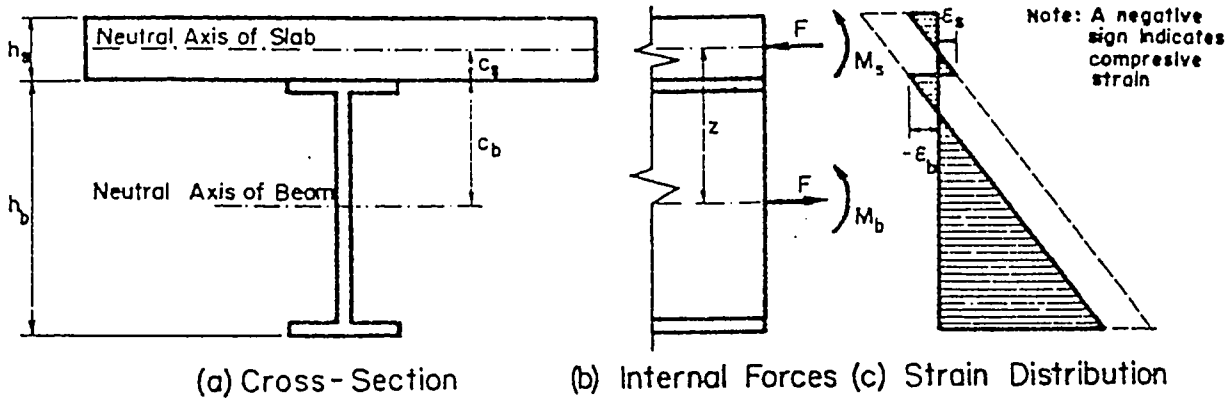

Figure 110: Composite beam consisting of I-Beam and concrete slab The axial force in the slab and the beam is same and is denoted by F.

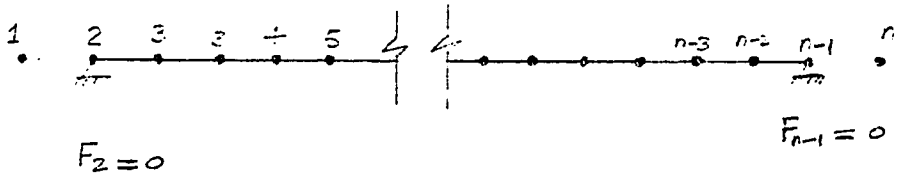

Figure 111: Figure showing boundary conditions for Newmark approach. Two extra nodes out side the boundaries are shown.

5.2.4 APPLICATIONS

By using the computer program NEW1 the slip at the interface between the beams and the slabs in composite beams can be determined.

In order to verify the program the slip at the interface was determined in the composite beam adopted from reference [22] for various loads and for various shear stiffnesses of the shear connection at the interface.

Figure 112 shows the cross-section of the composite beam adopted from reference [22] . The span length of this beam is 20 m. The elastic modulus of the slab is 21000 MPa. and the elastic modulus of the beam is 210000 MPa. The slip at the interface for this beam, has been determined for different values of loads and different values of shear stiffnesses at the interface of the composite beam. The results so obtained are presented in the following figures.

Figure 113 shows the distribution of slip at the interface of the composite beam for K_s=2180 N/mm/mm and for a uniformly distributed load of 12 N/mm.

Figure 114 shows the distribution of slip at the interface of the composite beam for shear stiffness K_s=2180 N/mm/mm and for a point load of 49.3 kN at the mid-span of the composite beam.

Figure 115 shows the distribution of slip at the interface of the composite beam for shear stiffness $K_s = 54.5$ N/mm/mm and for a uniformly distributed load of 12 N/mm.

Figure 116 shows the distribution of slip at the interface of the composite beam for $K_s = 54.5$ N/mm/mm and for a point load of 49.3 kN at the mid-span.

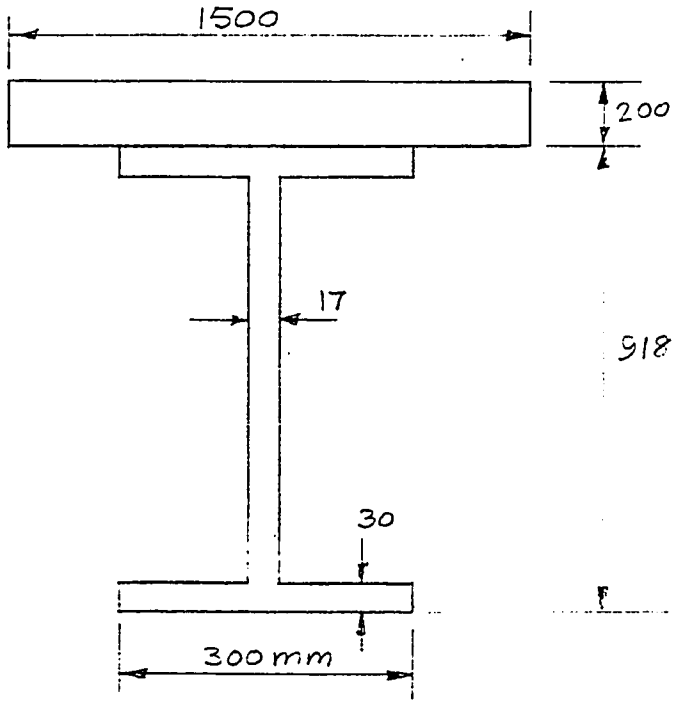

$E_s = 21000\ N/mm^2$

$E_b = 210,000\ N/mm^2$

SPAN LENGTH = 20m

Figure 112: Cross-sectional dimensions of the composite beam. This beam has been adopted from reference [22] .

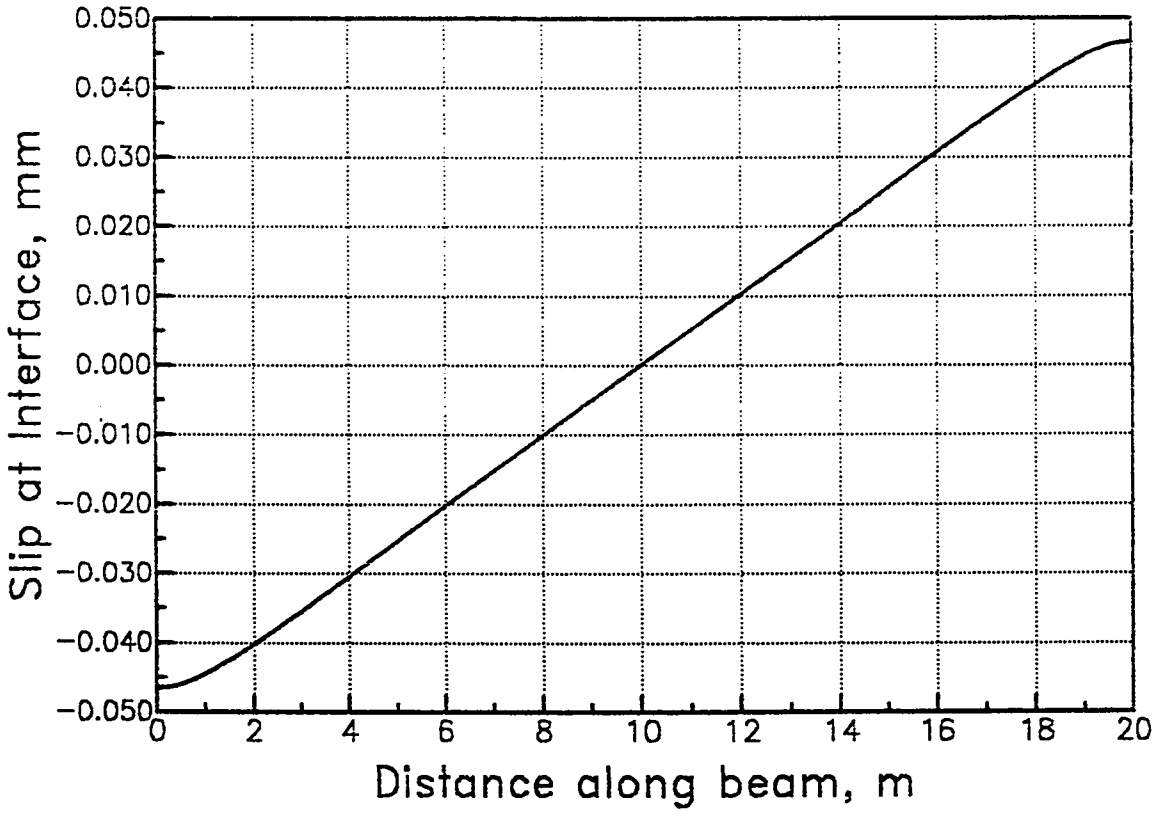

Figure 113: Distribution of slip at interface for Ks = 2180 N/mm/mm and for a uniformly distributed load of 12 N/mm.

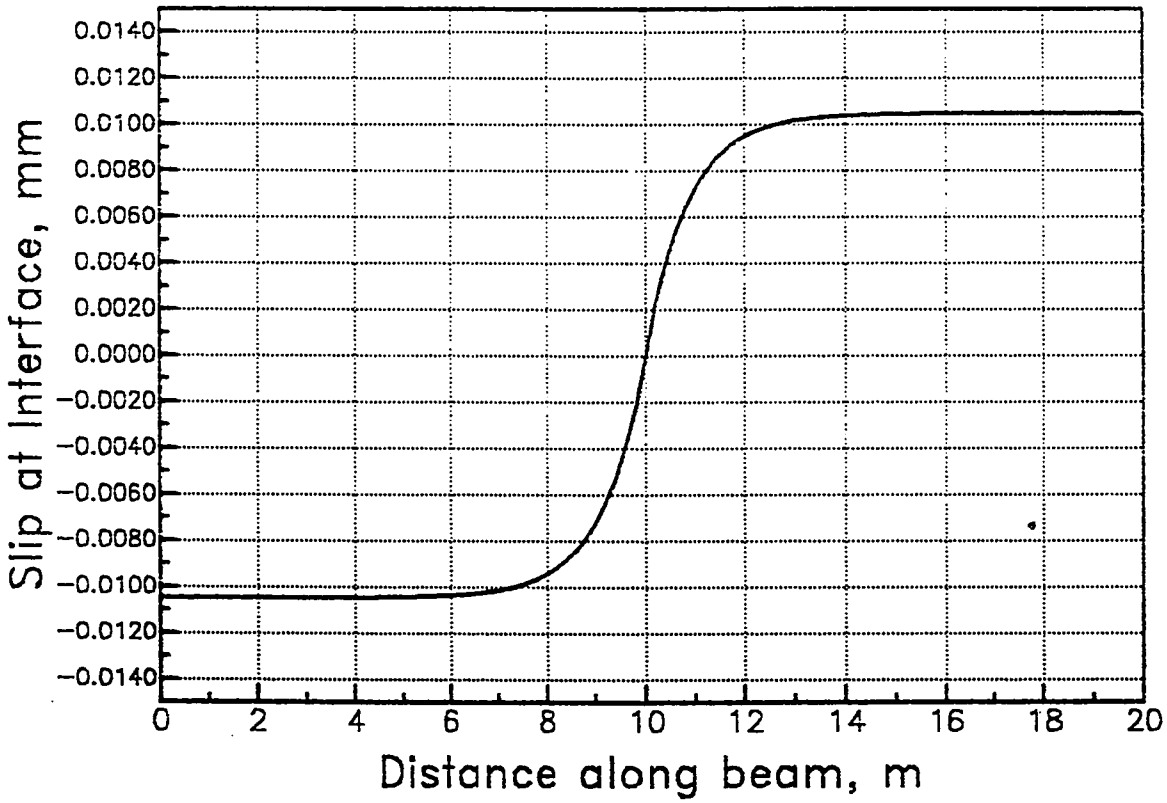

Figure 114: Distribution of slip at interface for Ks = 2180 N/mm/mm and for a central point load of 49.3 kN

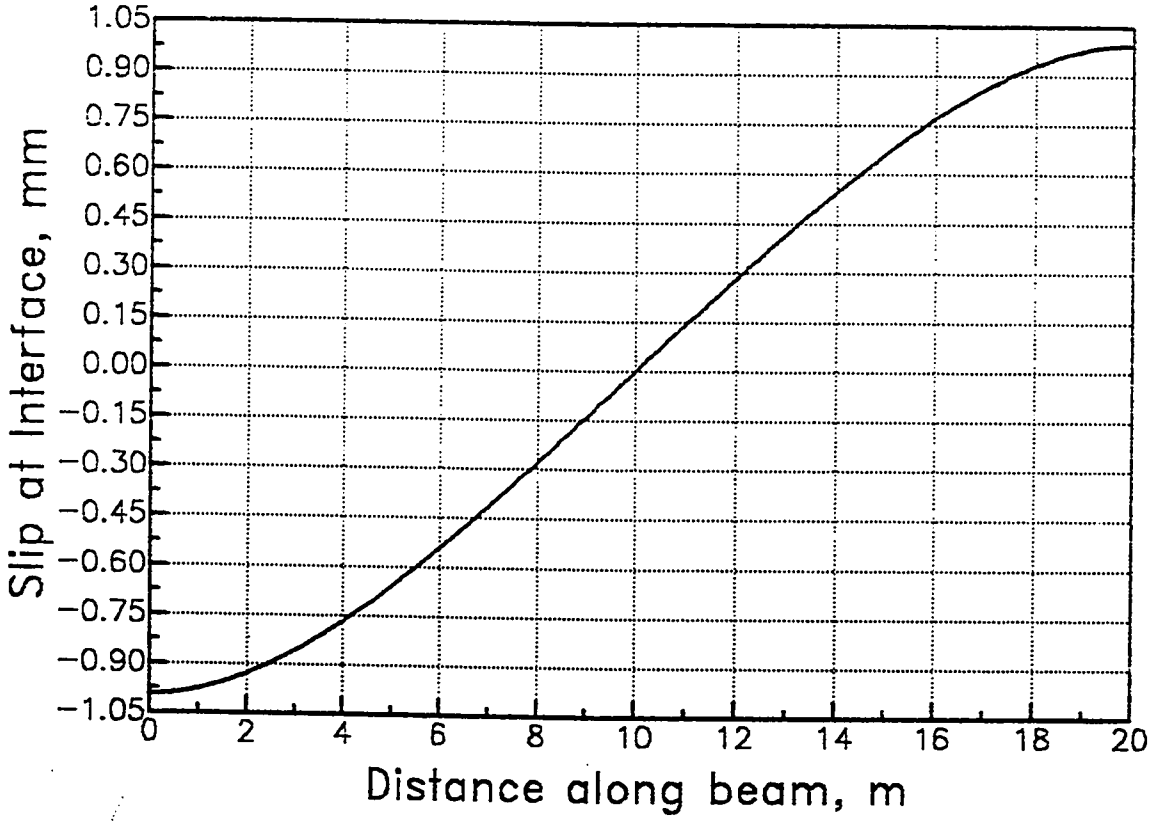

Figure 115: Distribution of slip at the interface for Ks = 54.5 N/mm/mm and for a uniformly distributed load of 12 N/mm/mm.

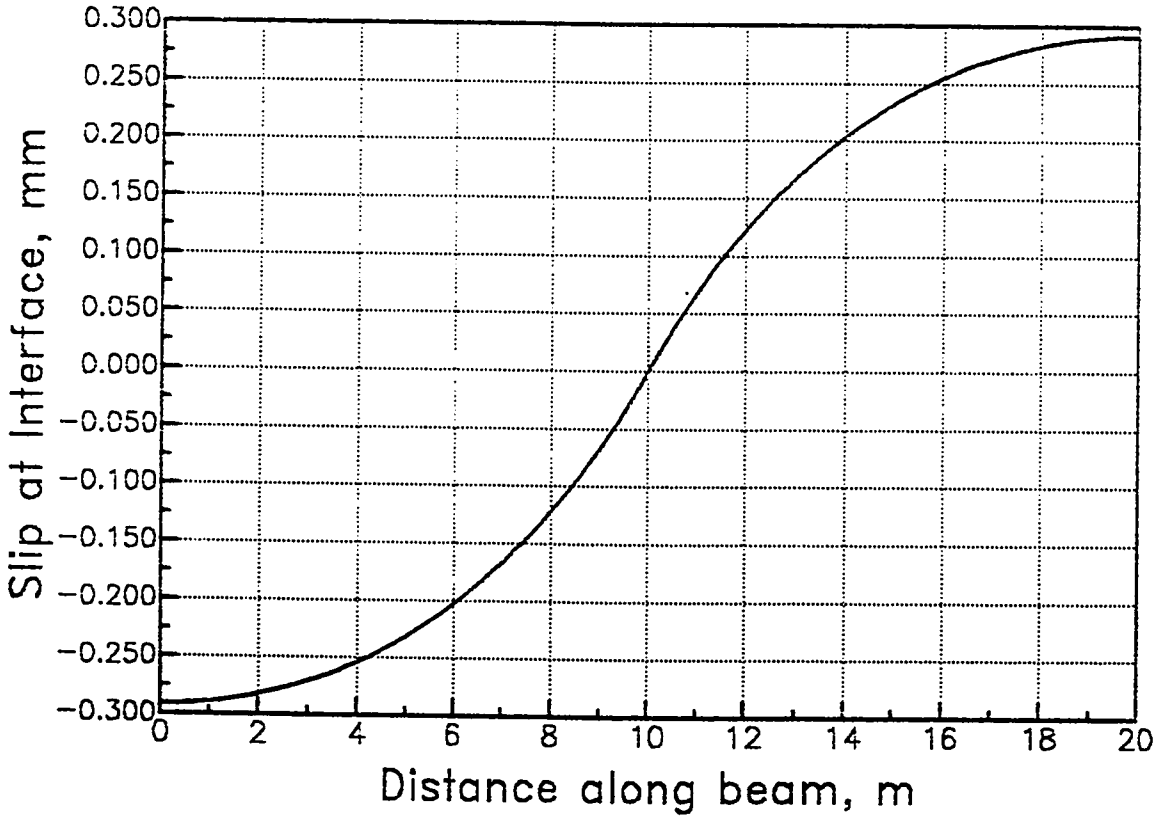

Figure 116: Distribution of slip at interface for Ks = 54.5 N/mm/mm and for a central point load of 49.3 kN.

5.3 ROBERTS APPROACH

For the derivations of the equilibrium and compatibility equations in Robert's approach [22] , consider a length δx of composite beam as shown in the Figure 117

The beam is made of two materials a and b joined by a medium of negligible thickness having finite normal and tangential stiffnesses. Assuming plane sections within each material remain plane, the strains can be expressed in terms of displacements u and w. Where u and w are the displacements with respect to x-axes and z-axes respectively. For material "a" the total displacement in the x direction at depth z_a , denoted by $\bar{u}_a$ is given by the following equation.

$$\bar{u}_a = u_a - z_a \frac{dw_a}{dx} \tag{30}$$

Similarly for the material b the total displacement in the x-direction, denoted by $\bar{u}_b$, is given by given by the following equation.

$$\bar{u}_b = u_b - z_b \frac{dw_a}{dx} \tag{31}$$

The derivatives of the total displacements in the x-direction for layer "a" and "b" respectively with respect to x-axis give the strains in the each layer.

$$\varepsilon_a = \frac{du_a}{dx} - z_a \frac{d^2 w_a}{dx^2} \tag{32}$$

$$\varepsilon_b = \frac{du_b}{dx} - z_b \frac{d^2 w_b}{dx^2} \tag{33}$$

Knowing the strains the stresses can be expressed as follows:-

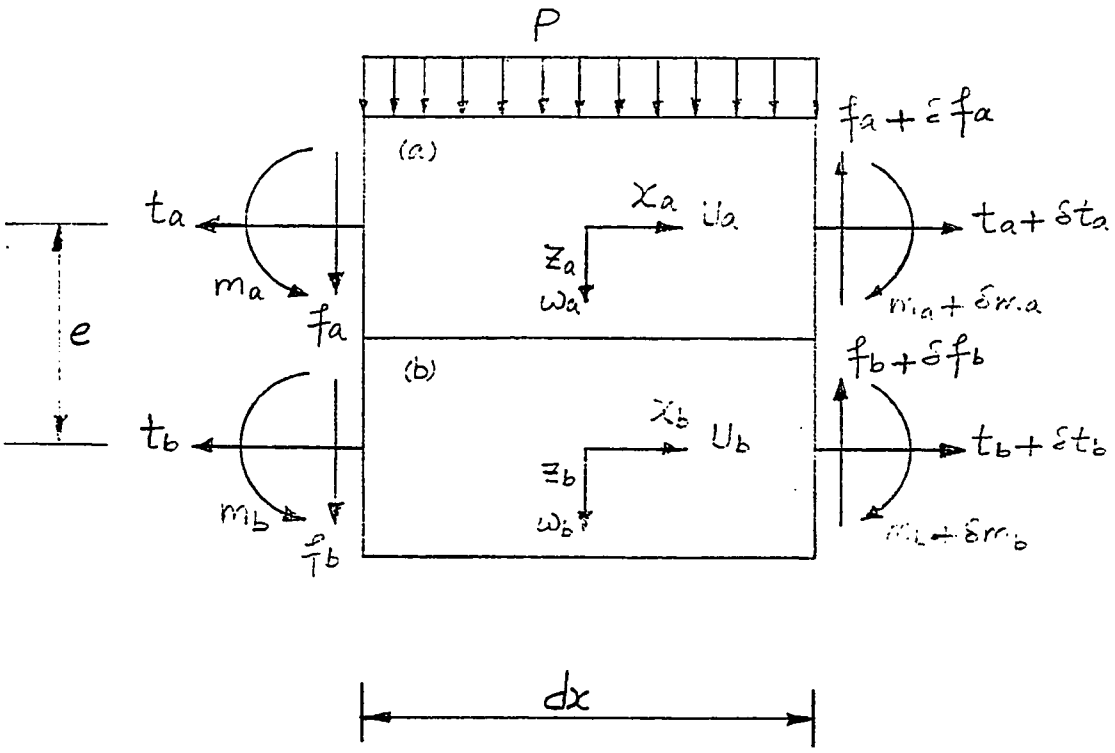

Figure 117: Element of a composite beam of length dx.

$$\sigma_a = E_a\left(\frac{du_a}{dx} - z_a\frac{d^2w_a}{dx^2}\right) \tag{34}$$

$$\sigma_b = E_b\left(\frac{du_b}{dx} - z_b\frac{d^2w_b}{dx^2}\right) \tag{35}$$

The axial forces t_a and t_b can be obtained by integrating the stresses over the cross section of the materials a and b, denoted by A_a and A_b respectively, as shown below.

$$t_a = \int\sigma_a dA_a \tag{36}$$

$$t_b = \int\sigma_b dA_b \tag{37}$$

and the moments m_a and m_b can be found by integrating the stresses multiplied by the appropriate lever arm over the cross-section of the materials a and b respectively, as shown below.

$$m_a = -\int\sigma_a z_a dA_a \tag{38}$$

$$m_b = -\int\sigma_b z_b dA_b \tag{39}$$

1. Taking the summation of forces in the x-direction with respect to Figure 117 on page 205 , we get

$$\frac{dt_a}{dx} + \frac{dt_b}{dx} = 0 \tag{40}$$

2. Taking the equilibrum of forces in the vertical direction with respect to Figure 117 on page 205., we get

$$\frac{df_a}{dx} + \frac{df_b}{dx} = p \tag{41}$$

Similarly equating the summation of moments about the origin of coordinates of upper layer equal to zero with reference to Figure 117 on page 205 , we get the following equation

$$\frac{dm_a}{dx} + \frac{dm_b}{dx} - \frac{dt_b}{dx}e = f_a + f_b \tag{42}$$

Combining the equations (41) and (42) we get the following equation

$$\frac{d^2m_a}{dx^2} + \frac{d^2m_b}{dx^2} - \frac{d^2t_b}{dx^2}e = p \tag{43}$$

Where p is the applied load per unit length and e is the distance between the origin of two coordinate systems.

3. The slip u_{ab} at the interface between materials a and b is the relative displacement in the x-direction of initially adjacent particles. K_s is the shear stiffness of the joint and it is equal to the force per unit length per unit slip. Taking the horizontal equilibrium of the upper layer as shown in the Figure 118 we get the following equation.

$$\frac{dt_a}{dx} = \bar{\tau} \tag{44}$$

where $\bar{\tau}$ is the force per unit length and this is also given by the following equation.

$$\bar{\tau} = K_s u_{ab} \tag{45}$$

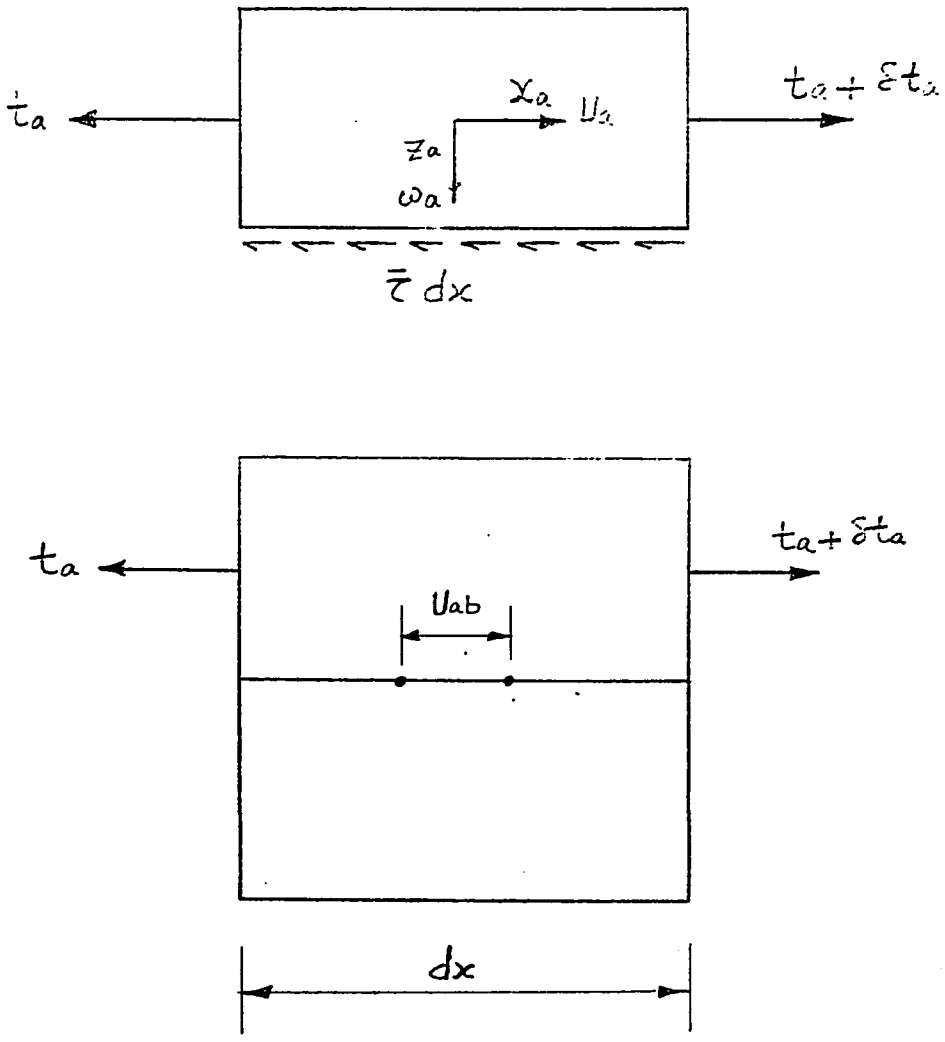

Figure 118: Free body diagram of the upper layer of Robert's model. Horizontal equilibrium of the upper layer.

Combining equations (44) and (45) and substituting the value of u_{ab} , we get the following equation.

$$\frac{dt_a}{dx} = K_s\left[(u_a - z_{ia}\frac{dw_a}{dx}) - (u_b - z_{ib}\frac{dw_b}{dx})\right] \tag{46}$$

Where z_{ia} and z_{ib} are the coordinates of the interface in the two materials.

4. The separation at the interface is the relative displacement in the z-direction between the material a and b respectively.

If K_n is the normal stiffness of the joint and it is defined as the normal force per unit length per unit separation. Then the normal force per unit length denoted by $\bar{\sigma}_n$ at the interface of the two materials with reference to Figure 119 can be written as

$$\bar{\sigma}_n = K_n(w_b - w_a) \tag{47}$$

Taking moment about the centroid of the upper layer with reference to free body diagram of the upper layer as shown in the Figure 118 on page 208 , we get the following equation.

$$\frac{dm_a}{dx} + \bar{\tau}z_{ia} - f_a = 0 \tag{48}$$

Vertical equilibrium of upper layer with respect to free body diagram of the upper layer as given in the Figure 119 , we get the following equation.

$$\frac{df_a}{dx} - (\bar{\sigma}_n + p) = 0 \tag{49}$$

Where f_a is the shear force in the material a.

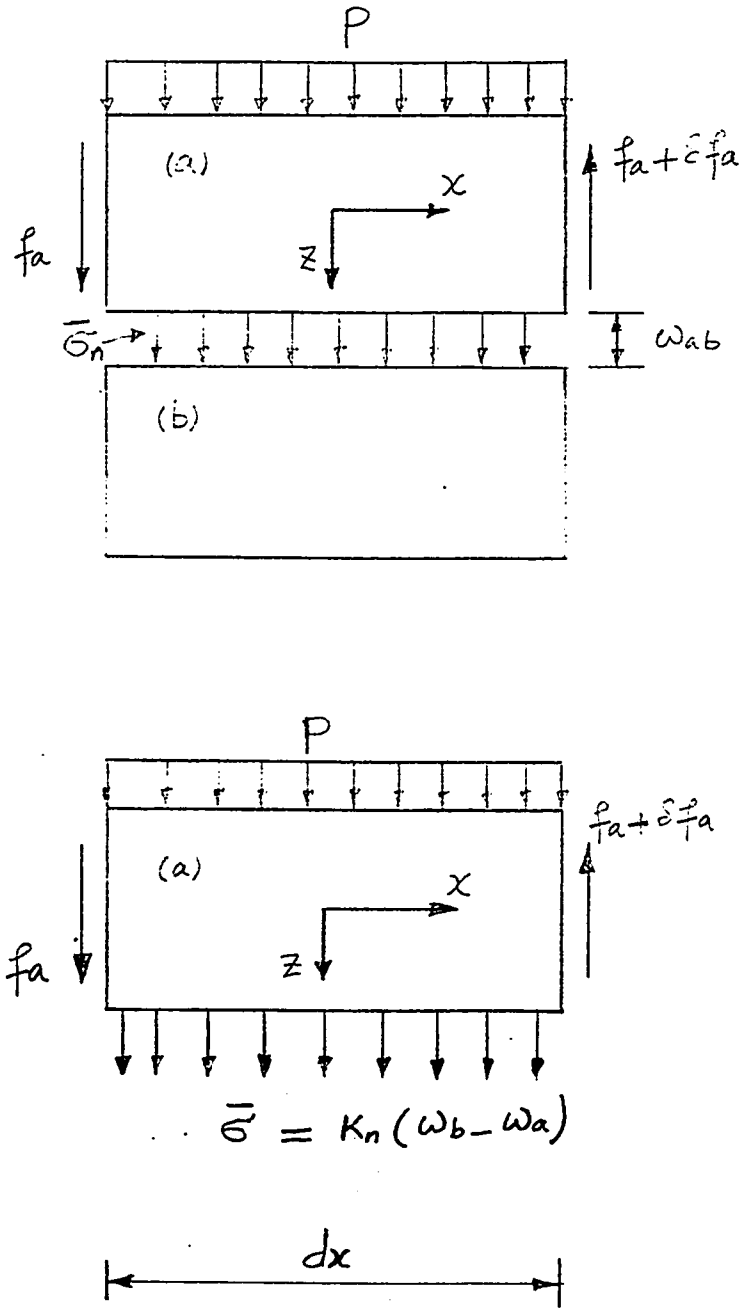

Figure 119: Free body diagram of the upper layer of Robert's model. Vertical equilibrium of the upper layer.

Combining (48) and (49) we get the following equation.

$$\frac{d^2 m_a}{dx^2} - K_n(w_b - w_a) + \frac{d^2 t_a}{dx^2} z_{ia} = p \tag{50}$$

The equations (40) , (43) , (46) and (50) can be simplified by following assuming

1. K_n to be very high.
2. That the coordinate systems x and y for each layer coincide with the respective centroids of the layers "a" and "b".
3. E_a and E_b to be constants.

Then the vertical displacement along the length of the beam for both layers becomes equal as shown below.

$$w_a = w_b = w \tag{51}$$

and the equation (50) becomes indeterminate and the basic equations take the following shapes.

$$t_a = E_a A_a \frac{du_a}{dx} \tag{52}$$

$$t_b = E_b A_b \frac{du_b}{dx} \tag{53}$$

$$m_a = E_a I_a \frac{d^2 w}{dx^2} \tag{54}$$

$$m_b = E_b I_b \frac{d^2 w}{dx^2} \tag{55}$$

And equilibrium and compatibility equations take the following shapes.

$$\frac{dt_b}{dx} + \frac{dt_b}{dx} = 0 \tag{56}$$

$$\frac{d^2 m_a}{dx^2} + \frac{d^2 m_b}{dx^2} - \frac{d^2 t_b}{dx^2} e = P \tag{57}$$

$$\frac{dt_a}{dx} - K_s(u_a - u_b - e\frac{dw}{dx}) = 0 \tag{58}$$

Where I_a and I_b are the second moments of areas of layers a and b about their centroidal axes. Substituting the values of t_a , t_b , m_a and m_b in the equations (56) , (57) and (58) we get the following equations:-

$$E_a A_a \frac{d^2 u_a}{dx^2} + E_b A_b \frac{d^2 u_b}{dx^2} = 0 \tag{59}$$

$$E_a I_a \frac{d^4 w}{dx^4} + E_b I_b \frac{d^4 w}{dx^4} - E_b I_b e \frac{d^3 u_b}{dx^3} = p \tag{60}$$

$$E_a A_a \frac{d^2 u_a}{dx^2} - K_s(u_a - u_b - e\frac{dw}{dx}) = 0 \tag{61}$$

At the boundaries in simply supported composite beams the bending moment and the axial force in both layers is zero and from Newmark equation (24) we get the following:-

$$\frac{d^2 F}{dx^2} = 0 \tag{62}$$

This condition in the Robert's approach takes the following shape.

$$\frac{d^2 t_b}{dx^2} = 0 \tag{63}$$

Substituting the value of t_b in the equation (63) we get the following equation

$$E_b A_b \frac{d^3 u_b}{dx^3} = 0 \tag{64}$$

Therefore, the above equations (59) , (60) and (61) at the boundaries will take the following forms:-

$$E_a A_a \frac{d^2 u_a}{dx^2} + E_b A_b \frac{d^2 u_b}{dx^2} = 0 \tag{65}$$

$$E_a I_a \frac{d^4 w}{dx^4} + E_b I_b \frac{d^4 w}{dx^4} = p \tag{66}$$

$$E_a A_a \frac{d^2 u_a}{dx^2} - K_s (u_a - u_b - e\frac{dw}{dx}) = 0 \tag{67}$$

The above mentioned equations at the boundaries and the equations at the interior zone of the composite beam as discussed before, can be solved by finite difference for u_a and u_b and w. Knowing u_a and u_b and w, the slip at the interface can be determined from the following equation.

$$u_{ab} = K_s [u_a - u_b - e\frac{dw}{dx}]$$

A computer program ROB1 was developed to solve these differential equations simultaneously with finite difference with the following boundary conditions. Boundary conditions on the left support are

$$w_3 = 0$$

$$(t_a)_3 = 0$$

$$(t_b)_3 = 0$$

$$m_3 = 0$$

Similarly boundary conditions on the right support are

$$w_{n-2} = 0$$

$$(t_a)_{n-2} = 0$$

$$(t_b)_{n-2} = 0$$

$$m_{n-2} = 0$$

These boundary conditions have been written with respect to Figure 120 . Here m represents the total external moment. In simply supported beams the external moment at the support is zero. The listing and a sample data file of the program ROB1 is given in the appendix F.

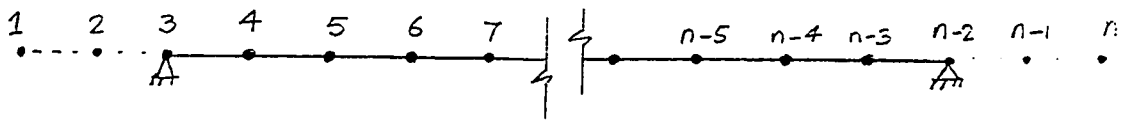

$w_3 = 0$

$(t_a)_3 = 0$

$(t_b)_3 = 0$

$m_3 = 0$

$w_{n-2} = 0$

$(t_a)_{n-2} = 0$

$(t_b)_{n-2} = 0$

$m_{n-2} = 0$

Figure 120: Boundary conditions for program ROB1.

5.3.1 VERIFICATION OF PROGRAM ROB1

In order to verify this program the composite beam given in reference [22] was analyzed for slip with different values of Ks and loads. The result so obtained were exactly similar to those shown in the Figure 113 on page 200 , Figure 114 on page 201 , Figure 115 on page 202 and Figure 116 on page 203 . From this comparison, it can be concluded that the boundary conditions used in the Robert's approach are correct.

Also this program was used to see the effect of variation of Ks on the central deflection. Same composite beam taken from reference [22] was used for this study. Figure 121 represents the effect of variation of Ks on the central deflection. The results are exactly similar to those given in the reference [22] .

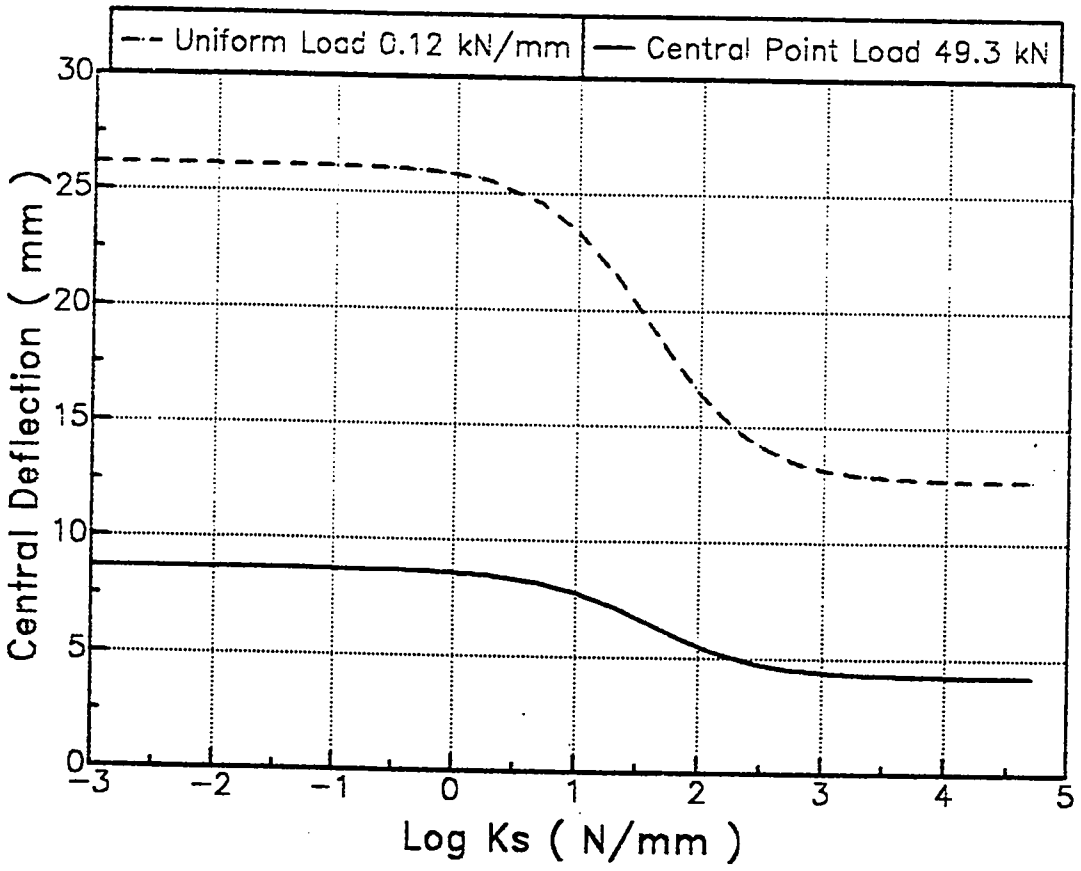

Figure 121: Effect of variation of Ks on the central deflection for the composite beam taken from reference [22]

5.4 STRESSES AT INTERFACE IN PLATED BEAMS

Program ROB1 was modified to program ROB9 to determine the shear and normal stresses at the interface in the epoxy bonded plated beams. The listing and a typical data file of the program ROB9 is given in the appendix G. This program can only handle simply supported epoxy bonded plated beams.

5.4.1 SHEAR STRESSES AT INTERFACE

In this section we will discuss the modifications at the boundaries in the Robert's model to determine shear stress distribution at the interface in the epoxy bonded plated beams. A typical epoxy bonded plated beam is shown in the Figure 122 . Where "l" is the span length of the beam and "a" is the length of the plate and "r" is the distance between the simple support and the end of the plate. These modifications at the boundaries in Robert's model [22] to determine shear stresses at the interface in epoxy bonded plated beams have been made by the author and these modifications are explained with the help of the Figure 123 . The shear stiffness K_s for the epoxy glue and I_b for the steel plate are taken equal to zero in the domain "r". Hence in domain "r", the equilibrium and compatibility equations (59) , (60) and (61) are modified to the following equations.

$$\frac{d^2u_a}{dx^2}=0 \tag{68}$$

and

$$\frac{d^2u_b}{dx^2}=0 \tag{69}$$

and

$$E_a I_a \frac{d^4 w}{dx^4} - eE_b A_b \frac{d^3 u_a}{dx^3} = p \tag{70}$$

and at the boundaries the equations (68) , (69) and (70) become

$$\frac{d^2 u_a}{dx^2} = 0 \tag{71}$$

$$\frac{d^2 u_b}{dx^2} = 0 \tag{72}$$

$$E_a I_a \frac{d^4 w}{dx^4} = p \tag{73}$$

In the bonded region the equations (59) , (60) and (61) remain valid and at the point of termination of plate, the average values of moment of inertia is used. By solving the differential equations for plated and unplated regions simultaneously by finite difference, u_a , u_b and w can be determined and then substituting the values of u_a and u_b and w in the following equation in the bonded region, that is, in the domain a, the slip at the interface can be determined.

$$u_{ab} = u_a - u_b - e\frac{dw}{dx} \tag{74}$$

Knowing the slip the force per unit length at the interface can be determined from the following equation.

$$\bar{\tau} = K_s(u_a - u_b - e\frac{dw}{dx}) \tag{75}$$

and the shear stress at the interface can be determined from the following equation.

$$\tau = K_s(u_a - u_b - e\frac{dw}{dx})/b \tag{76}$$

Where b is the width of the bonded plate.

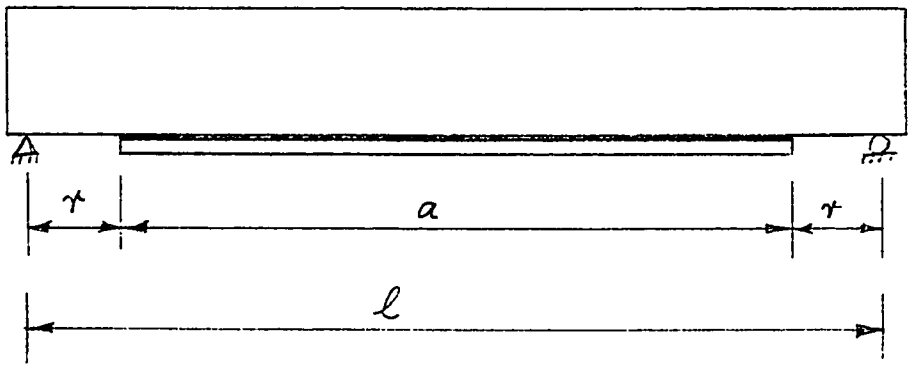

Figure 122: A typical epoxy bonded plated beam.

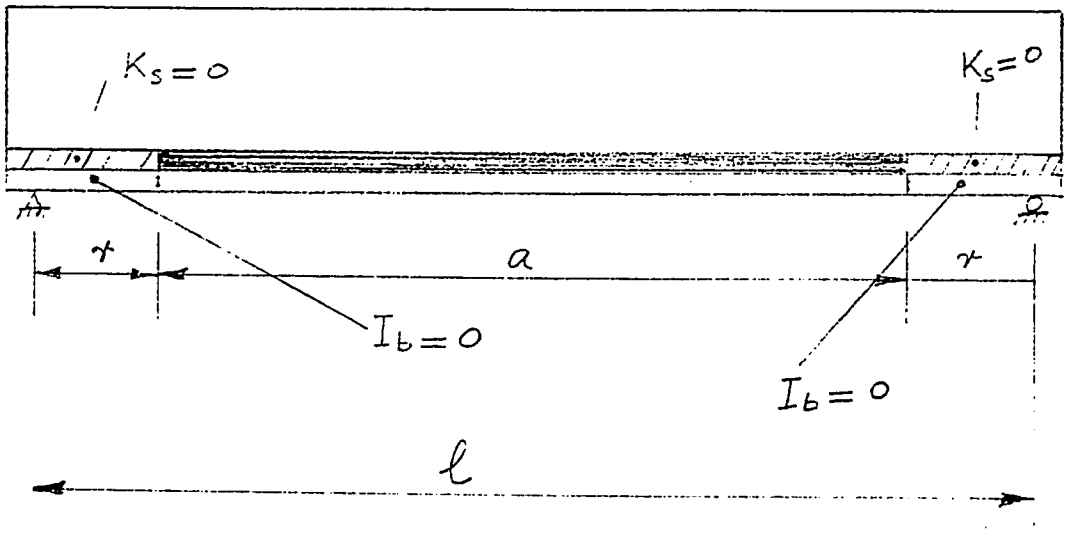

Figure 123: Boundary conditions to modify ROB1 to ROB9 to handle epoxy bonded plated beams.

5.4.2 PEELING STRESSES AT INTERFACE

This model for finding peeling stresses at the interface was suggested by Haji-Kazemi [21] . But in order to find peeling stresses at the interface by this model, we must know the shear stresses at the interface of the epoxy bonded plated beams. The procedure for finding the shear stresses at the interface has already been discussed.

When the material b is terminated before the end support, the solution of the Robert's equations [21] implies that a moment m_b and shear force f_b are applied to the free end of the plate. But in actual practice no moment and shear force act at the end of the bonded plate. In order to balance this moment and shear we must apply equal moment and shear force in opposite directions. This moment and shear is given by the following expressions:-

$$m_b = E_b I_b \frac{d^2 w}{dx^2} \tag{77}$$

and equilibrium of element of material b gives

$$f_b = E_b I_b \frac{d^3 w}{dx^3} - \bar{\tau} z_{ib} \tag{78}$$

It is recalled that it has been assumed that

$$w_a = w_b = w$$

Assuming the bending stiffness of the plate to be small as compared to the concrete beam, this problem can be analysed by considering the plate as flexible

beam on the elastic foundation, which possess only normal stiffness per unit length Kn. With reference to Figure 124 the governing differential equation for relative displacement of material b, denoted by w_b' is given by the following expression:-

$$\frac{d^4 w_b'}{dx^4} + (K_n / E_b I_b) w_b' = 0 \tag{79}$$

This equation was solved by finite difference by using the following boundary conditions.

$$E_b I_b \frac{d^2 w_b'}{dx^2} = M \tag{80}$$

$$E_b I_b \frac{d^3 w_b'}{dx^3} = F \tag{81}$$

Where M is the absolute value of m_b and F is the absolute value of shear force f_b

After finding the values of w_b from the differential equation of the beam on the elastic foundation, the normal force per unit length can be found from the relation.

$$\bar{\sigma} = K_n w_b' \tag{82}$$

and normal stress, also called peeling stress, becomes

$$\sigma = K_n \frac{w_b'}{b} \tag{83}$$

where b is the width of the plate.

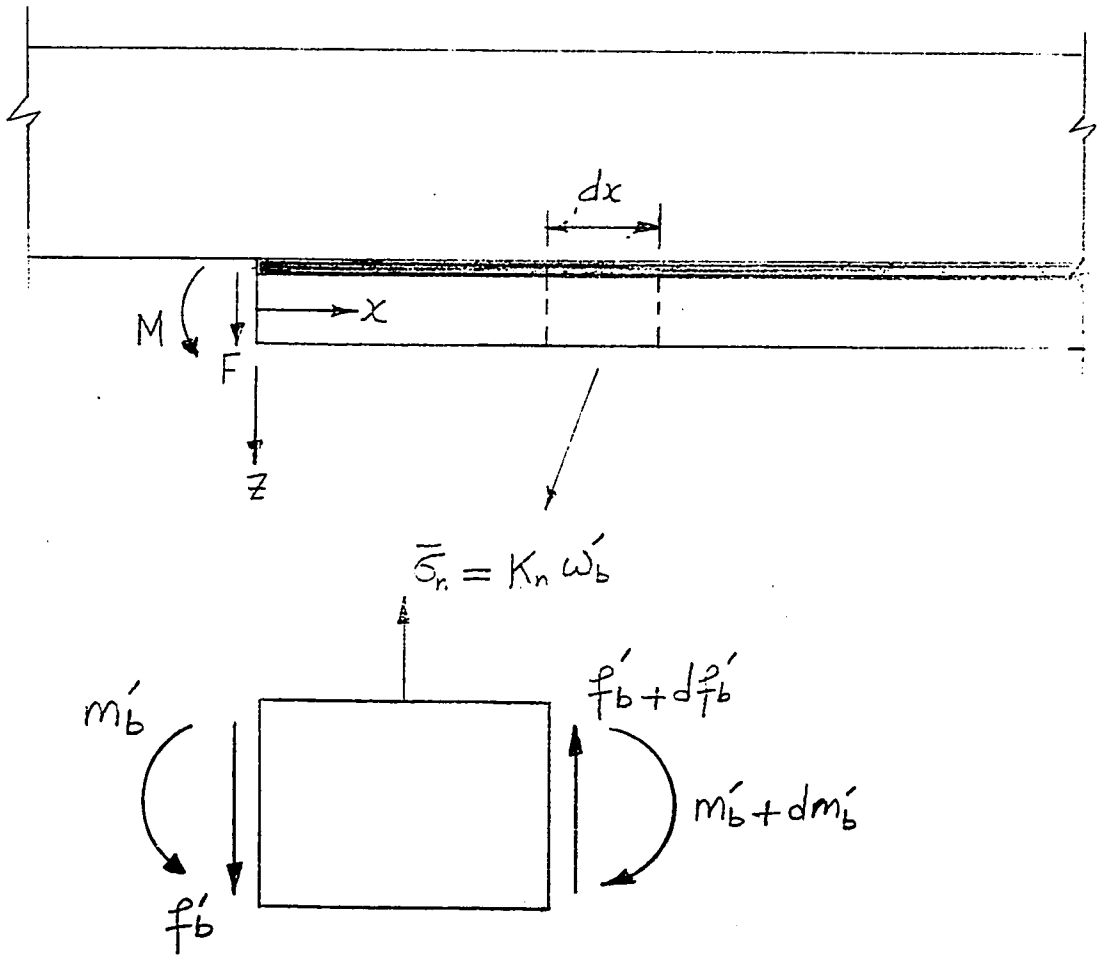

Figure 124: Model for determining peeling stresses at the interface. Considering the plate as the beam on the elastic foundation. Adhesive layer has been considered as an elastic foundation.

5.4.3 VERIFICATION OF THE PROGRAM ROB9

In order to verify the program the plated beam given in reference [21] was analyzed for shear and peeling stresses at the interface, tensile stresses in the bonded plate and various other parameters were studied. The dimensions of the beam, loading and properties of concrete and steel plate are given in the Figure 125 .

The span length "l" of the beam is 2400 mm over simple supports. The length of the plate is "a". Different values of the plate length "a" were used in these calculations. The beam is loaded to a uniformly distributed load of 15 N/mm. The shear stress and the peeling stress distributions at the interface and the tensile stress distribution along the length of the plate, for different values of Ks, Kn and a/l were determined and are shown in the following figures.

Figure 126 shows the shear stress distribution at interface for Ks = 20000 N/mm/mm and for a/l = 0.75. The results given by the program match with those given by Haji-Kazemi [21]

Figure 127 shows the peeling stress distribution at interface for Kn = 50000 N/mm/mm and for a/l = 0.75. The results match with those given by the Haji-Kazemi's solution. The peeling stress is very high at the end of the plate and diminishes rapidly to zero and then change to negative and then become zero again.

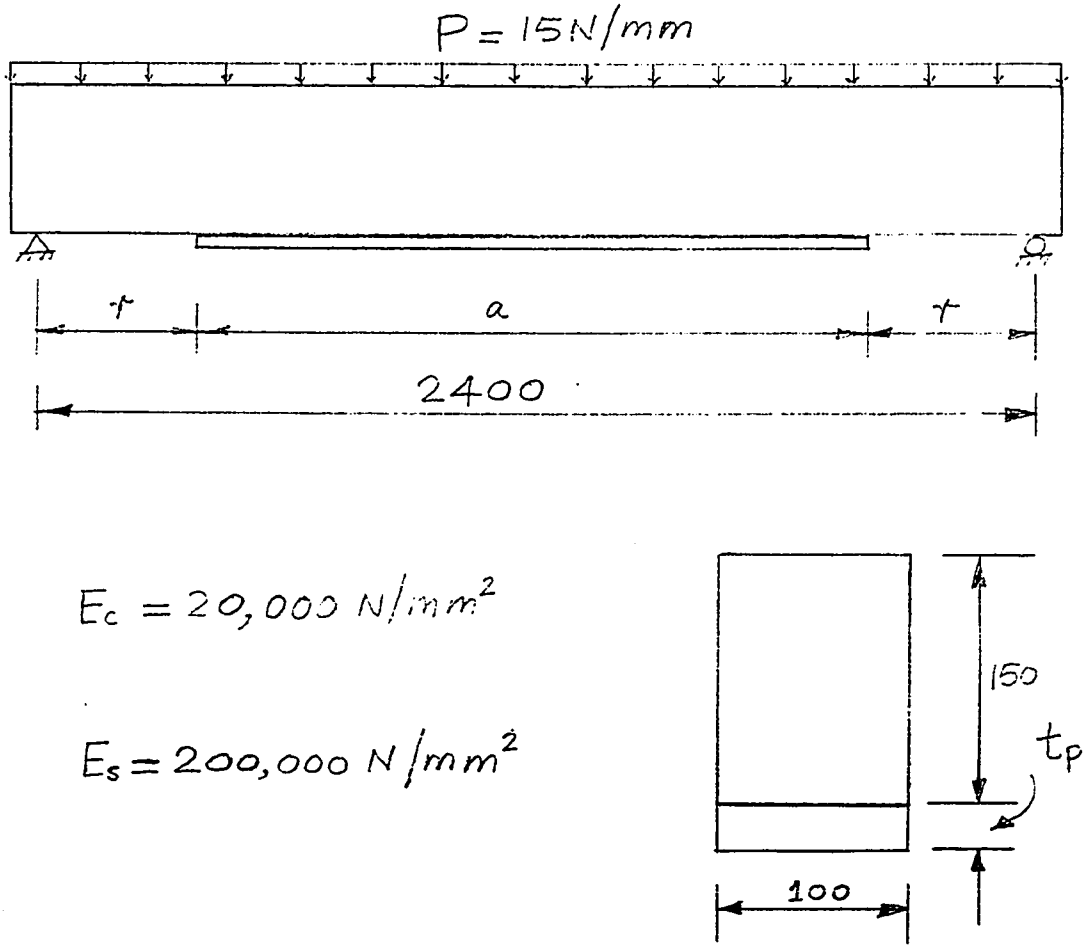

Figure 125: Dimensions, loading and material properties of the beam taken from the reference [21]

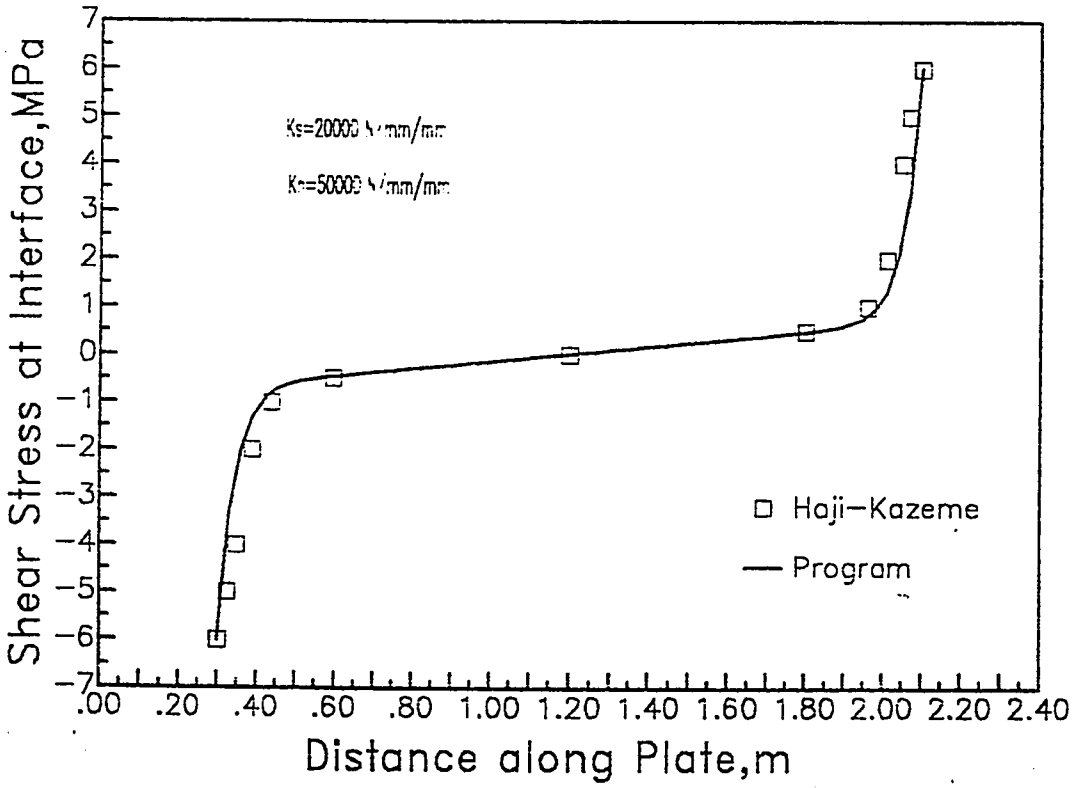

Figure 126: Shear stress distribution at interface for Ks=20000 N/mm/mm and for a/l=0.75.

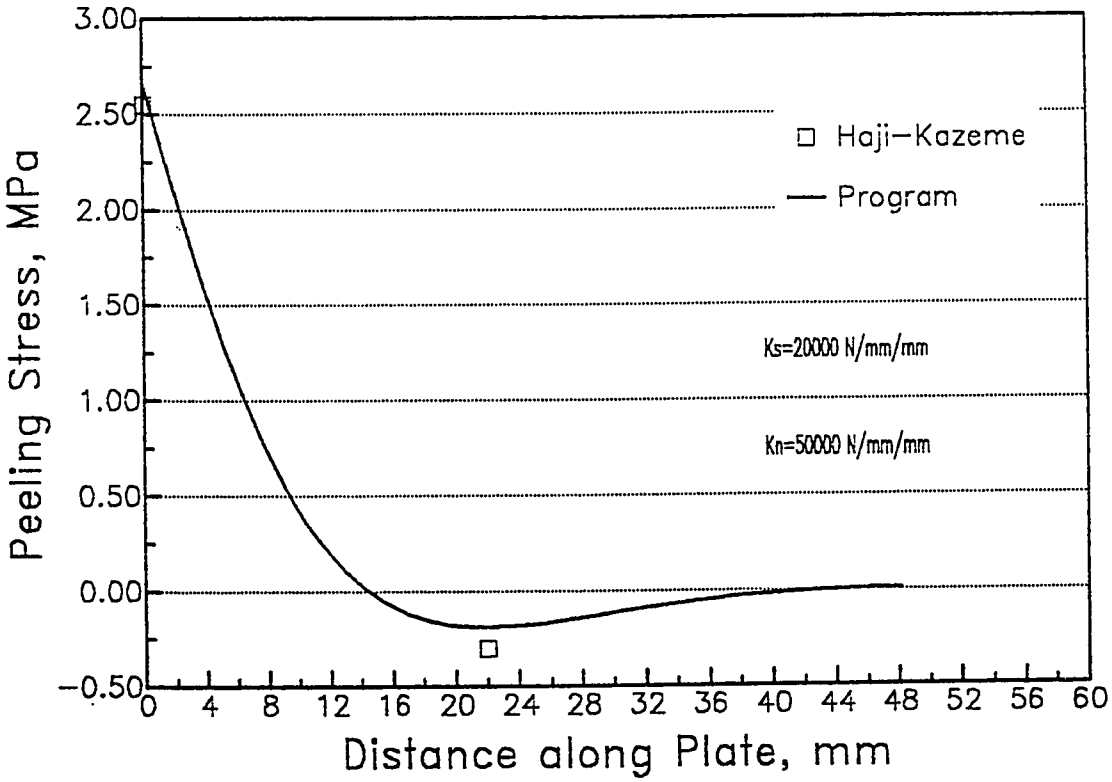

Figure 127: Peeling stress distribution at interface for Kn = 50000 N/mm/mm and for a/l = 0.75.

Figure 128 shows the tensile stress distributions along plate for Ks=20000 N/mm/mm, and for a/l=0.75 and a/l=0.50 respectively. The maximum tensile stress for both cases is same. The strain gradient at the end of the plate in case of shorter plate is more than that in case of longer plate.

Figure 129 shows the effect of the shear stiffness of the adhesive on the central deflection. With increasing the shear stiffness of the adhesive, the deflection of the beam decreases. This figure also shows that in case of longer plate, the central deflection is less than that in case of shorter plate.

Figure 130 shows the effect of shear stiffness of the adhesive on the maximum tensile stress of the steel plate for a/l=0.5 and 0.75 respectively.

Figure 131 shows the shear stress distributions along plate for Ks=20000 N/mm/mm and for a/l=0.5, a/l=0.75 and a/l=0.95 respectively. This figure shows that in case of shorter plate the shear stresses at the ends of the plate are higher than those in case of longer plate.

Figure 132 shows the shear stress distributions at interface for a/l=0.75 and for Ks=5000 N/mm/mm and Ks=40000 N/mm/mm respectively. In case of stiffer glue, the shear stresses at the ends of the plate are higher than those in case of softer glue.

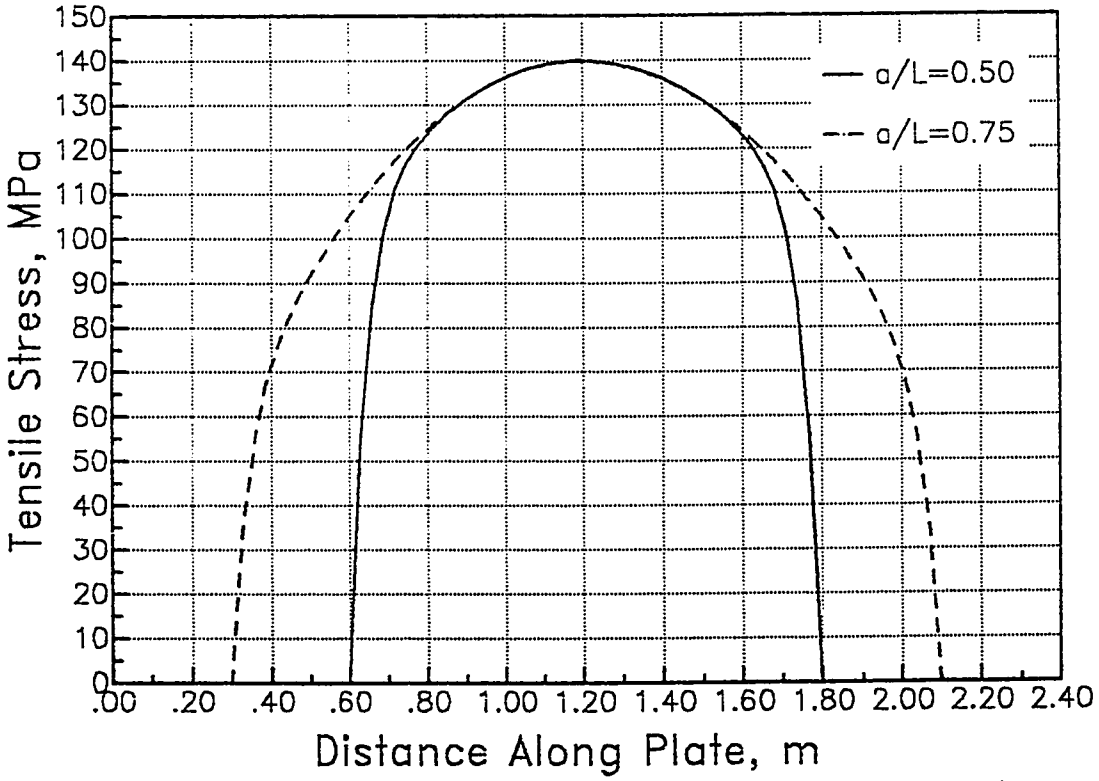

Figure 128: Tensile stress distributions along plate for a/l = 0.5 and 0.75 respectively and for Ks = 20000 N/mm/mm.

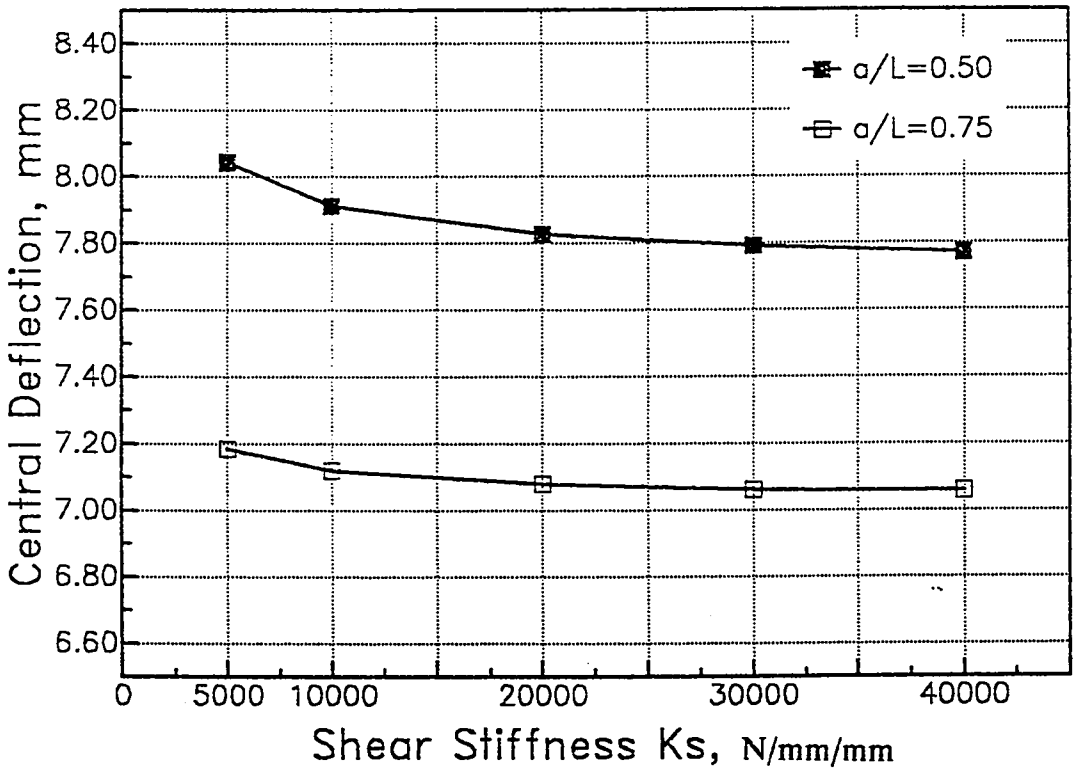

Figure 129: Effect of shear stiffness of the adhesive on the central deflection for a/l = 0.75 and 0.50 respectively.

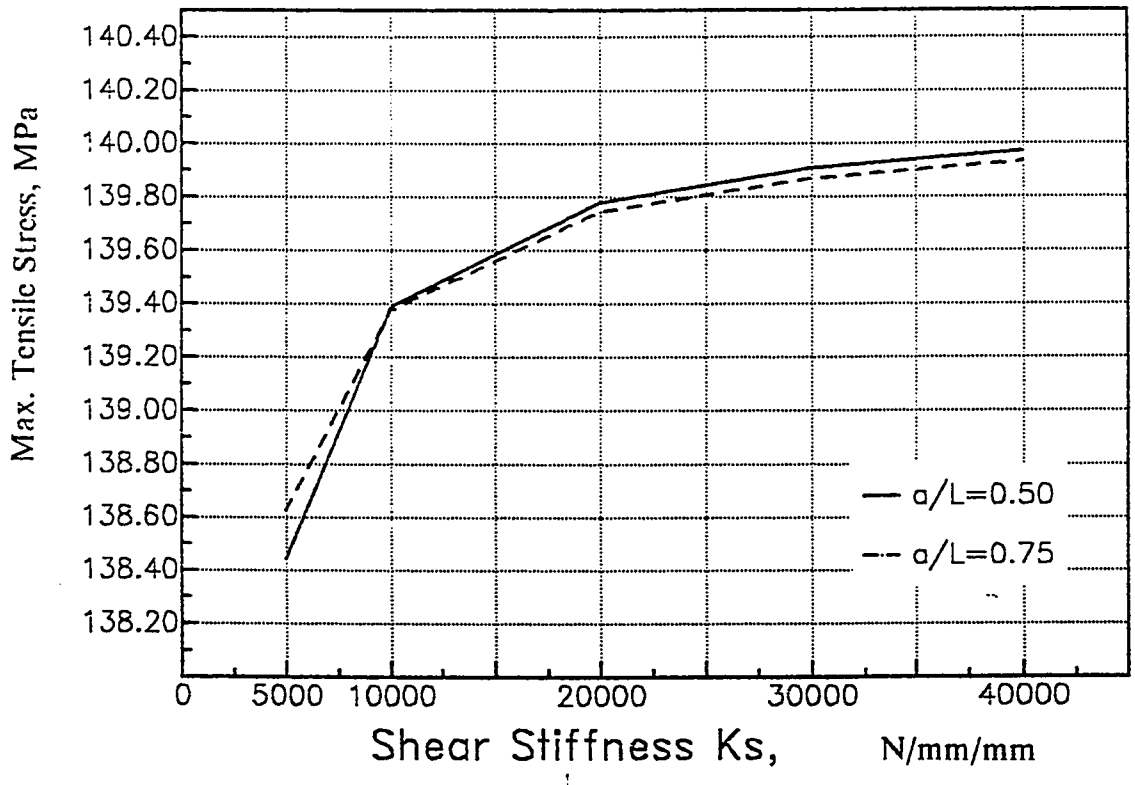

Figure 130: Effect of shear stiffness of the adhesive on the maximum tensile stress of the steel plate for a/l=0.5 and 0.75 respectively.

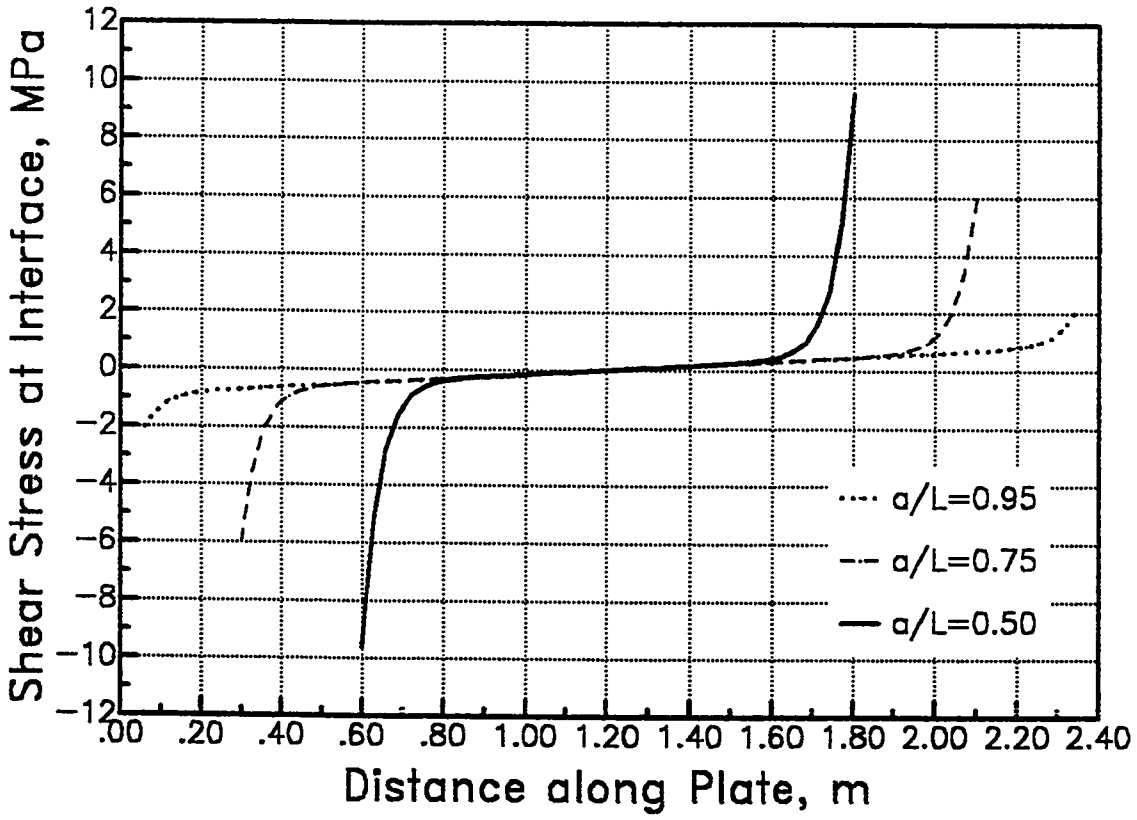

Figure 131: Shear stress distributions along plate for a/l=0.5, a/l=0.75 and a/l=0.95 respectively and for Ks=20000 N/mm/mm.

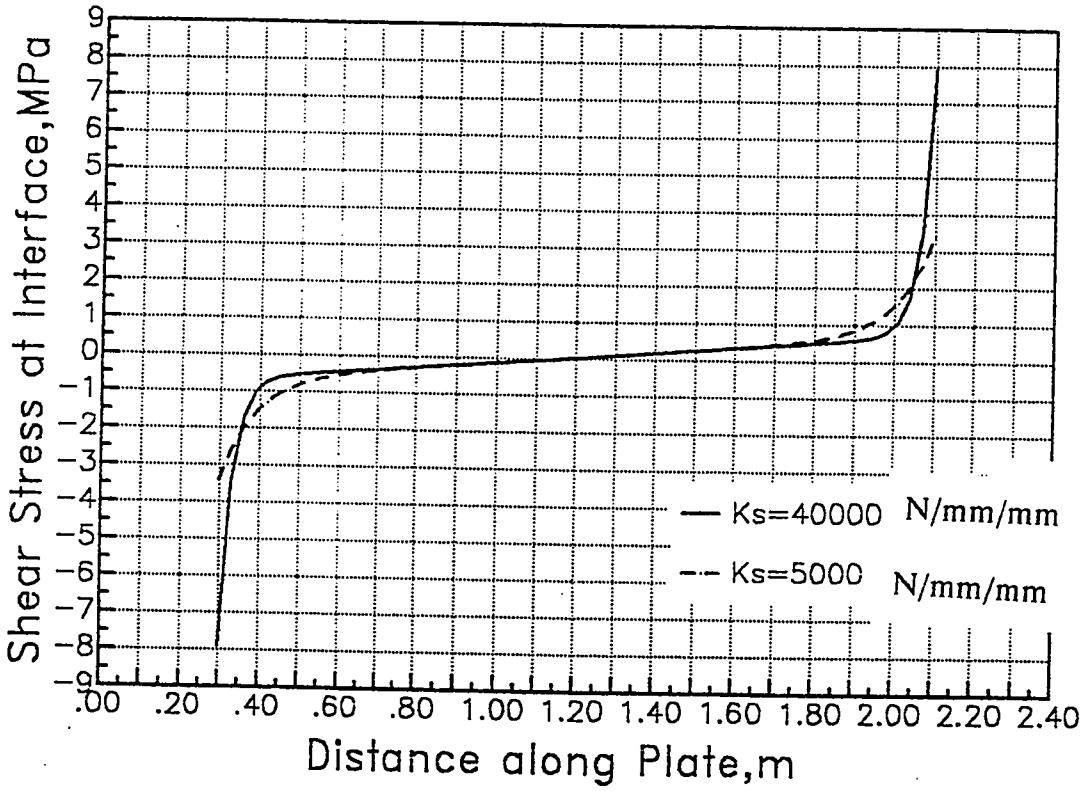

Figure 132: Shear stress distributions along plate for Ks = 5000 N/mm/mm and Ks = 40000 N/mm/mm respectively and for a/l = 0.75

Figure 133 shows the shear stress distributions at interface for a/l = 0.50 and for Ks = 5000 N/mm/mm and Ks = 40000 N/mm/mm respectively. In case of stiffer glue, the shear stresses at the ends of the plate are higher than those in case of softer glue.

Figure 134 shows the peeling stress distributions at interface for a/l = 0.50 and for Kn = 50000 N/mm/mm and Kn = 100000 N/mm/mm respectively. In case of stiffer glue, the peeling stresses at the ends of the plate are higher than those in case of softer glue. Also in case of stiffer glue the peeling stresses drop to zero more rapidly than those in case of softer glue.

Figure 135 shows the peeling stress distributions at interface for a/l = 0.75 and for Kn = 50000 N/mm/mm and Kn = 100000 N/mm/mm respectively. In case of stiffer glue, the peeling stresses at the ends of the plate are higher than those in case of softer glue. Also in case of stiffer glue the peeling stresses drop to zero more rapidly than those in case of softer glue.

Figure 136 shows the peeling stress distributions along plate for Kn = 50000 N/mm/mm and for a/l = 0.50, a/l = 0.75 and a/l = 0.95 respectively. In case of shorter plate, the peeling stresses at the ends of the plate are higher than those in case of longer plate.

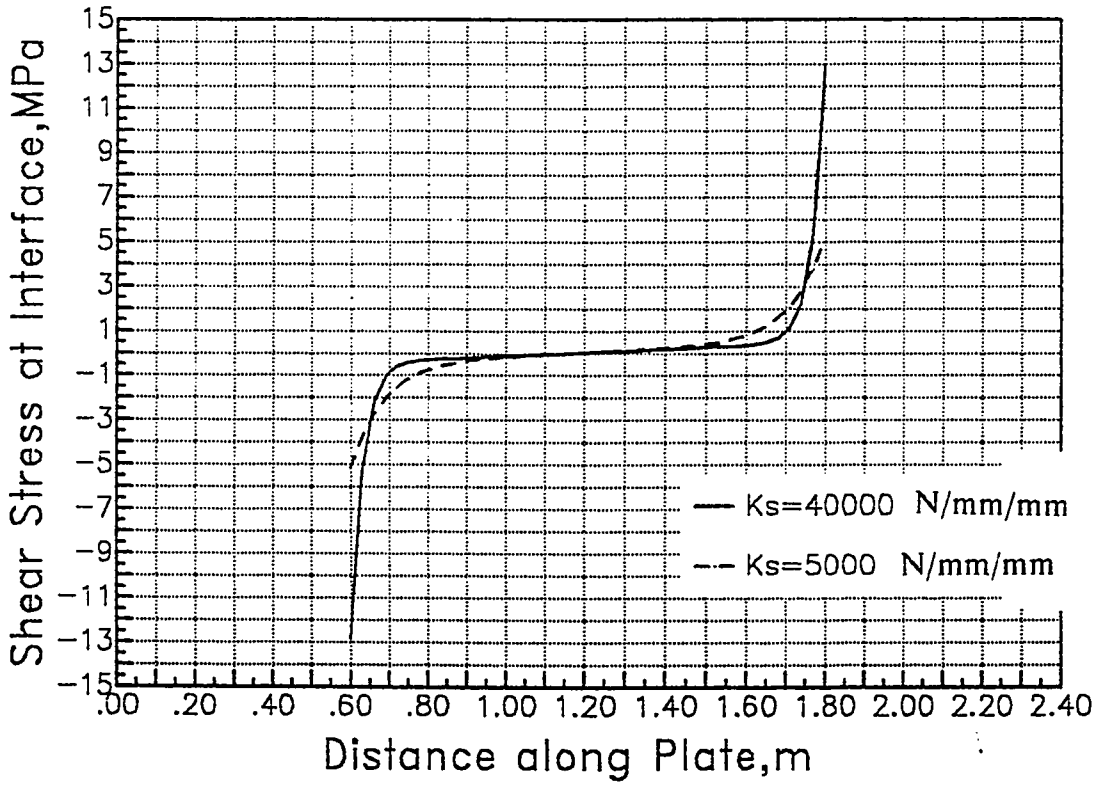

Figure 133: Shear stress distributions along plate for Ks = 5000 N/mm/mm and Ks = 40000 N/mm/mm respectively and for a/l = 0.50

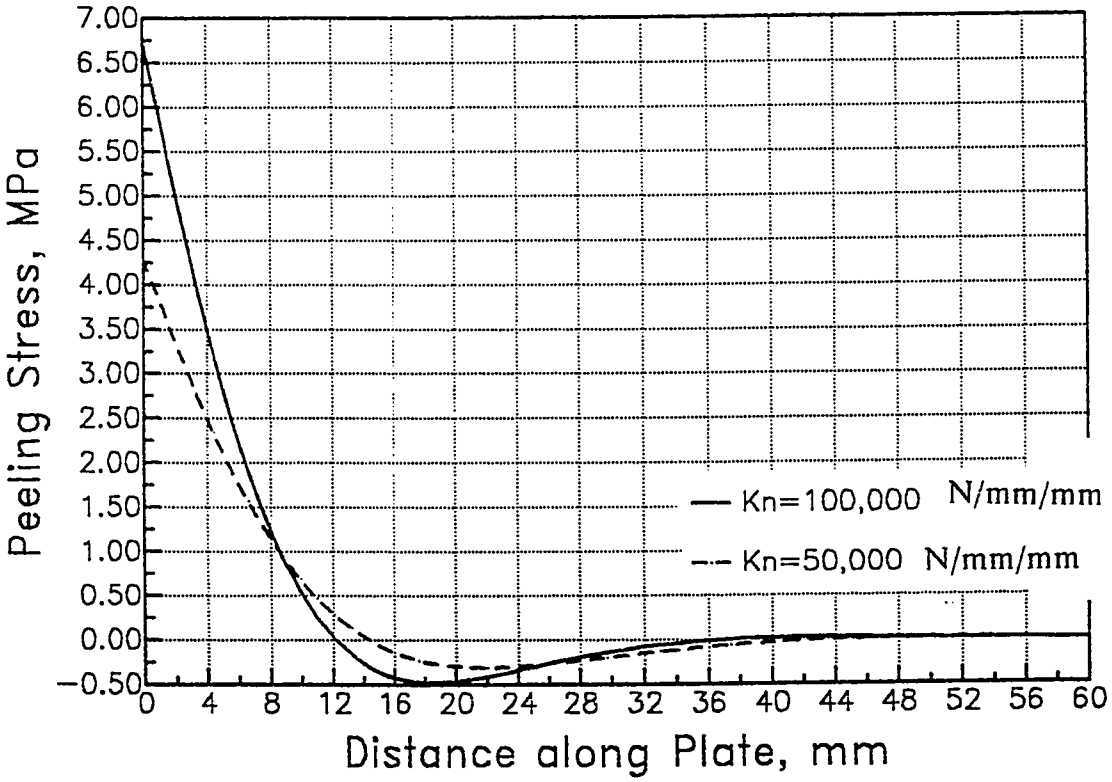

Figure 134: Peeling stress distributions along plate for Kn = 50,000 N/mm/mm and Kn = 100,000 N/mm/mm respectively, and for a/l = 0.50

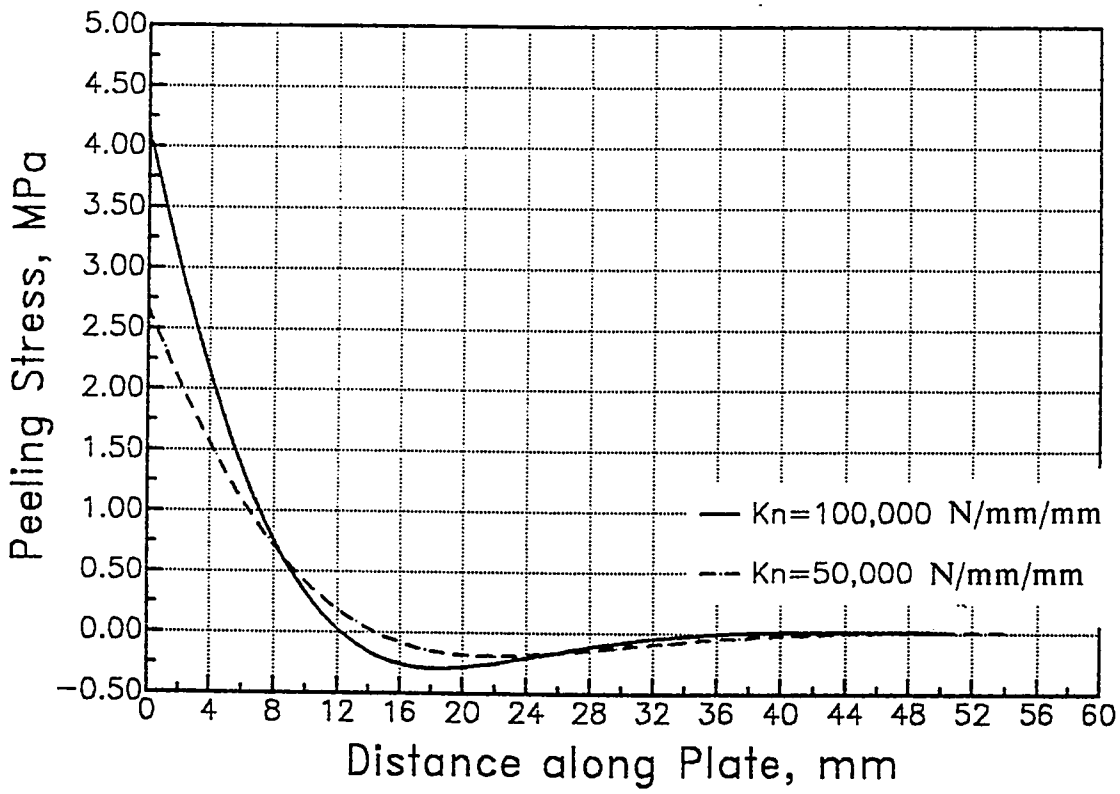

Figure 135: Peeling stress distributions along plate for Kn = 50,000 N/mm/mm and Kn = 100,000 N/mm/mm respectively, and for a/l = 0.75

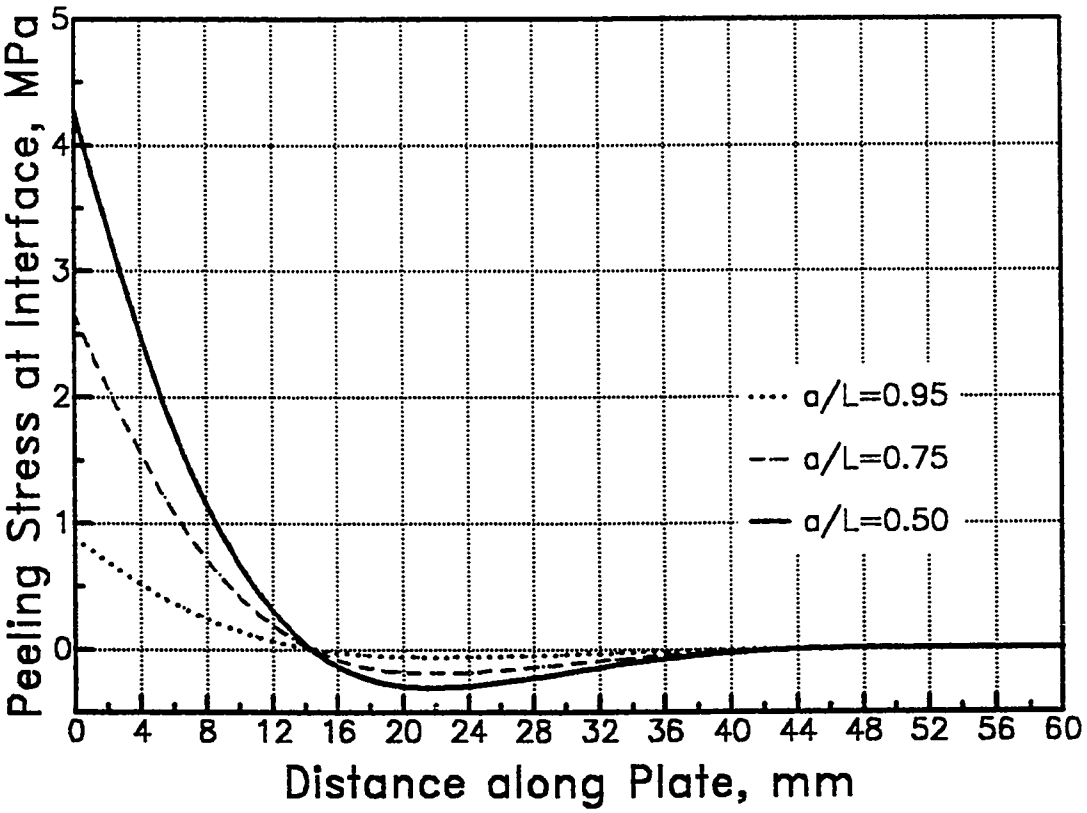

Figure 136: Peeling stress distributions along plate for a/l = 0.50, a/l = 0.75 and a/l = 0.95 respectively and for Kn = 50000 N/mm/mm.

Figure 137 shows the variation of the maximum shear stress at the ends of the plate with respect to the shear stiffness of the glue for a/l=0.5 and for a/l=0.75 respectively. This figure shows that with increasing the stiffness of the glue, the maximum shear stresses increase.

Figure 138 shows the variation of the maximum peeling stresses at the ends of the plate with respect to the normal stiffness of the glue for a/l=0.5 and 0.75 respectively. This figure shows that with increasing the stiffness of the glue, the peeling stresses increase.

Figure 139 shows the variation of the maximum shear stress with respect to the thickness of the bonded plate for a/l=0.75. This figure shows that with increasing the thickness of the plate, the maximum shear stress at the interface increases.

Figure 140 shows the effect of moving load on the shear stresses at the interface of the epoxy bonded plated beams. This figure shows the shear stress distribution at the interface for the plated beams taken from reference [21] for a point load of 30 kN placed at different positions along the span length for Ks=20000 N/mm/mm and for a/l=0.75. The span length of the beam is 2400 mm. When the load is at 1200 mm from the support, that is, the load is at mid-span, the shear stress distribution along the plate is symmetric. As the load is moved towards the the left support, the maximum shear stress on the left end of the

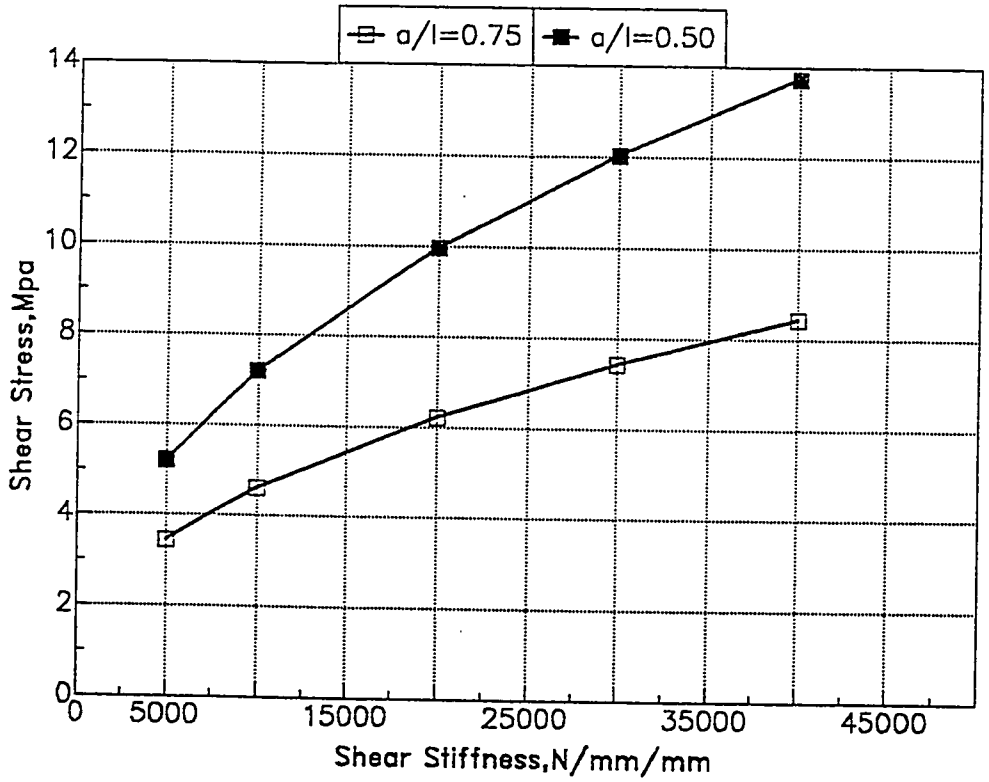

Figure 137: Variation of maximum shear stress at the ends of the plate with respect to shear stiffness of the Glue for a/l = 0.5 and a/l = 0.75 respectively.

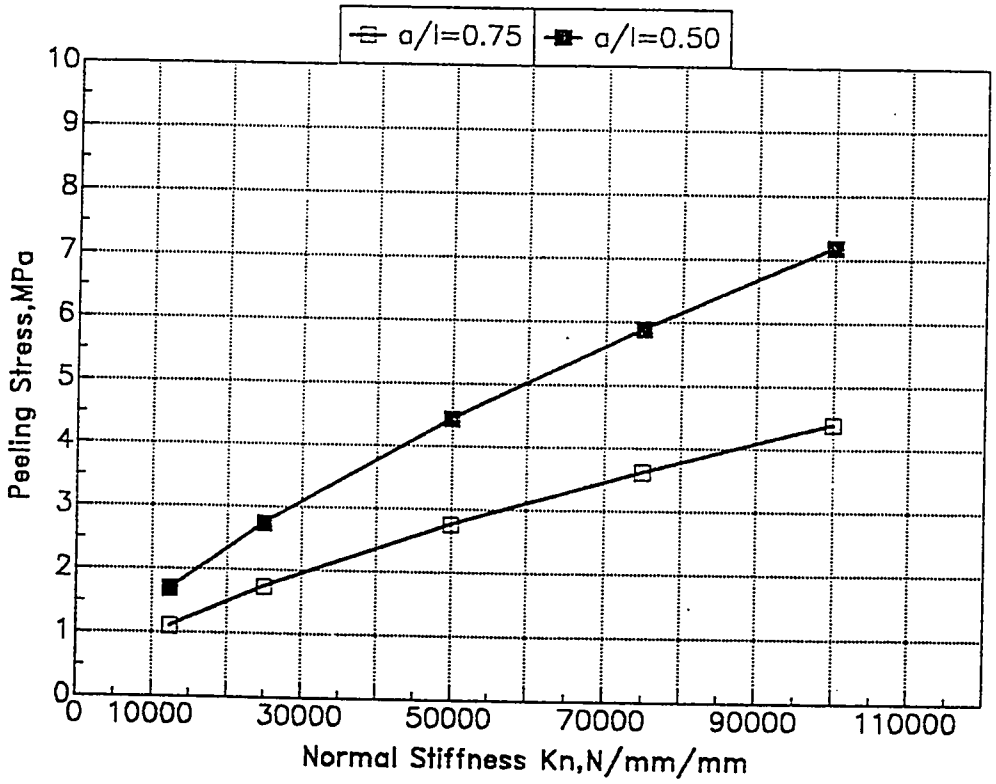

Figure 138: Variation of maximum peeling stresses at the ends of the plate with respect to Normal Stiffness Kn of the Glue for a/l=0.5 and a/l=0.75 respectively.

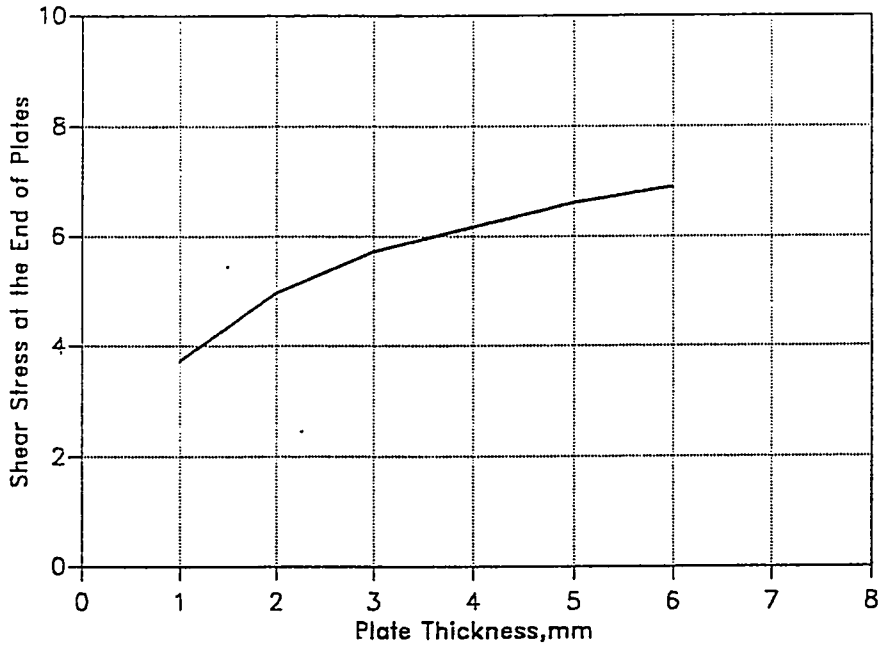

Figure 139: Variation of maximum shear stresses at the ends of the plate with respect to the thickness of the plate for a/l = 0.75.

plate increases and the maximum shear stress on the right end of the plate decreases. For example, when the point load is at 300 mm from the left support, the shear stress at the left end of the plate is about 8.9 MPa and at the right end of the plate is about 1.5 MPa. When the load is at 150 mm from the left support, the shear stress on the left end of the plate is 4.36 MPa and on the right end of the plate is 0.733 MPa. When the load is at 150 mm from the left support, it is in between the left end of the plate and the left support. When the load crosses the left end of the plate, the shear stress at the left of the plate has decreased as clear from the diagram. In brief, as the point load is moved towards left, the maximum shear stress at the left end of the plate increases provided the load does not cross the left end of the plate. When the load was placed in between the left end of the plate and the left support, the shear stress at the left end of plate was decreased.

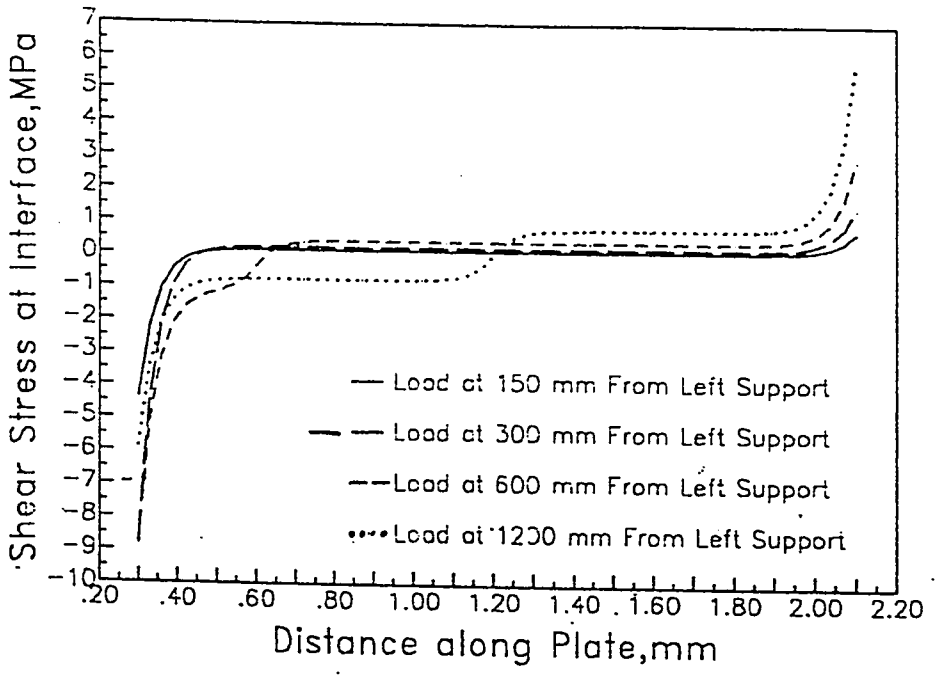

Figure 140: Effect of moving load on the shear stress at the interface.

5.5 COMPARISON OF EXPERIMENTAL AND THEORETICAL RESULTS

Table 13 shows the comparison of the theoretical and experimental results for the beams which were tested at KFUPM. For the concrete beam, upper layer, cracked transformed section was used in the program. Despite uncertainty in the properties of the glue and also this program can not handle the material and geometrical non-linearities, a good agreement exists between the experimental and theoretical values for deflections at loads just before the ultimate loads obtained from the testing of these beams. Beam B25 was bonded with 1.00 mm thick plate, beam B17 was bonded with 1.5 mm thick plate, beam B8 was bonded with 2.00 mm thick plate and beam B1 was bonded with 3.00 mm thick plate. The maximum shear and maximum peeling stresses, at the ends of the plates, at loads just before the ultimate loads, found from the program, for the beams B17, B8 and B1 fall within the range in which the separation of the plates takes place as suggested by R. Jones [19] based on the test results. Shear and peeling stresses at the interface for beam B25 were found at a load of 65 kN. In this beam pure flexure failure was obtained. The maximum shear and peeling stress at the interface for this beam as obtained from the program are 3.01 MPa and 0.715 MPa respectively. For separation to occur the maximum shear stress should be in the range of 3 to 5 MPa. and the maximum peeling stress should be in the range of 1 to 2 MPa as suggested by R. Jones [19] . In this beam (B25) the max. peeling stress is 0.715 MPa which is below the range of 1 to 2 MPa. From these stress values at the ends of the plate, it can be anticipated that in this beam separation of the plate should not occur upto the load at which program was run. Experimentally it has been proved that separation

of plate in this beam did not occurred at all. This beam failed by flexural crushing of the concrete. In case of beams B17, B8 and B1 strengthened by 1.5 mm, 2.0 mm and 3.00 plates failure occurred by the separation of the plate as observed from the testing of these beams. The maximum shear and peeling stresses at the ends of the plates, for these beams, as found from the program at loads just before the ultimate loads for these beams, fall within the ranges suggested by R. Jones [19] within which failure of the beam takes place by the separation of the plate.

Table 13: Comparison of theoretical and experimental results

Beam ID	Theo. max. shear stress (Mpa)	Theo. Max. Peel. Stress (MPa)	Theo. Defl. (mm)	Exp. Defl. (mm)	Prog. Run Load (kN)	Exp. Ult. Load (kN)	Mode of Failure
B25	3.01	0.715	5.75	5.5	65	69.0	Flexure
B17	4.00	1.061	5.54	5.5	72	75.0	Par.Flex.
B8	5.43	1.431	4.02	3.7	58	60.0	Separation
B1	6.43	2.090	3.25	3.6	56	58.0	Separation

Cracked Transformed Moment of Inertia for concrete beam was used

Shear Stiffness of Glue Ks = 8000 N/mm/mm ,That is, G = 120 MPa

Normal Stiffness of Glue Kn = 20000 N/mm/mm,that is, E = 300 MPa

R. Jones [19] recommended on the basis of test results that failure by the separation of plate occurs when the maximum shear stress range from 3 to 5 MPa and maximum peeling stress range from 1 to 2 MPa. Separation means the failure due to the tearing of the concrete at the end of the plate. However, these limits will depend on the strength of the concrete and the epoxy adhesive and on the method of surface preparation.

Chapter VI

LITERATURE SURVEY

(SHEAR PART)

6.1 INTRODUCTION

The main objective of our present study is to compare the various methods for repairing the RC beams damaged in shear. The comparison will be based on the improvement in ultimate strength and ductility. The ductility will be quantified by the modulus of toughness. Modulus of toughness is a good measure of ductility. The modulus of toughness is equal to the area under the load deflection curve of the beam up to failure. This area indicates the energy obsorbed by the beam upto failure. In this chapter shear force, shear stress based on linear flexure stress distribution, behaviour of beams without shear reinforcement and shear strength of the concrete beams based on ACI formula will also be discussed. The reason for reproducing the basic knowledge about the shear behaviour of the RC beams is to get acquaintance about the mechanisms of the different modes of shear failure of the RC beams.

6.1.1 SHEAR FORCE

Figure 141 shows a simply supported beam and a free-body diagram to the left of the section A-A. At section A-A of the free-body diagram, shear force V and moment M are acting. The shear force V and the moment M are the internal

forces provided by the beam. The value of V as shown in the free body diagram can be found by equating the sum of all the vertical forces acting on the free body diagram of the beam equal to zero. Similarly, the moment M shown on the free body diagram can be found by equating the sum of the moments about the point O equal to zero. Shear force V and moment M are the internal forces provided by the beam. Here we are concerned about the shear strength of the beam. Below the neutral axis there is only a state of pure shear which give rise to a stress of same magnitude acting at 45 degrees to the longitudinal axis of the beam. This tensile stress acting at 45 degrees to the longitudinal axis of the beam give rise to diagonal cracks. Shear failures are actually "tension failures" at the inclined cracks. This was first recognized by E. Morsey [35] in Germany in early 1900s. The factors influencing shear strength and formation of cracks are so numerous and complex that the definitive conclusion regarding the correct mechanism of inclined cracking which result from high shear stress are difficult to establish. Bresler and MacGregor [36] have given systematic correlation of the basic concepts.

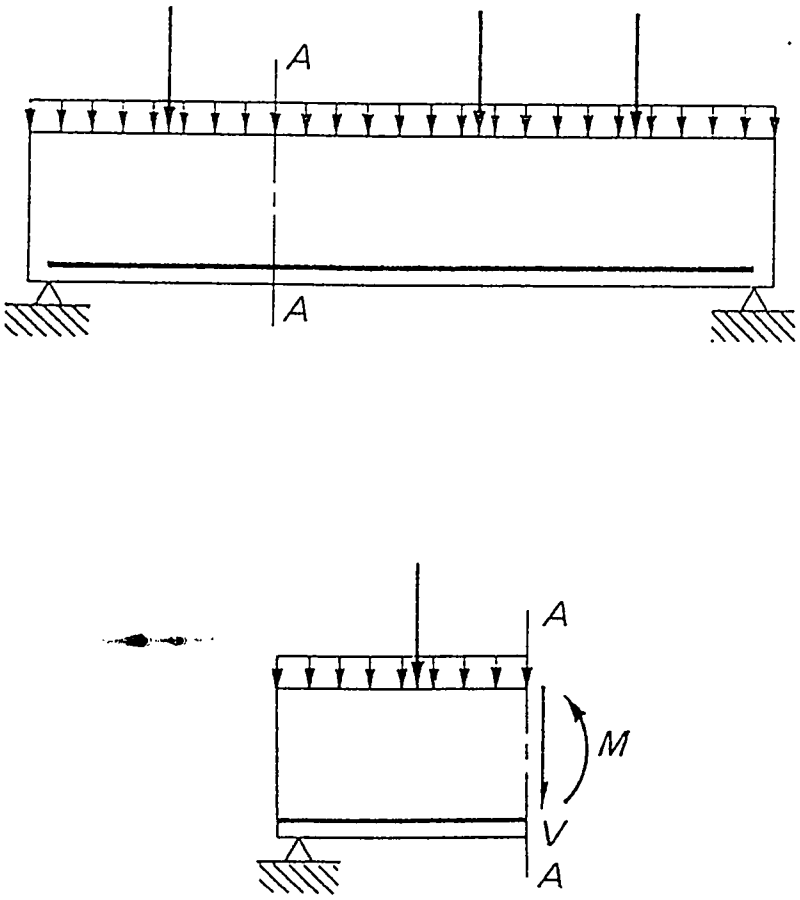

Figure 141: A typical simply supported beam and Free-Body diagram of the beam to the left of the section A-A.

6.1.2 SHEAR STRESS BASED ON LINEAR STRESS DISTRIBUTION

Figure 142 shows a simply supported beam. Consider the free body diagram of an element abcd. The depth of neutral axis is given by kd. Taking the equilibrium of horizontal forces on the element gives

$$v_y\, b\, dz = C_2 - C_1$$

where v_y is the unit horizontal shear stress on a plane at a distance y from the neutral axis. Within working stress limits we can have

$$C_1 = \frac{1}{2}(f_{c1} + f_{c2})\, b\, (kd\text{-}y)$$

$$f_{c1y} = \frac{y}{kd} f_{c1}$$

$$C_1 = \frac{M_1}{arm}\left(1 - \frac{y^2}{(kd)^2}\right)$$

$$C_2 = \frac{M_2}{arm}\left(1 - \frac{y^2}{(kd)^2}\right)$$

$$v_y = \left(\frac{M_2 - M_1}{dz}\right)\frac{1}{b(arm)}\left[1 - \frac{y^2}{(kd)^2}\right]$$

$$v_y = \frac{V}{b(arm)}\left[1 - \frac{y^2}{(kd)^2}\right]$$

At y = 0 we will get

$$v_y = \frac{V}{b\,(arm)} \qquad (84)$$

This formula is based on linear stress distribution. In strength design, the shear force V is the factored shear force and the distribution of flexural stress does not remain linear in the compression region of the beam. The tensile stress given by the equation (84) is not the actual tensile stress, however, the relative magnitude obtained by this equation is still a measure of the potential for inclined cracking. In ACI Code, the "arm" in the equation (84) has, thus, been replaced by effective depth "d" of the beam. The horizontal shear stress is also the vertical shear stress because the shear stress on two vertical planes must be equal. In regions where bending stress is low or where flexure cracks exist, the state of stress is pure shear stress. In such a case the maximum principal stress is the tensile stress acting at 45 degrees to the longitudinal axis of the beam of magnitude equal to shear stress. If at certain point below the neutral axis in a homogeneous beam the tensile stress is f_t, then the principal tensile stress will be

$$f_t(max) = \frac{1}{2} f_t + \sqrt{(\frac{1}{2} f_t)^2 + v^2}$$

This acts at an angle α with the beam axis. This angle for the principal tensile stress can be found from the following expression:-

$$\tan 2\alpha_{max} = \frac{2 \times v}{f_t}$$

These tensile stresses cause diagonal tension cracks in the concrete beams. Magnitude of the principal tensile stresses and their angle depend on the location of the point under consideration.

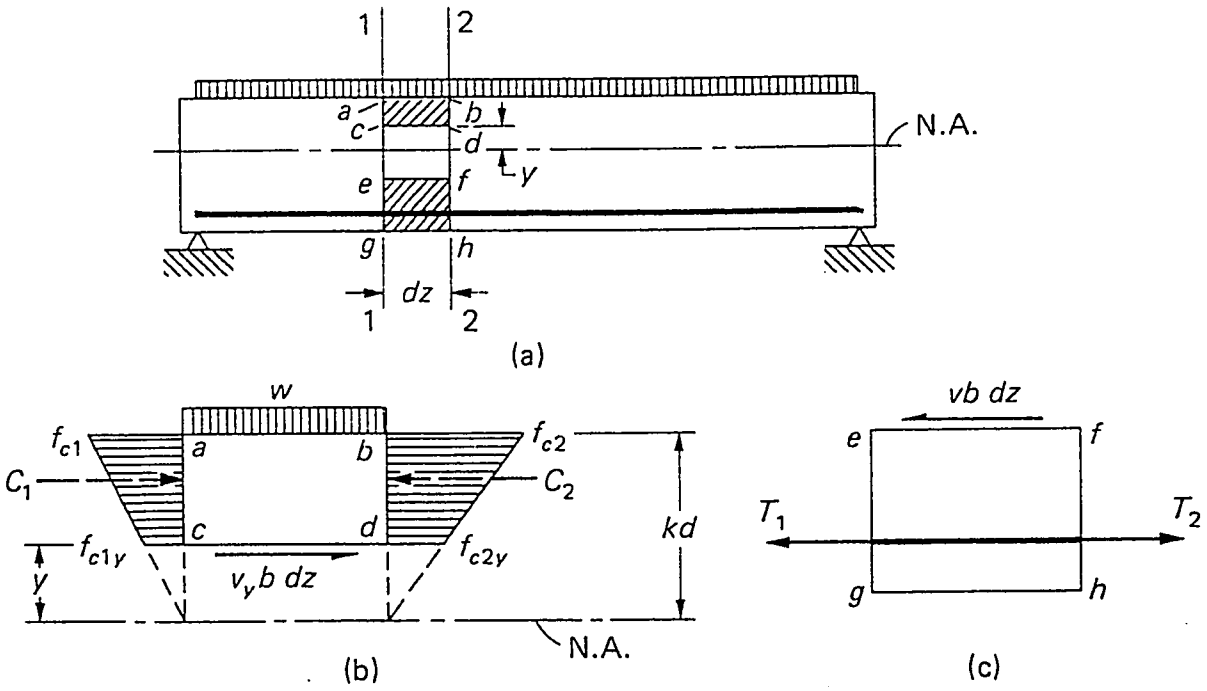

Figure 142: A Typical Simply Supported Beam. Free-Body Diagram of an Element abcd above the neutral axis.

6.1.3 BEHAVIOUR OF BEAMS WITHOUT SHEAR REINFORCEMENT

When a reinforced beam is loaded, two types of shear cracks could be produced.

1. WEB-SHEAR CRACKS

   An inclined crack occuring in a beam that was previously uncracked due to flexure is known as web shear crack.

2. FLEXURE-SHEAR CRACKS

   An inclined crack originating at the top of and becoming an extension to a previously existing flexure crack is known as flexure-shear crack. The critical flexure crack is known as an initiating crack.

Web-shear cracks are relatively rare in non-prestressed concrete beams. The cracks usually occur in thin-webbed beams having large flanges, commom only in prestressed construction. Web-shear cracks may also occur near the inflection points or bar cut-off points on the continuous reinforced concrete beams subjected to axial tension. Flexure-shear cracks are the usual type found in both reinforced and prestressed construction. In non-prestressed reinforced concrete beams flexure cracking occurs under service load. The flexure cracks extend vertically in the compression area of the beam. Due to shear stresses some of these flexure cracks transform into inclined shear crack. The rate of transformation of the initiating flexure crack into the flexure-shear cracks depends on the rate of growth and the height of flexure cracks as well as on the magnitude of shear stresses acting near the top of flexure cracks.

In reinforced concrete beams the shear force is resisted by the following mechanisms [37] as shown in the Figure 143

1. Shear resistance of the uncracked concrete, V_{cz}

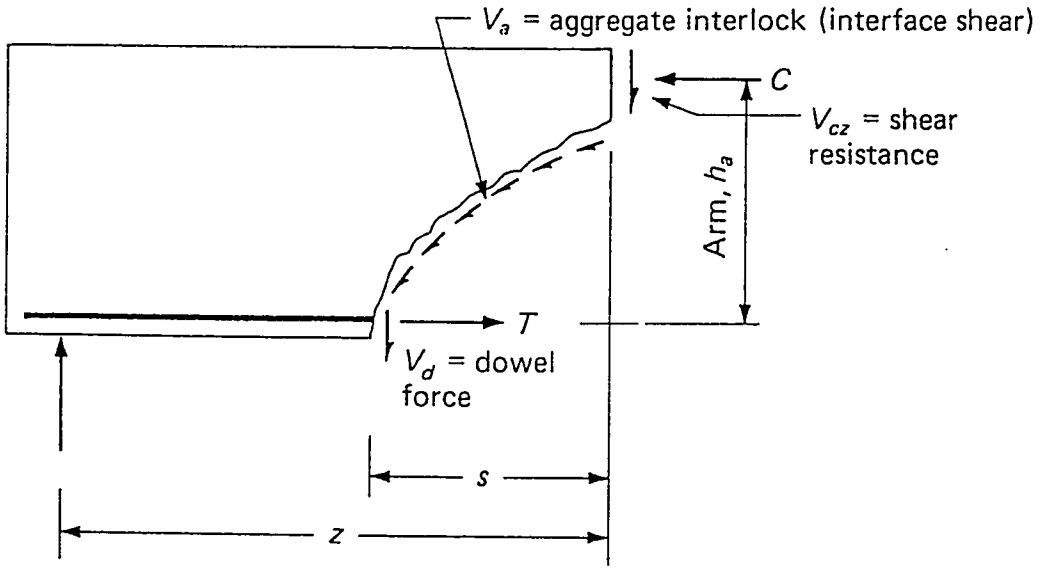

Figure 143: Redistribution of shear resistance after the formation of the inclined cracks.

2. Aggregate interlocking force. This acts tangentially along the crack and is similar to the frictional force due to irregular interlocking of the aggregate along the rough concrete surfaces on each side of the crack.
3. Dowel action, V_d , the resistance of the longitudinal reinforcement to a transverse force.
4. Arch action on relatively deep beams.
5. Resistance provided by the vertical and inclined stirrups.

The ability of a beam to carry additional load after inclined crack has formed depends whether or not the portion of the shear formerly carried by the uncracked concrete can be redistributed across the inclined crack. The mechanism 1 through 4 all participate in the redistribution, the success of which determines the shear capacity and degree of seriousness of the crack formation. ACI-ASCE Committee 426 [37] and H. P. J. Taylor [38] reported that for rectangular beams, after the formation of inclined crack, the transfer of shear by the various mechanisms is as follows

1. 15 % to 25 % is carried by the dowel action
2. 20 % to 40 % by the uncracked concrete in the compression zone.
3. 30 % to 50 % by the aggregate interlock.

The inclined cracks begin and grow depending on the relative magnitudes of shear stress and tensile stress. The shear and tensile stresses may be expressed as

$$v = k_1 \frac{V}{bd} \tag{85}$$

$$f_t = k_2 \frac{M}{bd^2} \tag{86}$$

where k_1 and k_2 are proportionality constants and dividing equation (86) by equation (85) we get the following equation

$$\frac{f_t}{v} = k_3(\frac{a}{d})$$

where constant k_3 is equal to $\frac{k_2}{k_1}$

The shear span to depth ratio (a/d) as has been shown experimentally is highly influential factor in determining the shear strength of the beams. This was reported by ACI-ASCE Committee 326 [35] , Boris Bresler and James G. Mac Gregor [36] , ACI Committee 426 [37] , JoDean Morrow and I. M. Viest [39] , G. N. J. Kani [40] and R. Diaz de Cossio and S. Loera [41] . Four general categories of failure may be established depending on the shear span to depth ratio (a/d) of the beams as shown in the Figure 144

1. DEEP BEAMS

   When a/d is less than 1, the beam is called deep beam. In deep beams , the shear stress has dominant effect. After inclined cracking, this type of beams tend to behave like a tied arch as shown in the Figure 145 in which the load is carried by the shaded area shown in this figure. Several modes of failure are possible for the tied arch as has been reported by H. A. Rawdon de Paiva and Chester P. Siess [42] , V. Ramakrishnan and Y. Ananthanarayana [43] , Howard P. J. Tayler [44] , R. F. Manual [45] and J. G. MacGregor and N. M. Hawkins [46] The possible modes of failure are indicated in the Figure 146

   a. Anchorage failure, that is, pull out of the tension reinforcement at the support.

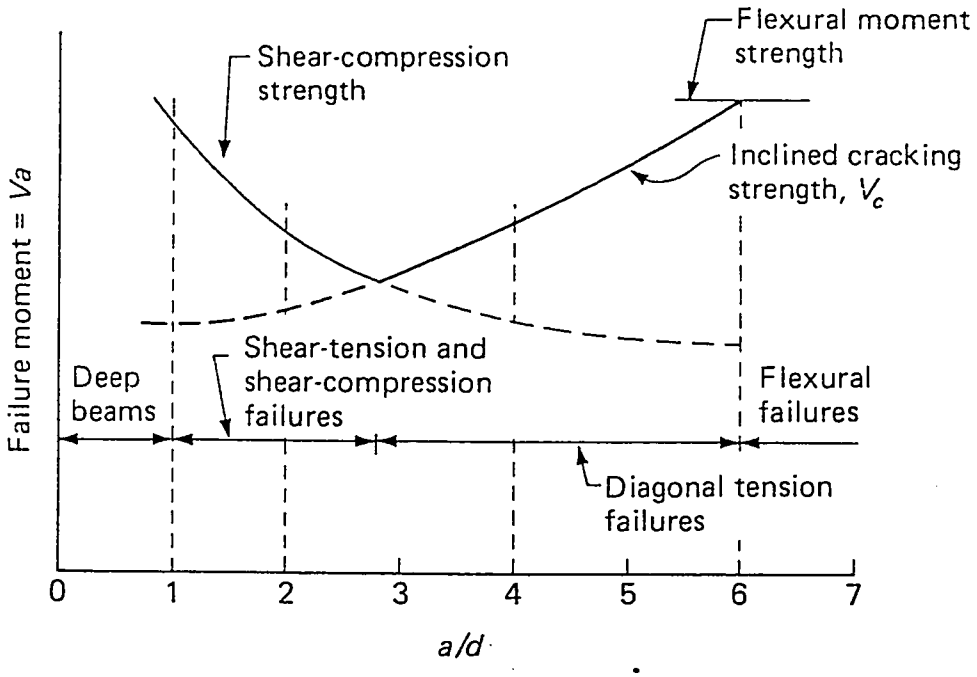

Figure 144: Variation in shear strength with a/d for rectagular beams. This figure has been taken from reference [36] .

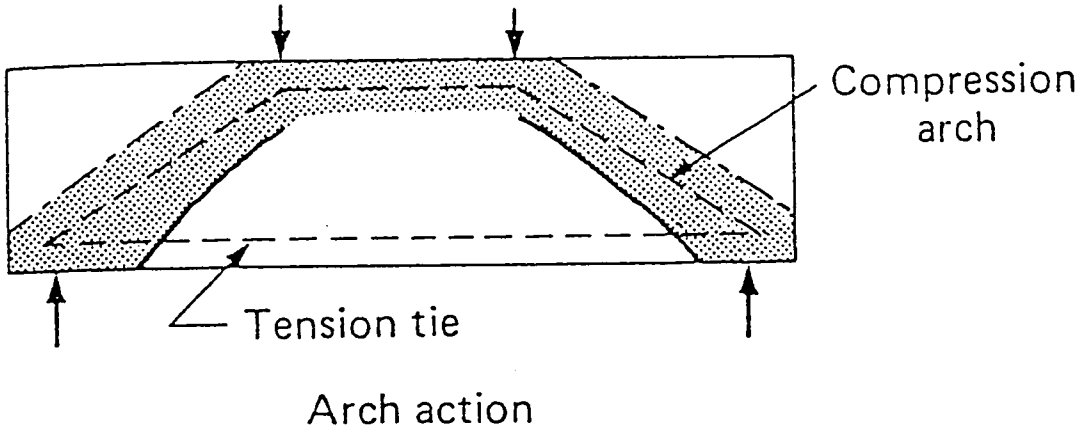

Figure 145: Arch Action in Deep Beams

b. A crushing failure at the reaction.

c. Flexure failure either due to crushing of the concrete or yielding of the tension reinforcement.

d. Failure of the arch rib due to an eccentricity of the arch thrust causing tension crack over the support or crushing of the concrete on the under side of the rib.

2. SHORT BEAMS

When a/d ratio is greater than 1 and less than or equal to 2.5, the beam is characterized as short beam. Short beams have shear strength more than the inclined cracking strength. After the flexure-shear crack develops, the crack extends further into the compression zone as the load increases. It also propagate as secondary crack towards the tension reinforcement. Failure occurs either by the anchorage failure at the tension reinforcement called shear-tension failure or by a crushing failure in the concrete near the compression face called shear compression failure as shown in the Figure 147 and Figure 148 respectively.

3. BEAMS OF INTERMEDIATE LENGTHS

When the a/d is greater than 2.5 and less than or equal to 6, the beams are called intermediate length beams. In intermediate length beams, first vertical flexure cracks are formed and then flexure shear cracks are formed. At the beginning, several flexure cracks tend to bend, making beam segments between the cracks as "teeth" as shown in the Figure 149 When the root of the tooth as a result of increasing number of flexure cracks, is so reduced [47] in size that it becomes unable to carry moment

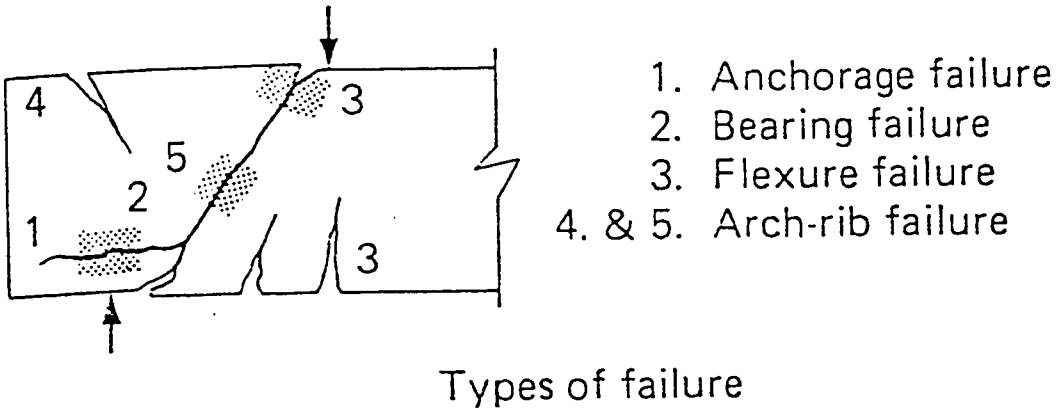

Figure 146: Modes of Failure in Deep Beams with a/d less than or equal to 1.00. Adopted from reference [36] .

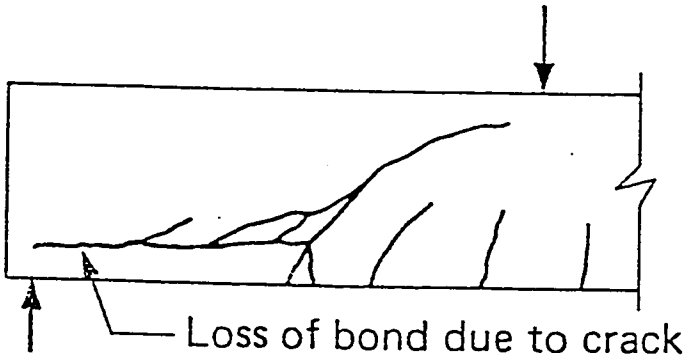

Figure 147: Shear Tension Failure in Short Beams

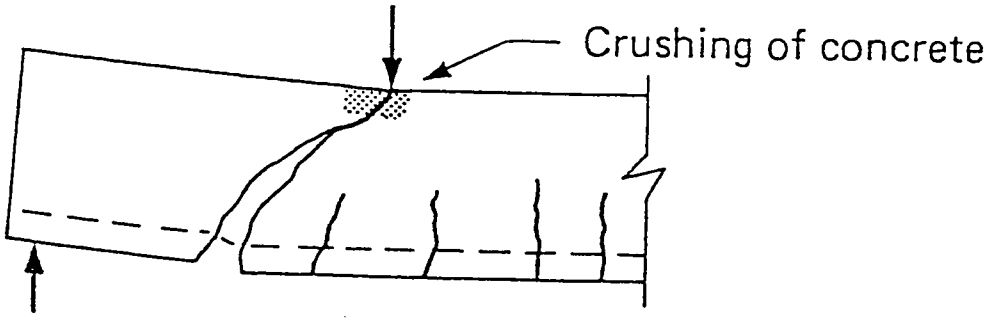

Figure 148: Shear Compression Failure in Short Beams

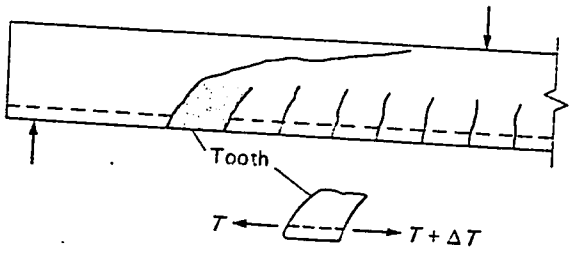

Figure 149: Diagonal Tension Failure or Tooth Cracking Failure. For Intermediate Length Beams; a/d about 2.5 to 6.

due to ΔT , it breaks to form flexure-Shear crack. At the sudden occurence of the inclined crack, the beam is not able to redistribute the load as in the situation of smaller a/d ratio. In other words, formation of the inclined crack represent shear strength of beams in this category. This type of failure is called diagonal tension failure.

4. LONG BEAMS

When a/d is greater than 6, the beams are called long beams. The failure of long beams start with the yielding of the tension reinforcement and ends by the crushing of the concrete at the section of maximum bending moment. In addition to the nearly vertical flexure cracks at the section of maximum bending moment, there may be slightly inclined cracks between the support and the section of maximum bending moment. However, the strength of the beam is entirely dependent on the magnitude of the maximum moment and is not dependent on the magnitude of shear force. Such beams may fail by the formation of inclined crack which is called diagonal tension failure as for the beams with a/d between 2.5 and 6.0

6.1.4 SHEAR STRENGTH OF CONCRETE BEAMS WITHOUT SHEAR REINFORCEMENT

The strength at which inclined crack forms, is taken to be the shear strength of the concrete beams without shear reinforcement. The shear strength depends on the strength of the concrete, reinforcement ratio of longitudinal steel, shear-span and the effective depth of the rectangular section. The following relationship for finding the the shear strength for beams of a/d varying from 2.5 to 6 was reported based on 440 tests [35] .

$$V_n = [1.9\sqrt{f_c'} + 2500\rho \frac{V_n d}{M_n}] b_w d$$

But V_n should not be greater than $3.5\sqrt{f_c'}bd$

Since 1963, ACI code has accepted this relation for finding the shear strength of the beams without shear reinforcement with small modification. The modified equation for finding the shear strength of RC beams is given below:-

$$V_c = [1.9\sqrt{f_c'} + 2500\rho_w \frac{V_u d}{M_u}] b_w d \qquad (87)$$

But V_c should not be greater than $3.5\sqrt{f_c'}b_w d$. Where V_c is the nominal strength of beams of a/d ratios of about 2.5 to 6. f_c' is the cylinder strength of the concrete in psi. ρ_w is the ratio of the longitudinal web steel. V_u is the factored shear force acting on the section, M_u is the factored moment acting on the section. b_w is the width of the concrete section at the neutral axis. d is the effective depth of the concrete section, that is, the distance between the centriod of the tension steel and the top edge of the beam.

The use of the factored shear force V_u and factored moment M_u instead of $V_n = \frac{V_u}{\Phi}$ and $M_n = \frac{M_u}{\Phi}$ in the equation (87) does not affect the end results because V_u/M_u remains approximately equal to the ratio V_n/M_n in spite of some difference in the strength reduction factor Φ for shear and for moment. The value of $V_u d/M_u$ shall not be taken greater than 1.00 except in the beams which are subjected to axial compression. In beams subjected to axial compression,

$\frac{V_u d}{M_u}$ may be greater than 1.00.

††††††††††††††††††††

This chapter has been written with the help of the book, "Reinforced Concrete Design Fourth Edition" by Chu-Kia Wang, Charles G. Salman, University of Wisconsin-Madison. Harper and Row Publishers, New York.

Chapter VII

EXPERIMENTAL PROGRAM

(SHEAR PART)

7.1 PREPARATION OF BEAMS

A total of twelve beams were cast, but only ten beams were used for our present study. These beams were named as MS-series beams. All the beams were 150 by 150 mm in cross-section and 1250 mm in length. These beams were designed such that under four point loading , as will be explained later, they should fail in shear. These beams were provided with 12 mm dia. bars at the bottom as longitudinal reinforcement. The clear cover upto the main steel was 30 mm. A total of four U-stirrups of 6 mm dia. bars were provided in these beams The reinforcement detail of these beams is given in the Figure 150

The casting of beams was done in the Ferrocement laboratory of KFUPM. Concrete cylinders 150 mm in diameter and 300 mm in length were also cast along the beams. The curing of concrete beams and cylinders was done for 28 days under gunny bags which were kept wet by sprinkling water over them intermittantly. After four months the beams were brought to Structural Mechanics laboratory for damaging them with the help of 25 tons INSTRON machine.

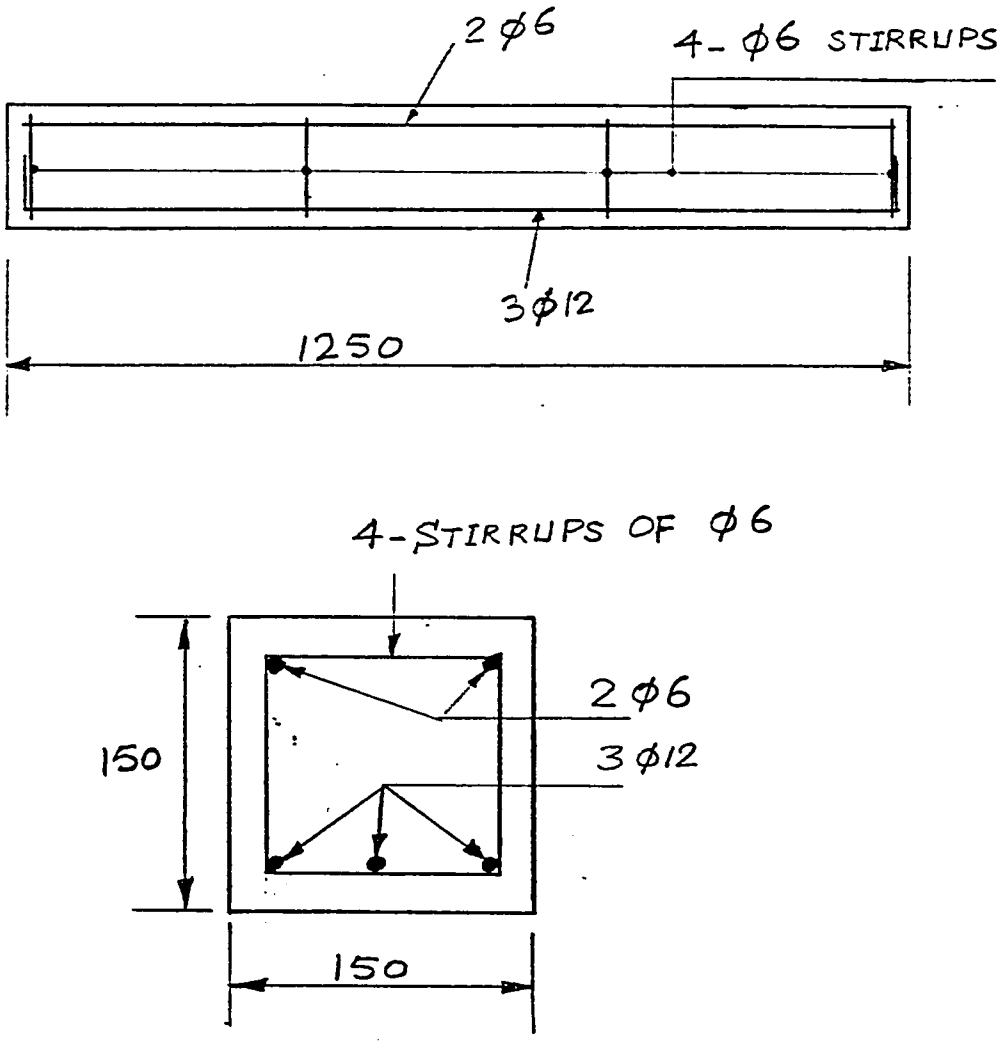

Figure 150: Reinforcement detail of beams of MS-series. A total of four U-stirrups were used, at the support and at third points.

7.2 MATERIAL PROPERTIES

Average concrete cylinder strength equal to 39.5 MPa was found for beams of MS-series. The plates were of mild steel and their yield strength was 269 MPa. However, for calculating the ultimate flexure strength of these beams actual stress-strain curve of the rebars steel was used which is also given in the Figure 151 . The elastic modulus of both steel plate and the steel bars is 200,000 MPa.

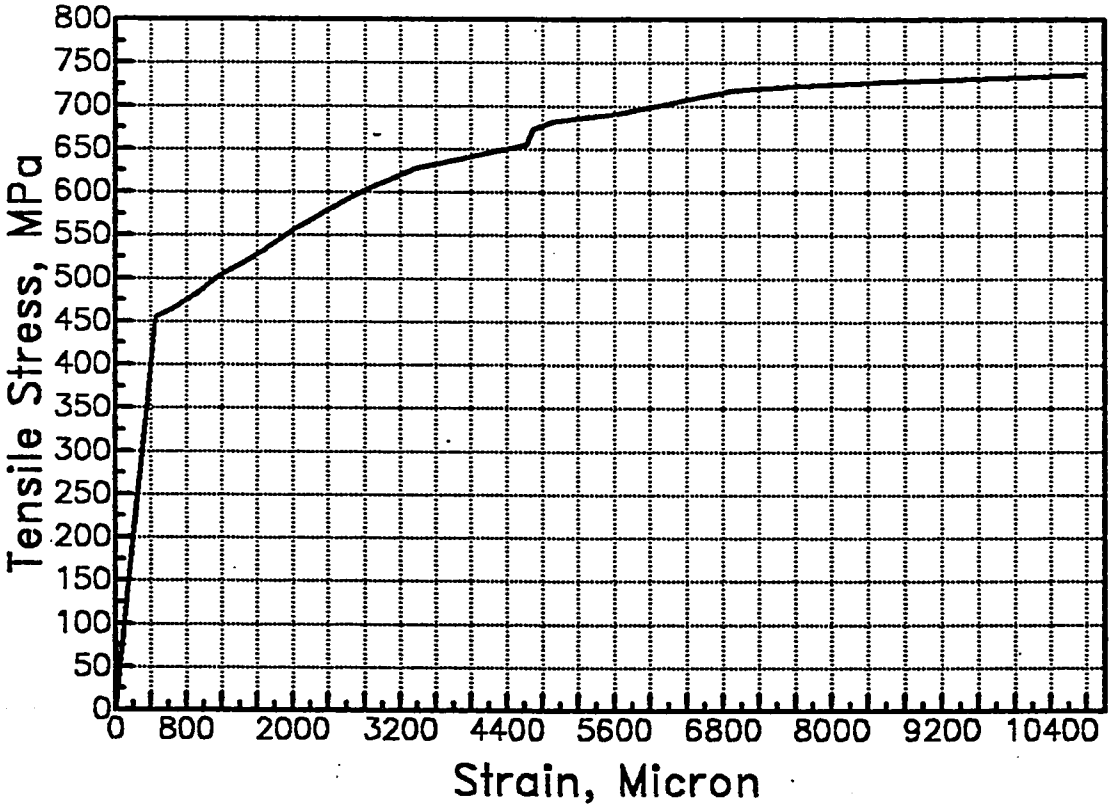

Figure 151: Stress-Strain curve of bar reinforcement.

7.3 DAMAGING THE BEAMS IN SHEAR

First of all, all the beams were marked at the support points and at the third points to help in placing the supports and LVDTs during loading. Figure 152 shows the loading setup and marking of the beams. All the beams were loaded to damage in shear. The loading was done upto about 5 mm central deflection. All the beams failed in shear upto this central deflection and then the load was gradually removed. The loading and unloading was done at the same rate, that is, 1 mm per minute to induce the shear damage in the beams. Diagonal cracks appeared in the shear spans and the widths of cracks at maximum load and after unloading were measured.

Figure 153 shows the load deflection curve of a typical beam for original loading.

Table 14 shows the maximum load, maximum central deflection and the residual deflection for original loading of all beams. Beam MS10 was badly damaged and it had a maximum crack width of 4 mm. Upon unloading this beam had a residual deflection of 3.143 mm as shown in the Table 14

Table 15 shows the average width of diagonal cracks at maximum central deflection and at residual deflection respectively.

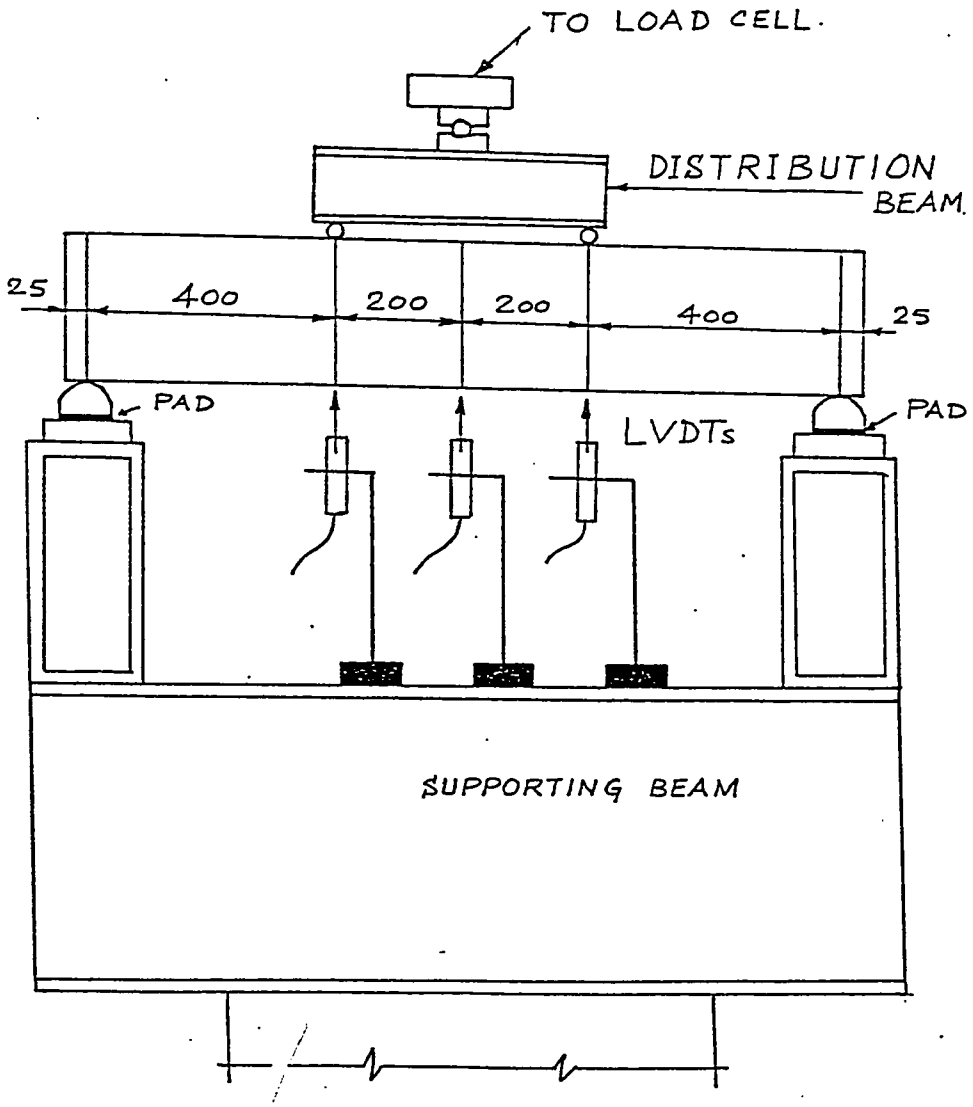

Figure 152: Marking of beams and loading SETUP for damaging and final testing respectively.

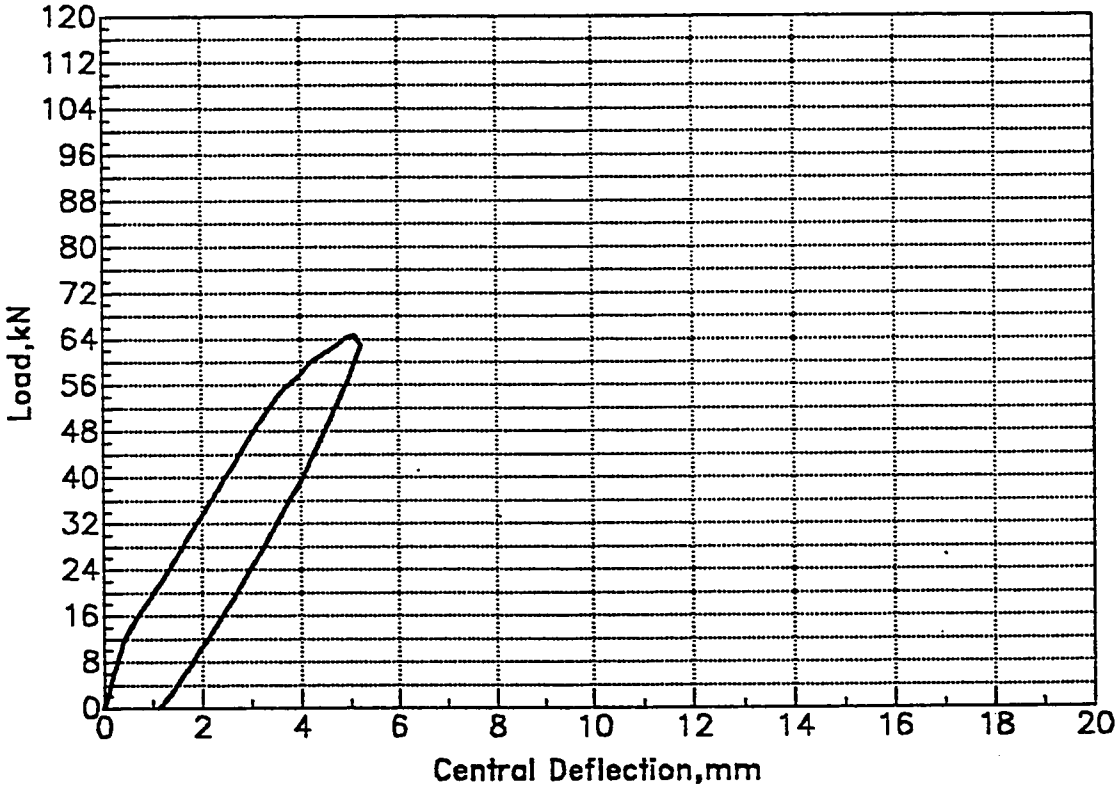

Figure 153: Load-deflection curve of a typical beam to induce shear damage.

Table 14: Original Loading

Beam Nos.	Maximum Load (kN)	Maximum Central Deflection (mm)	Residual Central Deflection (mm)
MS2	60.4	5.219	1.123
MS3	66.46	5.093	0.856
MS5	64.57	5.189	1.123
MS6	63.48	5.133	1.360
MS7	66.05	5.133	1.229
MS8	69.05	5.088	1.083
MS9	69.04	5.163	1.259
MS10	62.09	5.370	3.143
MS11	64.04	5.063	0.932

Note: For beam MS4 the file for loading for damaging the beam could not be saved. Therefore, the data for this beam is not given above.

Table 15: Average Width of Diagonal Cracks

Beam Nos.	Average crack width at maximum central Deflection (mm)	Average crack width at residual central deflection (mm)
MS3	0.50	-
MS5	0.55	0.25
MS6	1.00	-
MS7	0.80	0.40
MS9	0.90	0.30
MS10	4.00	4.00
MS11	0.30	0.10

In some beams more than one diagonal cracks appeared in the shear span so average values of diagonal cracks are given in this table at maximum central deflection and after unloading.

7.4 STRENGTHENING OF BEAMS

Reinforced concrete beams, damaged in shear, were repaired to restore and increase their shear capacity. The methods used in repair are explained below:-

1. JACKET A

   These were fabricated from 1.5 mm thick steel plates. The clear widths of these were 153 mm and the depths were 121.5 mm. The lengths of these were kept equal to the length of the shear span, that is, 400 mm.

2. JACKET B

These were also fabricated from 1.5 mm thick steel plate. The clear widths of these were 153 mm and depth was 61.5 mm. The lengths of these were equal to the length of the shear span, that is, 400 mm.

3. WINGS

These were 400 by 120 mm rectanglar plates bonded to the shear zone on both sides of the beams. These were also made from 1.5 mm thick steel plates.

4. U-STRIPS

These strips were fabricated from 1.5 mm thick steel plate. The width of these strips was 20 mm. The strip bend around the beam section from the sides. These were bonded to the beams at 40 mm clear spacing between them.

5. STRAIGHT STRIPS

These strips were fabricated from 1.5 mm thick steel plates. The width of these strips was 20 mm. The length of these strips was 150 mm. These strips were bonded to the sides of the beam in the shear zone. The clear spacing between them was kept equal to 40 mm.

The beams were prepared for bonding by sandblasting in shear span on both sides to expose the aggregate for proper adhesion of glue. Similarly the steel plates (jackets, wings, strips) were sandblasted to make them rough for proper adhesion. After sandblasting the beams and the plates were air blown to make them dust free.

The adhesive was a two part epoxy glue. First the each part was separately mixed in its own container with the help of stirrer. Then these parts were mixed in 1:2 ratio in an other container with the help of stirrer. The mixing of glue was done according to the quantity required. The mixed glue had a paste like consistency. After mixing the glue it was applied with the help of brushes to the sand-blasted concrete surface and strengthening plates (jackets, strips, wings) which were already cleaned. Then the plates were placed in proper position and clamps were used to hold the plates until the curing of glue.

7.5 INSTRUMENTATIN OF BEAMS

Strain gages were installed on the rebars at the mid-span for measuring rebar strain. Similarly, strain gages were installed on the top of the beams at mid-span for measuring concrete compression strain. Strain gages were also installed on the external reinforcement at different locations for measuring strains.

7.6 STRENGTHENING DETAIL OF BEAMS

Table 16 gives the the summary of the strengthening detail of the beams.

Figure 154 to figure 158 show the strengthening detail of the beams of MS-Series.

Table 16: Summary of the strengthening detail of beams

Beam ID	Strengthening Detail
MS6,MS10	Repaired By Jacket-A
MS3,MS8	Repaired By Jacket-B
MS4,MS9	Repaired By Wings
MS2,MS11	Repaired By U-strips
MS5,MS7	Repaired By Straight Strips

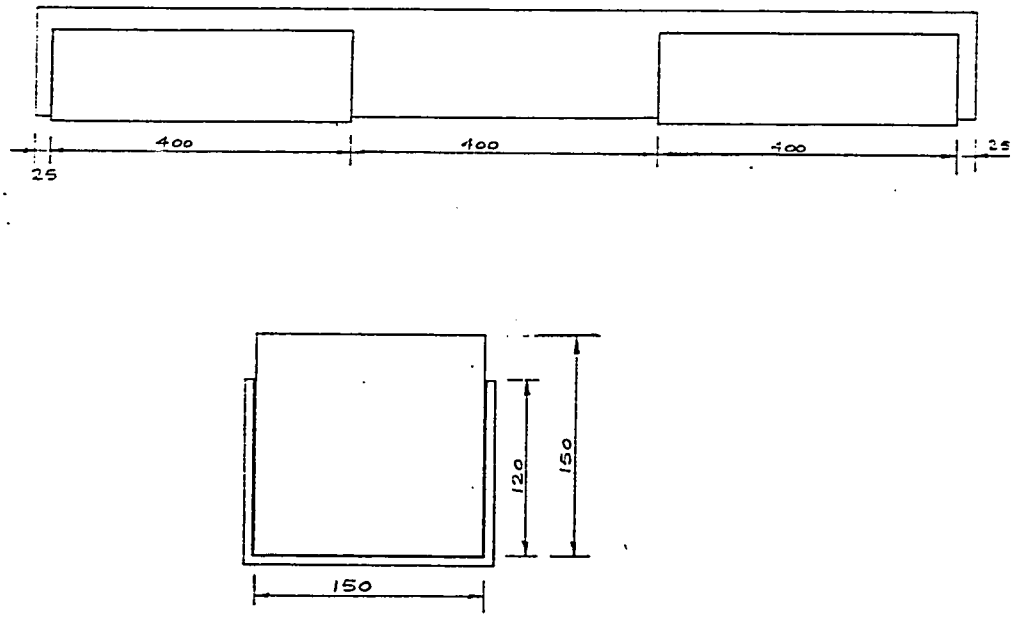

ALL DIMENSIONS ARE IN MILLIMETERS

Figure 154: Strengthening detail of beams MS6 and MS10 strengthened by Jacket A.

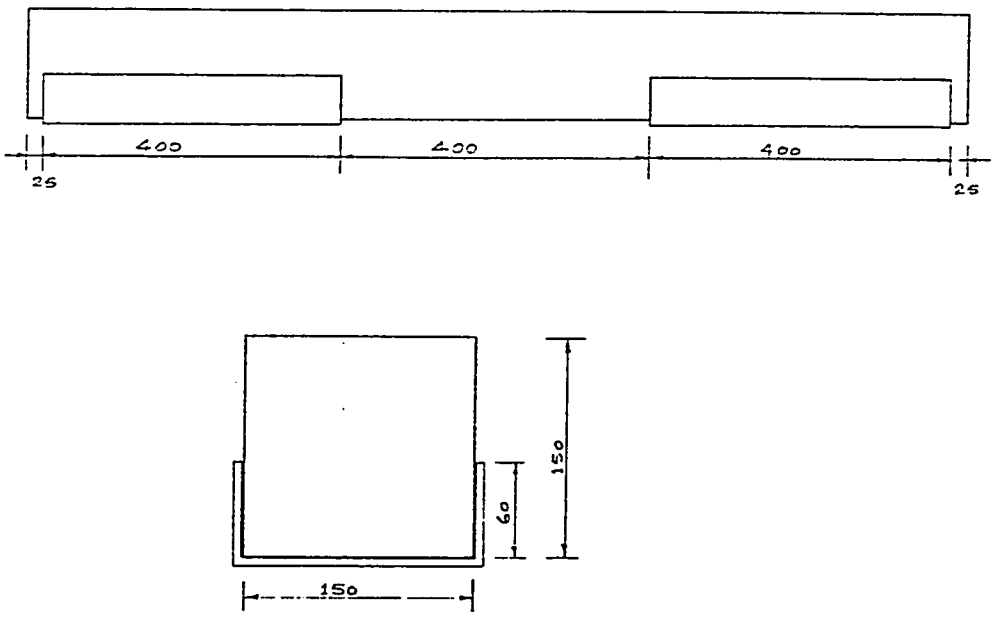

Figure 155: Strengthening detail of beams MS3 and MS8 strengthened by Jacket-B.

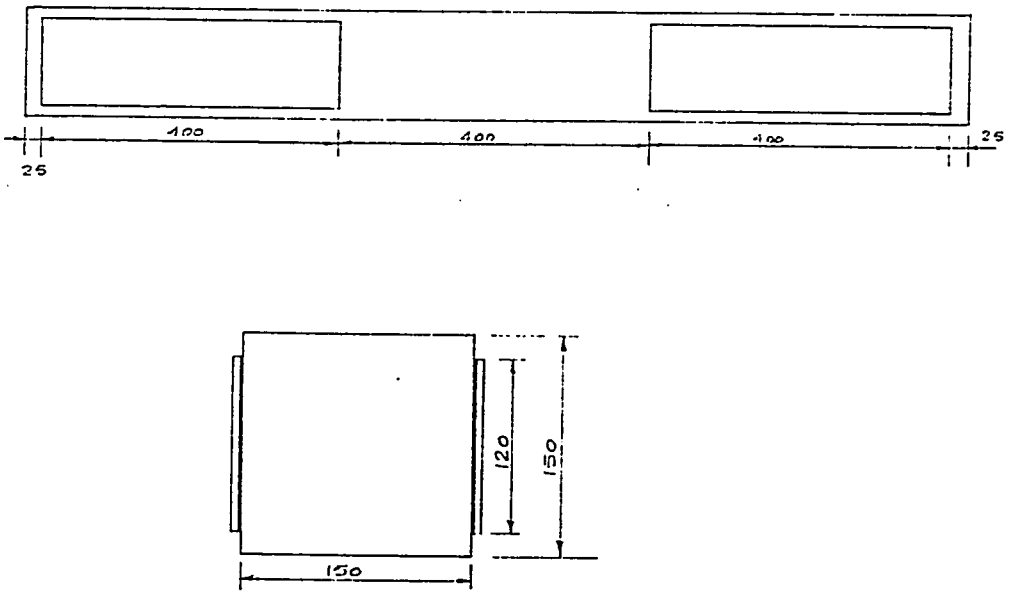

Figure 156: Strengthening detail of beams MS4 and MS9 strengthened by Wings.

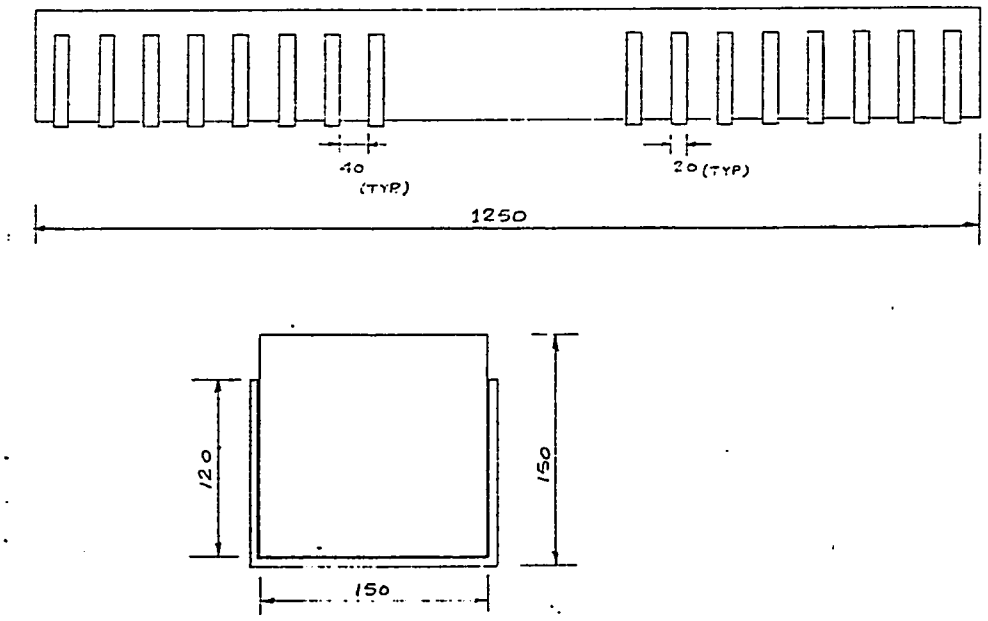

Figure 157: Strengthening detail of beams MS2 and MS11 strengthened by U-Strips.

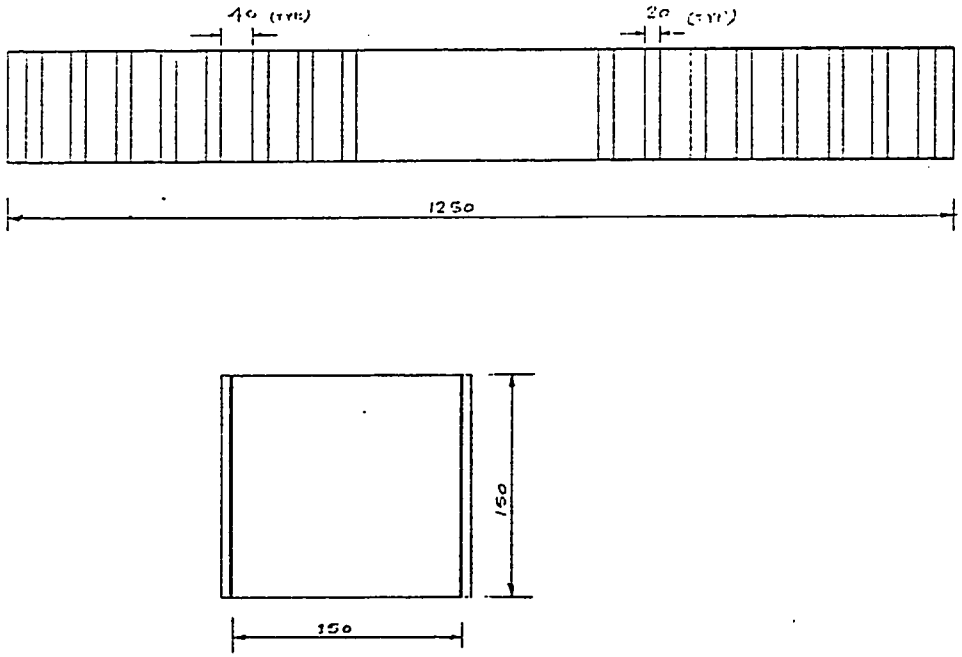

Figure 158: Strengthening detail of beams MS5 and MS7 strengthened By straight Strips.

7.7 TESTING OF THE REPAIRED BEAMS

Testing of repaired beams was done after the curing of epoxy glue. Generally the testing of the beams was done after not less than seven days of the gluing operation. The beams were tested under four point loading. Two point loads were applied at the ends of the middle third of the beam and the reactions were set at 25 mm from the ends of the beam. For loading 25 tons INSTRON machine was used. The loading was done at the rate of 1 mm per minute. Data acquisition system was used for recording readings.

Chapter VIII

TEST RESULTS AND DISCUSSION

(SHEAR PART)

8.1 LOAD VS CENTRAL DEFLECTION

Figure 159 through figure 168 show the load deflection curves for all the beams. These curves show that all the repaired beams showed improvement in ductility and strength with respect to unrepaired beams. All these figures show two cycles of loading. The first cycle is for damaging the beams and the second cycle represents the loading of the repaired beams upto ultimate. Figure 160 shows the load-deflection curve for beam MS10. This beam was strengthened by jacket-A as the beam MS6. The ultimate load obtained for this is very less than that of the beam MS6. The strengthening of this beam was not proper. Also this beam was badly damaged. So the results of this beam has not been included in the comparison.

Table 17 shows the summary of the test results. This table gives the ultimate load, ultimate concrete compression strain at mid-span, modulus of toughness and mode of failure of all the beams. This ultimate concrete compression strain is in addition to the residual concrete strain which was already there in these beams due to original loading. Modulus of toughness is a measure of ductility. This is equal to the area under the load deflection curve of the beam upto failure. In fact, this is the energy absorbed by the beam upto failure. The table

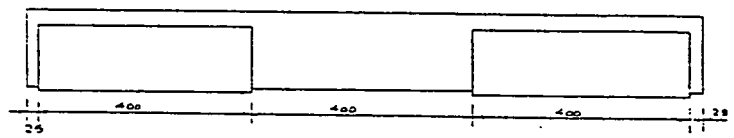

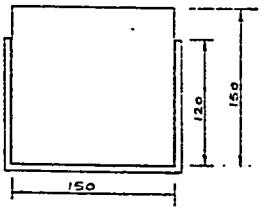

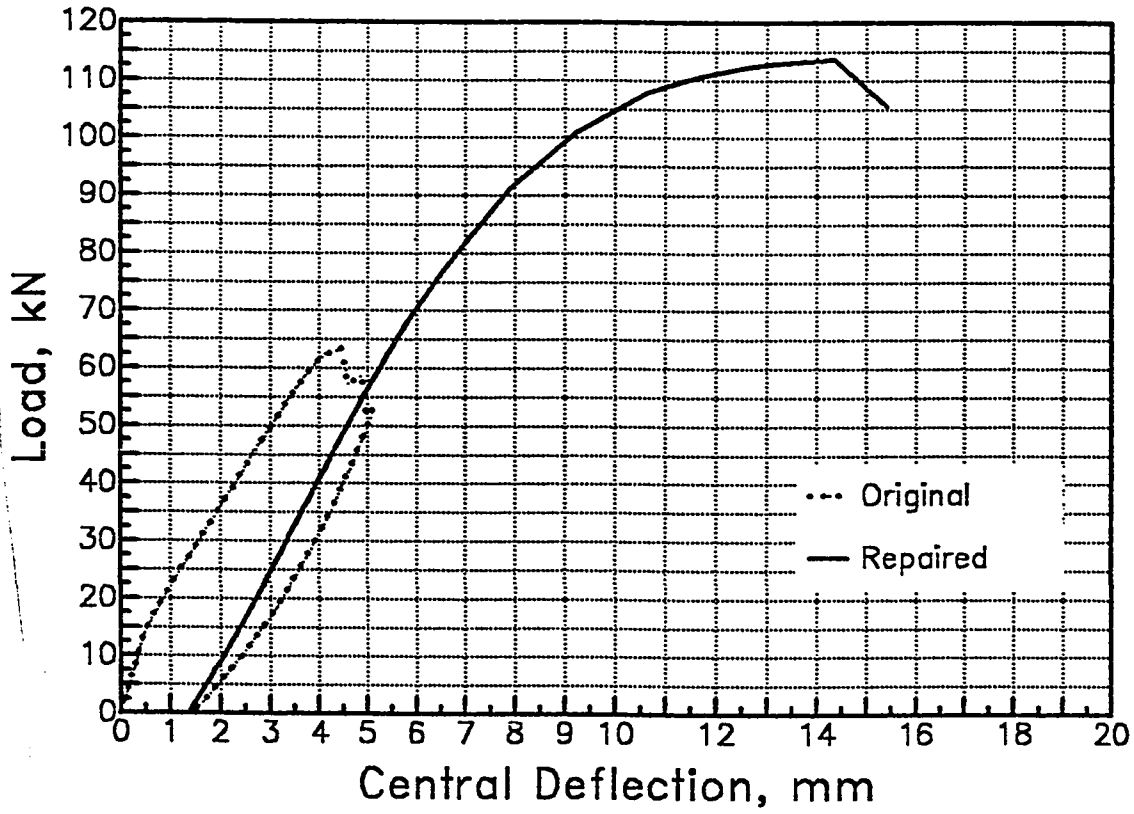

Figure 159: Load deflection curve for beam MS6 repaired by Jacket A

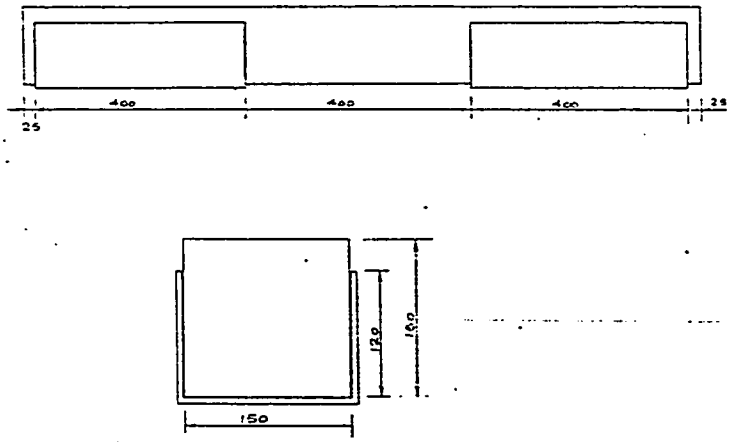

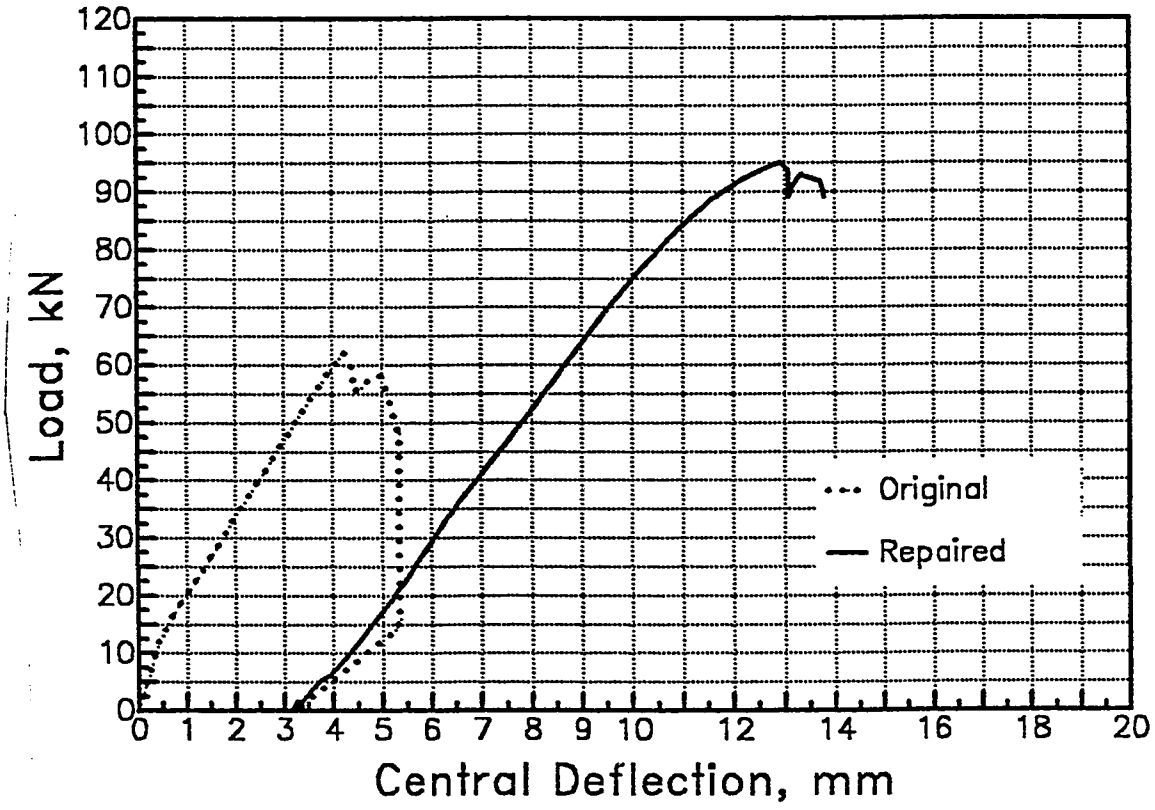

Figure 160: Load deflection curve for beam MS10 repaired by Jacket A

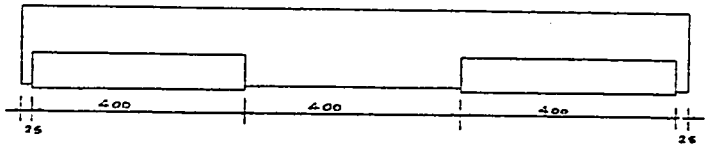

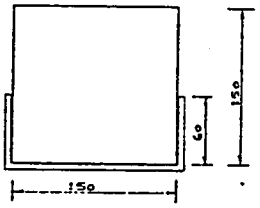

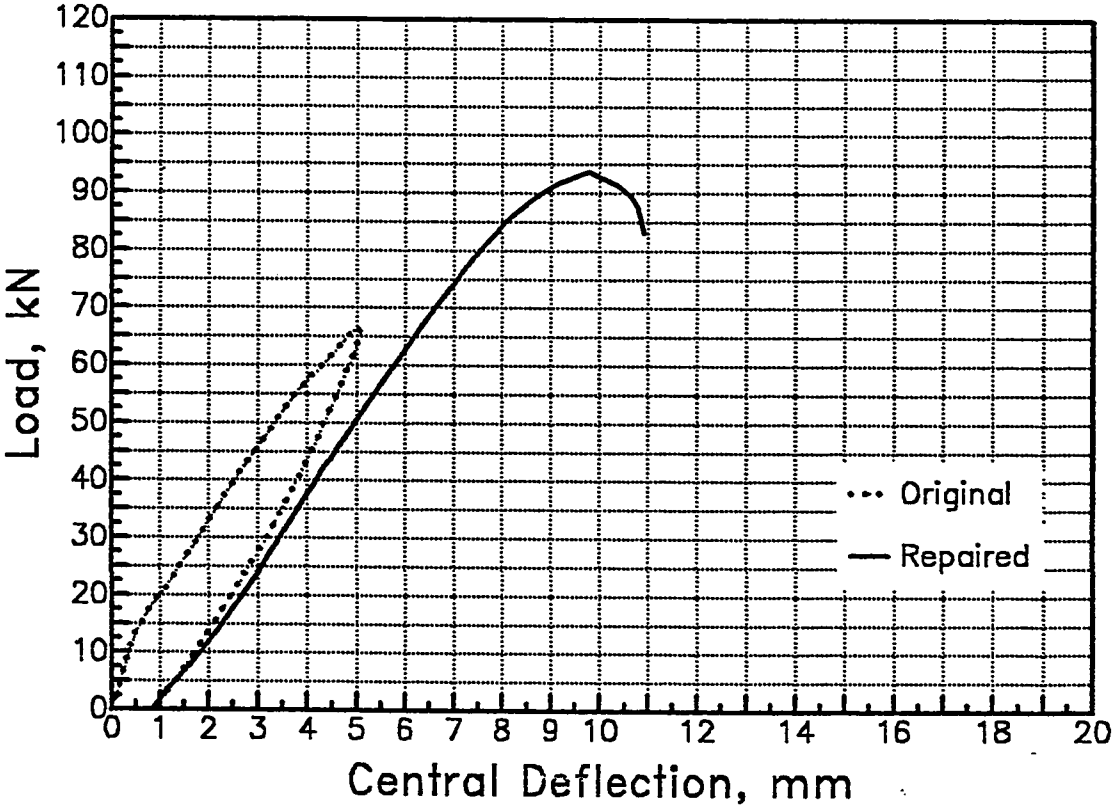

Figure 161: Load deflection curve for beam MS3 repaired by Jacket B

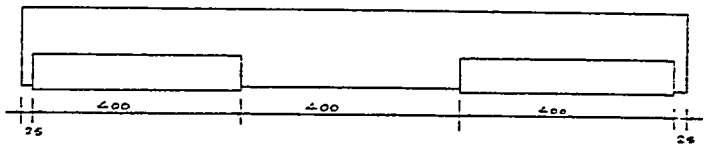

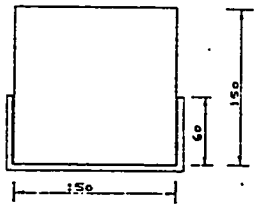

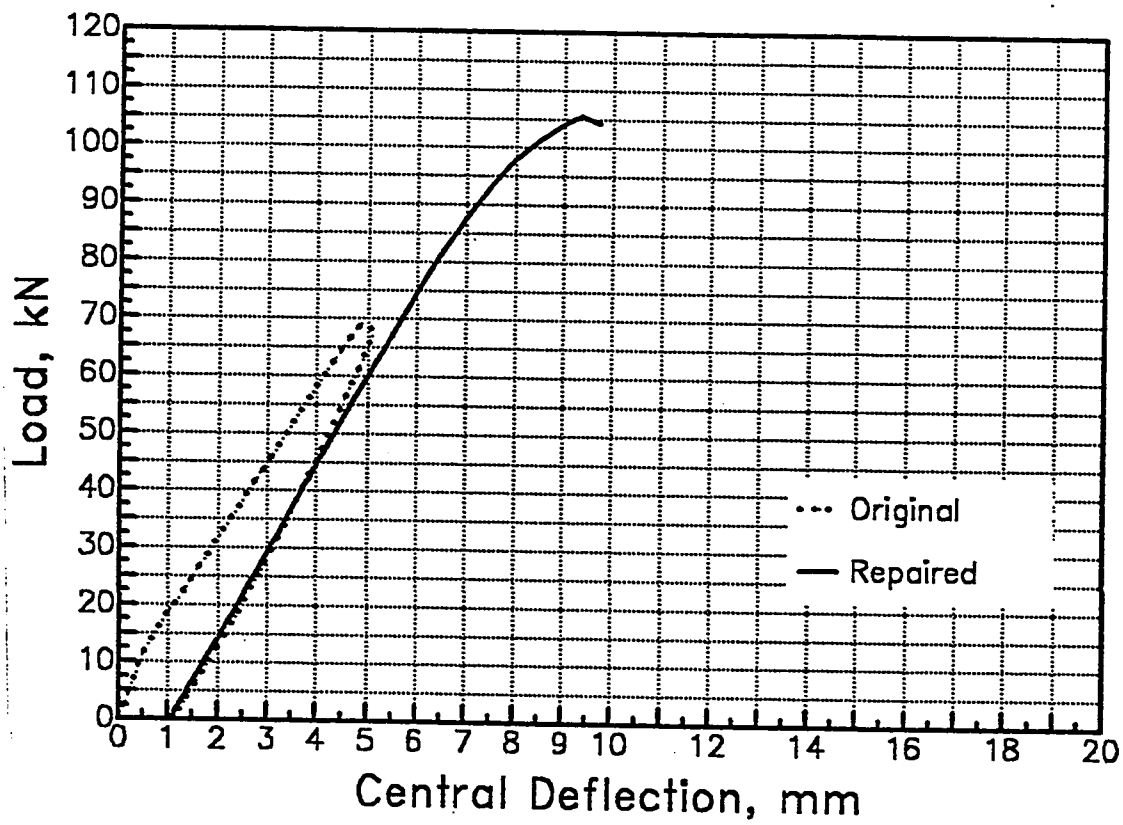

Figure 162: Load deflection curve for beam MS8 repaired by Jacket B

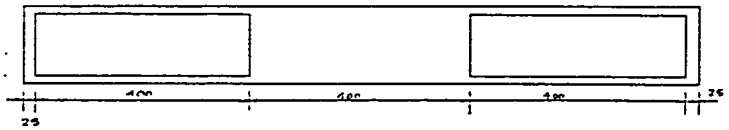

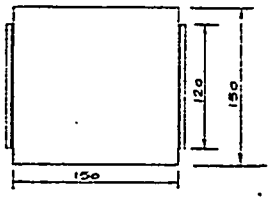

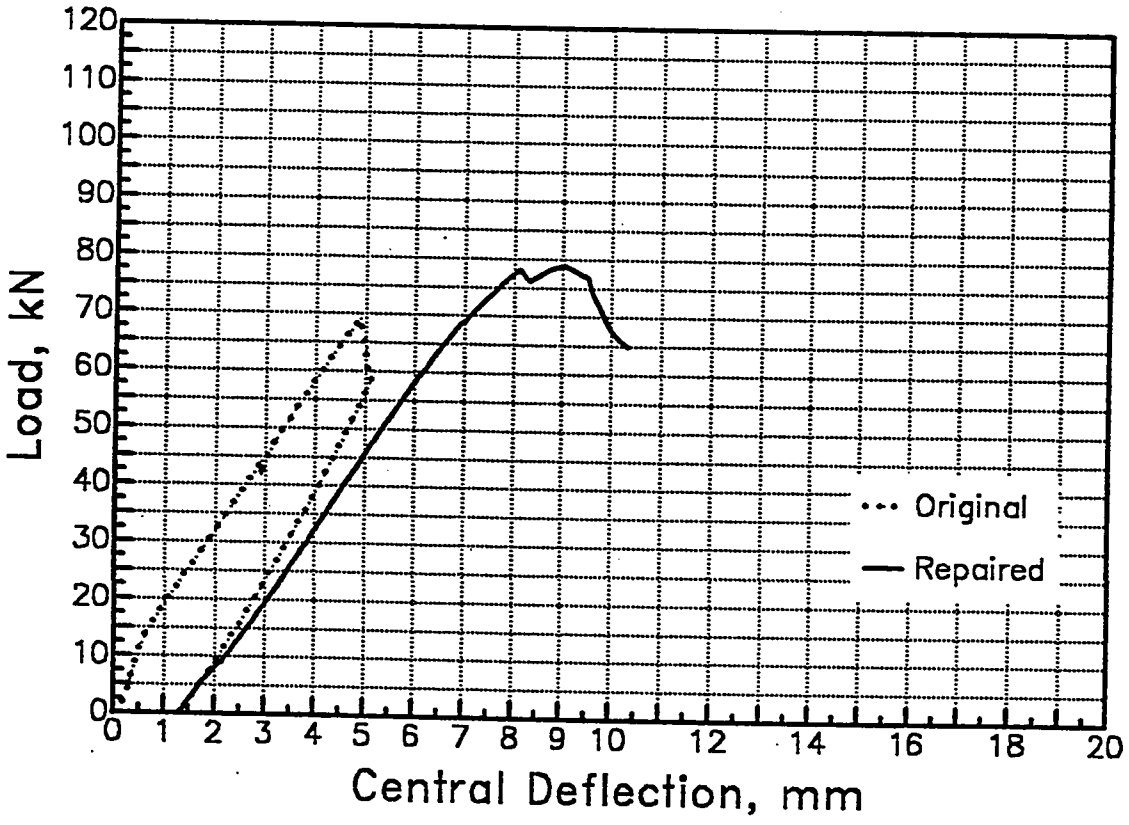

Figure 163: Load deflection curve for beam MS4 repaired by Wings

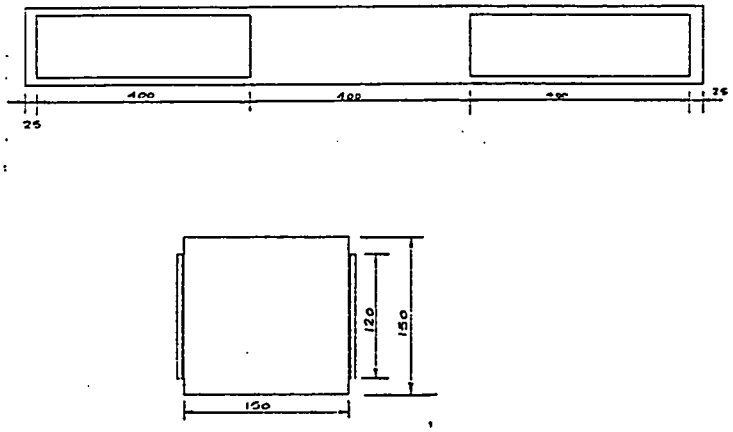

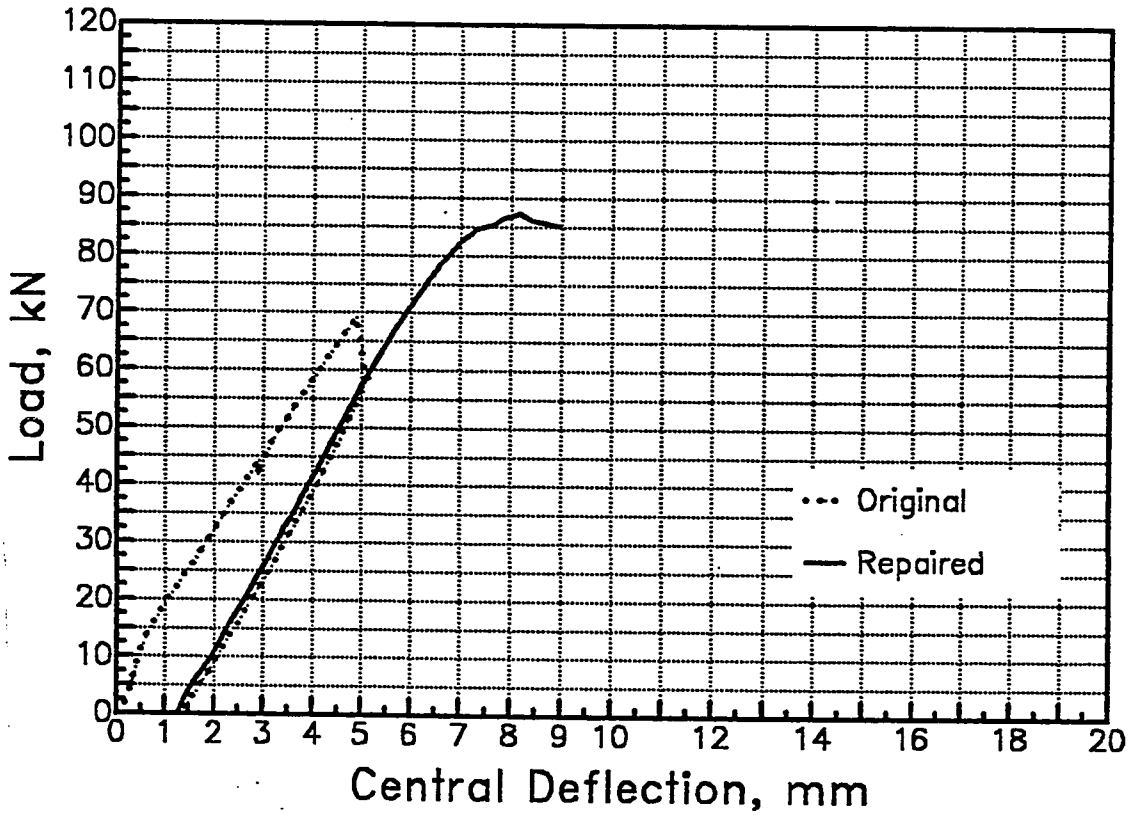

Figure 164: Load deflection curve for beam MS9 repaired by Wings

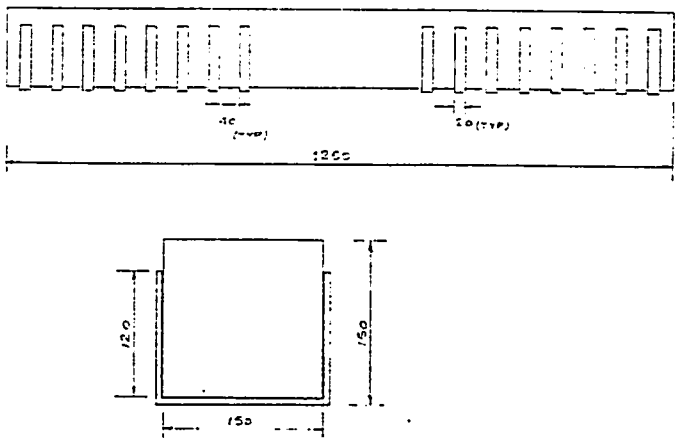

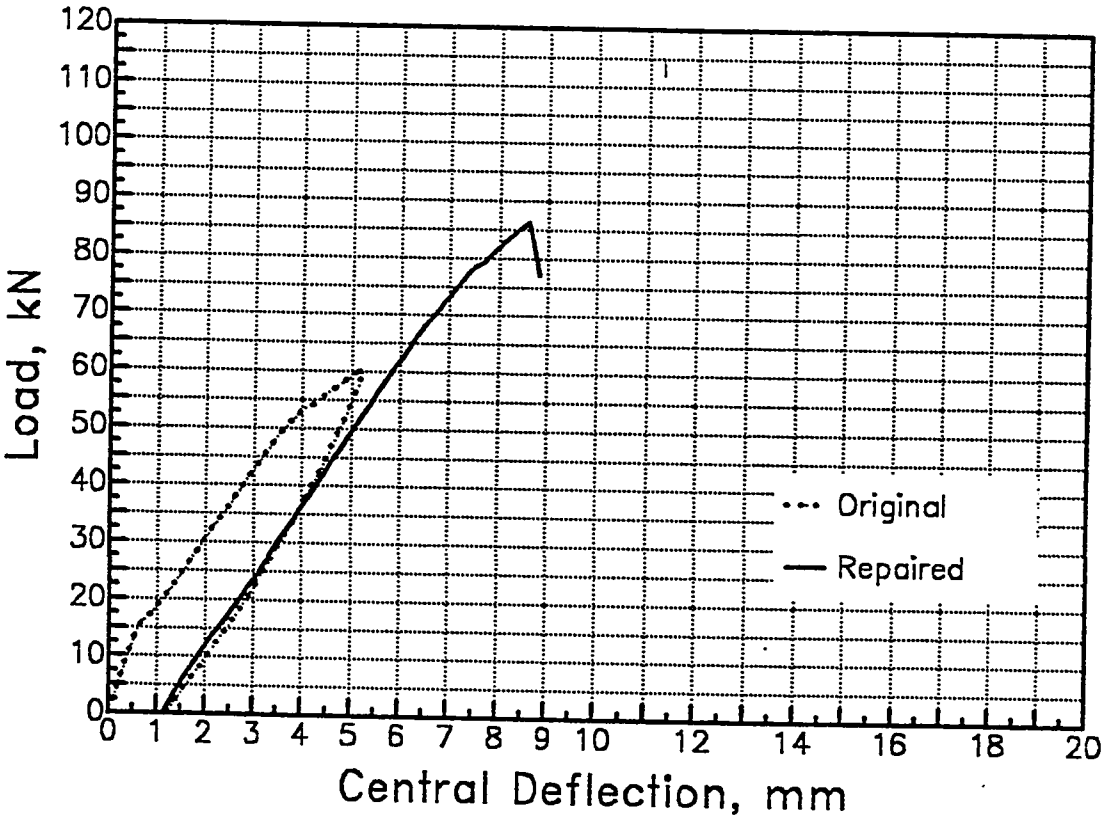

Figure 165: Load deflection curve for beam MS2 repaired by U-Strips

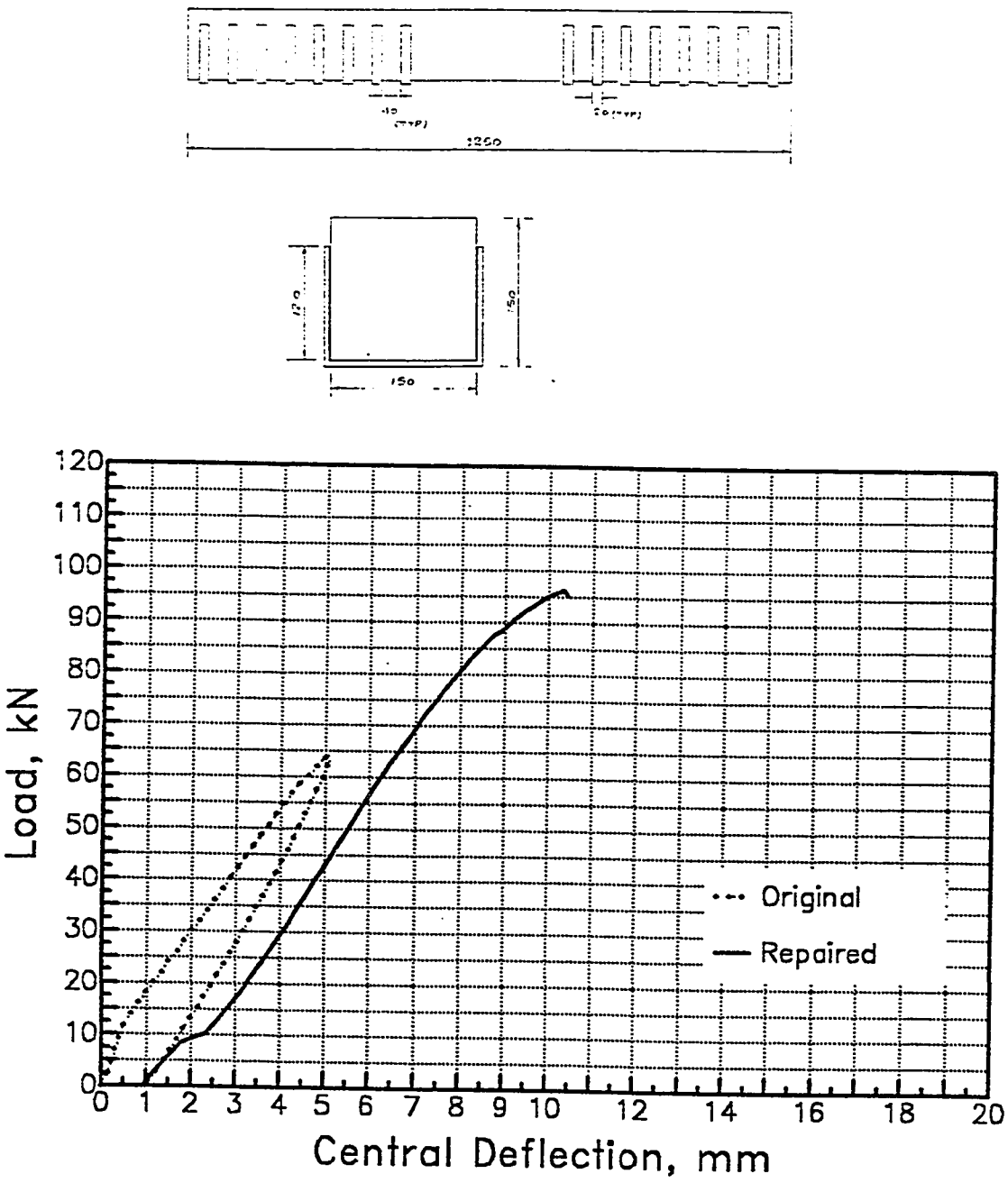

Figure 166: Load deflection curve for beam MS11 repaired by U-Strips

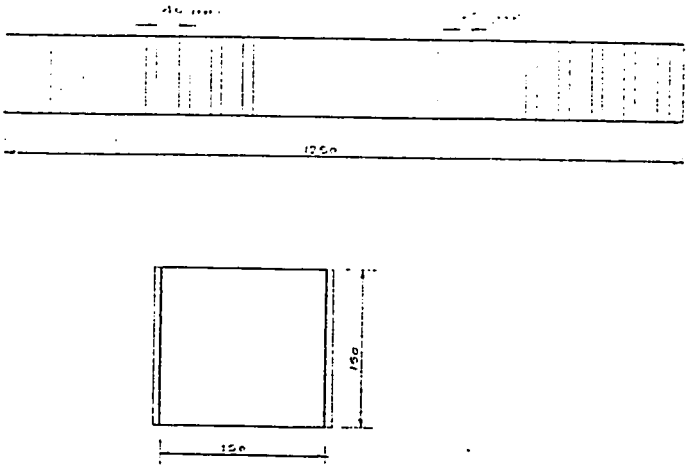

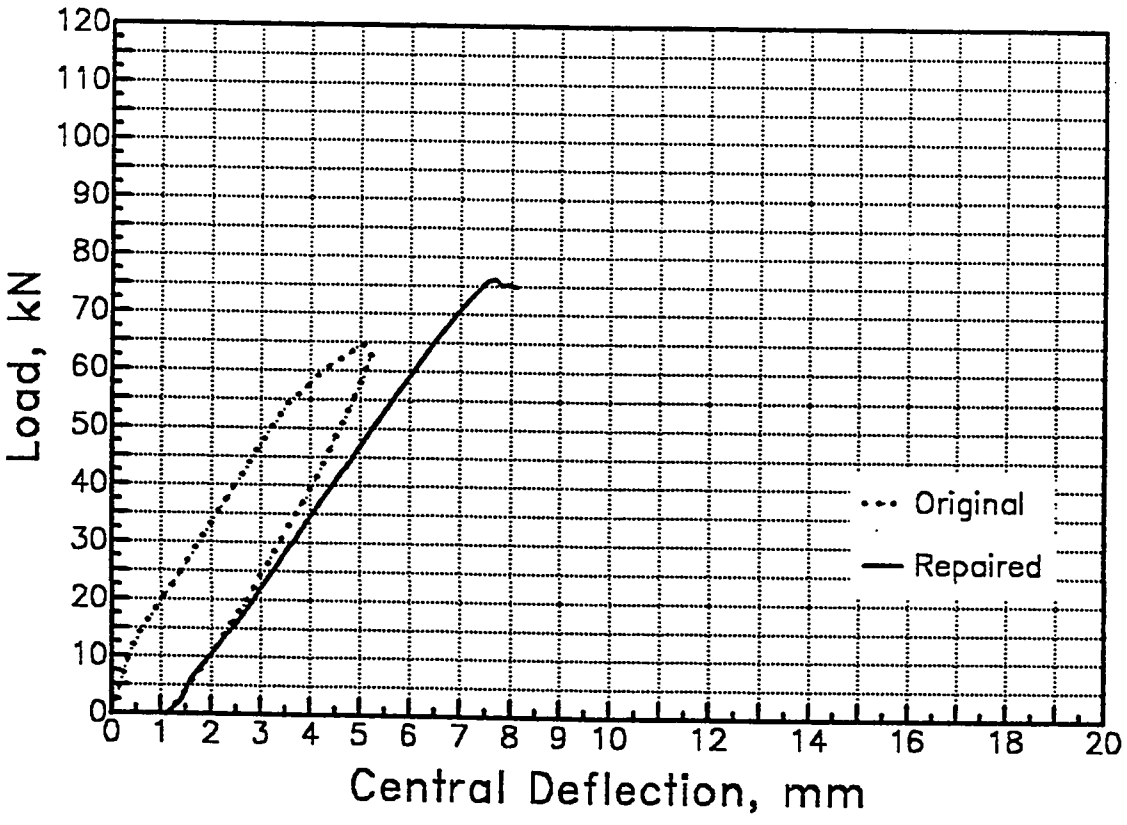

Figure 167: Load deflection curve for beam MS5 repaired by Straight Strips

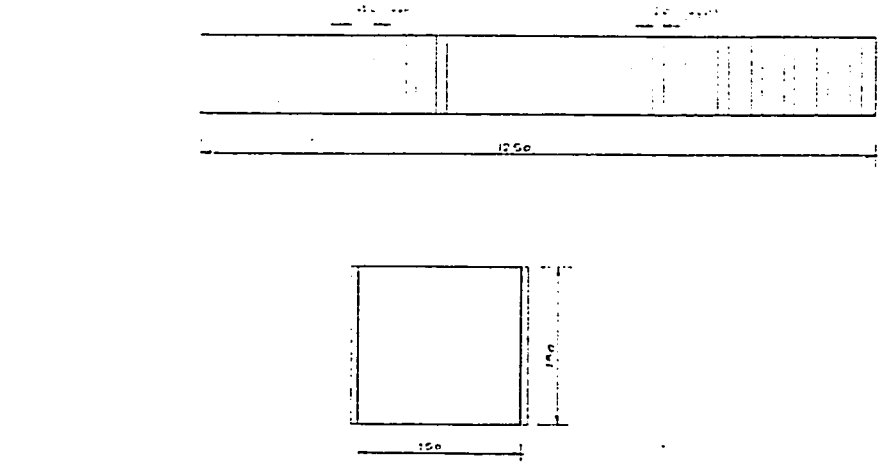

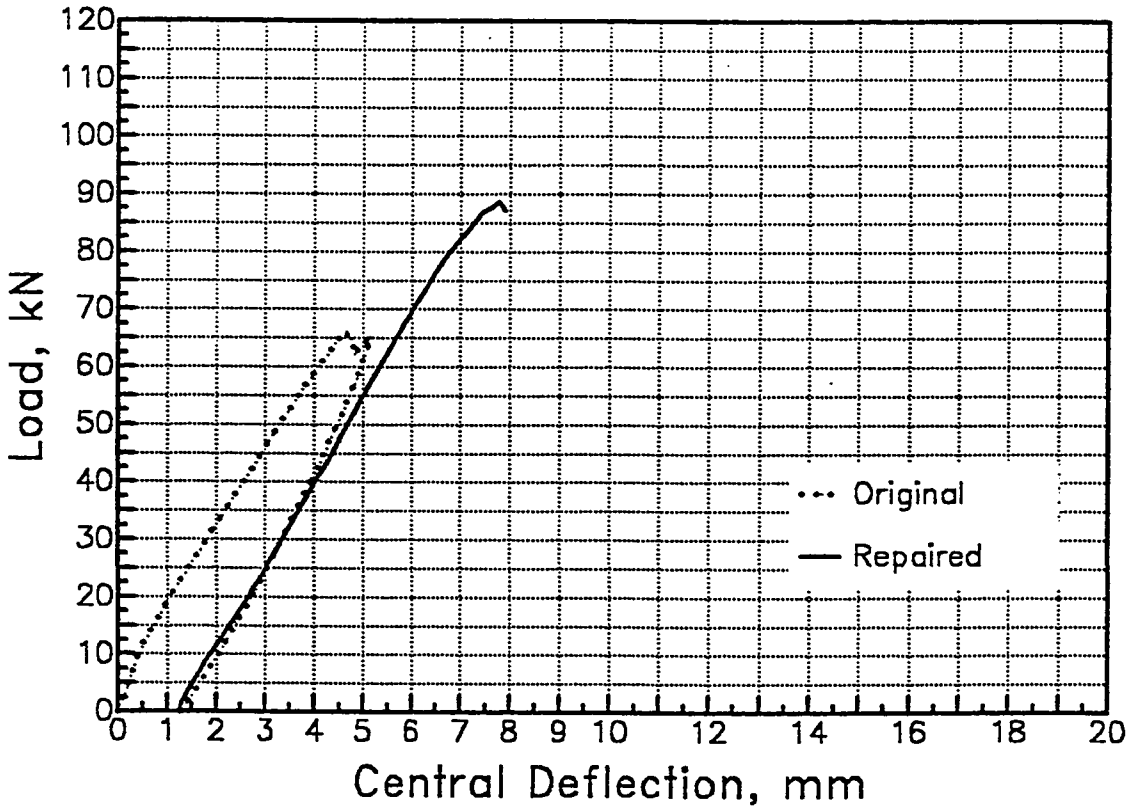

Figure 168: Load deflection curve for beam MS7 repaired by Straight Strips

shows the modulus of toughness of the repaired beams only, that is, area under the load deflection curve for the second cycle of loading.

Table 17: Summary of the test results

Beam ID.	Repair Type	Exper. Ult. Load (kN)	Mod. of Tough. N.mm	Maxi. Comp. (micron)	Mode of Failure
MSx	Virgin	64.6	193	*	Shear
MS6	Jac-A	113.70	1008	2700	Flexure
MS8	Jac-B	105.51	486	1600	Sep. of Jac.
MS3	=	93.60	448	1400	=
MS11	U-St.	96.24	465	1600	Ripping of St.
MS2	=	86.16	338	*	=
MS9	Wings	87.26	358	*	Sep. of Wings
MS4	=	78.85	358	1700	=
MS7	Strips	88.64	306	1500	Ripping of St.
MS5	=	76.10	243	1300	=

The theoretical ultimate flexure capacity of these beams is 98.5 kN based on the actual stress strain curve of the steel. MSx represents a typical original beam. The ultimate concrete compression strain given above is at the mid-span.

Table 18 shows the average ultimate load, average modulus of toughness for the beams with different types of repair arrangement. From this table it is clear that all types of repairs improve the strength and ductility of the beams, however, the improvement in strength and ductility for beams repaired by Jacket-A

is more than that for beams repaired by other repair arrangements. For beams strengthened by straight strips, the improvement in ductility and strength is less as compared to the improvement in strength and ductilty for beams repaired by other types of repair arrangements. After Jacket-A, Jacket-B is the best strengthening arrangement. The ultimate load and ductility for beams repaired by U-strips is less as compared to the beams repaired by Jacket-B. However, beams strengthened by U-strips showed higher strength and ductility as compared to beams repaired by Wings and Strips respectively.

Table 18: Average values of ultimate load and modulus of toughness

Repair Type	Experi. Ultimate Load (KN)	Modulus of Toughness (KN.mm)
Virgin	64.6	193
Jacket-A	113.7	1008
Jacket-B	99.5	467
U-Strips	91.2	402
Wings	83.1	358
Strips	82.7	275

The thoeretical ultimate flexure capacity of these beams is 98.50 kN based on the actual stress strain curve of the steel.

8.2 MODE OF FAILURES

In this section mode of failure of all the beams has been discussed. At failure, in all the beams the rebars at mid-span were yielding. In none of the beams external plate reinforcement was yielding at failure.

1. BEAMS STRENGTHENED WITH JACKET-A

Figure 169 shows the mode of failure for beam MS10. The failure of this beam took place due to separation of the sides of the Jacket-A. The failure was in the concrete adjacent to the glueline. The beam was badly damaged. Its diagonal crack width was 4 mm. Also there was a gap between concrete and bottom of the jacket because of warped jacket. The support was placed under the bottom of the jacket because there was not enough clearance between the support and the jacket. The reaction of the support was transferred to the beam through the sides of the jacket. The failure took place due to tearing of the concrete adjacent to the wings of the jacket with sound. The other beam repaired by the jacket A was MS6. This beam was properly repaired. There was enough clearance between the jacket and the support. In this beam pure flexure failure was obtained. At failure, the concrete in the compression zone under the point load at 3rd point started crippling and the concrete compression strain at mid-span was 2700 micron. This strain is in addition to the residual strain in the beam due to original loading. Unluckily, residual compression strain in original loading was not recorded. However, it is expected that the sum of residual strain and 2700 micron must be equal to or higher than 3000 micron, because this beam failed due to the crushing of concrete.

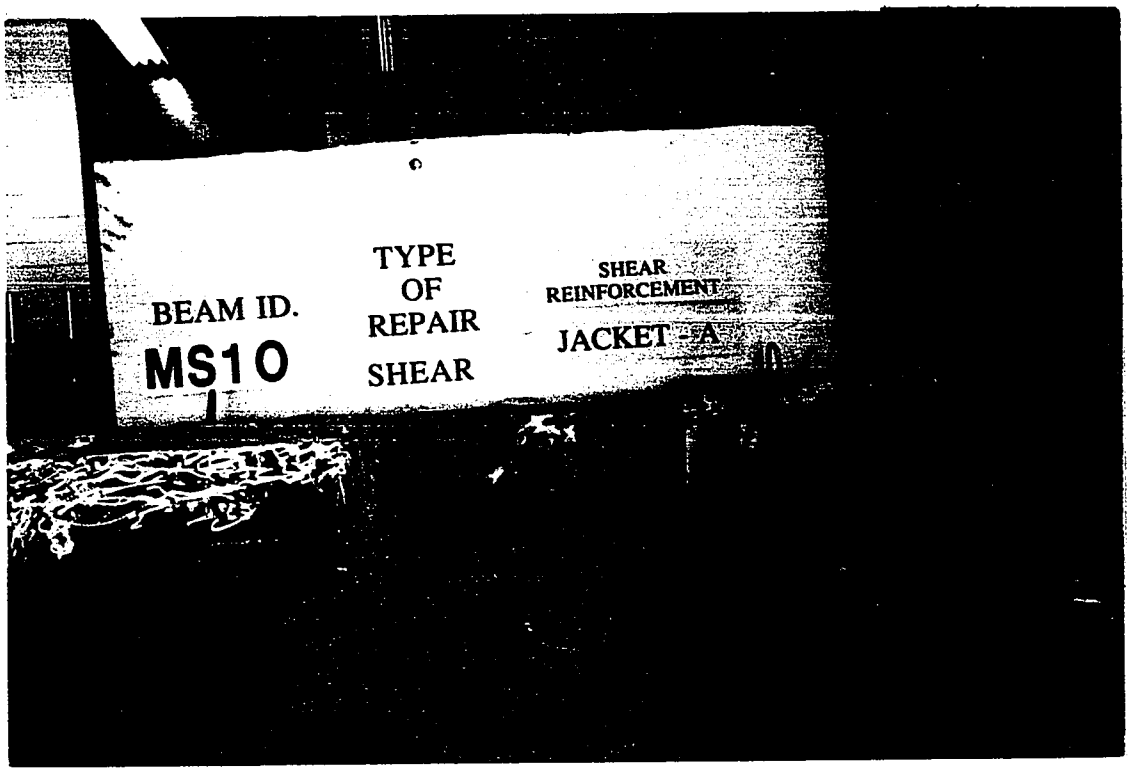

Figure 169: Photograph showing the cracks at failure for the beam MS10 repaired by Jacket-A.

2. BEAMS STRENGTHENED WITH JACKET-B

Figure 170 shows the mode of failure for beam MS8 repaired by jacket B. The failure was due to the tearing of the concrete and with that separation of the jacket took place. Also at failure, the original diagonal crack started to open.

Similary, beam MS3 was repaired by jacket B. The failure in this beam was simultaneously by the separation of the jacket and opening up the old diagonal shear crack.

3. BEAMS STRENGTHENED WITH WINGS

Figure 171 shows the mode of failure for beam MS4 repaired by the wings. The failure in this beam took place by the separation of the wings. The failure was due to tearing of the concrete. The failure started with the appearance of a vertical crack at the inner vertical edge of the wing, on both sides of the beams. These cracks moved inward from both sides and joined each other to make a single crack. Then the single crack moved towards the support and with that the separation of the wing took place. Similar failure occured in beam MS9 repaired by wings.

4. BEAMS STRENGTHENED WITH U-STRIPS

Figure 172 shows the mode of failure for beam MS2. This failure took place due to ripping of the U-strips on the open side of the U-strip. The failure was sudden. The failure was due to the tearing of the concrete. Exactly, similar failure occured in beam MS11 repaired by U-strips. In both of these beams strain in the strips in the vertical

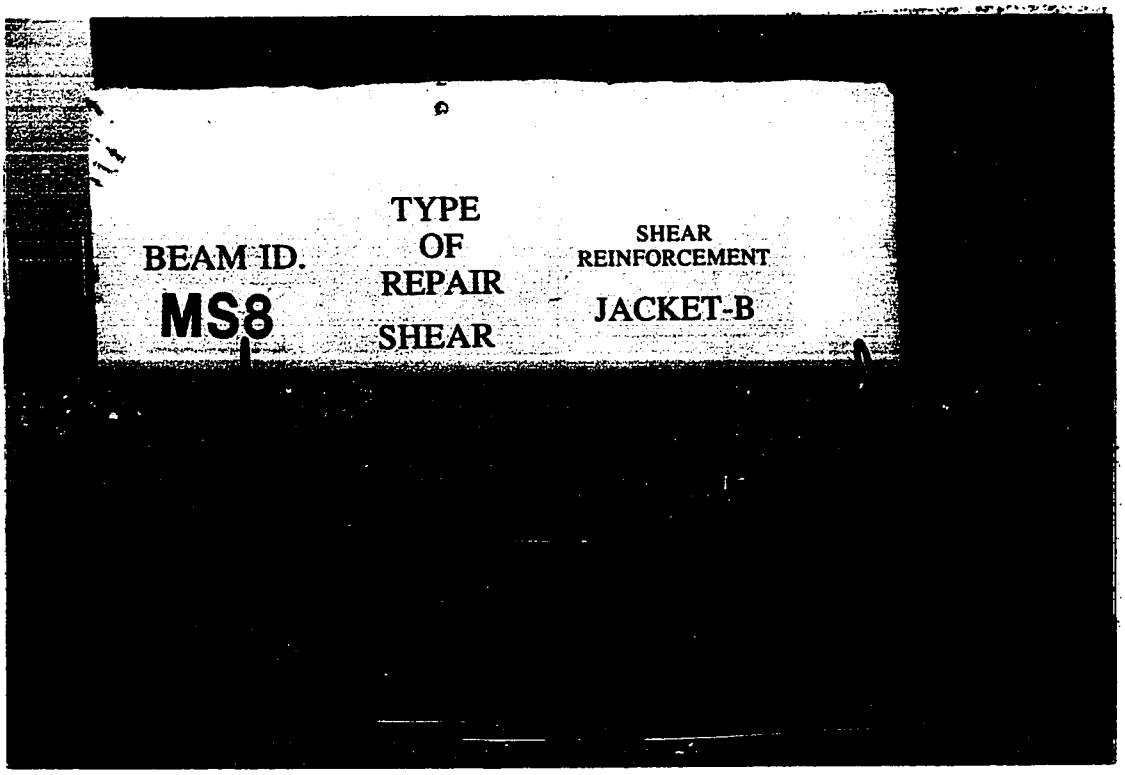

Figure 170: Photograph showing the cracks at failure for the beam MS8 repaired by Jacket-B

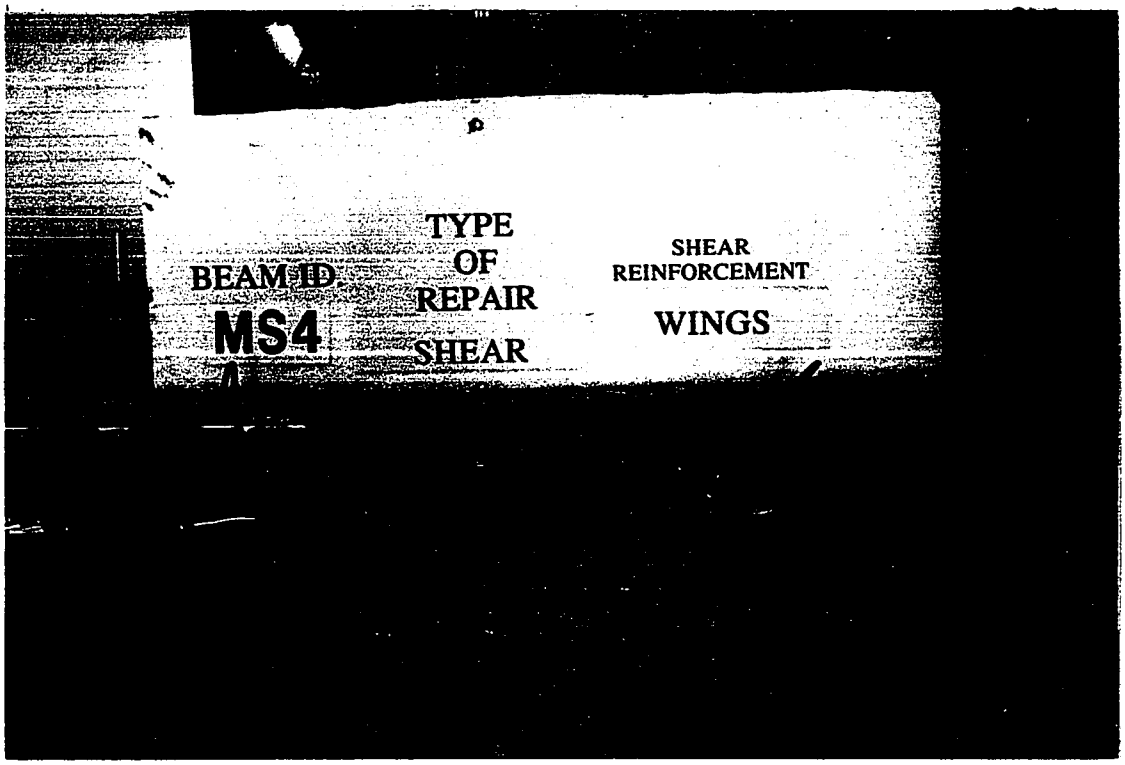

Figure 171: Photograph showing the cracks at failure for the beam MS4 repaired by Wings.

direction was measured. The strain in the strips was less than the yield strain.

5. BEAMS STRENGTHENED WITH STRAIGHT STRIPS

Figure 173 shows the mode of failure for beam MS5 repaired by strips. At failure, the strip on the back side of the beam started to separate as clear from this figure. This figure shows the back view of the beam. The figure shows that the crack was not properly trapped by the strips because the crack is very steep almost vertical. The strips on the back side started to open up, and the strips on the front side started to bend concavely. In beam MS7, repaired by strips, the failure was due to ripping of the strips suddenly. The strain in the strips in vertical direction in both of these beam was measured and it was found less than the yield strain at failure.

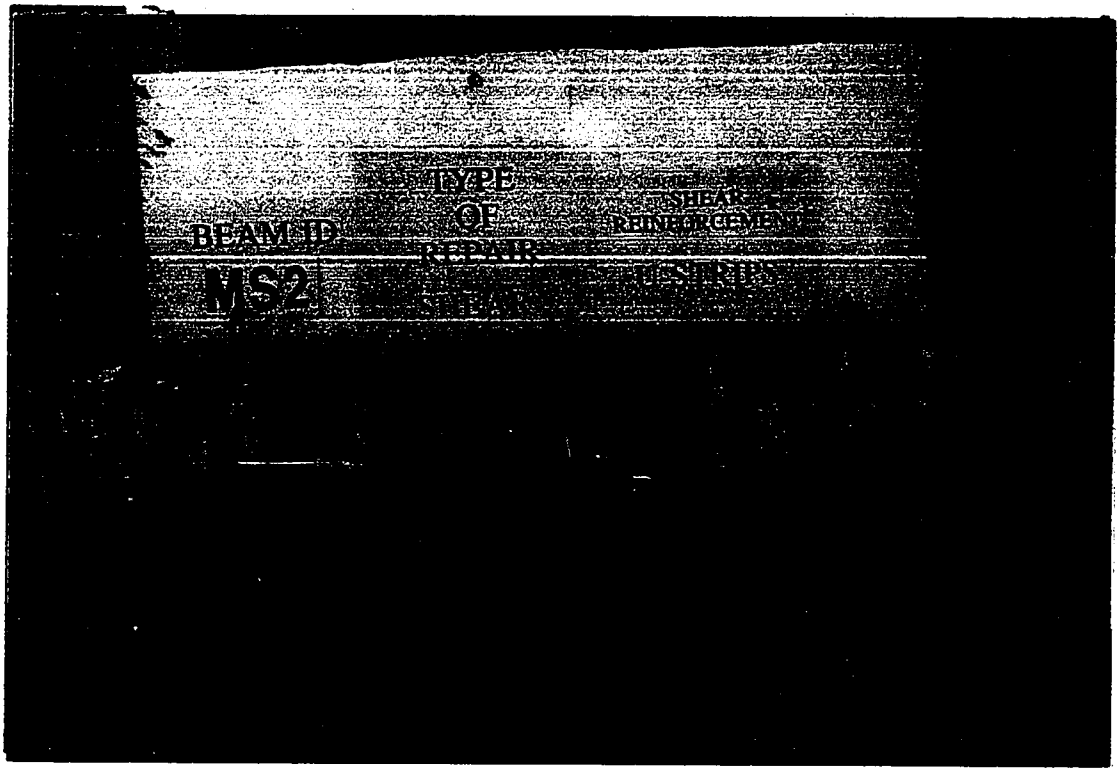

Figure 172: Photograph showing the cracks at failure for the beam MS2 repaired by U-strips

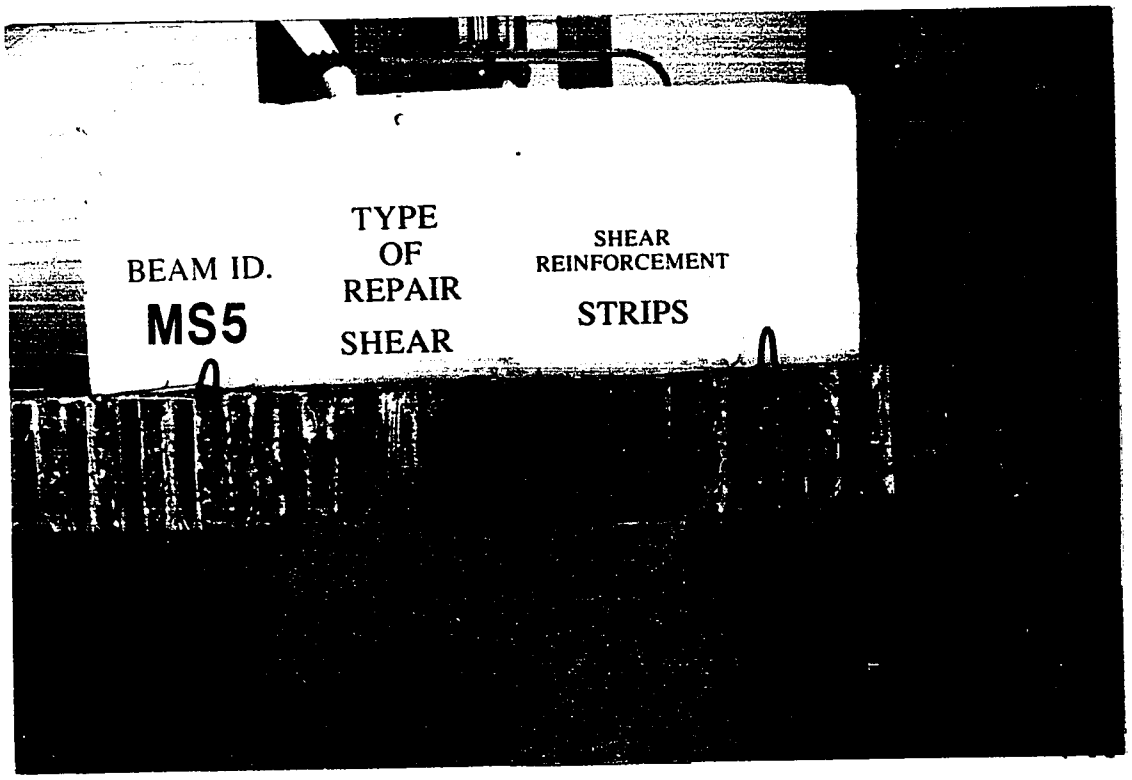

Figure 173: Photograph showing the cracks at failure for the beam MS5 repaired by Strips

Chapter IX

CONCLUSIONS AND RECOMMENDEDATIONS

9.1 CONCLUSIONS

9.1.1 FLEXURE PART

1. EXPERIMENTAL PART

a. The strength of the flexure damaged beams can be improved by bonding steel plates externally provided the plates are properly designed and bonding is done properly.

b. Full flexure failure was obtained in the beams bonded with 1.00 mm thick plates. The experimental ultimate load and theoretical ultimate load, calculated based on the actual stress strain curves of the reinforcing bars and the external steel plate, assuming full composite action between the steel plate and the concrete beam, were almost same. From this we conclude that full composite action between the steel plate and the concrete beam was obtained upto failure in beams bonded with 1.00 mm thick steel plates, that is, when b/t ratio for the plate was 100, full flexure failure was obtained. R. N. Swamy [30] suggested based on the

test results that in order to obtain pure flexure failure in the epoxy bonded plated beams the b/t ratio for the bonded plates should not be less than 50. Similarly, Macdonald [29] suggested based on the test results that in order to obtain full flexure failure in the epoxy bonded plated beams the b/t ratio for the bonded plates should not be less than 60.

c. In the beams bonded with 1.5 mm thick plates, full flexure failure could not be obtained. These beams failed prematurely due to the separation of the plates after the yielding of the plates showing less ductility. However, the ductility of these beams was improved by giving end anchorages to the steel plates. Different anchor bolt arrangements were used for end anchorage. It was observed that all types of anchor bolt arrangements improved the strength and ductility as compared to the beam with unachored plates of 1.5 mm thickness. However, the improvement in strength due to anchorage in beams bonded with 1.5 mm thick plates was marginal over the beams bonded with 1.5 mm thick unanchored plates. But there was considerable improvement in ductility by giving end anchorage to the plates. However, the mode of failure of these beams still remained by the appearance of the diagonal crack starting from the end of the plates.

d. The beams bonded with 2.00 mm and 3.00 mm thick steel plates failed prematurely due to the separation of the plates due to the high concentration of shear and peeling stresses at the ends of the plates. In these beams separation of the plates took place before yielding of the steel plates. By giving end anchorage to the plates in these beams both the ultimate strength and the ductility was improved. However, even by giving end anchorage to the plates, the theoretical ultimate capacity could not be obtained in these beams. The modes of failure of these beams remained by the appearance of the diagonal cracks starting generally from the ends of the plates. This is because of the high concentration of shear and peeling stresses at the ends of the thicker plates.

e. The effect of plate thickness on the stiffness of the beams was also studied. It was found that as the plate thickness increases, the stiffness of the beams increases.

f. The effect of, end anchorage to the plates, on the stiffness of the beams was also studied. It was observed that by giving end anchorage to the plates the stiffness of the beams increased as compared to the beams having unachored plates of the same thickness.

g. In epoxy bonded plated beams, the steel plates should terminate as close to the support as possible. Higher shear and peeling stresses occur at the ends of the bonded plates when the distance between the ends of the plates and the supports is more and hence the beams become more prone to failure by separation of the plates. The separation could be due to the tearing of the concrete above the glueline or at the glueline due to the failure of the glueline.

2. THEORETICAL PART

Using the finite difference computer program ROB9, based on the partial interaction theory to determine the shear and peeling stresses at the interface of the epoxy bonded plated beams, parametric study was done and based on that the following conclusions were drawn.

a. From the shear stress distribution along the plate, it was observed that, the shearing stresses at the ends of the plate are very high as compared to the interior portion of the plate, irrespective of the type of the load.

b. From the peeling stress distribution along the plate it was observed that, the peeling stresses are high close to the ends of the plate and suddenly dies down to zero, then become negative and then become zero again.

c. Maximum shear and the peeling stresses at the end of the bonded plate, in addition to other factors, depend on the distance between the support and the end of the bonded plate. If this distance is more, the shear and peeling stresses at the end of the bonded plate will be higher and vice versa.

d. With increasing the plate thickness, the shear and the peeling stresses increase provided the other parameters are kept constant.

e. With increasing the stiffness of the glue the shear and the peeling stresses at the interface increase provided the other parameters are kept constant.

f. With increasing the cross-sectional area of the bonded plates the stiffness of the beams increase provided the other parameters are kept constant.

g. The program ROB9 can be used to determine the size of the plate to be bonded to the concrete beam. For a certain plate size, which satisfy the strength requirements , determined from the strain compatibilty analysis, the shear and peeling stresses at the interface can be obtained by the program. The maximum shear and peeling stresses determined by the program are com-

pared to the limiting values of the shear and peeling stresses at which separation takes place due to the tearing of the concrete. But this should also be considered that this program does not take into account the material and geometrical non-linearities.

9.1.2 SHEAR PART

1. The RC beams damaged in shear can be repaired by bonding steel plates externally in the critical shear zone.

2. It was observed that all types of shear repair arrangements such as Jacket-A, Jacket-B, Wings, U-strips, Straight Strips improved the strength and ductility of the shear damaged beams. However, the improvement in strength and ductility in case of Jacket-A (Full encasement of the shear span) was more as compared to other strengthening arrangements.

3. The effectiveness of the repair depends on how effectively, the diagonal tension cracks in the shear damaged beams are trapped. If the diagonal tension cracks are not properly trapped by the external reinforcement, the improvement in the strength will be little irrespective of the repair type.

4. The ductility of the repaired beams damaged in shear was not enough except in the beams repaired by jacket-A.

5. In all other types of repair except Jacket-A. the failure was due to the separation of the fabricated steel plates. The separation was not in the glueline. But it was due to the tearing of the concrete adjacent to the glueline.

9.2 RECOMMENDATIONS

9.2.1 FLEXURE PART

1. EXPERIMENTAL PART

   a. The beams bonded with 2.00 mm and 3.00 mm thick anchored plates were tested. The end anchorage to the plates was given by one anchor bolt at each end in these beams.

      It will be interesting to test more beams bonded with 2.00 mm and 3.00 mm thick anchored plates. But this time end anchorage to the plates should not be given by single anchor bolt. Instead of that two anchor bolts at each end of the plate should be used for end anchorage. The two anchor bolts should be tried in lateral and axial direction as was done in beams bonded with 1.5 mm thick plates.

2. THEORETICAL PART

   a. With little work, the program ROB9 can be made capable of handling anchor bolts in epoxy bonded plated beams. The anchor bolts can be handled by defining node at the bolt location and by giving appropriate values of shear and normal stiffnesses to that node. The determination of the shear and peeling stiffnesses of the anchor bolt need some experimental work.

9.2.2 SHEAR PART

1. Although the improvement in strength and ductility in the beams repaired by jacket A, full encasement of the shear span, is maximum, but with respect to the ease of application in the field, the strips are the best.

NOMENCLATURE

f_{bp} is the glue/plate interface bond stress.

V is the shear force

A_p is the cross-sectional area of the plate.

y_p is the distance from the neutral axis to the mid-plane of the plate.

α_p is the modular ratio $E_{plate}/E_{conc.}$

I_T is the transformed second moment of area.

L is the distance from the support to the end of the plate.

$\bar{x}$ is the length of the anchorage zone

M_{xy} is the torsional moment on the plate in the anchorage zone.

t_g is the thickness of the glueline.

t_p is the thickness of the plate.

τ_0 is the shear stress at the interface at the end of the bonded plate.

σ_0 is the peeling stress at the interface at the end of the bonded plate.

F_0 is the shear force at the point of termination of the bonded plate.

M_0 is the bending moment at the point of termination of the bonded plate.

K_s is the shear stiffness of the adhesive per unit length.

K_n is the normal stiffness of the adhesive per unit length.

b_p is the width of the bonded plate.

d_p is the thickness of the bonded plate.

b_a is the width of the adhesive layer.

I is the moment of inertia of the fully composite transformed steel section.

E_p is the modulus of elasticity of the bonded plate.

h_p is the effective depth of the plate reinforcement.

h_s is the effective depth of the conventional steel reinforcement.

A_s is the area of the conventional steel reinforcement.

M is the total external moment acting on the composite beam.

M_s is the moment resisted by the slab of the composite beam.

M_b is the moment resisted by the I-beam of the composite beam.

Q is the load on the shear connector.

z is the distance between the centroidal axes of the slab and the I-beam.

s is the spacing of the shear connectors.

ε_s is the strain in the slab.

ε_b is the strain in the I-beam.

γ is the slip at the interface in the composite beam.

F is the axial force acting at the centroid of the slab and the I-beam in the composite beam.

k is the modulus of the shear connector. It is equal to the ratio of the load transmitted by the shear connector to the slip permitted by the shear connector.

u_a is the displacement in the x-direction in the layer a.

u_b is the displacement in the x-direction in the layer b.

$\overline{u}_a$ is the total displacement in the x-direction in the layer a.

$\overline{u}_b$ is the total displacement in the x-direction in the layer b.

w_a is the displacement in the y-direction in the layer a.

w_b is the displacement in the y-direction in the layer b.

ε_a is the strain in the layer a.

ε_b is the strain in the layer b.

σ_a is the stress in the layer a.

σ_b is the stress in the layer b.

t_a is the axial force in the layer a.

t_b is the axial force in the layer b.

m_a is the moment acting on the layer a.

m_b is the moment acting on the layer b.

A_a is the area of cross-section of the layer a.

A_b is the area of cross-section of the layer b.

I_a is the moment of inertia of the layer a.

I_b is the moment of inertia of the layer b.

f_a is the shear force resisted by the layer a.

f_b is the shear force resisted by layer b.

$\bar{\tau}$ is the force per unit length at the interface.

u_{ab} is the slip at the interface.

z_a is the depth of a point with respect to the coordinate system in the layer a.

z_b is the depth of a point with respect to the coordinate system in the layer b.

z_{ia} is the coordinate of interface with respect to the coordinate system in the layer a.

z_{ib} is the coordinate of interface with respect to the coordinate system in the layer b.

p is the uniformly distributed load on the composite beam.

y is the distance of a plane from the neutral axis.

v_y is the unit horizontal shear stress on a plane at distance y from the neutral axis.

M is the bending moment.

V is the shear force.

M_1 is the bending moment at section 1-1.

M_2 is the bending moment at section 2-2.

f_t is the tensile stress.

v is the shear stress.

α is the angle which the principal tensile stress makes with the beam axis.

V_{cz} is the shear resistance of the uncracked concrete.

V_d is the resistance of the longitudinal reinforcement to a transverse force.

a is the shear span.

d is the effective depth of the beam.

f_c is the cylinder strength of the concrete.

V_c represents the nominal strength of the concrete beams.

V_n is the total shear strength of the concrete beams.

M_n is the total flexure strength of the concrete beams.

V_u is the ultimate shear force acting at a particular section on the concrete beam.

M_u is the ultimate moment acting at a particular section of the concrete beam.

φ is the strength reduction factor.

REFERENCES

1. Van Gemert, D. A., "Repairing of concrete structures by externally bonded steel plates", Proceedings ICP/RILEM/IBK International Symposium on Plastics in Material and Structural Engineering, Prague, June 1981, Elsevier Scientific Publishing Company, 1982, pp. 519-526.

2. Bresson, J., "Realisation pratique d'un reinforcement par collage d'armatures", Annales de I, ITBTP, Suppl. 278, February 1971, PP. 50-52.

3. Bresson, J., "Reinforcement par collage d' armatures du passage inferieur du cd 126 sous l, Autoroute du sud. annales de l'Institute du batiment et des travaux publics", Supplement No. 297, September 1972. Concrete and reinforcement series No. 122

4. Iino, T., Otokawa, K., "Application of epoxy resins in strengthening of concrete structures", Proc. Third Internat. Congress on Polymers in Concrete, Koriyama, Japan, May 1981, Vol. II, pp. 997-1011.

5. Ryback, M., "Reinforcement of bridges by gluing reinforcing steel", RILEM Materials and Structures, 16, No. 91, January 1981, pp. 13-17

6. Fleming, C. J., King, G. E. M., "The development of the structural adhesives for three original uses in South Africa", RILEM International Symposium, Synthetic Resins in Building Construction, Paris, 1967, PP. 75-92.

7. Hugenschmidt, H., "Epoxy adhesive for concrete and steel", Proc. First International Congress on polymers in concrete , London, May 1975, The Construction Press Limited, Hornby, 1976, PP. 195-209.

8. Ladner, M., Weber, C., "Concrete structures with bonded external reinforcement", EMPA Report No. 206, Dubendorf, 1981.

9. Mander, R. F., "Bonded external reinforcement, a method of strengthening structures", Department of the Environment report on Quinton Interchange of the M5 motorway, 1974.

10. Davis, B. L., Powell, J., "Strengthening of Brinsworth road bridge, Rotherham", IABSE, 12th Congress, Vancouver, BC, September 1984, pp. 401-407.

11. Barrett, N., "Plates steel leads floor", New Civil Engineer, 20 June 1985, p. 18.

12. Ladner, M. and Flueler, P., Lauterbach, H., Tausky, R. u. a., "Verstarkung von Tragkonstruktionen mit geklebter Armierung. Schweizerische Bauzeitung", Vol. 92, No. 19, 9 May 1974. pp. 457-474.

13. "External Reinforcement of Concrete Structures" , CIBA-GEIGY Aspects June 1981.

14. Felix Hugenschmidt, "Strengthening of existing concrete structures with bonded reinforcements" , CIBA-GEIGY, June 1985.

15. "Reinforcing methods for bridges", Proceeding 23rd Annual Meeting of Civil Engineering, Nov. 1975, Public Works Institute, Ministry of Construction, Japan, (In Japanese).

16. L'Hermite, R., Devars du Mayne, R., "Le collage structural et le renforcement par resines des structures de la construction" , Annals de l'Institute technique du batiment et das travaux Publics, No. 349, April 1977. General construction series No. 62. 13 papers are summarized under the title "Le Renforcement du beton par resines" and "Les Applications du renforcement du Beton".

17. Sommerard, T., "Swanley steel Patch-Up", New Civil Engineer 1977, No. 247, 16 June 1977.

18. Raithby, K. D., "External strengthening of concrete bridges with bonded steel Plates", Department of the Environment, Department of the Transport, TRRL, Supplimentary Report 612, Crowthore, Birkshire, 1980.

19. R. Jones, R. N. Swamy and A. Charif, "Plate separation and anchorage of reinforced concrete beams strengthened by epoxy bonded-steel plates" , The Structual Engineer/Volume 66 / No. 5 / 1 March 1988.

20. T. M. Roberts, "Approximate analysis of shear and normal stress concentrations in the adhesive layer of plated RC beams.", The Structural Engineer / Volume 67 / No. 12 / June 1989.

21. T. M. Roberts, Haji-Kazemi, "Theoretical study of the behaviour of reinforced concrete beams strengthened by externally bonded steel plates.", Proc. Institute of Civil Engineers, Part 2, 1989, 87, March, 39-55 , Paper 9344, Structural Engineering Group.

22. T. M. Roberts, "Finite difference analysis of composite beams with partial interaction", Computers and Structures Vol. 21, No. 3, PP. 469-473, 1985, Printed in Great Britain.

23. L'Hermite, R. L., Bresson, J., "Beton arme par collage des armatures", RILEM International Symposium, Resins in Building Construction, part 2, Paris 1967, pp172-203.

24. Lerchental, H., "Bonded sheet metal reinforcement for concrete slabs", RILEM International Symposium, Resins in building construction, Paris 1967, pp165-173.

25. Kajfasz, S., "Concrete beams with external reinforcement bonded by gluing.", RILEM International Symposium, Resins in Building construction, Part 2, Paris 1967, pp142-151.

26. R. Jones, R. N. Swamy, J. Bloxham and Bouderbalah, "Composite behaviour of concrete beams with epoxy bonded external reinforcement", International Journal of cement composites, Volume 2, Number 2, May 1980.

27. R. Jones, R. N. Swamy and T. H. Ang, "Under- and over-reinforced concrete beams with glued steel plates", The International Journal of Cement Composites and light weight concrete, Volume 4, Number 1, February 1982.

28. Irwin, C. A. K., "The strengthening of concrete beams by bonded steel plates", TRRL Supplementary Report 160UC. Bridge Design Division, Structural Department, Crowthorne, Birkshire, 1975.

29. Macdonald, M. D. "The flexure behaviour of the concrete beams with bonded external reinforcement", TRRL Supplementary Report 415,

Transport and Road research Laboratory, Department of the environment, Crowthorne, 1978, p.13.

30. R. N. Swamy, R. Jones, J. W. Bloxham, "Structual behaviour of reinforced concrete beams strengthened by epoxy bonded steel plates", The Structural Engineer / Volume 65A / No. 2 / February 1987.

31. R. N. Swamy, R. Jones and A. Charif, "The effect of external plate reinforcement on the, Strengthening of structurally damaged RC beams" The Structural Engineer/Volume 67 / No. 3 / 7 February 1989.

32. Sadaatmanesh and M. R. Ehsani, "Epoxy-bonded glass fiber-reinforced plastic plates may provide a corrosion-free solution to increasing the load carrying capacities of concrete bridges", Concrete International, March 1990.

33. A. J. J. Calder, "Exposure tests on the externally reinforced concrete beams -First two years", Transport and Road Research Laboratory, Department of the Environment, Department of Transport.

34. G. O. Lioyd and A. J. J. Calder, "The microstructure of epoxy bonded steel-to-steel concrete joint ", Transport and Road Research Laboratory, Department of Transport, Department of Environment.

35. ACI-ASCE Committee 326, "ACI Journal, Proceedings, 59, January, February, and March 1962, 1-30, 277-344, and 352-396.

36. Boris Bresler and James G. MacGregor, "Review of concrete beams failing in shear", Journal of Structural Division, ASCE, 93, February 1967(ST1), 347-372.

37. ACI-ASCE Committee 426, "The shear strength of reinforced concrete members", Chapters 1-4, Journal of Structural Division, ASCE, 99, June 1973, 1091-1187

38. H. P. J. Taylor, "The fundamental behaviour of reinforced concrete beams in bending and shear", Shear in reinforced concrete, Vol. 1 (SP-42), Detroit: American Concrete Institute, 1974 (pp. 43-77)

39. JoDean Morrow and I. M. Viest, "Shear strength of reinforced concrete frame members without web reinforcement", ACI Journal Proceedings, 53, March, 1957, 833-869.

40. G. N. J. Kani, "Basic facts concerning shear failure", ACI Journal, Proceedings, 63, June 1966, 675-692. Disc. PP. 1511-1528.

41. R. Diaz De Cossio and S. Loera. Discussion of "Basic facts concerning shear failure" by G. N. J. Kani, ACI Jouranl, Proceedings, 63, December 1966, 1511-1544.

42. H. A. Rawdon de Paiva and Chester P. Siess, "Strength and behaviour of deep beams in shear", Journal of the Structural Division, ASCE, 91, October 1965 (ST5), 19-42.

43. V. Ramakrishnan and Y. Ananthanarayana, "Ultimate strength of deep beams in shear", ACI Journal, Proceedings, 65, February, 1968, 87-98.

44. Howard P. J. Taylor, "Shear strength of large beams ", Journal of Struc tural Division, ASCE, 98, November, 1972 (ST11), 2473-2490.

45. R. F. Manual, "Failure of deep beams", Shear in reinforecd concrete, Vol. 2 (SP-42), Detroit :American Concrete Institute, 1974 (PP.426-440)

46. J. G. MacGregor and N. M. Hawkins, "Suggested revision to ACI building code clauses dealing with shear friction and shear in deep beams and corbels", ACI Journal, Proceedings, 74, November, 1977, 537-545. Disc., 75, May 1998, 221-224.

47. G. N. J. Kani, "The riddle of shear failure and its solution", ACI Journal, Proceedings, 61, April, 1964, 441-467.

48. N. M. Newmark, C. P. Siess, I. M. Viest, "Tests and analysis of composite beams with incomplete interaction" , University of Illinois, Urbana, Illinois.

Appendix A

BEAMS OF SERIES B

In this appendix theoretical flexure and shear strengths of the beams of series B will be calculated. These beams were 150 by 150 mm in cross-section. These beams were reinforced with two 10 mm dia. bars as the main steel. The stirrups of 6 mm dia. were provided at 60 mm centre to centre throughout the lengths of the beams. The clear cover upto the stirrups was 30 mm in these beams. The average cylinder strength of the concrete for beams of this series was 31 MPa. For calculating the ultimate flexure strength, the ultimate concrete strain equal to 0.003 will be used. The rebars were of high strength steel. The actual stress strain curve of the rebar steel will be used for calculating the ultimate flexure strength of the beams of this series. Figure 174 shows the stress strain curve of the rebar steel.

The steel plates were of mild steel. The yield strength of the plate steel was 269 MPa. In order to take into account the strain hardening of the plate steel, a stress of 300 MPa for the steel plate will be used for calculating the flexure strengths of the beams of this series. For shear strength calculations, yield strength of 414 MPa will be used for the stirrups.

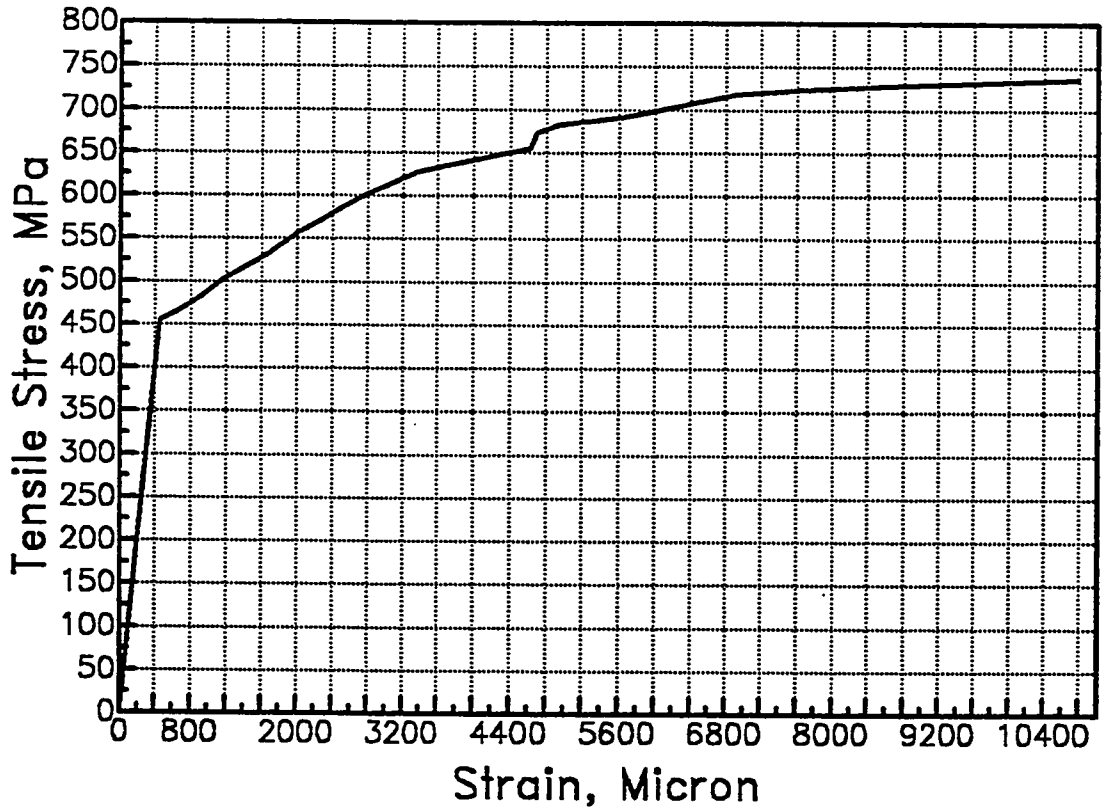

Figure 174: Stress strain curve of the rebar steel.

A.1 FLEXURE STRENGTH OF ORIGINAL BEAMS

h = 150 mm

d = 150 - effective cover

Effective cover = 41 mm.

Hence

d = 109 mm

$A_s = 157.08\ mm^2$

Assuming f_s equal to 700 MPa.

$$a = \frac{158.08 \times 700}{0.85 \times 31 \times 150}$$

By simplification we get

a = 27.98 mm

c = 27.98 / 0.823

c = 34.00

From the strain compatibilty analysis, the strain in the rebar steel equal to 0.00662 was found. The stress corresponding to this strain is about 700 MPa which match with our original assumption. Hence a steel stress equal to 700 MPa will be used for finding the ultimate flexure strength of the beams. The calculations for finding the ultimate flexure strength follows:-

$$M_n = A_s \times f_s \times (d - \frac{a}{2})$$

Substituting the values in the above equation and simplifying we get

$$M_n = 157.08 \times 700 \times (109 - \frac{27.98}{2})$$

$M_n = 10447$ kN-mm

$$\frac{P_n}{2} \times \text{shear-span} = M_n$$

$$P_n = \frac{10447}{200}$$

$$P_n = 52.23 \text{ kN}$$

Where shear span is equal to 400 mm.

A.2 FLEXURE STRENGTH OF BEAMS BONDED WITH 1.0 MM THICK PLATES

$$A_p = 100 \text{ mm}^2$$

$$A_s = 157.08 \text{ mm}^2$$

$$a = \frac{A_p \times f_{sp} + A_s \times f_s}{0.85 \times f_c \times b}$$

Assuming rebar steel stress equal to 680 MPa and plate steel stress equal to 300 MPa respectively, then we have the following.

$$a = \frac{100 \times 300 + 157.08 \times 680}{0.85 \times 31 \times 150}$$

$$a = 34.60 \text{ mm}$$

$$c = 34.60 / 0.823$$

$$c = 42.04 \text{ mm}$$

From the strain compatibility analysis the strain in the rebar steel was found equal to 0.004778. The stress corresponding to this strain is 680 MPa from the actual stress strain curve of the rebar steel which match with our assumption. So rebar stress equal to 680 MPa will be used for the flexure strength calculcations. Similarly, from the strain compatibility analysis the strain in the steel plate equal to 0.00774 was found which is above the yield strain of the steel

plate. So a stress of 300 MPa for the steel plate will be used for the flexure strength calculations. The flexure strength calculations are given below.

$$M_{n1} = A_p \times f_{sp} \times (d_p - \frac{a}{2})$$

$$M_{n1} = 100 \times 300 \times (150.5 - \frac{34.60}{2})$$

$$M_{n1} = 3996 \text{ kN.mm}$$

$$M_{n2} = A_s \times f_s \times (d - \frac{a}{2})$$

$$M_{n2} = 157.08 \times 680 \times (109 - \frac{34.60}{2})$$

$$M_{n2} = 9795 \text{ kN.mm}$$

$$M_n = M_{n1} + M_{n2}$$

$$M_n = 13791 \text{ kN.mm}$$

$$\frac{P_n}{2} \times 400 = 13791 \text{ kN.mm}$$

$$P_n = 69.00 \text{ kN}$$

A.3 FLEXURE STRENGTH OF BEAMS BONDED WITH 1.5 MM PLATES

$$A_p = 150 \text{ mm}^2$$

$$A_s = 157.08 \text{ mm}^2$$

$$a = \frac{A_p \times f_{sp} + A_s \times f_s}{0.85 \times f_c \times b}$$

Assuming rebar stress equal to 660 MPa and steel plate stress equal to 300 MPa, then we have the following.

$$a = \frac{150 \times 300 + 157.08 \times 660}{0.85 \times 31 \times 150}$$

$a = 37.60$ mm

$c = 37.60 / 0.823$

$c = 45.68$ mm

From strain compatibilty the strain in the rebar steel was found equal to 0.00416. The stress corresponding to this strain is 660 MPa in the actual stress strain curve of the rebar steel which match with our original assumption. Similarly from the strain compatibility the strain in the steel plate was found equal to 0.0069 which is above yield strain of the steel plate so a stress of 300 MPa will be used for finding the flexural strength. The flexure strength calculations follows:-

$$M_{n1} = A_p \times f_{sp} \times (d_p - \frac{a}{2})$$

$$M_{n1} = 150 \times 300 \times (150.75 - \frac{37.60}{2})$$

$M_{n1} = 5938.00$ kN.mm

$$M_{n2} = A_s \times f_s \times (d - \frac{a}{2})$$

$$M_{n2} = 157.08 \times 660 \times (109 - \frac{37.60}{2})$$

$M_{n2} = 9351$ kN.mm

$M_n = M_{n1} + M_{n2}$

$M_n = 15289$ kN.mm

$$\frac{P_n}{2} \times 400 = 15289 \text{ kN.mm}$$

$P_n = 76.50$ kN

A.4 FLEXURE STRENGTH OF BEAMS BONDED WITH 2.00 MM THICK PLATES

$A_p = 200\ mm^2$

$A_s = 157.08\ mm^2$

$$a = \frac{A_p \times f_{sp} + A_s \times f_s}{0.85 \times f_c \times b}$$

Assuming the rebar steel stress equal to 640 MPa and the steel plate stress equal to 300 MPa, then we have the following.

$$a = \frac{200 \times 300 + 157.08 \times 640}{0.85 \times 31 \times 150}$$

$a = 40.60\ mm$

$c = a / 0.823$

$c = 49.33\ mm$

From strain compatibilty analysis rebar strain was found equal to 0.00363 which corresponds to a stress of 640 MPa in the actual stress strain curve of the rebar steel which match with our assumption. So a stress of 640 MPa for the rebar steel will be used for calculating the flexure strength. Similarly, from the strain compatibility analysis the steel plate strain was found equal to 0.00618 which is above the yield strain so a stress of 300 MPa will be used for finding the flexural strength. The flexure strength calculations follows:-

$$M_{n1} = A_p \times f_{sp} \times (d_p - \frac{a}{2})$$

$$M_{n1} = 200 \times 300 \times (151.00 - \frac{40.60}{2})$$

$M_{n1} = 7842\ kN.mm$

$$M_{n2} = A_s \times f_s \times (d - \frac{a}{2})$$

$$M_{n2} = 157.08 \times 640 \times (109 - \frac{40.60}{2})$$

$$M_{n2} = 8917 \text{ kN.mm}$$

$$M_n = M_{n1} + M_{n2}$$

$$M_n = 16759 \text{ kN.mm}$$

$$\frac{P_n}{2} \times 400 = 16759 \text{ kN.mm}$$

$$P_n = 83.80 \text{ kN}$$

A.5 FLEXURE STRENGTH OF BEAMS BONDED WITH 3.0 MM THICK PLATES

$$A_p = 300 \text{ mm}^2$$

$$A_s = 157.08 \text{ mm}^2$$

$$a = \frac{A_p \times f_{sp} + A_s \times f_s}{0.85 \times f_c \times b}$$

Assuming the values of rebar stress equal to 600 MPa and steel plate stress equal to 300 MPa, then we have the following.

$$a = \frac{300 \times 300 + 157.08 \times 600}{0.85 \times 31 \times 150}$$

$$a = 46.60 \text{ mm}$$

$$c = a / 0.823$$

$$c = 56.62 \text{ mm}$$

From strain compatibilty analysis the strain in the rebar steel was found equal to 0.0028. The stress corresponding to this strain in the actual stress strain curve of the rebar steel is about 600 MPa which match with our assumption. So a stress of 600 MPa for the rebar steel will be used for the flexure strength calcu-

lations. Similarly, from the strain compatibility analysis, the strain in the steel plate was found equal to 0.00503 which is above the yield strain so a stress of 300 MPa will be used for the flexure strength calculations. The flexure strength calculations follows:-

$$M_{n1} = A_p \times f_{sp} \times (d_p - \frac{a}{2})$$

$$M_{n1} = 300 \times 300 \times (151.5 - \frac{46.60}{2})$$

$$M_{n1} = 11538 \text{ kN.mm}$$

$$M_{n2} = A_s \times f_s \times (d - \frac{a}{2})$$

$$M_{n2} = 157.08 \times 600 \times (109 - \frac{46.60}{2})$$

$$M_{n2} = 8077 \text{ kN.mm}$$

$$M_n = M_{n1} + M_{n2}$$

$$M_n = 19615 \text{ kN.mm}$$

$$\frac{P_n}{2} \times 400 = 19615 \text{ kN.mm}$$

$$P_n = 98 \text{ kN}$$

A.6 SHEAR STRENGTH OF BEAMS OF SERIES B

$$v_c = 0.166\sqrt{f_c'}$$

$$v_c = 0.166\sqrt{31}$$

$$v_c = 0.924 \text{ N/mm}^2$$

$$V_c = v_c bd$$

$$V_c = 0.924 \times 150 \times 109$$

$V_c = 15107.00\ N$

$$V_s = \frac{A_v f_y d}{s}$$

$A_v = 2 \times 28.274$

$A_v = 56.54\ mm^2$

$$V_s = \frac{56.54 \times 414 \times 109}{60}$$

$V_s = 42523.00\ N$

$V_n = V_c + V_s$

$V_n = 57630\ N$

$$\frac{P_n}{2} = V_n$$

$P_n = 2 \times V_n$

$P_n = 115.26\ kN$

Appendix B

BEAMS OF MF-SERIES

In this appendix theoretical flexure and shear strengths of the beams of this series will be calculated. These beams were 150 by 150 mm in cross-section. The beams of this series were reinforced with two 12 mm dia. bars at the bottom as the main steel. The links of 6 mm dia. bars were provided at the rate of 60 mm centre to centre throughout the lengths of the beams. The clear cover upto the main steel was 30 mm. The average cylinder strength of the concrete for beams of this series was 39.5 MPa. For calculating the ultimate flexure strength of the beams, the ultimate concrete strain equal to 0.003 will be used. The rebars were of high strength steel. The actual stress strain curve of the rebar steel will be used for calculating the ultimate flexure strength of the beams of this series. The stress strain curve of the rebar steel is shown in the Figure 175 . The steel plates were of mild steel. The yield strength of the plate steel is 269 MPa. In order to take into account the strain hardening of the plate steel, a stress of 300 MPa for the steel plate will be used for calculating the flexure strength of the beams when the plate strain is above the yield strain of the plate. For shear strength calculations yield strength of 414 MPa will be used for stirrups.

B.1 FLEXURE STRENGTH OF ORIGINAL BEAMS

h = 150 mm

d = 150 - effective cover

Effective cover = 36 mm

Hence

d = 114 mm

$A_s = 226\ mm^2$

Assuming f_s equal to 690 MPa.

$$a = \frac{226 \times 690}{0.85 \times 39.5 \times 150}$$

By simplification we get

a = 30.96 mm

c = 30.96 / 0.76

c = 40.73 mm

From the strain compatibilty analysis, the strain in the rebar steel equal to 0.0054 was found. The stress corresponding to this strain is about 690 MPa which match with our original assumption. Hence a steel stress equal to 690 MPa will be used for finding the ultimate flexure strength of the beams. The calculations for finding the ultimate flexure strength follows:-

$$M_n = A_s \times f_s \times (d - \frac{a}{2})$$

Substituting the values in the above equation and simplifying we get

$$M_n = 226 \times 690 \times (114 - \frac{30.96}{2})$$

$M_n = 15363$ kN-mm

$$\frac{P_n}{2} \times \text{shear-span} = M_n$$

$$P_n = \frac{15363}{200}$$

$$P_n = 76.80 \text{ kN}$$

Where shear span is equal to 400 mm.

B.2 FLEXURE STRENGTH OF BEAMS BONDED WITH 1.0 MM THICK PLATES

$$A_p = 100 \text{ mm}^2$$

$$A_s = 226 \text{ mm}^2$$

$$a = \frac{A_p \times f_{sp} + A_s \times f_s}{0.85 \times f_c \times b}$$

Assuming rebar steel stress equal to 650 MPa and steel plate stress equal to 300 MPa respectively, then we have the following.

$$a = \frac{100 \times 300 + 226 \times 650}{0.85 \times 39.5 \times 150}$$

$$a = 35.125 \text{ mm}$$

$$c = 35.125 / 0.76$$

$$c = 46.22 \text{ mm}$$

From the strain compatibility analysis the the strain in the rebar steel was found equal to 0.00438. With reference to actual stress strain curve of the rebar steel the stress corresponding to this strain is 650 MPa which match with our assumption. So a stress of 650 MPa will be used for the flexure strength calculations. Similarly, from the compatibility analysis the strain in the steel plate was found equal to 0.00677 which is above yield strain of the steel plate. So a stress

of 300 MPa for steel plate will be used for calculating the flexure strength of the beam. The flexure strength calculations follows:-

$$M_{n1} = A_p \times f_{sp} \times (d_p - \frac{a}{2})$$

$$M_{n1} = 100 \times 300 \times (150.5 - \frac{35.125}{2})$$

$$M_{n1} = 3988 \text{ kN.mm}$$

$$M_{n2} = A_s \times f_s \times (d - \frac{a}{2})$$

$$M_{n2} = 226 \times 650 \times (114 - \frac{35.125}{2})$$

$$M_{n2} = 14167 \text{ kN.mm}$$

$$M_n = M_{n1} + M_{n2}$$

$$M_n = 18155 \text{ kN.mm}$$

$$\frac{P_n}{2} \times 400 = 18155 \text{ kN.mm}$$

$$P_n = 90.77 \text{ kN}$$

B.3 FLEXURE STRENGTH OF BEAMS BONDED WITH 2.0 MM THICK PLATES

$$A_p = 200 \text{ mm}^2$$

$$A_s = 226 \text{ mm}^2$$

$$a = \frac{A_p \times f_{sp} + A_s \times f_s}{0.85 \times f_c \times b}$$

Assuming rebar steel stress equal to 630 MPa and steel plate stress equal to 300 MPa respectively, then we have the following.

$$a = \frac{200 \times 300 + 226 \times 630}{0.85 \times 39.5 \times 150}$$

$a = 40.18$ mm

$c = 40.18 / 0.76$

$c = 52.86$ mm

From the strain compatibility analysis the the strain in the rebar steel was found equal to 0.0035. With reference to actual stress strain curve of the rebar steel the stress corresponding to this strain is 630 MPa which match with our assumption. So a stress of 630 MPa will be used for the flexure strength calculations. Similarly, from the compatibility analysis the strain in the steel plate was found equal to 0.00557 which is above yield strain of the steel plate. So a stress of 300 MPa for steel plate will be used for calculating the flexure strength of the beam. The flexure strength calculations follows:-

$$M_{n1} = A_p \times f_{sp} \times (d_p - \frac{a}{2})$$

$$M_{n1} = 200 \times 300 \times (151 - \frac{40.18}{2})$$

$M_{n1} = 7855$ kN.mm

$$M_{n2} = A_s \times f_s \times (d - \frac{a}{2})$$

$$M_{n2} = 226 \times 630 \times (114 - \frac{40.18}{2})$$

$M_{n2} = 13371$ kN.mm

$M_n = M_{n1} + M_{n2}$

$M_n = 21226$ kN.mm

$$\frac{P_n}{2} \times 400 = 21226 \text{ kN.mm}$$

$P_n = 106.13$ kN

B.4 FLEXURE STRENGTH OF BEAMS BONDED WITH 3.0 MM THICK PLATES

$A_p = 300\ mm^2$

$A_s = 226\ mm^2$

$$a = \frac{A_p \times f_{sp} + A_s \times f_s}{0.85 \times f_c \times b}$$

Assuming rebar steel stress equal to 600 MPa and steel plate stress equal to 300 MPa respectively, then we have the following.

$$a = \frac{300 \times 300 + 226 \times 600}{0.85 \times 39.5 \times 150}$$

$a = 44.8$ mm

$c = 44.8 / 0.76$

$c = 59$ mm

From the strain compatibilty analysis, the strain in the rebar was found equal to 0.0028. The stress corresponding to this strain from the actual stress strain curve of the rebar steel was found equal to 600 MPa which match with our assumption. Similarly from the strain compatibility analysis the strain in the steel plate was found equal to 0.0047 which is above yield strain. So a stress of 300 MPa for steel plate will be used for calculating the flexure strength of the beam. The flexure strength calculations follows:-

$$M_{nl} = A_p \times f_{sp} \times (d_p - \frac{a}{2})$$

$$M_{nl} = 300 \times 300 \times (151.5 - \frac{44.80}{2})$$

$M_{nl} = 11619$ kN.mm

$$M_{n2} = A_s \times f_s \times (d - \frac{a}{2})$$

$$M_{n2} = 226 \times 600 \times (114 - \frac{44.80}{2})$$

$$M_{n2} = 12421 \text{ kN.mm}$$

$$M_n = M_{n1} + M_{n2}$$

$$M_n = 24040 \text{ kN.mm}$$

$$\frac{P_n}{2} \times 400 = 24040 \text{ kN.mm}$$

$$P_n = 120.20 \text{ kN}$$

B.5 SHEAR STRENGTH OF BEAMS OF MF-SERIES

$$v_c = 0.166\sqrt{f_c'}$$

$$v_c = 0.166\sqrt{39.50}$$

$$v_c = 1.0432 \text{ N/mm}^2$$

$$V_c = v_c bd$$

$$V_c = 1.0432 \times 150 \times 114$$

$$V_c = 17.84 \text{ kN}$$

$$V_s = \frac{A_v f_y d}{s}$$

$$A_v = 2 \times 28.274$$

$$A_v = 56.54 \text{ mm}^2$$

$$V_s = \frac{56.54 \times 414 \times 114}{60}$$

$$V_s = 44.47 \text{ kN}$$

$$V_n = V_c + V_s$$

$$V_n = 62.31 \text{ kN}$$

$$\frac{P_n}{2} = V_n$$

$$P_n = 2 \times V_n$$

$$P_n = 124.62 \text{ kN}$$

Appendix C

BEAMS OF MS-SERIES

In this appendix theoretical flexure and shear strengths of the beams of this series will be found. These beams were 150 mm by 150 mm in cross-section. These beams were reinforced with three 12 mm dia. bars at the bottom. The clear cover upto the main steel was 30 mm. The stirrups of 6 mm dia bars were provided at the ends of middle third and at the support points, that is, a total of four stirrups were provided throughout the lengths of the beams of this series. The average cylinder strength of the concrete for beams of this series was 39.5 MPa. For calculating the ultimate flexure strength of the beams, the ultimate concrete strain equal to 0.003 will be used. The rebars were of high strength steel. The actual stress strain curve of the rebar steel will be used for calculating the ultimate flexure strength of the beams. The steel plates were of mild steel. The yield strength of the plate steel was 269 MPa. In order to take into account the strain hardening of the plate steel, a stress of 300 MPa will be used for calculating the flexure strength of the beams. In these beams the stirrups do not contribute to the shear strength of the beams because the spacing between them was too high.

C.1 FLEXURAL STRENGTH OF BEAMS

Assuming a stress of 625 MPa in the rebars, then we have the following:-

$0.85f_c ab = A_s f_s$

$$a = \frac{A_s \times f_s}{0.85 \times f_c \times b}$$

$$a = \frac{339.29 \times 625}{0.85 \times 39.5 \times 150}$$

$a = 42.1$ mm

$c = 42.1 / 0.76$

$c = 55.4$ mm

From the strain compatibility analysis, the strain in th rebars was found equal to 0.0032. The stress corresponding to this strain from the actual stress strain curve of the rebar steel is equal to 625 MPa which match with our original assumption. So a stress of 625 MPa for rebar steel will be used for finding the flexure strength of the beams. The flexural strength calculations follows:-

$d = 114$ mm

$$M_n = A_s \times f_s \times (d - \frac{a}{2})$$

$$M_n = 339.29 \times 625 \times (114 - \frac{42.10}{2})$$

$M_n = 19711$ kN.mm

$$\frac{P_n}{2} \times 400 = 19711 \text{ kN.mm}$$

$P_n = 98.50$ kN

C.2 SHEAR STRENGTH OF BEAMS

In these beams the stirrups do not contribute to the shear strength of the beams because the spacing between the stirrups was too high. The shear strength calculations follows:-

$$V_c = 0.166 \times \sqrt{f_c'} \times b \times d$$

Substituting the values in the above equation

$$V_c = 0.166 \times \sqrt{39.5} \times 150 \times 114$$

$$V_c = 17.84 \text{ kN}$$

$$V_s = 0.0$$

$$V_n = V_s + V_c$$

$$\frac{P_n}{2} = V_n$$

$$P_n = 35.68 \text{ kN}$$

Appendix D

PRECEDURE FOR FINDING CURVATURE

The curvature of a beam is directly proportional to the bending moment provided the EI is constant as clear from the following equation.

$$\frac{M}{EI} = \varphi = \frac{1}{\rho}$$

In our loading set up the bending moment in the middle third of the beam is same every where. It means the curvature is same every where in the middle third of the beam. Therefore, the middle third of the beam can be considered as the segment of a circle. Knowing the deflection at three points in the middle third of the beam, the equation of circle can be fit to find the radius. The inverse of the radius will give the curvature of the beam. The procedure for finding the curvature follows:-

Figure 176 shows the segment of the deflected curve of the middle third of the beam in which the bending is constant. As the bending moment is constant in the middle third of the beam so this curve can be considered as the segment of a circle.

Let Δd be the difference between the mid-span deflection and average of the deflection at the third points.

Mathematically it can be written as follows:-

$$\Delta d = \Delta_c - \frac{\Delta_1 + \Delta_2}{2}$$

With the help of this figure the radius of the circle, shear span a and Δd can be related by the following equation.

$$\rho^2 = (\frac{a}{2})^2 + (\rho - \Delta d)^2$$

By simplification we get the following equation.

$$\rho = \frac{(a/2)^2 + (\Delta d)^2}{2 \times \Delta d}$$

where a is the shear span and ρ is the radius of curvature. The reciprocal of the radius is equal to the curvature of the beam. So the curvature of the beam in the middle third of the beam is given by the following equation.

$$\Phi = \frac{1}{\rho} = \frac{2 \times \Delta d}{(a/2)^2 + (\Delta d)^2}$$

where Φ is the curvature of the beam.

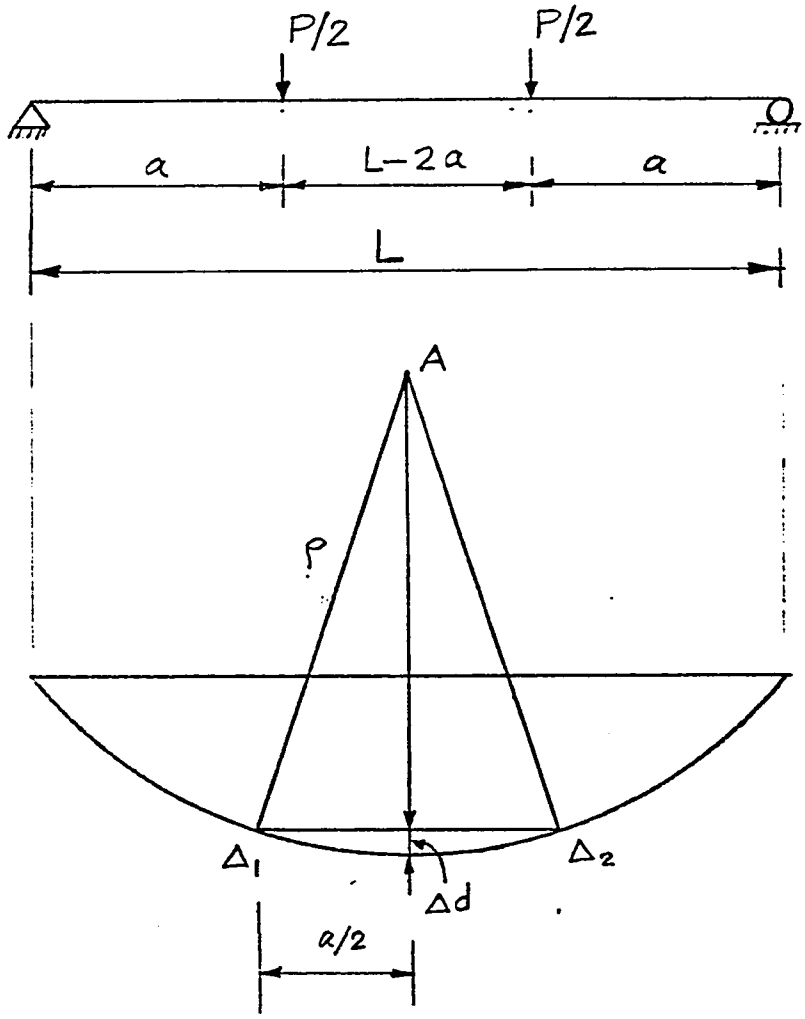

Figure 176: Elastic curve of the beam in the constant moment region. This curve has constant curvature.

Appendix E

LISTING AND A TYPICAL DATA FILE FOR PROGRAM NEW1

E.1 PROGRAM NEW1

This program is for finding the slip at interface in simply supported composite beams. This program is based on the partial interaction theory Newmark approach [48] . With the help of this program the shear connectors for the composite beams can be designed.

E.2 EXPLANATION OF THE TERMS IN THE DATA FILE

1. TLENG

   This term represents the total length of the composite beam to be analysed.

2. NDIVS

   This term represents the total number of segments in which the beam is divided. Any number can be used. For more accuracy, the number of segments are increased.

3. NCL

This term represents the number of concentrated loads to be placed on the beam for analysis.

4. Z

This term represents the distance between the centroid of the upper and lower layer respectively.

5. XKS

This term represents the shear stiffness of the interface. It is equal to force per unit length per unit slip at the interface.

6. W

This term represents the uniformly distributed load on the beam.

7. AA, XIA, EA

These terms represent the area, moment of inertia about the centroidal axis and modulus of elasticity of the upper layer respectively.

8. AB, XIB, EB

These terms represent the area, moment of inertia about the centroidal axis and modulus of elasticity of the lower layer respectively.

9. NODE

This term represents the node at which the concentrated load is placed. More than one point loads can be placed on the beam.

FILE: NEW1 FORTRAN A1 KING FAHD UNIVERSITY OF PETROLEUM AND MINERALS, DHAHRAN

```
C*************************************************************************NEW00010
C   PROGRAM FOR THE ANALYSIS OF  SLIP IN THE COMPOSITE BEAMS              NEW00020
C   BASED ON NEWMARK APPROACH USING FINITE DIFFERENCE METHOD              NEW00030
C            WRITTEN BY :MUNAWAR HUSSAIN (ST#890481)                      NEW00040
C*************************************************************************NEW00050
      IMPLICIT REAL*8(A-H,O-Z)                                            NEW00060
      DIMENSION PCL(150),ACL(150),PLOAD(150)                              NEW00070
      DIMENSION ABM(150,150),BM(150),SLIP(150)                            NEW00080
      DIMENSION AFM(150,150),VF(150),AF(150)                              NEW00090
      READ (20,10) TITLE                                                  NEW00100
      WRITE(21,10) TITLE                                                  NEW00110
10    FORMAT(18A4)                                                        NEW00120
      READ (20,10) WORDS                                                  NEW00130
      READ (20,10) WORDS                                                  NEW00140
      READ (20,*) TLENG,NDIVS,NCL,Z,XKS,W                                 NEW00150
      READ (20,10) WORDS                                                  NEW00160
      READ (20,10) WORDS                                                  NEW00170
      READ (20,*) AA,XIA,EA                                               NEW00180
      READ (20,10) WORDS                                                  NEW00190
      READ (20,*) AB,XIB,EB                                               NEW00200
      READ (20,10) WORDS                                                  NEW00210
      READ (20,10) WORDS                                                  NEW00220
      NPOIN=NDIVS+1                                                       NEW00230
      NTOT=NPOIN+2                                                        NEW00240
      H=TLENG/NDIVS                                                       NEW00250
      SIGEI=EA*XIA+EB*XIB                                                 NEW00260
      EABAR=EA*AA*EB*AB/(EA*AA+EB*AB)                                     NEW00270
      EIBAR=SIGEI+EABAR*Z**2                                              NEW00280
      C1=XKS*EIBAR/EABAR/SIGEI                                            NEW00290
      C2=XKS*Z/SIGEI                                                      NEW00300
C-------------------------------------------------------------------------NEW00310
      DO 40 K=1,NTOT                                                      NEW00320
      PCL(K)=0                                                            NEW00330
40    ACL(K)=0                                                            NEW00340
      DO 60 I=1,NCL                                                       NEW00350
60    READ (20,*)J,ACL(J)                                                 NEW00360
      DO 65 K=1,NTOT                                                      NEW00370
65    PCL(K)=W*H                                                          NEW00380
      PCL(1)=PCL(1)/2.0                                                   NEW00390
      PCL(NTOT)=PCL(NTOT)/2.0                                             NEW00400
      DO 70 K=1,NTOT                                                      NEW00410
70    ACL(K)=-ACL(K)-PCL(K)                                               NEW00420
      ACL(2)=0                                                            NEW00430
      ACL(NTOT-1)=0                                                       NEW00440
      WRITE(21,*)'ACL FOLLOWS'                                            NEW00450
      WRITE(21,100)(ACL(K),K=1,NTOT)                                      NEW00460
C-------------------------------------------------------------------------NEW00470
100   FORMAT(5E25.8)                                                      NEW00480
      WRITE(21,120) TLENG                                                 NEW00490
120   FORMAT(//15X,'TLENG=',E15.6)                                        NEW00500
      WRITE(21,125) NDIVS                                                 NEW00510
125   FORMAT(/15X,'NDIVS=',I3)                                            NEW00520
      WRITE(21,130) NCL                                                   NEW00530
130   FORMAT(/15X,'  NCL=',I3)                                            NEW00540
      WRITE(21,135) Z                                                     NEW00550
```

```
135   FORMAT(/15X,' Z=',E15.6)                                          NEW00560
      WRITE(21,140) XKS                                                 NEW00570
140   FORMAT(/15X,'KS=',E15.6)                                          NEW00580
      WRITE(21,145)AA                                                   NEW00590
145   FORMAT(/15X,'AA=',E15.6)                                          NEW00600
      WRITE(21,150) XIA                                                 NEW00610
150   FORMAT(/15X,'IA=',E15.6)                                          NEW00620
      WRITE(21,155) EA                                                  NEW00630
155   FORMAT(/15X,'EA=',E15.6)                                          NEW00640
      WRITE(21,165)AB                                                   NEW00650
165   FORMAT(/15X,'AB=',E15.6)                                          NEW00660
      WRITE(21,170) XIB                                                 NEW00670
170   FORMAT(/15X,'IB=',E15.6)                                          NEW00680
      WRITE(21,175) EB                                                  NEW00690
175   FORMAT(/15X,'EB=',E15.6)                                          NEW00700
      WRITE(21,190) H                                                   NEW00710
190   FORMAT(/15X,'H=',E15.6)                                           NEW00720
      WRITE(21,195)W                                                    NEW00730
195   FORMAT(/15X,'UDL=',E15.6)                                         NEW00740
      CALL GABM(NTOT,ABM)                                               NEW00750
      CALL MINVT(ABM,NTOT,ISTAB)                                        NEW00760
      CALL ALOAD(NTOT,H,ACL,PLOAD)                                      NEW00770
      CALL MATMC(ABM,PLOAD,BM,NTOT)                                     NEW00780
      CALL GAFM(NTOT,H,C1,AFM)                                          NEW00790
      CALL MINVT(AFM,NTOT,ISTAB)                                        NEW00800
      CALL GVF(NTOT,H,C2,BM,VF)                                         NEW00810
      CALL MATMC(AFM,VF,AF,NTOT)                                        NEW00820
      CALL GSLIP(NTOT,H,XKS,AF,SLIP)                                    NEW00830
      WRITE(21,*)'BM FOLLOWS'                                           NEW00840
      WRITE(21,100)(BM(K),K=1,NTOT)                                     NEW00850
      WRITE(21,*)'AF FOLLOWS'                                           NEW00860
      WRITE(21,100)(AF(K),K=1,NTOT)                                     NEW00870
      WRITE(21,*)'SLIP FOLLOWS'                                         NEW00880
      WRITE(21,100)(SLIP(K),K=2,NTOT-1)                                 NEW00890
      STOP                                                              NEW00900
      END                                                               NEW00910
C-----------------------------------------------------------------------NEW00920
C-----SUBROUTINE FOR MULPLICATION OF MATRIX                             NEW00930
C-----------------------------------------------------------------------NEW00940
      SUBROUTINE MATMUL(A,B,C,L,M,N)                                    NEW00950
      IMPLICIT REAL*8 (A-H,O-Z)                                         NEW00960
      DIMENSION A(150,150),B(150,150),C(150,150)                        NEW00970
C     DOUBLE PRECISION A,B,C                                            NEW00980
      DO 20 I=1,L                                                       NEW00990
      DO 20 J=1,N                                                       NEW01000
      C(I,J)=0                                                          NEW01010
      DO 20 K=1,M                                                       NEW01020
20    C(I,J)=C(I,J)+A(I,K)*B(K,J)                                       NEW01030
      RETURN                                                            NEW01040
      END                                                               NEW01050
C-----------------------------------------------------------------------NEW01060
C-----SUBROUTINE FOR MULTIPLICATION OF A VECTOR WITH MATRIX             NEW01070
C-----------------------------------------------------------------------NEW01080
      SUBROUTINE MATMC(A,B,C,M)                                         NEW01090
      IMPLICIT REAL*8 (A-H,O-Z)                                         NEW01100
```

```
      DIMENSION A(150,150),B(150),C(150)                                NEW01110
C     DOUBLE PRECISION A,B,C                                            NEW01120
      DO 10  I=1,M                                                      NEW01130
      C(I)=0                                                            NEW01140
      DO 10 J=1,M                                                       NEW01150
10    C(I)=C(I)+A(I,J)*B(J)                                             NEW01160
      RETURN                                                            NEW01170
      END                                                               NEW01180
C SUBROUTINE MATRIX INVERSION                                           NEW01190
      SUBROUTINE MINVT(A,N,ISTAB)                                       NEW01200
      IMPLICIT REAL*8 (A-H,O-Z)                                         NEW01210
      DIMENSION A(150,150)                                              NEW01220
C     DOUBLE PRECISION A                                                NEW01230
      ISTAB=0                                                           NEW01240
      DO 40 I=1,N                                                       NEW01250
      PIVOT=A(I,I)                                                      NEW01260
      IF(ABS(PIVOT).EQ.(0.0)) THEN                                      NEW01270
      ISTAB=1                                                           NEW01280
      RETURN                                                            NEW01290
      ENDIF                                                             NEW01300
      PIVR=1./PIVOT                                                     NEW01310
      DO 10 NCOL=1,N                                                    NEW01320
      A(I,NCOL)=A(I,NCOL)/PIVOT                                         NEW01330
10    CONTINUE                                                          NEW01340
      DO 30 K=1,N                                                       NEW01350
      IF(K.NE.I) THEN                                                   NEW01360
      PIVOT=A(K,I)                                                      NEW01370
      DO 20 NCOL=1,N                                                    NEW01380
      A(K,NCOL)=A(K,NCOL)-A(I,NCOL)*PIVOT                               NEW01390
20    CONTINUE                                                          NEW01400
      A(K,I)=-PIVOT*PIVR                                                NEW01410
      ENDIF                                                             NEW01420
30    CONTINUE                                                          NEW01430
      A(I,I)=PIVR                                                       NEW01440
40    CONTINUE                                                          NEW01450
      RETURN                                                            NEW01460
      END                                                               NEW01470
C=====================================================================NEW01480
C=====================================================================NEW01490
C=====================================================================NEW01500
C=====================================================================NEW01510
C=====================================================================NEW01520
      SUBROUTINE GABM(NTOT,ABM)                                         NEW01530
      IMPLICIT REAL*8 (A-H,O-Z)                                         NEW01540
      DIMENSION ABM(150,150)                                            NEW01550
C---------------------------------------------------------------------NEW01560
      DO 10 J=1,NTOT                                                    NEW01570
      DO 10 K=1,NTOT                                                    NEW01580
10    ABM(J,K)=0                                                        NEW01590
C---------------------------------------------------------------------NEW01600
      K=2                                                               NEW01610
      ABM(K-1,K+1)=1.0                                                  NEW01620
      ABM(K-1,K)=-2.0                                                   NEW01630
      ABM(K-1,K-1)=1.0                                                  NEW01640
C---------------------------------------------------------------------NEW01650
```

```
      K=2                                                                NEW01660
      ABM(K,K)=1.0                                                       NEW01670
C-----------------------------------------------------------------------NEW01680
      DO 200 K=3,NTOT-2                                                  NEW01690
      ABM(K,K+1)=1.0                                                     NEW01700
      ABM(K,K)=-2.0                                                      NEW01710
      ABM(K,K-1)=1.0                                                     NEW01720
200   CONTINUE                                                           NEW01730
C-----------------------------------------------------------------------NEW01740
      K=NTOT-1                                                           NEW01750
      ABM(K,K)=1.0                                                       NEW01760
C-----------------------------------------------------------------------NEW01770
      K=NTOT-1                                                           NEW01780
      ABM(K+1,K+1)=1.0                                                   NEW01790
      ABM(K+1,K)=-2.0                                                    NEW01800
      ABM(K+1,K-1)=1.0                                                   NEW01810
      RETURN                                                             NEW01820
      END                                                                NEW01830
C=======================================================================NEW01840
C=======================================================================NEW01850
C=====GENERATES AMATRX FOR AXIAL FORCE=================================NEW01860
C=======================================================================NEW01870
C=======================================================================NEW01880
      SUBROUTINE GAFM(NTOT,H,C1,AFM)                                     NEW01890
      IMPLICIT REAL*8 (A-H,O-Z)                                          NEW01900
      DIMENSION AFM(150,150)                                             NEW01910
C-----------------------------------------------------------------------NEW01920
      DO 10 J=1,NTOT                                                     NEW01930
      DO 10 K=1,NTOT                                                     NEW01940
10    AFM(J,K)=0                                                         NEW01950
C-----------------------------------------------------------------------NEW01960
      K=2                                                                NEW01970
      AFM(K-1,K+1)=1.0                                                   NEW01980
      AFM(K-1,K)=-2.0-C1*H*H                                             NEW01990
      AFM(K-1,K-1)=1.0                                                   NEW02000
C-----------------------------------------------------------------------NEW02010
      K=2                                                                NEW02020
      AFM(K,K)=1.0                                                       NEW02030
C-----------------------------------------------------------------------NEW02040
      DO 200 K=3,NTOT-2                                                  NEW02050
      AFM(K,K+1)=1.0                                                     NEW02060
      AFM(K,K)=-2.0-C1*H*H                                               NEW02070
      AFM(K,K-1)=1.0                                                     NEW02080
200   CONTINUE                                                           NEW02090
C-----------------------------------------------------------------------NEW02100
      K=NTOT-1                                                           NEW02110
      AFM(K,K)=1.0                                                       NEW02120
C-----------------------------------------------------------------------NEW02130
      K=NTOT-1                                                           NEW02140
      AFM(K+1,K+1)=1.0                                                   NEW02150
      AFM(K+1,K)=-2.0-C1*H*H                                             NEW02160
      AFM(K+1,K-1)=1.0                                                   NEW02170
      RETURN                                                             NEW02180
      END                                                                NEW02190
                                                                         NEW02200
```

```
C=======================================================================NEW02210
C=======================================================================NEW02220
C=====GENERATES LOAD VECTOR=FOR FORCE==================================NEW02230
C=======================================================================NEW02240
C=======================================================================NEW02250
      SUBROUTINE GVF(NTOT,H,C2,BM,VF)                                   NEW02260
      IMPLICIT REAL*8 (A-H,O-Z)                                         NEW02270
      DIMENSION BM(150),VF(150)                                         NEW02280
      DO 10 K=1,NTOT                                                    NEW02290
10    VF(K)=0                                                           NEW02300
C-----------------------------------------------------------------------NEW02310
      VF(1)=-BM(2)*C2*H*H                                               NEW02320
      VF(2)=0                                                           NEW02330
      DO 20 K=3,NTOT-2                                                  NEW02340
20    VF(K)=-BM(K)*C2*H*H                                               NEW02350
      VF(NTOT-1)=0                                                      NEW02360
      VF(NTOT)=-BM(NTOT-1)*C2*H*H                                       NEW02370
C-----------------------------------------------------------------------NEW02380
      RETURN                                                            NEW02390
      END                                                               NEW02400
C=======================================================================NEW02410
C=======================================================================NEW02420
C=====CALCULATES SLIP==================================================NEW02430
C=======================================================================NEW02440
C=======================================================================NEW02450
      SUBROUTINE GSLIP(NTOT,H,XKS,AF,SLIP)                              NEW02460
      IMPLICIT REAL*8 (A-H,O-Z)                                         NEW02470
      DIMENSION SLIP(150),AF(150),COOR(150)                             NEW02480
      DO 10 K=1,NTOT                                                    NEW02490
10    SLIP(K)=0                                                         NEW02500
      DO 20 K=2,NTOT-1                                                  NEW02510
20    SLIP(K)=(-AF(K+1)+AF(K-1))/2.0/H/XKS                              NEW02520
      DO 30 K=2,NTOT-1                                                  NEW02530
30    COOR(K-1)=(K-2)*H/1000                                            NEW02540
      WRITE(22,40)(COOR(K-1),SLIP(K),K=2,NTOT-1)                        NEW02550
40    FORMAT(5X,2F20.5)                                                 NEW02560
      RETURN                                                            NEW02570
      END                                                               NEW02580
C=======================================================================NEW02590
C=======================================================================NEW02600
C=====GENERATES LOAD VECTOR FOR BENDING MOMENT==========================NEW02610
C=======================================================================NEW02620
C=======================================================================NEW02630
      SUBROUTINE ALOAD(NTOT,H,ACL,PLOAD)                                NEW02640
      IMPLICIT REAL*8 (A-H,O-Z)                                         NEW02650
      DIMENSION ACL(150),PLOAD(150)                                     NEW02660
      DO 10 K=1,NTOT                                                    NEW02670
10    PLOAD(K)=0                                                        NEW02680
      DO 20 K=1,NTOT                                                    NEW02690
20    PLOAD(K)=ACL(K)*H                                                 NEW02700
      RETURN                                                            NEW02710
      END                                                               NEW02720
```

FILE: NEW1 DATA A1 KING FAHD UNIVERSITY OF PETROLEUM AND MINERALS, DHAHRAN

PROBLEN NO. 1

CONTROL INFORMATION

TLENG	NDIVS	NCL	Z	XKS	W
20000	99	1	559	54.5	0.00

MATERIAL PROPERTIES

AA	XIA	EA
3.0E5	1.0E9	21000

AB	XIB	EB
3.26E4	4.44E9	210000

CONCENTRATED LOADS FOLLOWS

NODE	CONCENTRATED LOAD
51	49300

Appendix F

LISTING AND A TYPICAL DATA FILE FOR PROGRAM ROB1

F.1 PROGRAM ROB1

This program is for determining the slip at the interface of the simply supported composite beams. This program is based on partial interaction theory, Robert's approach [22] .

F.2 EXPLANATION OF THE TERMS IN THE DATA FILE

1. XKS

   This term represents the shear stiffness of the interface. Its unit is force per unit length per unit slip.

2. NDIVS

   This term represents the number of segments in which the beam is divided. For more accuracy, the number of segments are increased.

3. NCL

   This term represents the number of concentrated loads to be placed on the beam for the analysis.

4. ECCEN

This term represents the distance between the centroids of the upper and lower layer respectively in the composite beam.

5. TLENG

This term represents the total length of the composite beam.

6. AA, AB

These terms represent the areas of upper and lower layer respectively, in the composite beam.

7. XIA, XIB

These terms represent the moments of inertias of the upper and lower layer respectively, about their own centroidal axes.

8. EA, EB

These terms represent the modulus of elasticity of the upper and lower layer respectively.

9. ZIA

This term represents the distance from the centroid of the upper layer to the interface. This is positive because it is measured in the positive direction of the z-axis.

10. ZIB

This term represents the distance between the centroid of the bottom layer to the interface. This will be negative when measured upward because the positive direction of the z-axis was taken downward in the derivations of the differential equations.

11. PS

This term represents the uniformly distributed load on the beam.

12. NODE

This term represents the node at which point load is to be placed. The point loads could be more than one.

FILE: ROB1 FORTRAN A1 KING FAHD UNIVERSITY OF PETROLEUM AND MINERALS, DHAHRAN

```
C*************************************************************************ROB00010
C   PROGRAM FOR THE ANALYSIS OF SLIP IN THE COMPOSITE BEAMS                ROB00020
C   BASED ON ROBERT'S APPROACH USING FINITE DIFFERENCE METHOD              ROB00030
C            WRITTEN BY :MUNAWAR HUSSAIN (ST#890481)                       ROB00040
C*************************************************************************ROB00050
      IMPLICIT REAL*8(A-H,O-Z)                                             ROB00060
      DIMENSION AMATX(450,450),TITLE(18),PCL(120),ACL(120)                 ROB00070
      DIMENSION PLOAD(450),DISP(450),UAB(120),AMT1(450,450)                ROB00080
      DIMENSION UA(120),UB(120),W(120),COOR(120),AMT(450,450)              ROB00090
C *** READ AND WRITE CONTROL DATA                                          ROB00100
C                                                                          ROB00110
      READ (20,10) TITLE                                                   ROB00120
      WRITE(21,10) TITLE                                                   ROB00130
10    FORMAT(18A4)                                                         ROB00140
      READ (20,10) WORDS                                                   ROB00150
      READ (20,10) WORDS                                                   ROB00160
      READ (20,*) XKS,NDIVS,NCL,E,TLENG                                    ROB00170
      READ (20,10) WORDS                                                   ROB00180
      READ (20,10) WORDS                                                   ROB00190
      READ (20,*) AA,XIA,EA,ZIA                                            ROB00200
      READ (20,10) WORDS                                                   ROB00210
      READ (20,*) AB,XIB,EB,ZIB                                            ROB00220
      READ(20,10)WORDS                                                     ROB00230
      READ(20,10)WORDS                                                     ROB00240
      READ(20,*)PS                                                         ROB00250
      WRITE(21,20) TLENG                                                   ROB00260
20    FORMAT(/5X,'TLENG=',E20.6)                                           ROB00270
                                                                           ROB00280
      WRITE(21,25) NDIVS                                                   ROB00290
25    FORMAT(/5X,'NUMBER OF SEGMENTS......NDIVS=',I3)                      ROB00300
                                                                           ROB00310
      WRITE(21,30) E                                                       ROB00320
30    FORMAT(/5X,'.............................E=',E15.6)                  ROB00330
                                                                           ROB00340
      WRITE(21,35) XKS                                                     ROB00350
35    FORMAT(/5X,'............................KS=',E15.6)                  ROB00360
                                                                           ROB00370
                                                                           ROB00380
      WRITE(21,45)AA                                                       ROB00390
45    FORMAT(/5X,'............................AA=',E15.6)                  ROB00400
      WRITE(21,50) XIA                                                     ROB00410
50    FORMAT(/5X,'............................IA=',E15.6)                  ROB00420
      WRITE(21,55) EA                                                      ROB00430
55    FORMAT(/5X,'............................EA=',E15.6)                  ROB00440
      WRITE(21,60) ZIA                                                     ROB00450
60    FORMAT(/5X,'...........................ZIA=',E15.6)                  ROB00460
      WRITE(21,65) AB                                                      ROB00470
65    FORMAT(/5X,'AB=',E15.6)                                              ROB00480
      WRITE(21,70) XIB                                                     ROB00490
70    FORMAT(/5X,'IB=',E15.6)                                              ROB00500
      WRITE(21,75) EB                                                      ROB00510
75    FORMAT(/5X,'EB=',E15.6)                                              ROB00520
      WRITE(21,80) ZIB                                                     ROB00530
80    FORMAT(/5X,'ZIB=',E15.6)                                             ROB00540
      NPOIN=NDIVS+1                                                        ROB00550
```

```
      WRITE(21,85) NPOIN                                                ROB00560
85    FORMAT(/5X,'NPOIN=',I3)                                           ROB00570
      H=TLENG/FLOAT(NDIVS)                                              ROB00580
      WRITE(21,90) H                                                    ROB00590
90    FORMAT(///5X,'.............................H=',E15.6)             ROB00600
      WRITE(21,100) PS                                                  ROB00610
100   FORMAT(///5X,'..........................  ..PS=',E15.6)          ROB00620
      WRITE(21,116)NCL                                                  ROB00630
116   FORMAT(/5X,'NUMBER OF CONCENTRATED LOADS.=',I5)                   ROB00640
C-----------------------------------------------------------------------ROB00650
      NUA=NPOIN+2                                                       ROB00660
      NUB=NPOIN+2                                                       ROB00670
      NW=NPOIN+4                                                        ROB00680
      NTOT=NUA+NUB+NW                                                   ROB00690
       DO 440 K=1,NW                                                    ROB00700
440    PCL(K)=0                                                         ROB00710
       READ (20,10) WORDS                                               ROB00720
       DO 600 K=1,NCL                                                   ROB00730
600    READ (20,*)J,PCL(J)                                              ROB00740
       DO 610 K=1,NW                                                    ROB00750
610    PCL(K)=PCL(K)/H                                                  ROB00760
       DO 650 K=1,NW                                                    ROB00770
650    PCL(K)=PCL(K)+PS                                                 ROB00780
       PCL(1)=PCL(1)/2.0                                                ROB00790
       PCL(2)=0                                                         ROB00800
       PCL(3)=0                                                         ROB00810
       PCL(NW-2)=0                                                      ROB00820
       PCL(NW-1)=0                                                      ROB00830
       PCL(NW)=PCL(NW)/2.0                                              ROB00840
C      WRITE(21,*)'PCL FOLLOWS'                                         ROB00850
C      WRITE(21,630)(PCL(K),K=1,NW)                                     ROB00860
 630   FORMAT(5E25.6)                                                   ROB00870
      DO 700 K=1,NW                                                     ROB00880
      C=EA*XIA+EB*XIB                                                   ROB00890
      C=H**4/C                                                          ROB00900
700   PCL(K)=C*PCL(K)                                                   ROB00910
C-----------------------------------------------------------------------ROB00920
C     GENERATION OF AMATRIX  FOLLOWS:-                                  ROB00930
C-----------------------------------------------------------------------ROB00940
      DO 130 I=1,NTOT                                                   ROB00950
      DO 130 J=1,NTOT                                                   ROB00960
      AMATX(I,J)=0.0                                                    ROB00970
130   CONTINUE                                                          ROB00980
C=======================================================================ROB00990
C=======================================================================ROB01000
C=====SLIP EQUATION FOLLOWS============================================ROB01010
C=======================================================================ROB01020
C=======================================================================ROB01030
C-------------------------------------------------------------          ROB01040
      J=2                                                               ROB01050
      AMATX(J-1,J+1)=1.0                                                ROB01060
      AMATX(J-1,J-1)=-1.0                                               ROB01070
C-------------------------------------------------------------          ROB01080
      DO 170 J=2,NUA-1                                                  ROB01090
      K=J+1                                                             ROB01100
```

```
      C=XKS*H**2/EA/AA                                                  ROB01110
      AMATX(J,J+1)=1                                                    ROB01120
      AMATX(J,J)=-2.0-C                                                 ROB01130
      AMATX(J,J-1)=1                                                    ROB01140
      AMATX(J,NUA+J)=C                                                  ROB01150
      C=XKS*E*H/EA/AA/2.0                                               ROB01160
      AMATX(J,NUA+NUB+K+1)=C                                            ROB01170
      AMATX(J,NUA+NUB+K-1)=-C                                           ROB01180
170   CONTINUE                                                          ROB01190
C-----------------------------------------------------------------      ROB01200
      J=NUA-1                                                           ROB01210
      AMATX(J+1,J+1)=1.0                                                ROB01220
      AMATX(J+1,J-1)=-1.0                                               ROB01230
C=================================================================      ROB01240
C=================================================================      ROB01250
C=====HORIZONTAL EQUILIBRIUM                                           ROB01260
C=================================================================      ROB01270
C=================================================================      ROB01280
C-----------------------------------------------------------------      ROB01290
      J=2                                                               ROB01300
      AMATX(NUA+J-1,NUA+J+1)=1.0                                        ROB01310
      AMATX(NUA+J-1,NUA+J-1)=-1.0                                       ROB01320
C-----------------------------------------------------------------      ROB01330
      DO 180  J=2,NUB-1                                                 ROB01340
      AMATX(NUA+J,J+1)=1.0                                              ROB01350
      AMATX(NUA+J,J)=-2.0                                               ROB01360
      AMATX(NUA+J,J-1)=1.0                                              ROB01370
      C=EB*AB/EA/AA                                                     ROB01380
      AMATX(NUA+J,NUA+J+1)=C                                            ROB01390
      AMATX(NUA+J,NUA+J)=-2.0*C                                         ROB01400
      AMATX(NUA+J,NUA+J-1)=C                                            ROB01410
180   CONTINUE                                                          ROB01420
C-----------------------------------------------------------------      ROB01430
      J=NUB-1                                                           ROB01440
      AMATX(NUA+J+1,NUA+J+1)=-1.0                                       ROB01450
      AMATX(NUA+J+1,NUA+J-1)=1.0                                        ROB01460
C=================================================================      ROB01470
C=================================================================      ROB01480
C--  VERTICAL EQUILIBRIUM                                              ROB01490
C=================================================================      ROB01500
C=================================================================      ROB01510
      K=3                                                               ROB01520
      AMATX(NUA+NUB+K-2,NUA+NUB+K-2)=1                                  ROB01530
      AMATX(NUA+NUB+K-2,NUA+NUB+K-1)=-4                                 ROB01540
      AMATX(NUA+NUB+K-2,NUA+NUB+K)=6                                    ROB01550
      AMATX(NUA+NUB+K-2,NUA+NUB+K+1)=-4                                 ROB01560
      AMATX(NUA+NUB+K-2,NUA+NUB+K+2)=1                                  ROB01570
C-----------------------------------------------------------------      ROB01580
      K=3                                                               ROB01590
      AMATX(NUA+NUB+K-1,NUA+NUB+K-1)=1                                  ROB01600
      AMATX(NUA+NUB+K-1,NUA+NUB+K)=-2                                   ROB01610
      AMATX(NUA+NUB+K-1,NUA+NUB+K+1)=1                                  ROB01620
C-----------------------------------------------------------------      ROB01630
      K=3                                                               ROB01640
      AMATX(NUA+NUB+K,NUA+NUB+K)=1                                      ROB01650
```

FILE: ROB1 FORTRAN A1 KING FAHD UNIVERSITY OF PETROLEUM AND MINERALS, DHAHRAN

```
C-----------------------------------------------------------------------ROB01660
      DO 190 K=4,NW-3                                                  ROB01670
      J=K-1                                                            ROB01680
      C=EA*XIA+EB*XIB                                                  ROB01690
      C=2.0*C                                                          ROB01700
      C=E*H*EA*AA/C                                                    ROB01710
      AMATX(NUA+NUB+K,J+2)=C                                           ROB01720
      AMATX(NUA+NUB+K,J+1)=-2.0*C                                      ROB01730
      AMATX(NUA+NUB+K,J-1)=2.0*C                                       ROB01740
      AMATX(NUA+NUB+K,J-2)=-C                                          ROB01750
      AMATX(NUA+NUB+K,NUA+NUB+K-2)=1                                   ROB01760
      AMATX(NUA+NUB+K,NUA+NUB+K-1)=-4                                  ROB01770
      AMATX(NUA+NUB+K,NUA+NUB+K)=6                                     ROB01780
      AMATX(NUA+NUB+K,NUA+NUB+K+1)=-4                                  ROB01790
      AMATX(NUA+NUB+K,NUA+NUB+K+2)=1                                   ROB01800
190   CONTINUE                                                         ROB01810
C-----------------------------------------------------------------------ROB01820
      K=NW-2                                                           ROB01830
      AMATX(NUA+NUB+K,NUA+NUB+K)=1                                     ROB01840
C-----------------------------------------------------------------------ROB01850
      K=NW-2                                                           ROB01860
      AMATX(NUA+NUB+K+1,NUA+NUB+K-1)=1                                 ROB01870
      AMATX(NUA+NUB+K+1,NUA+NUB+K)=-2                                  ROB01880
      AMATX(NUA+NUB+K+1,NUA+NUB+K+1)=1                                 ROB01890
C-----------------------------------------------------------------------ROB01900
      K=NW-2                                                           ROB01910
      AMATX(NUA+NUB+K+2,NUA+NUB+K-2)=1                                 ROB01920
      AMATX(NUA+NUB+K+2,NUA+NUB+K-1)=-4                                ROB01930
      AMATX(NUA+NUB+K+2,NUA+NUB+K)=6                                   ROB01940
      AMATX(NUA+NUB+K+2,NUA+NUB+K+1)=-4                                ROB01950
      AMATX(NUA+NUB+K+2,NUA+NUB+K+2)=1                                 ROB01960
C-----------------------------------------------------------------------ROB01970
C-----------------------------------------------------------------------ROB01980
C-----------------------------------------------------------------------ROB01990
C-----------------------------------------------------------------------ROB02000
      DO 290  I=1,NTOT                                                 ROB02010
      DO 290  J=1,NTOT                                                 ROB02020
290   AMT(I,J)=AMATX(I,J)                                              ROB02030
                                                                       ROB02040
C     WRITE(21,235)                                                    ROB02050
CC235  FORMAT(10X,'MATRIX OF COEFFICIENTS FOLLOWS:-')                  ROB02060
C     DO 240 I=1,NTOT                                                  ROB02070
C     WRITE(21,245)I                                                   ROB02080
C245  FORMAT(/5X,'ROW NUMBER OF AMATRIX=',I4)                          ROB02090
C     WRITE(21,*)'COEFFICIENTS        FOR          UA       FOLLOWS;-'  ROB02100
C     WRITE(21,250)(AMATX(I,J),J=1,NUA)                                ROB02110
C     WRITE(21,*)'COEFFICIENTS FOR                 UB       FOLLOWS;-'  ROB02120
C     WRITE(21,250)(AMATX(I,J),J=NUA+1,NUA+NUB)                        ROB02130
C     WRITE(21,*)'COEFFICIENTS  FOR                W     FOLLOWS;-'    ROB02140
C     WRITE(21,250)(AMATX(I,J),J=NUA+NUB+1,NTOT)                       ROB02150
C250  FORMAT(5E25.4)                                                   ROB02160
C240  CONTINUE                                                         ROB02170
C     WRITE(21,*)'DIAGONAL OF AMATX FOLLOWS'                           ROB02180
C     WRITE(21,251)(AMATX(J,J),J=1,NTOT)                               ROB02190
C     WRITE(21,261)                                                    ROB02200
```

FILE: ROB1 FORTRAN A1 KING FAHD UNIVERSITY OF PETROLEUM AND MINERALS, DHAHRAN

```
C261   FORMAT(5X,'INVERSE  OF  AMATX FOLLOWS')                          ROB02210
C      DO 241 I=1,NTOT                                                  ROB02220
CC      WRITE(21,246)I                                                  ROB02230
C246   FORMAT(/5X,'ROW NUMBER OF AMATRIX=',I4)                          ROB02240
C      WRITE(21,*)'COEFFICIENTS        FOR          UA        FOLLOWS;-'  ROB02250
C      WRITE(21,251)(AMATX(I,J),J=1,NUA)                                ROB02260
C      WRITE(21,*)'COEFFICIENTS FOR                 UB        FOLLOWS;-'  ROB02270
C      WRITE(21,251)(AMATX(I,J),J=NUA+1,NUA+NUB)                        ROB02280
C     WRITE(21,*)'COEFFICIENTS  FOR                W      FOLLOWS;-'    ROB02290
C     WRITE(21,251)(AMATX(I,J),J=NUA+NUB+1,NUA+NUB+NW)                  ROB02300
251    FORMAT(5E25.4)                                                   ROB02310
C241    CONTINUE                                                        ROB02320
       CALL MINVT(AMATX,NTOT,ISTAB)                                     ROB02330
C      WRITE(21,*)'DIAGONAL OF INVERSE OF AMATX FOLLOWS'                ROB02340
C      WRITE(21,251)(AMATX(J,J),J=1,NTOT)                               ROB02350
       CALL MATMUL(AMATX,AMT,AMT1,NTOT,NTOT,NTOT)                       ROB02360
C      WRITE(21,*)'DIAGONAL OF RESULTANT MATRIX FOLLOWS'                ROB02370
C      WRITE(21,251)(AMT1(J,J),J=1,NTOT)                                ROB02380
C-----------------------------------------------------------------------ROB02390
       CALL ALOAD(PCL,NPOIN,PLOAD)                                      ROB02400
       CALL MATMC(AMATX,PLOAD,DISP,NTOT)                                ROB02410
       DO 300 K=1,NUA                                                   ROB02420
300    UA(K)=DISP(K)                                                    ROB02430
       DO 310 K=1,NUB                                                   ROB02440
310    UB(K)=DISP(NUA+K)                                                ROB02450
       DO 320 K=1,NW                                                    ROB02460
320    W(K)=DISP(NUA+NUB+K)                                             ROB02470
C-----------------------------------------------------------------------ROB02480
C-----------------------------------------------------------------------ROB02490
C      WRITE(21,*)'UA FOLLOWS'                                          ROB02500
C      WRITE(21,251)(UA(K),K=1,NUA)                                     ROB02510
C      WRITE(21,*)'UB FOLLOWS'                                          ROB02520
C      WRITE(21,251)(UB(K),K=1,NUB)                                     ROB02530
C      WRITE(21,*)'W FOLLOWS'                                           ROB02540
C      WRITE(21,999)(W(K),K=1,NW)                                       ROB02550
       WRITE(24,999)(W(K),K=1,NW)                                       ROB02560
999    FORMAT(F8.3)                                                     ROB02570
C-----------------------------------------------------------------------ROB02580
       DO 370 K=3,NPOIN+2                                               ROB02590
       J=K-1                                                            ROB02600
       I=K-2                                                            ROB02610
       C=E/H/2.0                                                        ROB02620
370    UAB(I)=UA(J)-UB(J)-C*W(K+1)+C*W(K-1)                             ROB02630
C      WRITE(21,*)'UAB FOLLOWS'                                         ROB02640
C      WRITE(21,251)(UAB(K),K=1,NPOIN)                                  ROB02650
C-----------------------------------------------------------------      ROB02660
C-----------------------------------------------------------------------ROB02670
       DO 400 K=1,NPOIN                                                 ROB02680
400    COOR(K)=H*(K-1)/1000                                             ROB02690
       WRITE(22,380)(COOR(K),UAB(K),K=1,NPOIN)                          ROB02700
380    FORMAT(2F25.6)                                                   ROB02710
C-----------------------------------------------------------------------ROB02720
       STOP                                                             ROB02730
       END                                                              ROB02740
C-----------------------------------------------------------------------ROB02750
```

```
C-----SUBROUTINE FOR MULPLICATION OF MATRIX                              ROB02760
C-------------------------------------------------------------------------ROB02770
      SUBROUTINE MATMUL(A,B,C,L,M,N)                                     ROB02780
      IMPLICIT REAL*8 (A-H,O-Z)                                          ROB02790
      DIMENSION A(450,450),B(450,450),C(450,450)                         ROB02800
      DO 20 I=1,L                                                        ROB02810
      DO 20 J=1,N                                                        ROB02820
      C(I,J)=0                                                           ROB02830
      DO 20 K=1,M                                                        ROB02840
20    C(I,J)=C(I,J)+A(I,K)*B(K,J)                                        ROB02850
      RETURN                                                             ROB02860
      END                                                                ROB02870
C-------------------------------------------------------------------------ROB02880
C-----SUBROUTINE FOR MULTIPLICATION OF A VECTOR WITH MATRIX              ROB02890
C-------------------------------------------------------------------------ROB02900
      SUBROUTINE MATMC(A,B,C,M)                                          ROB02910
      IMPLICIT REAL*8 (A-H,O-Z)                                          ROB02920
      DIMENSION A(450,450),B(450),C(450)                                 ROB02930
      DO 10  I=1,M                                                       ROB02940
      C(I)=0                                                             ROB02950
      DO 10 J=1,M                                                        ROB02960
10    C(I)=C(I)+A(I,J)*B(J)                                              ROB02970
      RETURN                                                             ROB02980
      END                                                                ROB02990
C SUBROUTINE MATRIX INVERSION                                            ROB03000
      SUBROUTINE MINVT(A,N,ISTAB)                                        ROB03010
      IMPLICIT REAL*8 (A-H,O-Z)                                          ROB03020
      DIMENSION A(450,450)                                               ROB03030
      ISTAB=0                                                            ROB03040
      DO 40 I=1,N                                                        ROB03050
      PIVOT=A(I,I)                                                       ROB03060
      IF(ABS(PIVOT).EQ.(0.0)) THEN                                       ROB03070
      ISTAB=1                                                            ROB03080
      RETURN                                                             ROB03090
      ENDIF                                                              ROB03100
      PIVR=1./PIVOT                                                      ROB03110
      DO 10 NCOL=1,N                                                     ROB03120
      A(I,NCOL)=A(I,NCOL)/PIVOT                                          ROB03130
10    CONTINUE                                                           ROB03140
      DO 30 K=1,N                                                        ROB03150
      IF(K.NE.I) THEN                                                    ROB03160
      PIVOT=A(K,I)                                                       ROB03170
      DO 20 NCOL=1,N                                                     ROB03180
      A(K,NCOL)=A(K,NCOL)-A(I,NCOL)*PIVOT                                ROB03190
20    CONTINUE                                                           ROB03200
      A(K,I)=-PIVOT*PIVR                                                 ROB03210
      ENDIF                                                              ROB03220
30    CONTINUE                                                           ROB03230
      A(I,I)=PIVR                                                        ROB03240
40    CONTINUE                                                           ROB03250
      RETURN                                                             ROB03260
      END                                                                ROB03270
C==SUBROUTINE FOR LOAD VECTOR FOLLOWS ==================================ROB03280
      SUBROUTINE ALOAD(PCL,NPOIN,PLOAD)                                  ROB03290
      IMPLICIT REAL*8 (A-H,O-Z)                                          ROB03300
```

```
      DIMENSION PLOAD(450),PCL(120)                                    ROB03310
      NUA=NPOIN+2                                                      ROB03320
      NUB=NPOIN+2                                                      ROB03330
      NW=NPOIN+4                                                       ROB03340
      NTOT=NUA+NUB+NW                                                  ROB03350
C-----------------------------------------------------------------     ROB03360
      DO 260 K=1,NTOT                                                  ROB03370
260   PLOAD(K)=0                                                       ROB03380
C-----------------------------------------------------------------     ROB03390
      DO  270  K=1,NW                                                  ROB03400
270   PLOAD(NUA+NUB+K)=PCL(K)                                          ROB03410
C-----------------------------------------------------------------     ROB03420
C     WRITE(21,*)'LOAD VECTOR FOLLOWS'                                 ROB03430
C     WRITE(21,251)(PLOAD(K),K=1,NTOT)                                 ROB03440
      RETURN                                                           ROB03450
      END                                                              ROB03460
```

FILE: ROB1 DATA A1 KING FAHD UNIVERSITY OF PETROLEUM AND MINERALS, DHAHRAN

PROBLEN NO. 1
CONTROL INFORMATION

XKS	NDIVS	NCL	ECCEN	TLENG
50000.0	16	1	559	20000

MATERIAL PROPERTIES

AA	XIA	EA	ZIA
3.0E5	1.00E9	21000	100
AB	XIB	EB	ZIB
3.26E4	4.44E9	210000	-459

LOADS

PS
0.0

NODE	CONCENTRATED LOAD
11	49300

Appendix G

LISTING AND A TYPICAL DATA FILE FOR PROGRAM ROB9

G.1 PROGRAM ROB9

This program is based on the partial interaction theory. This can be used for finding the shear and peeling stresses at the interface in the epoxy bonded plated beams. This program can not handle the material and geometrical non-linearities.

G.2 EXPLANATION OF THE TERMS IN THE DATA FILE

1. TLENG

   This term represents the total length of the beam strengthened by plate bonding.

2. NDIVS

   This term represents the total number of segments in which the beam is divided. Any number can be used. For increasing accuracy, the number of segments are increased.

3. NCL

This term represents the number of concentrated loads to be placed on the beam.

4. ECCEN

This is the distance between the centroids of the concrete beam and the steel plate.

5. XKS, XKN

These are the shear and normal stiffnesses of the interface respectively.

6. AA, AB

These terms represent the areas of the concrete beam and the bonded plate respectively.

7. XIA, XIB

These terms represent the moments of inertias about their centroidal axis for the concrete beam and the bonded plate respectively.

8. EA, EB

These terms represent the modulli of elasticities of the upper and lower layer respectively.

9. ZIA, ZIB

ZIA is the distance from the centroid of the upper layer to the interface and ZIB represent the distance from the centroid of the lower layer to the interface. ZIB will be negative when measured upward because the positive direction of the z-axis was taken downward in the derivations of the differential equations.

10. AWID, BWID

These terms represent the widths of the upper and lower layer respectively.

11. PS

This term represents the uniformly distributed load placed on the beam.

12. JPL, JPR

These terms represent the nodes at which the bonded plate terminate. JPL is the node at which the left end of the plate terminates and JPR is the node at which the right end of the plate terminates. For the time being, this program can handle symmetrically bonded plates. But with very little work, the program can be made capable of handling unsymmetrically bonded plates.

13. MIDD, DH

These are variables used in the subroutine which determine the distribution of peeling stresses at the interface. As the peeling stresses dies down to zero very rapidly, therefore, there is no need to run the whole plate length in this subroutine, which takes a lot of computation time. Only a small length of the plate at the end is needed to run for finding the peeling stress distribution at the interface knowing that the peeling stresses towards the mid-span are zero. MIDD multiplied by DH represents the length of the plate over which the peeling stress distribution is to be determined. MIDD is an arbitrarily chosen number and DH represents the distance between the nodes. It is to be noted that this DH has no relation with the NDIVS. This is independent of the previous node

numbering system which was used for finding the shear stress distribution at the interface. For this subroutine to give good results for peeling stress distribution at the interface of the epoxy bonded plated beams, the node interval should be kept small.

```
C*************************************************************************ROB00010
C          PROGRAM  FOR THE DETERMINATION OF SHEAR AND PEELING            ROB00020
C          STRESSES AT THE INTERFACE IN THE EPOXY BONDED PLATED BEAMS     ROB00030
C                  WRITTEN BY :MUNAWAR HUSSAIN (ST#890481)                ROB00040
C*************************************************************************ROB00050
      IMPLICIT REAL*8(A-H,O-Z)                                            ROB00060
      DIMENSION TITLE(18),ACL(105)                                        ROB00070
251   FORMAT(4F20.3)                                                      ROB00080
      READ(20,10)TITLE                                                    ROB00090
      WRITE(21,10)TITLE                                                   ROB00100
10    FORMAT(18A4)                                                        ROB00110
      READ(20,10)WORDS                                                    ROB00120
      READ(20,10)WORDS                                                    ROB00130
      READ(20,*)TLENG,NDIVS,NCL,E,XKS,XKN                                 ROB00140
      READ(20,10)WORDS                                                    ROB00150
      READ(20,10)WORDS                                                    ROB00160
      READ(20,*)AA,XIA,EA,ZIA,AWID                                        ROB00170
      READ(20,10)WORDS                                                    ROB00180
      READ(20,*)AB,XIB,EB,ZIB,BWID                                        ROB00190
      READ(20,10)WORDS                                                    ROB00200
      READ(20,10)WORDS                                                    ROB00210
      READ(20,*)PS,JPL,JPR,MIDD,DH                                        ROB00220
      WRITE(21,20) TLENG                                                  ROB00230
20    FORMAT(/5X,'TLENG=',F15.3)                                          ROB00240
      WRITE(21,25) NDIVS                                                  ROB00250
25    FORMAT(/5X,'NUMBER OF SEGMENTS.....NDIVS=',I3)                      ROB00260
      WRITE(21,30) E                                                      ROB00270
30    FORMAT(/5X,'.............................E=',E15.6)                 ROB00280
      WRITE(21,35) XKS                                                    ROB00290
35    FORMAT(/5X,'.............................KS=',E15.6)                 ROB00300
      WRITE(21,45)AA                                                      ROB00310
45    FORMAT(/5X,'.............................AA=',E15.6)                 ROB00320
      WRITE(21,50) XIA                                                    ROB00330
50    FORMAT(/5X,'.............................IA=',E15.6)                 ROB00340
      WRITE(21,55) EA                                                     ROB00350
55    FORMAT(/5X,'.............................EA=',E15.6)                 ROB00360
      WRITE(21,60) ZIA                                                    ROB00370
60    FORMAT(/5X,'.............................ZIA=',E15.6)                ROB00380
      WRITE(21,65) AB                                                     ROB00390
65    FORMAT(/5X,'AB=',E15.6)                                             ROB00400
      WRITE(21,70) XIB                                                    ROB00410
70    FORMAT(/5X,'IB=',E15.6)                                             ROB00420
      WRITE(21,75) EB                                                     ROB00430
75    FORMAT(/5X,'EB=',E15.6)                                             ROB00440
      WRITE(21,80) ZIB                                                    ROB00450
80    FORMAT(/5X,'ZIB=',E15.6)                                            ROB00460
      NPOIN=NDIVS+1                                                       ROB00470
      WRITE(21,85) NPOIN                                                  ROB00480
85    FORMAT(/5X,'NPOIN=',I3)                                             ROB00490
      H=TLENG/FLOAT(NDIVS)                                                ROB00500
      WRITE(21,90) H                                                      ROB00510
90    FORMAT(///5X,'.............................H=',F15.3)               ROB00520
      WRITE(21,100) PS                                                    ROB00530
100   FORMAT(///5X,'.............................PS=',F15.3)              ROB00540
      WRITE(21,116)NCL                                                    ROB00550
```

```
116   FORMAT(/5X,'NUMBER OF CONCENTRATED LOADS.=',I5)                    ROB00560
      WRITE(21,98)JPL                                                    ROB00570
98    FORMAT(/5X,'LEFT JOINT OF PLATE.=',I5)                             ROB00580
      WRITE(21,99)JPR                                                    ROB00590
99    FORMAT(/5X,'RIGHT JOINT OF PLATE.=',I5)                            ROB00600
C-----------------------------------------------------------------       ROB00610
      WRITE(*,*)'THE STARTS TO CALCULATE'                                ROB00620
      NUA=NPOIN+2                                                        ROB00630
      NUB=NPOIN+2                                                        ROB00640
      NW=NPOIN+4                                                         ROB00650
      NTOT=NUA+NUB+NW                                                    ROB00660
C-----------------------------------------------------------------       ROB00670
      DO 440 K=1,NW                                                      ROB00680
440   ACL(K)=0                                                           ROB00690
      READ (20,10) WORDS                                                 ROB00700
      DO 600 K=1,NCL                                                     ROB00710
600   READ (20,*)J,ACL(J)                                               ROB00720
      DO 610 K=1,NW                                                      ROB00730
610   ACL(K)=ACL(K)/H                                                    ROB00740
      DO 650 K=1,NW                                                      ROB00750
650   ACL(K)=ACL(K)+PS                                                   ROB00760
      ACL(1)=ACL(1)/2.0                                                  ROB00770
      ACL(2)=0                                                           ROB00780
      ACL(3)=0                                                           ROB00790
      ACL(NW-2)=0                                                        ROB00800
      ACL(NW-1)=0                                                        ROB00810
      ACL(NW)=ACL(NW)/2.0                                                ROB00820
C     WRITE(21,*)'ACL FOLLOWS'                                           ROB00830
C     WRITE(21,630)(ACL(K),K=1,NW)                                       ROB00840
630   FORMAT(4E18.3)                                                     ROB00850
      CALL DEFL(ACL,EA,XIA,EB,XIB,JPL,JPR,H,XKS,NPOIN,AA,AB,E,           ROB00860
     .BWID,ZIA,ZIB,XKN,XFL,XML)                                          ROB00870
      WRITE(28,631)XFL                                                   ROB00880
631   FORMAT('XFL=',F10.3)                                               ROB00890
      WRITE(28,632)XML                                                   ROB00900
632   FORMAT('XML=',F10.3)                                               ROB00910
      CALL SIG(DH,MIDD,XML,XFL,XKN,EB,XIB,BWID)                          ROB00920
      STOP                                                               ROB00930
      END                                                                ROB00940
C-----------------------------------------------------------------------ROB00950
      SUBROUTINE DEFL(ACL,EA,XIA,EB,XIB,JPL,JPR,H,XKS,NPOIN,AA,AB,E,     ROB00960
     .BWID,ZIA,ZIB,XKN,XFL,XML)                                          ROB00970
      IMPLICIT REAL*8(A-H,O-Z)                                           ROB00980
      DIMENSION AMATX(310,310),PLOAD(310),DISP(310)                      ROB00990
      DIMENSION ACL(105),PCL(105),UA(105),UB(105),W(105)                 ROB01000
      DIMENSION COOR(105),UAB(105),STRESS(105),TAU(105),SIGMA(105)       ROB01010
C-----------------------------------------------------------------       ROB01020
      NUA=NPOIN+2                                                        ROB01030
      NUB=NPOIN+2                                                        ROB01040
      NW=NPOIN+4                                                         ROB01050
      NTOT=NUA+NUB+NW                                                    ROB01060
C-----------------------------------------------------------------------ROB01070
251   FORMAT(5F14.2)                                                     ROB01080
C-----------------------------------------------------------------------ROB01090
      DO 700 K=1,JPL-1                                                   ROB01100
```

```
      C=EA*XIA                                                          ROB01110
      C=H**4/C                                                          ROB01120
700   PCL(K)=C*ACL(K)                                                   ROB01130
C-----------------------------------------------------------------------ROB01140
      K=JPL                                                             ROB01150
      C=EA*XIA+EB*XIB*0.5                                               ROB01160
      C=H**4/C                                                          ROB01170
      PCL(K)=C*ACL(K)                                                   ROB01180
C-----------------------------------------------------------------------ROB01190
      DO 701 K=JPL+1,JPR-1                                              ROB01200
      C=EA*XIA+EB*XIB                                                   ROB01210
      C=H**4/C                                                          ROB01220
701   PCL(K)=C*ACL(K)                                                   ROB01230
C-----------------------------------------------------------------------ROB01240
      K=JPR                                                             ROB01250
      C=EA*XIA+EB*XIB*0.5                                               ROB01260
      C=H**4/C                                                          ROB01270
      PCL(K)=C*ACL(K)                                                   ROB01280
C-----------------------------------------------------------------------ROB01290
      DO 702 K=JPR+1,NW                                                 ROB01300
      C=EA*XIA                                                          ROB01310
      C=H**4/C                                                          ROB01320
702   PCL(K)=C*ACL(K)                                                   ROB01330
C-------------------------------------------------------------          ROB01340
      DO 703 K=1,NTOT                                                   ROB01350
703   PLOAD(K)=0                                                        ROB01360
C-------------------------------------------------------------          ROB01370
      DO  704  K=1,NW                                                   ROB01380
704   PLOAD(NUA+NUB+K)=PCL(K)                                           ROB01390
C-----------------------------------------------------------------------ROB01400
C     GENERATION OF AMATRIX  FOLLOWS:-                                  ROB01410
C-----------------------------------------------------------------------ROB01420
      DO 130 I=1,NTOT                                                   ROB01430
      DO 130 J=1,NTOT                                                   ROB01440
      AMATX(I,J)=0.0                                                    ROB01450
130   CONTINUE                                                          ROB01460
C=======================================================================ROB01470
C=====HORIZONTAL EQUILIBRIUM OF UPPER LAYER=============================ROB01480
C=======================================================================ROB01490
      JPL=JPL-1                                                         ROB01500
      JPR=JPR-1                                                         ROB01510
C=======================================================================ROB01520
      J=2                                                               ROB01530
      AMATX(J-1,J+1)=1.0                                                ROB01540
      AMATX(J-1,J-1)=-1.0                                               ROB01550
C-------------------------------------------------------------          ROB01560
      DO 165 J=2,JPL-1                                                  ROB01570
      AMATX(J,J+1)=1.0                                                  ROB01580
      AMATX(J,J)=-2.0                                                   ROB01590
      AMATX(J,J-1)=1.0                                                  ROB01600
165   CONTINUE                                                          ROB01610
C-------------------------------------------------------------          ROB01620
      J=JPL                                                             ROB01630
      K=J+1                                                             ROB01640
      C=XKS*H*H/EA/AA/2.0                                               ROB01650
```

```
      AMATX(J,J+1)=1                                                    ROB01660
      AMATX(J,J)=-2.0-C                                                 ROB01670
      AMATX(J,J-1)=1                                                    ROB01680
      AMATX(J,NUA+J)=C                                                  ROB01690
      C=XKS*E*H/EA/AA/4.0                                               ROB01700
      AMATX(J,NUA+NUB+K+1)=C                                            ROB01710
      AMATX(J,NUA+NUB+K-1)=-C                                           ROB01720
C-----------------------------------------------------------------      ROB01730
      DO 170 J=JPL+1,JPR-1                                              ROB01740
      K=J+1                                                             ROB01750
      C=XKS*H*H/EA/AA                                                   ROB01760
      AMATX(J,J+1)=1                                                    ROB01770
      AMATX(J,J)=-2.0-C                                                 ROB01780
      AMATX(J,J-1)=1                                                    ROB01790
      AMATX(J,NUA+J)=C                                                  ROB01800
      C=XKS*E*H/EA/AA/2.0                                               ROB01810
      AMATX(J,NUA+NUB+K+1)=C                                            ROB01820
      AMATX(J,NUA+NUB+K-1)=-C                                           ROB01830
170   CONTINUE                                                          ROB01840
C-----------------------------------------------------------------      ROB01850
      J=JPR                                                             ROB01860
      K=J+1                                                             ROB01870
      C=XKS*H*H/EA/AA/2.0                                               ROB01880
      AMATX(J,J+1)=1                                                    ROB01890
      AMATX(J,J)=-2.0-C                                                 ROB01900
      AMATX(J,J-1)=1                                                    ROB01910
      AMATX(J,NUA+J)=C                                                  ROB01920
      C=XKS*E*H/EA/AA/4.0                                               ROB01930
      AMATX(J,NUA+NUB+K+1)=C                                            ROB01940
      AMATX(J,NUA+NUB+K-1)=-C                                           ROB01950
C-----------------------------------------------------------------      ROB01960
      DO 175 J=JPR+1,NUA-1                                              ROB01970
      AMATX(J,J+1)=1                                                    ROB01980
      AMATX(J,J)=-2                                                     ROB01990
      AMATX(J,J-1)=1                                                    ROB02000
175   CONTINUE                                                          ROB02010
C-----------------------------------------------------------------      ROB02020
      J=NUA-1                                                           ROB02030
      AMATX(J+1,J+1)=1.0                                                ROB02040
      AMATX(J+1,J-1)=-1.0                                               ROB02050
C=================================================================      ROB02060
C=====HORIZONTAL EQUILIBRIUM                                           ROB02070
C=================================================================      ROB02080
      J=2                                                               ROB02090
      AMATX(NUA+J-1,NUA+J+1)=1.0                                        ROB02100
      AMATX(NUA+J-1,NUA+J-1)=-1.0                                       ROB02110
C-----------------------------------------------------------------      ROB02120
      DO 180  J=2,JPL-1                                                 ROB02130
      AMATX(NUA+J,NUA+J+1)=1                                            ROB02140
      AMATX(NUA+J,NUA+J)=-2.0                                           ROB02150
      AMATX(NUA+J,NUA+J-1)=1                                            ROB02160
180   CONTINUE                                                          ROB02170
C-----------------------------------------------------------------      ROB02180
      DO 184  J=JPL,JPR                                                 ROB02190
      AMATX(NUA+J,J+1)=1.0                                              ROB02200
```

```
      AMATX(NUA+J,J)=-2.0                                              ROB02210
      AMATX(NUA+J,J-1)=1.0                                             ROB02220
      C=EB*AB/EA/AA                                                    ROB02230
      AMATX(NUA+J,NUA+J+1)=C                                           ROB02240
      AMATX(NUA+J,NUA+J)=-2.0*C                                        ROB02250
      AMATX(NUA+J,NUA+J-1)=C                                           ROB02260
184   CONTINUE                                                         ROB02270
C-----------------------------------------------------------------------ROB02280
      DO 186  J=JPR+1,NUB-1                                            ROB02290
      AMATX(NUA+J,NUA+J+1)=1.0                                         ROB02300
      AMATX(NUA+J,NUA+J)=-2.0                                          ROB02310
      AMATX(NUA+J,NUA+J-1)=1                                           ROB02320
186   CONTINUE                                                         ROB02330
C-----------------------------------------------------------------------ROB02340
      J=NUB-1                                                          ROB02350
      AMATX(NUA+J+1,NUA+J+1)=-1.0                                      ROB02360
      AMATX(NUA+J+1,NUA+J-1)=1.0                                       ROB02370
C=======================================================================ROB02380
C     VERTICAL EQUILIBRIUM  AND  MOMENT EQUILIBRIUM                    ROB02390
C=======================================================================ROB02400
      JPL=JPL+1                                                        ROB02410
      JPR=JPR+1                                                        ROB02420
C=======================================================================ROB02430
      K=3                                                              ROB02440
      AMATX(NUA+NUB+K-2,NUA+NUB+K-2)=1                                 ROB02450
      AMATX(NUA+NUB+K-2,NUA+NUB+K-1)=-4                                ROB02460
      AMATX(NUA+NUB+K-2,NUA+NUB+K)=6                                   ROB02470
      AMATX(NUA+NUB+K-2,NUA+NUB+K+1)=-4                                ROB02480
      AMATX(NUA+NUB+K-2,NUA+NUB+K+2)=1                                 ROB02490
C-----------------------------------------------------------------------ROB02500
      K=3                                                              ROB02510
      AMATX(NUA+NUB+K-1,NUA+NUB+K-1)=1                                 ROB02520
      AMATX(NUA+NUB+K-1,NUA+NUB+K)=-2                                  ROB02530
      AMATX(NUA+NUB+K-1,NUA+NUB+K+1)=1                                 ROB02540
C-----------------------------------------------------------------------ROB02550
      K=3                                                              ROB02560
      AMATX(NUA+NUB+K,NUA+NUB+K)=1                                     ROB02570
C-----------------------------------------------------------------------ROB02580
      DO 185 K=4,JPL-1                                                 ROB02590
      J=K-1                                                            ROB02600
      C=EA*XIA                                                         ROB02610
      C=2.0*C                                                          ROB02620
      C=E*H*EA*AA/C                                                    ROB02630
      AMATX(NUA+NUB+K,J+2)=C                                           ROB02640
      AMATX(NUA+NUB+K,J+1)=-2.0*C                                      ROB02650
      AMATX(NUA+NUB+K,J-1)=2.0*C                                       ROB02660
      AMATX(NUA+NUB+K,J-2)=-C                                          ROB02670
      AMATX(NUA+NUB+K,NUA+NUB+K-2)=1                                   ROB02680
      AMATX(NUA+NUB+K,NUA+NUB+K-1)=-4                                  ROB02690
      AMATX(NUA+NUB+K,NUA+NUB+K)=6                                     ROB02700
      AMATX(NUA+NUB+K,NUA+NUB+K+1)=-4                                  ROB02710
      AMATX(NUA+NUB+K,NUA+NUB+K+2)=1                                   ROB02720
185   CONTINUE                                                         ROB02730
C-----------------------------------------------------------------------ROB02740
      K=JPL                                                            ROB02750
```

```
      J=K-1                                                          ROB02760
      C=EA*XIA+EB*XIB*0.5                                            ROB02770
      C=2.0*C                                                        ROB02780
      C=E*H*EA*AA/C                                                  ROB02790
      AMATX(NUA+NUB+K,J+2)=C                                         ROB02800
      AMATX(NUA+NUB+K,J+1)=-2.0*C                                    ROB02810
      AMATX(NUA+NUB+K,J-1)=2.0*C                                     ROB02820
      AMATX(NUA+NUB+K,J-2)=-C                                        ROB02830
      AMATX(NUA+NUB+K,NUA+NUB+K-2)=1                                 ROB02840
      AMATX(NUA+NUB+K,NUA+NUB+K-1)=-4                                ROB02850
      AMATX(NUA+NUB+K,NUA+NUB+K)=6                                   ROB02860
      AMATX(NUA+NUB+K,NUA+NUB+K+1)=-4                                ROB02870
      AMATX(NUA+NUB+K,NUA+NUB+K+2)=1                                 ROB02880
C-----------------------------------------------------------------------ROB02890
      DO 190 K=JPL+1,JPR-1                                           ROB02900
      J=K-1                                                          ROB02910
      C=EA*XIA+EB*XIB                                                ROB02920
      C=2.0*C                                                        ROB02930
      C=E*H*EA*AA/C                                                  ROB02940
      AMATX(NUA+NUB+K,J+2)=C                                         ROB02950
      AMATX(NUA+NUB+K,J+1)=-2.0*C                                    ROB02960
      AMATX(NUA+NUB+K,J-1)=2.0*C                                     ROB02970
      AMATX(NUA+NUB+K,J-2)=-C                                        ROB02980
      AMATX(NUA+NUB+K,NUA+NUB+K-2)=1                                 ROB02990
      AMATX(NUA+NUB+K,NUA+NUB+K-1)=-4                                ROB03000
      AMATX(NUA+NUB+K,NUA+NUB+K)=6                                   ROB03010
      AMATX(NUA+NUB+K,NUA+NUB+K+1)=-4                                ROB03020
      AMATX(NUA+NUB+K,NUA+NUB+K+2)=1                                 ROB03030
190   CONTINUE                                                       ROB03040
C-----------------------------------------------------------------------ROB03050
      K=JPR                                                          ROB03060
      J=K-1                                                          ROB03070
      C=EA*XIA+EB*XIB*0.5                                            ROB03080
      C=2.0*C                                                        ROB03090
      C=E*H*EA*AA/C                                                  ROB03100
      AMATX(NUA+NUB+K,J+2)=C                                         ROB03110
      AMATX(NUA+NUB+K,J+1)=-2.0*C                                    ROB03120
      AMATX(NUA+NUB+K,J-1)=2.0*C                                     ROB03130
      AMATX(NUA+NUB+K,J-2)=-C                                        ROB03140
      AMATX(NUA+NUB+K,NUA+NUB+K-2)=1                                 ROB03150
      AMATX(NUA+NUB+K,NUA+NUB+K-1)=-4                                ROB03160
      AMATX(NUA+NUB+K,NUA+NUB+K)=6                                   ROB03170
      AMATX(NUA+NUB+K,NUA+NUB+K+1)=-4                                ROB03180
      AMATX(NUA+NUB+K,NUA+NUB+K+2)=1                                 ROB03190
C-----------------------------------------------------------------------ROB03200
      DO 195 K=JPR+1,NW-3                                            ROB03210
      J=K-1                                                          ROB03220
      C=EA*XIA                                                       ROB03230
      C=2.0*C                                                        ROB03240
      C=E*H*EA*AA/C                                                  ROB03250
      AMATX(NUA+NUB+K,J+2)=C                                         ROB03260
      AMATX(NUA+NUB+K,J+1)=-2.0*C                                    ROB03270
      AMATX(NUA+NUB+K,J-1)=2.0*C                                     ROB03280
      AMATX(NUA+NUB+K,J-2)=-C                                        ROB03290
      AMATX(NUA+NUB+K,NUA+NUB+K-2)=1                                 ROB03300
```

```
      AMATX(NUA+NUB+K,NUA+NUB+K-1)=-4                                   ROB03310
      AMATX(NUA+NUB+K,NUA+NUB+K)=6                                      ROB03320
      AMATX(NUA+NUB+K,NUA+NUB+K+1)=-4                                   ROB03330
      AMATX(NUA+NUB+K,NUA+NUB+K+2)=1                                    ROB03340
195   CONTINUE                                                          ROB03350
C-----------------------------------------------------------------------ROB03360
      K=NW-2                                                            ROB03370
      AMATX(NUA+NUB+K,NUA+NUB+K)=1                                      ROB03380
C-----------------------------------------------------------------------ROB03390
      K=NW-2                                                            ROB03400
      AMATX(NUA+NUB+K+1,NUA+NUB+K-1)=1                                  ROB03410
      AMATX(NUA+NUB+K+1,NUA+NUB+K)=-2                                   ROB03420
      AMATX(NUA+NUB+K+1,NUA+NUB+K+1)=1                                  ROB03430
C-----------------------------------------------------------------------ROB03440
      K=NW-2                                                            ROB03450
      AMATX(NUA+NUB+K+2,NUA+NUB+K-2)=1                                  ROB03460
      AMATX(NUA+NUB+K+2,NUA+NUB+K-1)=-4                                 ROB03470
      AMATX(NUA+NUB+K+2,NUA+NUB+K)=6                                    ROB03480
      AMATX(NUA+NUB+K+2,NUA+NUB+K+1)=-4                                 ROB03490
      AMATX(NUA+NUB+K+2,NUA+NUB+K+2)=1                                  ROB03500
C-----------------------------------------------------------------------ROB03510
      CALL MINVT(AMATX,NTOT,ISTAB)                                      ROB03520
C-----------------------------------------------------------------------ROB03530
      CALL MATMC(AMATX,PLOAD,DISP,NTOT)                                 ROB03540
      DO 300 K=1,NUA                                                    ROB03550
300   UA(K)=DISP(K)                                                     ROB03560
      DO 310 K=1,NUB                                                    ROB03570
310   UB(K)=DISP(NUA+K)                                                 ROB03580
      DO 320 K=1,NW                                                     ROB03590
320   W(K)=DISP(NUA+NUB+K)                                              ROB03600
C-----------------------------------------------------------------------ROB03610
      DO 400 K=1,NPOIN                                                  ROB03620
400   COOR(K)=H*(K-1)/1000                                              ROB03630
C     WRITE(21,*)'UA FOLLOWS'                                           ROB03640
C     WRITE(21,251)(UA(K),K=1,NUA)                                      ROB03650
C     WRITE(21,*)'UB FOLLOWS'                                           ROB03660
C     WRITE(21,251)(UB(K),K=1,NUB)                                      ROB03670
C     WRITE(21,*)'W FOLLOWS'                                            ROB03680
C     WRITE(21,251)(W(K),K=1,NW)                                        ROB03690
      WRITE(27,381)(COOR(K),W(K+2),K=1,NW-2)                            ROB03700
381   FORMAT(2F15.5)                                                    ROB03710
C-----------------------------------------------------------------------ROB03720
      DO 370 K=3,NPOIN+2                                                ROB03730
      J=K-1                                                             ROB03740
      I=K-2                                                             ROB03750
      C=E/H/2.0                                                         ROB03760
370   UAB(I)=UA(J)-UB(J)-C*W(K+1)+C*W(K-1)                              ROB03770
C     WRITE(21,*)'UAB FOLLOWS'                                          ROB03780
C     WRITE(21,251)(UAB(K),K=1,NPOIN)                                   ROB03790
      WRITE(22,380)(COOR(K),UAB(K),K=1,NPOIN)                           ROB03800
380   FORMAT(2F15.5)                                                    ROB03810
C-----------------------------------------------------------------------ROB03820
      DO 371 K=2,NUB-1                                                  ROB03830
      J=K-1                                                             ROB03840
371   STRESS(J)=(UB(K+1)-UB(K-1))*EB/H/2.0                              ROB03850
```

```
      WRITE(24,380)(COOR(K),STRESS(K),K=1,NPOIN)                        ROB03860
C-----------------------------------------------------------------------ROB03870
      JPL=JPL-1                                                         ROB03880
      JPR=JPR-1                                                         ROB03890
C-----------------------------------------------------------------------ROB03900
      DO 372 J=2,NUA-1                                                  ROB03910
      I=J-1                                                             ROB03920
372   TAU(I)=0.0                                                        ROB03930
C-----------------------------------------------------------------------ROB03940
      DO 374 J=JPL,JPR                                                  ROB03950
      I=J-1                                                             ROB03960
374   TAU(I)=UAB(I)*XKS/BWID                                            ROB03970
C-----------------------------------------------------------------------ROB03980
      WRITE(25,380)(COOR(K),TAU(K),K=1,NPOIN)                           ROB03990
C-----------------------------------------------------------------------ROB04000
      JPL=JPL+1                                                         ROB04010
      JPR=JPR+1                                                         ROB04020
      K=JPL                                                             ROB04030
      XFL=EB*XIB*(W(K+2)-2.0*W(K+1)+2.0*W(K-1)-W(K-2))/H/H/H/2.0        ROB04040
      XFL=XFL-TAU(JPL-2)*ZIB*BWID                                       ROB04050
      XML=EB*XIB*(W(K+1)-2.0*W(K)+W(K-1))/H/H                           ROB04060
      K=JPR                                                             ROB04070
      XFR=EB*XIB*(W(K+2)-2.0*W(K+1)+2.0*W(K-1)-W(K-2))/H/H/H/2.0        ROB04080
      XFR=XFR-TAU(JPR-2)*ZIB*BWID                                       ROB04090
      XMR=EB*XIB*(W(K+1)-2.0*W(K)+W(K-1))/H/H                           ROB04100
321   FORMAT(I4)                                                        ROB04110
      WRITE(21,*)'XML FOLLOWS'                                          ROB04120
      WRITE(21,251)XML                                                  ROB04130
      WRITE(21,*)'XMR FOLLOWS'                                          ROB04140
      WRITE(21,251)XMR                                                  ROB04150
      WRITE(21,*)'XFL FOLLOWS'                                          ROB04160
      WRITE(21,251)XFL                                                  ROB04170
      WRITE(21,*)'XFR FOLLOWS'                                          ROB04180
      WRITE(21,251)XFR                                                  ROB04190
      WRITE(21,*)'JPL FOLLOWS'                                          ROB04200
      WRITE(21,321)JPL                                                  ROB04210
      WRITE(21,*)'JPR FOLLOWS'                                          ROB04220
      WRITE(21,321)JPR                                                  ROB04230
      RETURN                                                            ROB04240
      END                                                               ROB04250
C-----------------------------------------------------------------------ROB04260
C-----SUBROUTINE FOR MULTIPLICATION OF A VECTOR WITH MATRIX             ROB04270
C-----------------------------------------------------------------------ROB04280
      SUBROUTINE MATMC(A,B,C,M)                                         ROB04290
      IMPLICIT REAL*8 (A-H,O-Z)                                         ROB04300
      DIMENSION A(310,310),B(310),C(310)                                ROB04310
      DO 10  I=1,M                                                      ROB04320
      C(I)=0                                                            ROB04330
      DO 10 J=1,M                                                       ROB04340
10    C(I)=C(I)+A(I,J)*B(J)                                             ROB04350
      RETURN                                                            ROB04360
      END                                                               ROB04370
C SUBROUTINE MATRIX INVERSION                                           ROB04380
      SUBROUTINE MINVT(A,N,ISTAB)                                       ROB04390
      IMPLICIT REAL*8 (A-H,O-Z)                                         ROB04400
```

```
      DIMENSION A(310,310)                                              
      ISTAB=0                                                           ROB04410
      DO 40 I=1,N                                                       ROB04420
      PIVOT=A(I,I)                                                      ROB04430
      IF(ABS(PIVOT).EQ.(0.0)) THEN                                      ROB04440
      ISTAB=1                                                           ROB04450
      RETURN                                                            ROB04460
      ENDIF                                                             ROB04470
      PIVR=1./PIVOT                                                     ROB04480
      DO 10 NCOL=1,N                                                    ROB04490
      A(I,NCOL)=A(I,NCOL)/PIVOT                                         ROB04500
10    CONTINUE                                                          ROB04510
      DO 30 K=1,N                                                       ROB04520
      IF(K.NE.I) THEN                                                   ROB04530
      PIVOT=A(K,I)                                                      ROB04540
      DO 20 NCOL=1,N                                                    ROB04550
      A(K,NCOL)=A(K,NCOL)-A(I,NCOL)*PIVOT                               ROB04560
20    CONTINUE                                                          ROB04570
      A(K,I)=-PIVOT*PIVR                                                ROB04580
      ENDIF                                                             ROB04590
30    CONTINUE                                                          ROB04600
      A(I,I)=PIVR                                                       ROB04610
40    CONTINUE                                                          ROB04620
      RETURN                                                            ROB04630
      END                                                               ROB04640
      SUBROUTINE SIG(DH,MIDD,XML,XFL,XKN,EB,XIB,BWID)                   ROB04650
      IMPLICIT REAL*8 (A-H,O-Z)                                         ROB04660
      DIMENSION AMATX(310,310),PLOAD(310),W(310)                        ROB04670
      DIMENSION SIGMA(310),COOR(310)                                    ROB04680
      XML=ABS(XML)                                                      ROB04690
      XFL=ABS(XFL)                                                      ROB04700
      XMR=XML                                                           ROB04710
      XFR=-XFL                                                          ROB04720
      DO 5 J=1,MIDD                                                     ROB04730
      DO 5 K=1,MIDD                                                     ROB04740
5     AMATX(J,K)=0.0                                                    ROB04750
C-----------------------------------------------------------------------ROB04760
      K=3                                                               ROB04770
      AMATX(K-2,K+2)=1.0                                                ROB04780
      AMATX(K-2,K+1)=-2.0                                               ROB04790
      AMATX(K-2,K-1)=2.0                                                ROB04800
      AMATX(K-2,K-2)=-1.0                                               ROB04810
C-----------------------------------------------------------------------ROB04820
      K=3                                                               ROB04830
      AMATX(K-1,K+1)=1.0                                                ROB04840
      AMATX(K-1,K)=-2.0                                                 ROB04850
      AMATX(K-1,K-1)=1.0                                                ROB04860
C-----------------------------------------------------------------------ROB04870
      DO 10 K=3,MIDD-2                                                  ROB04880
      AMATX(K,K+2)=1.0                                                  ROB04890
      AMATX(K,K+1)=-4.0                                                 ROB04900
      AMATX(K,K)=6.0+XKN*(DH**4)/EB/XIB                                 ROB04910
      AMATX(K,K-1)=-4.0                                                 ROB04920
      AMATX(K,K-2)=1.0                                                  ROB04930
10    CONTINUE                                                          ROB04940
                                                                        ROB04950
```

```
C-----------------------------------------------------------------------ROB04960
      K=MIDD-2                                                          ROB04970
      AMATX(K+1,K+1)=1.0                                                ROB04980
C-----------------------------------------------------------------------ROB04990
      K=MIDD-2                                                          ROB05000
      AMATX(K+2,K+2)=1.0                                                ROB05010
C-----------------------------------------------------------------------ROB05020
C     WRITE(21,*)'AMATX FOLLOWS'                                        ROB05030
C     WRITE(21,30)((AMATX(J,K),K=1,MIDD),J=1,MIDD)                      ROB05040
C-----------------------------------------------------------------------ROB05050
      CALL MINVT(AMATX,MIDD,ISTAB)                                      ROB05060
C-----------------------------------------------------------------------ROB05070
      DO 15 K=1,MIDD                                                    ROB05080
15    PLOAD(K)=0.0                                                      ROB05090
      PLOAD(1)=2*XFL*DH**3/EB/XIB                                       ROB05100
      PLOAD(2)=XML*DH*DH/EB/XIB                                         ROB05110
      WRITE(21,*)'PLOAD IN BEAM ON ELASTIC FOUNDATION'                  ROB05120
      WRITE(21,30)(PLOAD(K),K=1,MIDD)                                   ROB05130
C-----------------------------------------------------------------------ROB05140
      CALL MATMC(AMATX,PLOAD,W,MIDD)                                    ROB05150
C-----------------------------------------------------------------------ROB05160
      WRITE(21,*)'W OF BEAM ON THE ELASTIC FOUNDATION'                  ROB05170
      WRITE(21,30)(W(K),K=1,MIDD)                                       ROB05180
30    FORMAT(5F14.3)                                                    ROB05190
C-----------------------------------------------------------------------ROB05200
      DO 81 K=3,MIDD                                                    ROB05210
      J=K-2                                                             ROB05220
81    SIGMA(J)=W(K)*XKN/BWID                                            ROB05230
      DO 91 K=3,MIDD                                                    ROB05240
      J=K-2                                                             ROB05250
91    COOR(J)=(K-3)*DH                                                  ROB05260
      WRITE(26,101)(COOR(K-2),SIGMA(K-2),K=3,MIDD)                      ROB05270
101   FORMAT(2F15.3)                                                    ROB05280
      WRITE(21,*)'SIGMA    FOLLOWS'                                     ROB05290
      WRITE(21,31)(SIGMA(K),K=1,MIDD)                                   ROB05300
31    FORMAT(5F14.3)                                                    ROB05310
      RETURN                                                            ROB05320
      END                                                               ROB05330
```

PROBLEN NO. 1
CONTROL INFORMATION

TLENG	NDIVS	NCL	ECCEN	XKS	XKN
2400	80	1	77.0	20000	50000

MATERIAL PROPERTIES

AA	XIA	EA	ZIA	AWID
15000	28125000	20000	75	100
AB	XIB	EB	ZIB	BWID
400	533.33	200000	-2.0	100

LOADS AND PLATE TERMINATION NODES

PS	JPL	JPR	MIDD	DH
15.0	13	73	200	1.3

NODES	CONCENTRATED LOADS
34	0.00